Genotoxicity assessment of andrographolide.

Sharifuddin, Yusrizam

Genotoxicity Assessment of Andrographolide

By

Yusrizam Sharifuddin

Yr Ysgol Feddygaeth, Prifysgol Abertawe
School of Medicine, Swansea University

A thesis submitted in partial fulfilment of the requirement for the degree of Doctor of Philosophy

ProQuest LLC.
789 East Eisenhower Parkway
P.O. Box 1346
Ann Arbor, MI 48106 – 1346

DECLARATION

This work has not previously been accepted in substance for any degree and is not being concurrently submitted in candidature for any degree.

Signed ..... (Yusrizam Sharifuddin)

Date 8th August 2008.

FIRST STATEMENT

This thesis is the result of my own investigations, except where otherwise stated. Where correction services have been used, the extent and nature of the correction is clearly marked in a footnote(s).

Other sources are acknowledged by footnotes giving explicit references. A bibliography is appended.

Signed .... (Yusrizam Sharifuddin)

Date 8th August 2008.

SECOND STATEMENT

I hereby give consent for my thesis, if accepted, to be available for photocopying and for inter-library loan, and for the title and summary to be made available to outside organisations.

Signed ..... (Yusrizam Sharifuddin)

Date 8th August 2008.

To my parents and my family for everything they had done for me

"Amser dyn yw ei gynhysgaeth-a gwae y sawl a'l gwey'n ofer"

"Time is man's greatest inheritance and woe betide he who spends it wantonly"

- Morgan Llywd o Wynedd,
Welsh philosopher.

ACKNOWLEDGEMENTS

Firstly, I would like to thank my supervisors Professor James Parry and Dr. Elizabeth Parry, whom I have known since my undergraduate years in Abertawe, whose lectures, advice and guidance I will always treasure. Professor Parry usually claims that I have no sense of humour but I found that pursuing a research degree under the watchful eyes of a distinguish scientist, his words were and still are important to me, that I frequently did not realise he was sharing a joke. I was certainly impressed when he correctly identified the D'deridex Class Romulan Warbird!

My thanks also go to my lecturers at the School of Biological Sciences, Abertawe during my undergraduate years for what they had taught me especially Professor David Skibinski, Professor Norman Ratcliffe, Dr. Hugh Jones and the late Professor John Gallon. It must have been a real challenge for them to teach a late bloomer like me. Not to forget is Dr. Philip Judson who has been helpful with my work.

One of my best friends, Dr. Dalia Saidely deserves a special credit for her unwavering support in my studies and my wellbeing. I would not be surprised should she win the Nobel Prize one day. My special thanks also goes to Dr. George Johnson for being there for me during good times as well as turbulent ones and whom I am proud to claim as a close friend. I also wish to express my gratitude to Dr. Gareth Jenkins and Dr. Shareen Doak for their much valued opinions, their achievements have always been a source of motivation for me to work harder.

To the Ladies of the Laboratory, I thank Mrs. Margaret Clatworthy and Mrs. Sally James whose presence were indispensable to my daily work, whose company I will not forget and certainly for tolerating my tantrums when some of the other patrons were 'involved in temporally transient but consistent actions that affected the operational harmony of the laboratory'. I surely will not forget Mrs. Cherrill Laws and Mrs. Diane Elwell for always cheering me up and for all the cherished conversations.

I like to thank my friends namely Dr. James Cronin, Dr. Athanassios Roussos, Dr. Sarah Prior, Dr. Emma Quick, Jane Mikhail, Nurul Hamidi and the 'younglings' who recently joined the laboratory namely James 'The Diving Snowman' Davies, Beverley 'Sunshine' Jones and Elizabeth 'Flintoff' McAdam, I thank all of you for your friendship and for tolerating my 'Godzilla' moments.

My record of gratitude are also reserved for Dr. Vivienne Jenkins and Dr. Diane Kelly for their invaluable assistance, support and interests in my research.

Last but not least, I thank all the scientists particularly those in genetic toxicology, some of whom I had the pleasure to meet or listen to in person and others whose names are familiar to my lips. Their work has been inspirational.

Finally, I like to thank myself for my hard work and perseverance in my inextinguishable desire to better myself despite all the trials and tribulations in life. Otherwise, this thesis would not have seen daylight.

SUMMARY

In this thesis, the genotoxic potential of andrographolide, which is a primary phytochemical of an annual herb *Andrographis paniculata*, was assessed and the possible mechanisms of action were elucidated.

In silico predictions showed that andrographolide may be capable of inducing skin sensitisation and chromosome damage in mammals *in vitro* and the identification of possible metabolites.

Andrographolide was demonstrated to induce micronuclei formation *in vitro* in three cell lines tested namely AHH-1, MCL-5 and V-79. In AHH-1 and V-79 cell lines, the highest frequency of micronuclei was recorded at 30 μM whereas in MCL-5 cell line, 50 μM of the compound was necessary to elicit similar damage, which may be due differences in cellular metabolism capacity. The phytochemical was shown to cause dose-dependent cellular cytotoxicity in all the cell lines tested with cells dying primarily via necrosis compared to apoptosis and effectively reduced cell number.

Kinetochore labelling on MCL-5 cells challenged with increasing doses of andrographolide revealed that the phytochemical acts in aneugenic manner evident from the increment in kinetochore-positive micronuclei.

The compound of interest was also found to disrupt segregation fidelity via centrosome amplification resulting in chromosomal aberration. The presence of extra microtubule organising centres may play a role in the promotion of aberrant mitoses. Disruption to normal cell division was observed even after the removal of the compound *in vitro*.

Mammalian *HPRT* point mutation assay using AHH-1 cell line revealed that andrographolide induced mutation evident from *HPRT*$^-$ mutant colonies formation between 5μM and 30μM. The phytochemical was also found to exert cytotoxicity in a concentration-dependent manner between 1μM and 50μM.

Thus, andrographolide is capable of disrupting normal mammalian cell division and causing dose-dependent cytotoxicity *in vitro*.

ABBREVIATIONS

γ-TuRC.	γ-tubulin ring complex.
ADP.	Adenosine diphosphate.
AHH.	Aryl hydrocarbon hydroxilase.
AP-1.	Activator protein-1.
APE.	*Andrographis paniculata* extract.
APC/C.	Anaphase promoting complex/cyclosome.
ATCC.	American Type Culture Collection.
ATM.	Ataxia telangiectasia mutated.
ATP.	Adenosine triphosphate.
BER.	Base excision repair.
BSA.	Bovine serum albumin.
BBR.	Brilliant blue R.
BFB.	Breakage-fusion-bridge.
CBMA.	Cytokinesis-block micronucleus assay.
CDK-1.	Cyclin-dependent kinase-1.
CDK-2.	Cyclin-dependent kinase-2.
COM.	Committee on Mutagenicity of Chemicals in Food, Consumer Products and the Environment (Department of Health, UK).
COX.	Cyclooxygenase.
CREST.	Calcinosis, Raynaud phenomenon, esophageal dismotility, sclerodactyly and telangiectasia.
CS.	Cockayne syndrome.
CSAR.	Computer-assisted structure activity relationship.
CYP.	Cytochrome P450.
DAPI.	4,6-diamidine-2-phenyl-indoledihydrochloride.
DEREK.	Deductive estimation of risk from existing knowledge.
DHFR.	Dihydrofolate reductase.
DMAPP.	Dimethylallyl pyrophosphate.
DMEM.	Dulbecco's modified E medium.
DMSO.	Dimethylsulfoxide.

DNA.	Deoxyribonucleic acid.
DSB.	Double-strand break.
ECACC.	European Collection of Cell Cultures.
ERK.	Extra-cellular signal-related kinase.
EU.	The European Union.
FAP.	Familial Ademato us Polyposis
FDA.	Food and Drugs Administration (US).
FISH.	Fluorescence *in situ* hybridisation.
FPP.	Farnesyl pyrophosphate.
FSA.	Food Standards Agency (UK).
$G_{0/1/2}$	Gap 0/1/2.
GGPP.	Geranyl geranyl pyrophosphate.
GLP.	Good Laboratory Practice.
GRO.	Growth-related oncogene.
GSH.	Glutathione
GST.	Glutathione S-transferases.
GSSG.	Oxidised glutathione.
HAT.	Hypoxanthine-aminopterin-thymidine.
HT.	Hypoxanthine-thymidine.
HBSS.	Hank's balanced salt solution.
HPRT.	Hypoxanthine phosphoribosyl transferase.
HR.	Homologous recombination.
HTS.	High-throughput screening.
IARC.	International Agency for Research on Cancer.
ICH.	International Conference on Harmonisation of Technical Requirements for Registration of Pharmaceuticals for Human Use.
IMDM.	Iscove's modified Dulbecco media.
IPP.	Isopentenyl pyrophosphate.
IUPAC.	International Union of Pure and Applied Chemistry.
IWGT.	International Workshops on Genotoxicity Testing.
LPS.	Lipopolysaccharide.
MAO.	Monoamine oxidases.
MAPK.	Mitogen-activated protein kinases.
MCASE.	Multiple computer automated structure evaluation.

MCC.	Mitotic checkpoint complex.
MF.	Mutation frequency.
MFI.	Mean fluorescence intensity.
MFO.	Mixed-function oxygenase.
MHC.	Major histocompatibility complex.
MHRA.	Medicines and Healthcare products Regulatory Agency (UK).
MMP.	Mitochondrial membrane potential.
MMR.	Mismatched repair.
MTOC.	Microtubule-organising centre.
NAPQI.	*N*-acetyl-*p*-benzoquinone imine.
NCE.	New chemical entity.
NER.	Nucleotide excision repair.
NF-κB.	Nuclear factor-κB
NHEJ.	Non-homologous end joining.
NO.	Nitric oxide.
NOEL	No observed effect levels.
NPB.	Nucleoplasmic bridge.
OECD.	Organisation of Economic Co-operation and Development.
PAF.	Platelet aggregation factor.
PAH.	Polycyclic aromatic hydrocarbon.
PAPS.	3′-phosphoadenosine-5′-phosphosulfate.
PAR.	Poly-ADP-ribosylation.
PARP.	Poly(ADP-ribose) polymerase.
PBS.	Phosphate-buffered saline.
PBT.	Phosphate-buffered saline with Tween 20.
PCR.	Polymerase chain reaction.
PCM.	Pericentriolar matrix.
PCNA.	Proliferating cell nuclear antigen.
PE.	Plating efficiency.
QSAR.	Qualitative structure-activity relationships.
RANTES.	Regulated upon activation normal T-cell expressed and secreted.
Rb.	Retinoblastoma.
REACH.	Registration, Evaluation and Authorisation of Chemicals.
RNA.	Ribonucleic acid.

RTG.	Relative total growth.
SDS.	Sodium dodecyl sulphate.
SO.	Safranin O.
SOM.	Self-organising map.
SULT.	Sulfotransferases.
TOPKAT.	Toxicity Prediction by Komputer Assisted Technology.
UDS.	Unscheduled DNA synthesis.
UGT.	UDP-glucuronosyltransferases.
UK.	The United Kingdom.
US.	The United States.
VCAM.	Vascular cell adhesion molecule.
WHO.	World Health Organisation.
XP.	Xeroderma pigmentosum

MAIN CONTENTS

Chapter 2. Part 2. *IN SILICO* PREDICTION OF ANDROGRAPHOLIDE BIOTRANSFORMATION ROUTES

Chapter 3. ASSESSMENT OF ANDROGRAPHOLIDE GENOTOXICITY POTENTIAL USING THE *IN VITRO* CYTOKINESIS BLOCK MICRONUCLEUS ASSAY

MATERIALS USED AND SOURCES

Cell lines

AHH-1 human lymphoblastoid cell line.	Gentest Corporation, USA.
MCL-5 human lymphoblastoid cell line.	Gentest Corporation, USA.
V-79 chinese hamster fibroblast cell line.	ECACC.

Chemicals

6-thioguanine (6-TG).	Sigma, UK.
Andrographolide (98.0%).	Sigma, UK.
Acridine orange.	Sigma, UK.
Acetic acid glacial.	Fisher Scientific, UK.
Coomassie Brilliant Blue R stain.	Sigma, UK.
Calcium chloride dehydrate ($CaCl_2$ $2H_2O$).	Sigma, UK.
Colchicine (95.0%).	Sigma, UK.
Cytochalasin-B.	Sigma, UK.
DAPI stain	Sigma, UK
DPX mountant solution.	Fisher Scientific, UK.
Dimethylsulfoxide.	Sigma, UK.
DMEM growth medium.	Gibco, UK.
Ethanol.	Fisher Scientific, UK.
Foetal bovine serum.	Gibco, UK.
F2168 (Monoclonal anti-α-tubulin conjugate).	Sigma, UK.
Giemsa stain solution (improved R66).	BDH Lab Supplies, UK.

HAT solution (50x strength).	Gibco, UK.
HBSS/Ca/Mg.	Gibco, UK.
Horse serum.	Gibco, UK.
HT solution (50x strength).	Gibco, UK.
Hygromycin-B.	Sigma, UK.
L-Glutamine (100x strength).	Gibco, UK.
Magnesium chloride hexahydrate($MgCl_2$ $6H_2O$)	Fisher Chemicals, UK.
Methanol (99.99%).	Fisher Scientific, UK.
Mitomycin-C.	Sigma, UK.
MycoAlert Detection Kit.	Cambrex, UK.
Perchloric acid (60%).	Fisher Scientific, UK.
Phosphate-buffered saline (PBS).	Sigma, UK.
RPMI-1640 growth medium.	Gibco, UK.
Safranin-O stain.	Sigma, UK.
T6557 (Monoclonal anti-γ-tubulin).	Sigma, UK.
T7782 (Anti-mouse IgG Fab-specific TRITC conjugate)	Sigma, UK.
Trypan Blue (0.4%)	Sigma, UK.
Trypsin-EDTA (in HBSS)	Gibco, UK.
Tween 20.	BDH Lab Supplies, UK.
Xylene (99.99%)	Fisher Scientific, UK.
Vectorshield.	Vector Laboratories, USA.

Non-chemical consumables

Petri dishes.	Sterilin, UK.
T-25 ($25cm^2$) , T-80 ($80cm^2$) culture flasks	Nunc, Denmark.

Non-consumables

IEC Centra-3M centrifuge.	Intl. Equipment Co., UK.
Class II Lamina Flow Hood.	Medical Air Technology Ltd.,UK
Cytospin 4.	ThermoShandon, UK.
Kelvinator.	Forma Scientific.
Milli-Q PF Ultrapure Water Purification System.	Millipore, Watford, UK.
Nikon TMS phase contrast microscope	Nikon, Japan.
Olympus BH-2 light microscope	Olympus, Japan.
Olympus BH2-RCF fluorescent microscope	Olympus, Japan.
Waterbath	Grant Instruments, UK.
Luminometer Anthos Lucy 1.	Anthos Instruments, UK.

List of Figures Available In This Thesis

Chapter 1. Part 1: Introduction to the Importance of Phytochemicals and the Needs to Assure Their Safety

Chapter 1. Part 2: Introduction to Genetic Toxicology in Mammalian Cells and Its Importance

Chapter 2. Part 2: *In Silico* Prediction of Andrographolide Biotransformation

Chapter 3. Assessment of Andrographolide Genotoxicity Potential Using the *In Vitro* Cytokinesis-Block Micronucleus Assay

Chapter 4. Induction of Centrosome Amplification and Its Consequences in Cells Challenged with Andrographolide

List of Tables Available In This Thesis

Chapter 1. Part 1: Introduction to the Importance of Phytochemicals and the Needs to Assure Their Safety

Chapter 3. Assessment of Andrographolide Genotoxicity Potential Using the *In Vitro* Cytokinesis-Block Micronucleus Assay

CHAPTER 1

PART 1. INTRODUCTION TO THE IMPORTANCE OF PHYTOCHEMICALS AND THE NEED TO ASSURE THEIR SAFETY

PART 2. INTRODUCTION TO GENETIC TOXICOLOGY IN MAMMALIAN CELLS AND ITS IMPORTANCE

CHAPTER 1

PART 1: INTRODUCTION TO THE IMPORTANCE OF PHYTOCHEMICALS AND THE NEEDS TO ASSURE THEIR SAFETY

"It does not matter that rhubarb is a purgative. The question is, what purges? Names do not have virtues. Substances do."

Paracelsus; in Archidoxa of the Arcanum, circa 1524.

1.1 Phytochemicals and Herbal Applications in Traditional Medicines

Traditional medicines captivate a wide spectrum of reactions in general, ranging from uninformed scepticism to abiding enthusiasm from the general public as well as the scientific community. Traditional medicines are still widely used in developing countries and are increasingly popular in developed countries. In certain parts of the world, it is the only geographically accessible and economically feasible mode of healthcare. Globally the public, health professionals and policy-makers are wrestling with the questions about the quality, efficacy, safety, preservation and further development of this type of health care. This thesis is focusing on herbal applications in traditional medicine and highlighting the need to ensure safe application of medicines derived from plants.

Modern pharmaceutical drugs are based on chemicals with active properties and many drugs used today have been discovered through research into the physiological effects of phytochemicals, which are chemicals derived from plant sources. The primacy of plants as the source of new drug discoveries throughout human civilisation remained unrivalled until the recent competition from combinatorial chemistry (Schreiber, 2000) and computational drug design (Clark and Pickett, 2000), which effectively reduced its influence in drug discovery process. During the 20th century especially since the Industrial Revolution, efforts gradually shifted from producing medicinal plant extracts to synthetically producing these phytochemicals or their active analogues. Figure 1.1 highlights the factors that contribute to the decline of natural products in drug discovery and development. Although many can now be synthesised, such as aspirin, which is a safer analogue of salicylic acid derived from *Salix alba,* some of these drugs are still derived directly from plants (e.g.

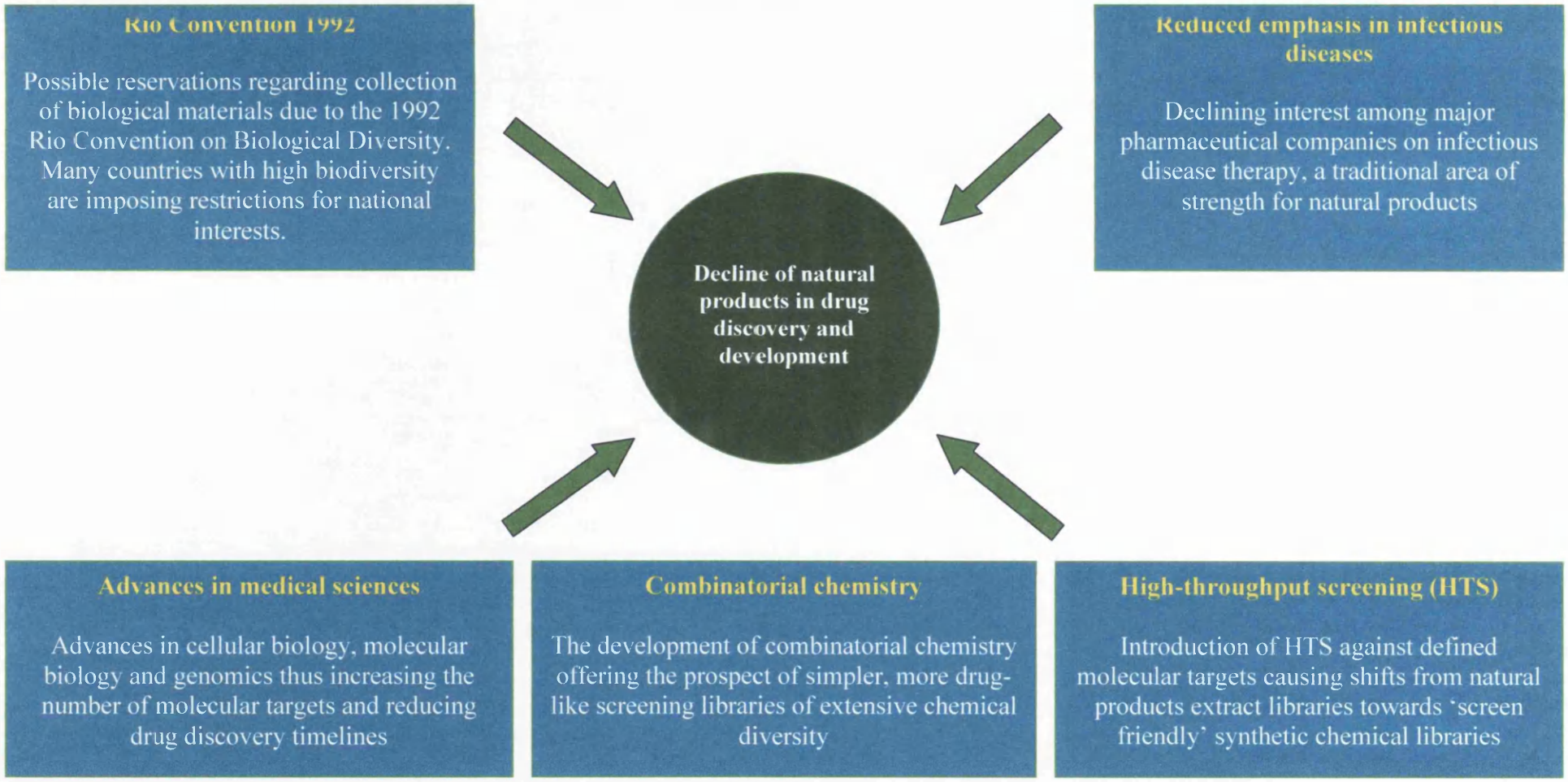

Fig. 1.1. Factors contributing to declining emphasis in the pharmaceutical industry on using natural products in drug discovery and development.

digitalin from foxglove, *Digitalis sp.*). Chemicals in some plants are extracted and transformed, providing the building blocks of drugs (e.g. progesterone, synthesised from chemicals found in some species of wild yam, *Dioscorea sp.*). Generally, phytochemicals are referred to as new chemical entities (NCEs) especially in the industry circle and viewed as templates for structure optimisation in making perfect new drugs. Other compounds are potentially useful to humans or are of toxicological relevance.

Although synthetic chemistry is currently more appealing as an approach to produce new drugs, flora's contribution in preventing and treating diseases cannot be ignored. At the beginning of the 21st century, it was reported that 11% of the 252 drugs regarded as vital by the World Health Organisation (WHO) and about 25% of drugs prescribed worldwide were solely derived from plants (Rates, 2001). Furthermore, 49% of 877 new chemical entities introduced between 1981 and 2002 were natural products, semi-synthetic natural products or mimics based on natural-products (Newman *et al.*, 2003). As shown in Figure 1.2, there was an increasing trend in natural product patents worldwide whereas Table 1.1 lists the percentage of identified medicinal plant species in selected countries and the world in general.

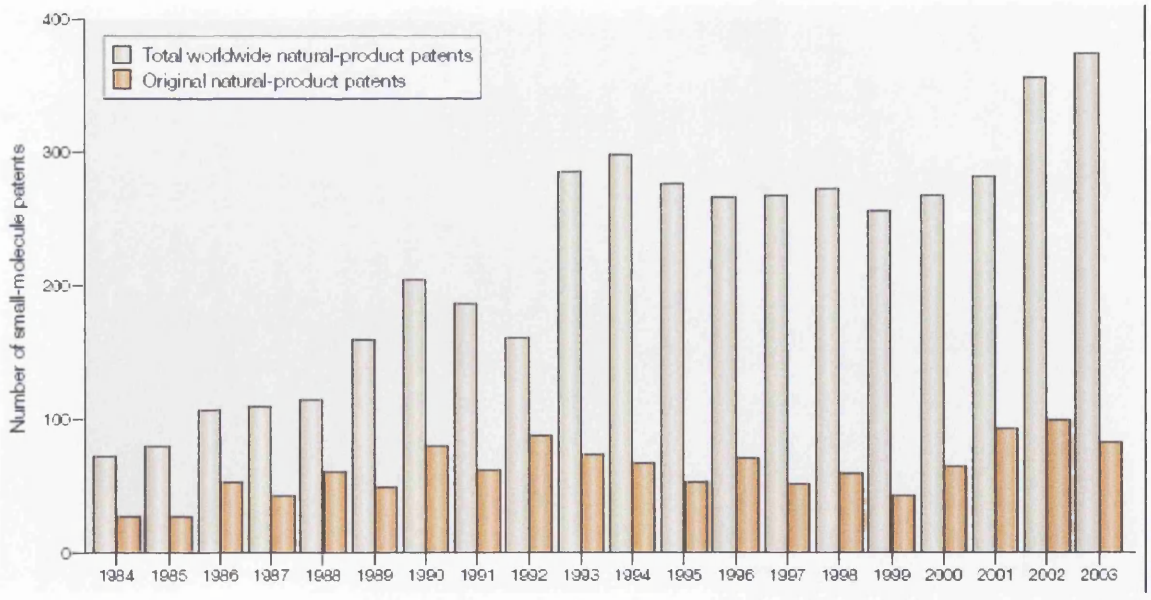

Fig 1.2. Worldwide pharmaceutical natural product patents. Original natural product patents refer to all first-time grants of patents for novel composition of small molecule natural products as pharmaceuticals. Whereas those for total worldwide natural products are global grants for patents asserting composition-of-matter or small natural products applications as therapeutics. One single natural product can generate several patents based on multiple filings in different countries or for different indications. (Adopted from Koehn & Carter, 2005.)

Table 1.1. The percentage of identified medicinal plant species in selected countries and the world in general.

Country	Plant species	Medicinal plant species	Percentage
India	15,000	3000	20.0
China	26,092	4941	18.9
United States	21,641	2564	11.8
Malaysia	15,500	1200	7.7
World	422,000	52,885	12.5

Data obtained from Schippmann *et al*, 2002.

The idea that evolution has been selecting and improving phytochemicals longer than any pharmaceutical companies and in greater diversity than any chemical library made by humans should be recognised. This is especially true in areas where there are insufficient synthetic leads. Furthermore, plants have utilised a more holistic tactic in their biochemical defence against pathogens by producing arrays of structurally and functionally diverse anti-pathogenic compounds that act in concert, not only to neutralise the threat but also in averting the development of resistance in the future. For example, *Berberis fremontii* (Fremont barberry) produces both anti-microbial berberine alkaloid and inhibitors of a bacterial pump that strongly potentiate the activity of berberines (Hsiang & Lewis, 2000). It is for the same reason that made herbal medicines appealing not only to the scientific community but also to the public, where multi-factorial nature of many complex diseases such as psychiatric disorders and cancers cannot be ideally solve with a 'single golden molecular bullet'. Most of these diseases are not a result of one single factor but from a combination of genetic, behavioural and environmental influences. Furthermore, many proteins and molecular targets are involved in complex biochemical and cellular processes. Thus, carelessly tampering with one reaction might affect the others.

Pharmacognosy (derived from Greek words *pharmakon*, 'remedy', and *gignosco*, 'knowledge') is the science of biogenic or nature-derived pharmaceuticals and poisons. It concerns all medicinal plants including those yielding complex mixtures, those used in the crude forms or extracts (phytotherapy), pure compounds such as morphine, and foods having additional health benefits (nutraceuticals). Phytomedicines generally refer to herbal medicinal products used in phytotherapy. Phytotherapy should not be confused with other "special therapeutic disciplines" that also utilise plant materials such as anthroposophy and homeopathy. Homeopathy, whose efficacy is still being critically assessed, was proposed by Samuel Hahnemann and works on the principle of '*similia similibus curentur*'- similar

symptoms are healed by similar medicines. Furthermore, homeopathy mainly involves really low doses where 'efficacy' is believed to increase with dilutions, in stark contrast to current scientific comprehension.

There are various ways in which plants can be used as therapeutics as listed in Table 1.2. Herbal teas and other homemade remedies are very popular. Crude or standardised extracts can be prepared in pills or capsules and can also be use as tinctures. Ultimately, as mentioned briefly before, successive extraction and purification procedures to isolate phytochemicals from plants of interests, that is bioactive and can be used straight away as drugs (e.g. ergotamine and digoxin) or use as leads in hemisynthetic processes.

Table 1.2. A variety of ways in which phytochemicals can be used.

Therapeutic	Description	Availability	Example
Drugs	Primarily single active pharmaceutical compounds originating from plants.	Via prescription or over-the-counter purchases.	Aspirin, vinblastine and taxol.
Botanical drugs	Standardised phytochemical mixtures that are clinically proven.	Via prescription or over-the-counter purchases.	*Hypericum perforatum.*
Dietary supplements	A plant component with health benefits.	Over-the counter purchases.	Garlic or *Echinacea* extract.

Phytochemicals can also be use as reference models for total synthesis with well-defined pharmacological activity or structure activity relationship studies determining a prototype drug (e.g. morphine). One good example would be artemisinin. Artemisinin, a sesquiterpene trioxane lactone containing a peroxide bridge that is necessary for its activity, was first isolated by Chinese researchers from *Artemisia annua* (sweet wormwood) and its structure was elucidated in 1979 (Klayman, 1985). Various soluble and more active forms of artemisinin have been synthesised to combat malaria. The phytochemical and its derivatives kills *Plasmodium* in all stages of life cycle by interacting with heme resulting in carbon-centred free radicals, which alkylate protein thus damaging the membrane and microorganelles of the parasites (Meshnick, 1998). Up to this day and to the best of the author's knowledge, there are no known cases of artemisinin-resistant malaria in humans

(Balint, 2001). Figure 1.3 highlights the evolution of *Artemisia annua* application starting with traditional medicine to modern drug discovery and Figure 1.4 shows the similar passage of the senna plant. The variety of development and use of natural products is shown in Figure 1.5.

1.2 Increasing Public Interest in Phytomedicines and Phytotherapy

It is widely accepted that there is an increasing use of phytomedicines by the general public to replace or complement allopathic medicines (Newall *et al.*, 1996). This revival of interest in phytomedicines is largely driven by the public's increasing interest and confidence in self-medication (Blenkinsopp and Bradley, 1996). There are many reasons for the increasing popularity of phytotherapy and most likely to include the following:

- Increasing consumer interest in self-medication.
- Increasing consumer interest in using herbal remedies as daily supplements.
- As a complementary to allopathic medicine.
- The popular notion that phytomedicines are safe and natural.
- Growing concern about the adverse effects of synthetic drugs.
- Disappointment with the efficacy of conventional drugs, especially in chronic conditions.
- The desire for a more natural lifestyle.
- Cost factor. Herbal medications are normally available over the counter and are cheaper than prescribed modern drugs.

The world market for phytomedicines is estimated to be £38 billion (UNCTAD, 2000). It is estimated that Europe imports about 400,000 tonnes of medicinal plants annually with Germany as the largest market and consumer of medicinal plants, spending about £1.4 billion, followed by France with £116 million (Masood, 1997). The UK is third in place.

As highlighted in the House of Lords Select Committee's report on complementary and alternative medicine, comprehensive information on the use of herbal medicines in the UK is insufficient (House of Lords, 2000). There are several estimates available but it is difficult to make an accurate determination as many products could be categorised as food

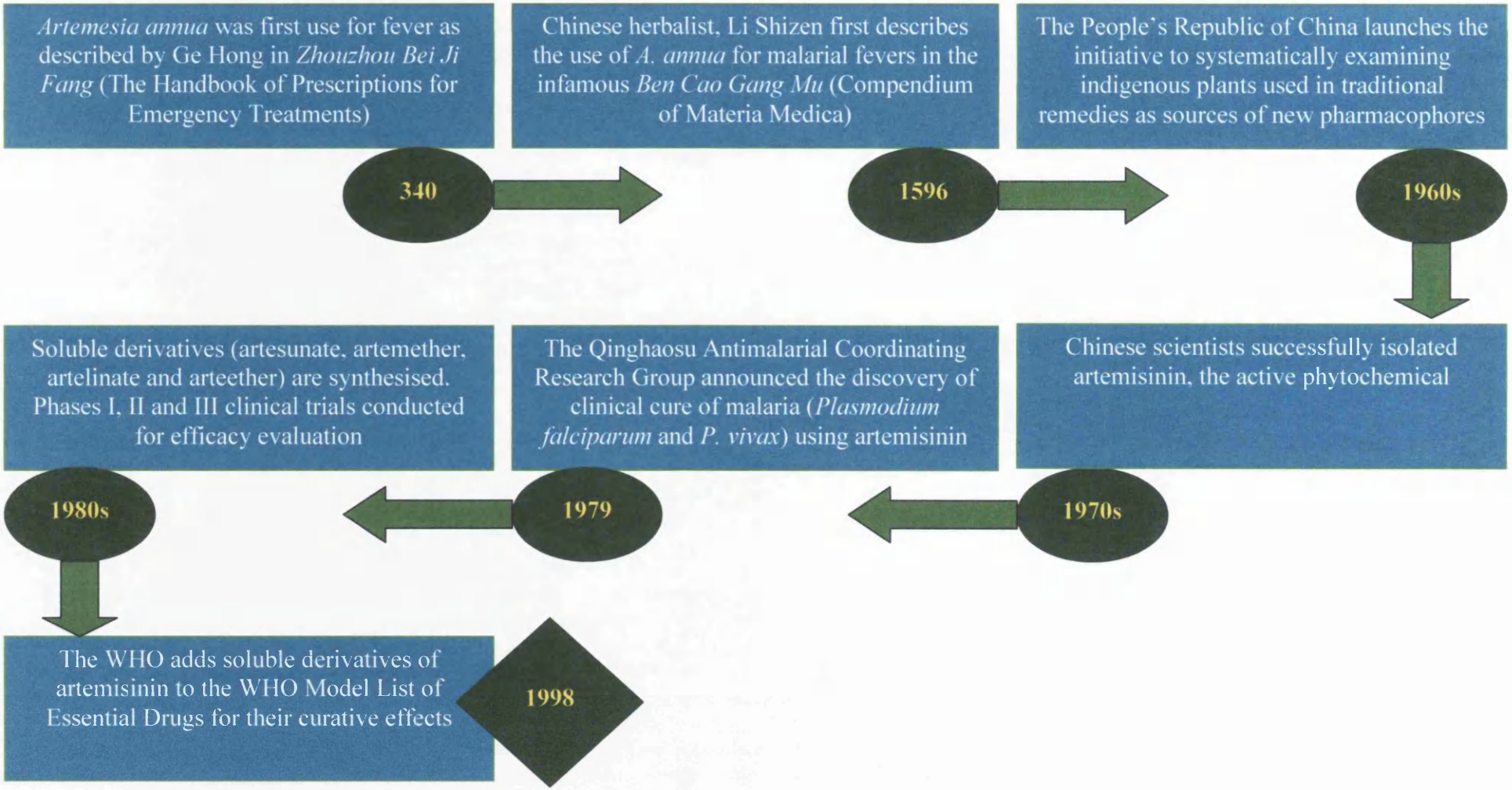

Fig. 1.3. Highlighting the application of *Artemisia annua* beginning with traditional medicine to modern drug discovery. Page 7.

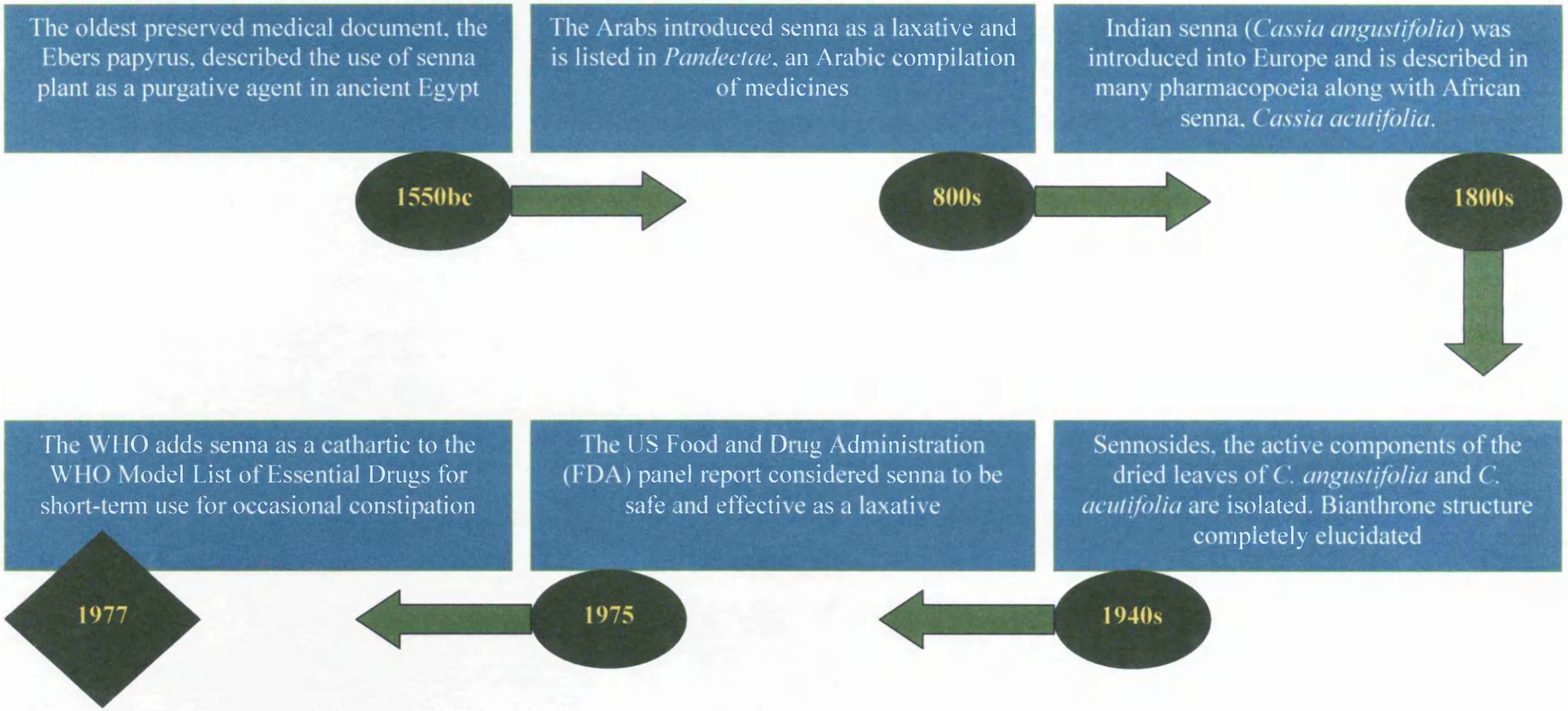

Fig. 1.4. Highlighting the application of the senna plant beginning with traditional medicine to modern drug discovery. Page 8.

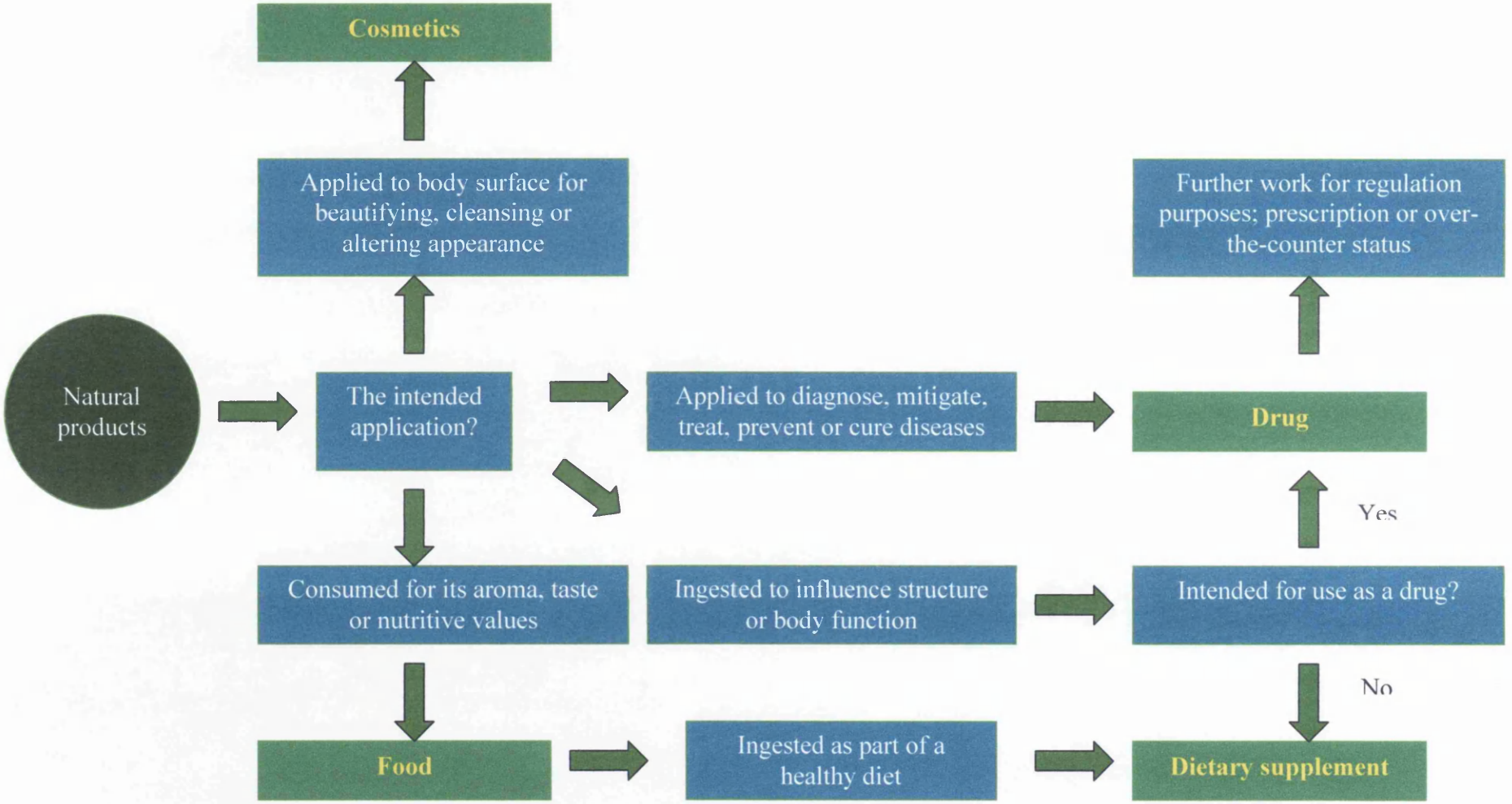

Fig. 1.5. Various development routes and applications of natural products. Page 9.

supplements rather than medicines mainly for regulatory purposes, effectively the public in many cases are unable to differentiate phytomedicines for dietary supplements or therapeutic applications. A report by the Mintel market research group on retail sales of licensed homeopathic, herbal remedies and essential oils showed that phytomedicines make up more than 50% of the total complementary market in the United Kingdom with estimated value of £38 million in 1996 compared to £27.2 million in 1991 (Mintel, 1997). However, the total market value is likely to be higher since the study excluded ginkgo and unlicensed herbal products from its analysis.

Another report estimated the phytomedicines market to be over £60 million (Mintel, 2000). More recent reports estimated the market value of herbal remedies (excluding traditional Chinese and Ayurvedic medicines) had grown to £75 million in 2002, dominating the UK natural health market and accounting for almost 60% of the sector value (Mintel, 2003). Another Mintel report in 2005 noted that herbal medicines have shown greatest growth over the last two years with value sales hitting £87 million in 2004, accounting for half of overall category sales. All these estimates should be considered as broad brush since some companies might not always have an accurate view as to which of their products would be classified as medicines.

The analysis of the market structure for unlicensed phytomedicines is complicated by several factors such as:

- Most phytomedicines possess borderline status as to whether they should be categorised as medicines or fall within other regulatory classification such as supplements, cosmetics or general consumer products.
- A number of companies supply herbal ingredients (e.g. for herbalists' use or by manufacturers) rather than manufacture the product themselves.
- Under existing regulations, companies are not required to submit products to the Medicines and Healthcare products Regulatory Agency (MHRA) for determining their status.

One must recognised the fact that future growth in the industry remains vulnerable to adverse publicity arising from issues over the safety and quality of phytomedicines.

1.3 The Regulation of Phytomedicines in the United Kingdom and the European Union

The House of Lord's Select Committee on Science and Technology 6th report (2000) stressed for a need of a more effective guidance to the public regarding the safety and efficacy of alternative medicines. The absence of central information provision for healthcare practitioners and the general public, effectively gave the media and other unregulated information sources unchecked influence in shaping opinions in the field. Over 25% of consumers believed that pharmacists should provide more information on herbal medicines highlighting increasing consumer concern, with about 20% of consumers worried about the possible side-effects from alternative medications (Mintel, 2003).

Whilst the government and the industry need to address this consumer concern, Mintel's report also found that around 1 in 5 UK consumers worry about the possible side effects from standard medication too. And 18% admitted they have tried conventional medicine which did not work, suggesting a significant opening for the phytomedicine industry (Mintel, 2003).

Phytomedicines intended for general retail sale reach the UK market by two different routes. First, an authorisation can be obtained from the licensing authority for marketing purposes under the Medicines for Human Use (Marketing Authorisation Use) Regulations 1994 (SI3144/1994) that fundamentally transposed European Directive 2001/83/EC into UK law. Under these Regulations, authorisation is requisite for most industrially produced medicines that are to be marketed. Such authorisation is obtained by providing standards of quality, efficacy and safety.

Alternatively, exemption from product licence requirement (compulsory under the Medicines Act) can be obtained under Section 12(2) of the Medicines Act 1968 [and regulation 1(3) of the 1994 Regulations] for phytomedicines that do not need marketing authorisation, providing that the remedy meets various conditions. There are restrictions or prohibitions on certain ingredients, but generally there are no specific requirements for quality, safety and efficacy. Written medical claims are not permitted for these herbal remedies and specific requirement to provide the consumers with systematic information about the safe application of the product is absent.

Even though several hundred phytomedicines posses marketing permission in the UK, most herbal medicines were marketed on general sale by utilising the exemption provided in Section 12(2) of the Medicines Act as explained above.

The primary piece of European legislation is Directive 2001/83/EC of the European Parliament and of the Council of 6 November 2001 on the Community code regarding medicinal products intended for human use. Thus, there was no distinction in the European legislation for medicines made from non-herbal ingredients and phytomedicine. Medicinal products are also subjected to some non-specific legislation, such as Directive 85/374/EEC on product viability, which was transposed into the UK law as Consumer Protection Act 1987 and applies in part to medicinal products for consumer protection.

On 30th October 2005, the MHRA introduced a new scheme, the Traditional Herbal Medicines Registration Scheme implemented through the Medicines (Traditional Herbal Medicinal Products for Human Use) Regulations 2005 (SI 2005 No. 2750), which is required by the European Directive on Traditional Herbal Medicinal Products 2004/24/EC. This scheme will assist in protecting public health, consumer confidence and the industry itself by requiring specific standards to be met relating to the product namely quality, safety, manufacturing standards, patient information, wholesale and import. However, the key feature of this scheme is the requirement for evidence of traditional application in the EU for 30 years. Evidence for up to 15 years of traditional applications outside the Union is admissible. This new EU Directive effectively amends Directive 2001/83/EC, to introduce the scheme and applies many existing requirements of the later to traditional herbal medicinal products. Another separate new EU Directive 2004/27/EC is simultaneously amending Directive 2001/83/EC. All manufactured traditional herbal medicines that marketed with exemption under Section 12(2) of the Medicines Act, will be required to be registered under this new scheme.

However, for unlicensed herbal medicines that were legally on the market by 30 April 2004, Her Majesty's Government has opted for a seven-year transitional period that ends on 30 April 2011, a flexibility accorded to EU member States under Directive 2004/24/EC intended to allow companies to adjust to the new regulations.

Herbal products that are not classified as medicines are still subject to other regulations. The fact that a product is not medicinal in nature thus not necessarily means that it is safe or acceptable from a legal standpoint. Food and supplements are regulated by the Food Standards Agency (FSA) while cosmetics or other consumer products fall under the jurisdiction of the Department of Trade and Industry. The MHRA accepts no responsibilities on these points. The Food Safety Act (1990) states that food sold in the United Kingdom cannot be injurious to health and according to the FSA, herbal ingredients that do not possess a history of significant consumption within the European Union prior to May 1997 may be subject to Novel Food Regulation (EC) 258/97.

1.4 The Importance of Natural Products and Phytomedicines

Natural products have enjoyed an undisputedly important role as new chemical entities (NCEs). Between the years 1981 and 2002, approximately 28% of NCEs were natural products or derived from natural products, with another 20% were considered as synthetics based on natural product pharmacophores (Newman *et al.*, 2003).

Natural products (phytochemicals) have many common structural features such as chiral centres, degree of molecule saturation, complex ring systems and aromatic rings that have been demonstrated to be highly applicable in drug discovery process (Koehn & Carter, 2005). Furthermore, the realisation that combinatorial chemistry may not always provide high degree of compound diversity led to the exploration of combining the natural product and natural product-like libraries with the potential of combinatorial chemistry in drug discovery and Table 1.3 shows some of the well-known phytochemicals in use today.

The existence and application of new technologies such as combinatorial synthesis, genomics and screening technology allow new research and development strategies to be adopted and contributed to revival of interest in phytochemicals. Table 1.4 listed some phytochemicals with their known molecular targets which might pave the way for better comprehension on their mode of action(s) and possible development into clinically applicable drugs.

Table 1.3. Shows some medicinally and chemically important phytochemicals known, their source(s), chemical type and application.

Compound name	Source(s)	Type	Therapeutic application
Artemisinin	*Artemisia annua*	Sesquiterpene lactone	Antimalarial
Camptothecin	*Camptotheca acuminata*	Indol alkaloid	Antineoplastic
Cocaine	*Erythroxylum coca*	Cocaine alkaloid	Local anasthetic
Codeine, morphine	*Papaver somniferum*	Opium alkaloid	Analgesic, antitussive
Digitoxin, digoxin	*Digitalis spp.*	Steroidal glycosides	Cardiotonic
Quinine	*Cinchona spp.*	Quinoline alkaloid	Antimalarial
Reserpine	*Rauwolfia serpentina*	Indole alkaloid	Antihypertensive
Sennosides A& B	*Cassia angustifolia*	Hydroxy-anthracene glycosides	Laxative
Taxol	*Taxus brevifolia, T. bacata*	Diterpenes	Antineoplastic
Vinblastine, vincristine	*Catharanthus roseus*	Bis-indole alkaloid	Antineoplastic

Table 1.4. A short list of phytochemical compounds and their reported molecular targets.

Compound	Molecular Target	Authors
Betulinic acid	Selective melanoma cytotoxicity via p38 activation	Pisha *et al.*, 1995; Tan *et al.*, 2003; Cichewicz & Kouzi, 2004.
Cucurbitacin I	Highly selective in inhibiting the JAK/STAT3 pathway in tumours with activated STAT3	Blaskovich *et al.*, 2003.
Indirubin	Selectively inhibits cyclin-dependent kinases	Hoessel *et al.*, 1999; Eisenbrand *et al.*, 2004.
Kamebakaurin	Inhibition of NFκB	Lee *et al.*, 2002.
B-lacaphone	Kills cancer cells selectively via direct checkpoint activation during cell cycle	Li *et al.*, 2003.

Recently, a well-known pharmaceutical company, Novartis has set up the so-called Novartis Institutes for Biomedical Research in Shanghai's Zhanjiang Park and collaborating with the Chinese Academy of Sciences to harness purified natural compounds from plants and fungi normally used in traditional Chinese medicine. In May 2007, another pharmaceutical heavyweight, GlaxoSmithKline (GSK) announced the establishment of its own drug research and development facility in Shanghai, China (Corporate Press Releases,

Novartis and GSK respectively, 2007). Embracing phytochemicals again and re-designing strategies for discovering new molecules from plants including studying those described in traditional medicine texts such as in China, is understandable since the new chemical entities pipeline of pharmaceutical companies were reported to be at historically low levels (Bolten & DeGregorio, 2002).

1.5 The Efficacy of Phytomedicines

The extraordinary level of phytomedicines popularity in recent years made it ethically imperative to elucidate its efficacy. There were opinions that the criteria for efficacy as well as safety of herbal medicines should be on par as those for conventional medicines and the author concur with these views. Many phytomedicines possess a long history of traditional use but most are of unproven efficacy by acceptable scientific standards, and traditional use does not necessarily confer safety usage mark. Insufficient evidence does not mean that phyomedicines are unsafe and ineffective, but that rigorous scientific investigation has not been carried out. Base on the same line of argument, the lack of evidence cannot be use to justify that all phytomedicines are safe.

The accepted 'gold standard' for testing the efficacy of medicines, whether it is synthetic or herbal, is the randomised clinical trials. Depending on the research objectives, these trials can be conducted against reference medications should one exists, or against placebo or no treatment at all. There is good evidence of efficacy for some phytomedicines but usually such an evaluation is scientifically inadequate. Figure 1.6 shows the percentage of randomised clinical trials highlighting the benefit of phytomedicines based on 50 trials with 10 herbal medicines for 18 therapeutic indications, where only 34% exhibited benefit when compared against placebo and 18% showed the same activity as placebo. Almost half (48%) of the results from the trials has an unlikely benefit due to discrepancies in experimental design or data analysis.

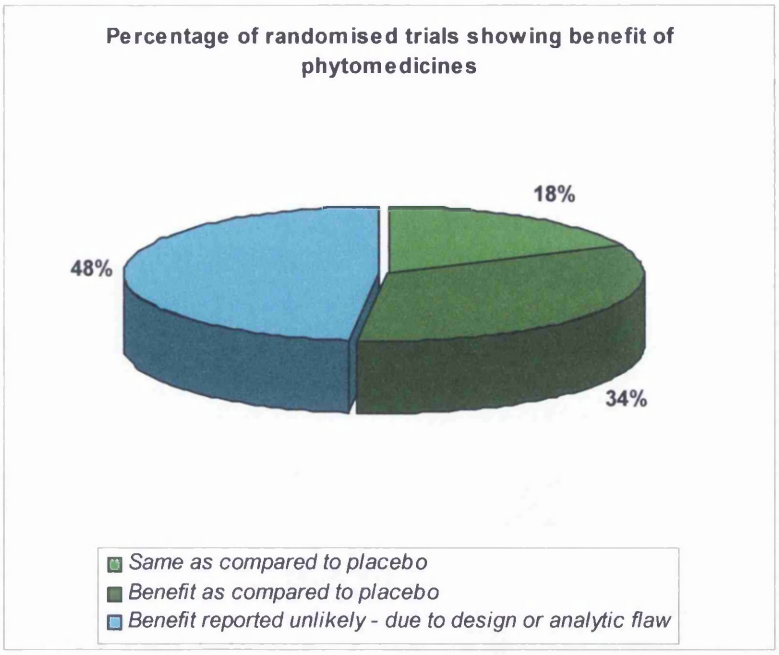

Fig. 1.6. Percentage of randomised trials showing benefit of phytomedicines.
Based on data in Herbal Medicines: an evidence-based look.
(Therapeutics Letter, Issue 25, June-July 1998.)

However, in order to provide a fair estimate of overall efficacy of a particular herbal medication, relying on the data generated from randomised trials alone is not sufficient. Only the totality of the available data that can be achieved by performing systematic reviews and meta-analyses can provide the most reliable evidence while minimising bias and random error. Determining the efficacy of an herbal product against its safety is important.

1.6 Safety of Phytomedicines: Clear and Hidden Risks

The advances in organic chemistry, biological and medical sciences in the 20th century had paved the way for the introduction and consumption of powerful synthetic drugs, resulting in the decline of phytomedicines usage in modern medicine. However, the current revival of interest in phytotherapy had caused the pharmaceutical industry to start marketing an increasing amount of new phytomedicines to accommodate the needs of consumers. This makes the need to ensure the quality, efficacy and safety of phytomedicines even more pressing since these products are generally self-prescribed, used to treat minor and often

chronic conditions. The assumption that they only possess beneficial effects has proven to be inaccurate.

Furthermore, traditional medicines have developed in many different regions, having been very much influenced by historical conditions and local cultures within which they first evolved. Thus, there has been no parallel development of methods and standards, both at national or international level that are suitable for evaluation purposes.

Safety evaluation of phytomedicines is difficult. Identifying plants accurately is essential as well as isolation of active ingredients, which is far more complex since the properties of phytochemicals are influenced by several factors such as environmental conditions. A single medicinal plant can also contain hundreds of phytochemicals and elucidating the individual effect of each can therefore be prohibitively expensive. Unsurprisingly, research effort has been inadequate, resulting in inadequate methodology development and paucity of reliable data. Although many phytomedicines showed promising potential and are increasingly used, many of them are untested and their use by the public not properly monitored leading to limited knowledge of their side-effects. Benefit-risk assessment can also be difficult due to insufficient information in several areas relevant to safety. Consequently, proper development of legislation and regulation of herbal medicines has been impaired at the public expense.

Generally, data are currently lacking on:

- The active constituents and/or metabolites
- Pharmacology
- Pharmacokinetics
- Toxicology
- Possibilities of drug-herb interactions, as well as interactions with food and alcohol
- Frequency of possible adverse effects, and effects of long term use
- Possible effects in specific patient groups e.g. children, the elderly
- Possible effects for use during pregnancy and lactation

Insufficient data on the factors stated above also makes it hard to compare and contrast the risk-benefit profile of several phytomedicines with that of conventional drugs, where effectiveness has been reported.

Toxicity related to the use of phytomedicines may have multiple causes but generally can be divided into two distinguishable categories as highlighted in Tables 1.5 and 1.6 respectively. The first category can be designated as extrinsic or non-plant associated, where toxic effects or adverse reactions occurred due to accidental or deliberate substitution or contamination of the plant material described on the label. On the other hand, the second category is more intrinsic or plant-associated in nature. In this category, the plant material itself or the phytochemicals present, thus an active agent in the herbal medicinal products, which causes the health risks.

Table 1.5. Extrinsic or non-plant-associated causative factors involved in adverse drug reactions.

Adulteration • Accidental or deliberate substitution of the original plant material by other plant species
Contamination • Micro-organisms (bacteria including *Salmonella, E.coli*, yeasts, moulds) • Microbial toxins (aflatoxins, lipopolysaccharides) • Heavy metals (mercury, lead, etc.) • Pesticides and/or herbicides • Fumigants • Radioactive particles
Substitution • Synthetic drugs (anti-inflammatory agents, corticosteroids etc.) • Animal substances (enzymes, hormones etc.)

Table 1.6. Intrinsic or plant-associated causative factors; health risks related to the medicinal herb itself as active ingredient in the phytomedicine.

- Use of plants containing constituents that are known to affect bioavailability and/or pharmacokinetics of other compounds or drugs
- Ignored toxicity of plant constituent(s) present in the product
- Use of plants, either as raw material or in processed form, of which at present no or insufficient data regarding safety are available
- Use of highly concentrated or specifically processed extracts

Although the number of side effects attributed to the use of phytomedicines represents only a small proportion of the total amount of adverse drug reactions in the WHO database (Barnes, 1998), reports on toxic effects of or adverse reactions to herbal preparations have regularly been published over the past years (Barnes, 1998). Proponents of phytotherapy usually present long-standing experience in traditional medicine as evidence of their safety, unfortunately this type of evidence has considerable deficiencies. Determining botanicals that contain phytochemicals, which manifest their toxicities and acute adverse effects in a large fraction of users is relatively easy. A 5-year toxicological study by the UK National Poisons Unit from 1991 to 1995 on potentially serious adverse reactions attributed to exposure to herbal remedies, showed there were 785 cases of possible or definitive positive poisoning out of 1297 inquiries (Shaw *et al.*, 1997). Although the study concluded that the overall risk to public health was low, there were clusters of cases that deserve serious attention where there were 21 incidents of hepatotoxicity including two deaths due to the use of traditional medicines although no causative agent was identified.

The harder task is recognising subtle adverse effects that develop over time and occur infrequently, for example hypokalemia from the use of anthranoid laxatives (Blumenthal, 1998), or that are readily ascribed to an underlying disease such as hepatitis from celandine, a bile duct remedy derived from *Chelidonium majus* (Benninger *et al.*, 1999). Hypothetically, for a herb that caused an adverse reaction in 1 for every 1000 users, a traditional practitioner would have to prescribed the herb to 4800 patients, that is 1 new user per day for more than 18 years, in order to obtain a 95% probability of observing such reaction in more than 1 user (De Smet, 1995).

Thus, the more chronic but subtle form of toxicity such as mutagenicity and carcinogenicity effects of phytochemicals will remain unrecognised if their applications in traditional settings were left unexamined, as these may have been undetermined by previous generations. For example, although *Aristolochia fangchi* have been used for centuries in Chinese traditional medicine, its nephrotoxicity and potential to induce urothelial carcinoma by DNA-adduct formation has only recently been elucidated (Nortier *et al.*, 2000; Lord *et al.*, 2001) and it was the same case with the hepatotoxicity potential of *Piper methysticum* (Escher *et al.*, 2001).

Furthermore, there is always a belief among the general public that herbal medicines or supplements are safe primarily because they are derived from nature, compared to synthetic compounds. Therefore, it was often considered harmless by the public that the consumption of these herbal products would not cause profound injury directly or vice-versa. Herb-drugs interactions for example, can occur at the pharmaceutical, pharmacodynamic and/or pharmacokinetic levels (Beijnen & Schellens, 2004). The application of herbal medicines in combination with conventional therapeutics may increase the risk for undesired interactions primarily due to the narrow therapeutic window of many oncolytic drugs. Alarmingly, more than 72% of cancer patients in the US for example, failed to inform their doctors about herbal products consumption when undergoing conventional therapy at the same time (Sparreboom *et al.*, 2004). One of the well-known examples of a clinically significant effect displayed by herbs on the pharmacokinetic of chemotherapeutic drugs is *Hypericum perforatum* (St. John's wort), which is popular among cancer patients due to its suggested activity on mild to moderate levels of depression (Mathijssen *et al.*, 2002). The plasma levels of SN-38, the active metabolite of irinotecan was 42% lower in cancer patients who took *Hypericum* at the same time. Co-administration of cyclosporin with *Hypericum* leads to decrease cyclosporin plasma concentration (Barone *et al.*, 2000) and disrupts hormonal contraception with irregular bleeding when taken together with ethynylestradiol (Schwarz *et al.*, 2003). Even the innocently looking grapefruit (*Citrus paradisi*) juice, has been shown to caused 26.2% reduction in etoposide bioavailability (Reif *et al.*, 2002) and the culprit is bergamottin, a major furanocoumarin that reversibly inhibited the activities of CYP1A2, 2A6, 2C9, 2C19, 2D6, 2E1 and 3A4 in human liver microsomes (He *et al.*, 1998), which may last up to 24 hours. It also alters the concentration of many drug substrates for CYP3A4 when taken simultaneously (Quo *et al.*, 2000). These examples highlight the need for more research not only into direct detrimental

effects pose by phytochemicals but also indirect effects or impacts that are not clearly manifested including mutations and metabolic enzymes manipulation. The public may not be aware of these hidden risks due to the 'naturally safe' paradigm long held about herbal products.

Although phytomedicines are not devoid of risk, they could still be safer than synthetic drugs. Currently, the relative safety of phytomedicines is undefinable, many existing data indicate that adverse reactions, especially serious ones, occur less frequently than with prescribed synthetic drugs. Kava (*Piper methysticum*), an herbal anxiolytic (Pittler & Ernst, 2003) that raised serious concern due to its hepatotoxicity effect, could be safer than benzodiazepines, according to preliminary data (Schulze *et al.*, 2003) and herbal antidepressant St. John's wort (*Hypericum perforatum*), has only about half the rate of possible adverse reactions compared to conventional antidepressants (Linde *et al*, 1996; Stevinson & Ernst, 1999). However, its use is only recommended for weak and mild depression and was found not to be effective for major depression cases compared to placebo (Linde *et al.*, 1996; Shelton *et al.*, 2001; Hypericum Depression Trial Study Group, 2002) The World Health Organization's monitoring centre collected 8985 reports of adverse reaction events associated with phytomedicines from 55 countries between 1968 and 1997 (Farah & Edwards, 2000). Even though this figure may seem impressively high, it amounts to only a small fraction of adverse events associated with synthetic drugs held in the same database (Farah & Edwards, 2000). However, one must recognise the fact that relative paucity could also be due to a relatively higher level of underreporting due to the perceived safety of natural herbs among the general population and more conclusive evidence on the relative safety risks of phytomedicines against conventional drugs is scarce.

1.7 Plants and Secondary Metabolites

As briefly stated before, plants have evolved various defence mechanisms including chemical, mechanical or even mimicry to improve their survival and reproduction by reducing the impact of herbivory and infection. Over billions of years of evolution, plants continually produce the necessary metabolites to out-manoeuvre pathogens in their local environment or to repel herbivores. If the metabolites were useful to the plant, the biosynthetic genes were retained, with subsequent genetic modifications and improving the process yielding exotic structures rich in functional groups and stereochemistry. Chemical defence involved the production of organic compounds that are not essential to metabolic, photosynthetic or other physiologically crucial activities and are known as secondary metabolites. They are usually synthesised as by-products during the production of primary metabolic process and play a major role in deterring herbivores.

Plants have developed various secondary metabolites and can generally be classified into three sub-groups namely nitrogen compounds (including alkaloids and glucosinolates), terpenes and phenolics.

1.8 Brief Introduction to *Andrographis paniculata*

Andrographis paniculata is a shrub that is found throughout tropical and sub-tropical Asia and is locally known in Malaysia as 'Hempedu bumi' and 'Akar cerita bidara'. This herbaceous, annual herb is from the family Acanthaceae with a slightly, characteristic odour and an intensely bitter taste, hence commonly known as 'king of bitter'. Pictures of various parts of the plant is shown in Figure 1.7 and Table 1.7 shows the systematic position of *Andrographis paniculata.*

Fig. 1.7. Pictures of various parts of *Andrographis paniculata*. (a) The whole plant can grow up to 1m in height. (b) The flowering part of the plant. (c) Seeds.

Table 1.7. Systematic position of *A. paniculata*

Division:	Angiosperms
Class:	Dicotyledonae
Subclass:	Gamopetalae
Series:	Bicarpellatae
Order:	Personales
Tribe:	Justicieae
Family:	Acanthaceae
Genus:	*Andrographis*
Species:	*paniculata*

The aerial part of the herb contains several diterpenoids and diterpene glycosides especially andrographolide, a major constituent which is not less than 6% of the total diterpene lactones present and is mainly responsible for its bitter taste. Other diterpene lactones present free and in glycosidic forms include 14-deoxyandrographolide, 14-deoxy-11,12-didehydroandrographolide, neoandrographolide, andrographiside, deoxyandrographiside and andropanoside (Kleipool, 1952). Table 1.8 listed the reported medical properties of andrographolide or extracts obtained from the herb.

Table 1.8. Reported medical properties of *A. paniculata.*

Properties	Authors
Anti-cancer	Siripong *et al.*, 1992; Rajagopal *et al.*, 2003; Kumar *et al.*, 2004.
Anti-inflammatory	Shen *et al.*, 2002.
Immuno-stimulatory	Puri *et al.*, 1993; Rajagopal *et al.*, 2003; Kumar *et al.*, 2004.
Anti-bacterial	Singha *et al.*, 2003.
Anti-viral	Chang *et al.*, 1991; Calabrese *et al.*, 2000.
Anti-pyretic	Deng *et al.*, 1982; Vedavathy & Rao, 1991; Madav *et al.*, 1995.
Anti-diarrheal	Gupta *et al.*, 1990; Gupta *et al.*, 1993; Chiou *et al.*, 1998.
Anti-venom	Misra *et al.*, 1992; Nik A. Rahman *et al.*, 1999.

Coon and Ernst (2004) conducted a systematic review on the safety and efficacy of *Andrographis paniculata* in the treatment of upper respiratory tract infections. It was found that the data collectively showed that *A. paniculata* is superior to placebo in alleviating the subjective symptoms of uncomplicated upper respiratory tract infection. The authors also found a few spontaneous reports of adverse events and *A. paniculata* may be a safe and efficacious treatment for the relief of symptoms of uncomplicated upper tract infection but more research is warranted. However, there were several shortcomings of the review that need to be addressed (Coon & Ernst, 2004).

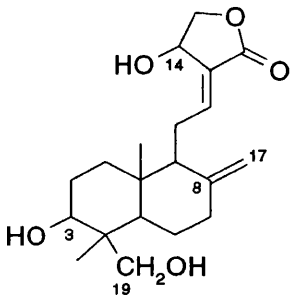

Fig. 1.8. The chemical structure of andrographolide with numbered carbon positions.

1.9 The Compound of Interest: Andrographolide

Andrographolide (CAS no: 5508-58-7) with IUPAC designation 3-{2-[decahydro-6-hydroxy-5-(hydroxymethyl)-5,8a-dimethyl-2-methylene-1-napthalenyl]-ethylidene}dihydro-4-hydroxy-2(3H)-furanone is the major bioactive constituent found in various parts of *Andrographis paniculata* particularly in the leaves. It is a labdane diterpene harbouring a γ-lactone ring attached to a decahydronapthalene ring system via an unsaturated C-2 moiety. As shown above in Figure 1.8, it contains an α-alkylidene γ-butyrolactone moiety as well as three hydroxyl groups located at C-3, C-14 and C-19 with these being secondary, allylic and primary respectively. These hydroxyls are responsible for the bioactivities of andrographolide (Nanduri *et al.*, 2004). The stereochemistry of this phytochemical has been previously elucidated with the furan ring adopting an envelope conformation whereas the two bicyclic rings adopt a chair conformation (Smith *et al.*, 1982; Fujita *et al.*, 1984; Spek *et al.*, 1987). Andrographolide was considered to be the most active constituent present in *A. paniculata* extract (Kumar *et al.*, 2004; Nanduri *et al.*, 2004)

Terpenes are ubiquitous in nature and occur in most species including humans and are sometimes referred to as isoprenes due to a common repetitive structural motif, the branched 5-carbon (C_5) unit or isopentane skeleton that is comparable to isoprene. They are a good example of a class of natural compound where many members are chiral, structurally diverse and have many functional group chemistry. Terpenes contribute to many of the aromas associated with plants and range in complexity from C_5 units to polyisoprenes that includes leaf waxes, latex and rubber. This class of compounds are derived from a number of extensive reactions between two C_5 units namely dimethylallyl pyrophosphate (DMAPP) and isopentenyl pyrophosphate (IPP) whose chemical structures are depicted in Figure 1.9. Thus,

the products of these reactions shall possess multiples of five carbons (C_5). DMAPP and IPP are biosynthesised from two sources, either deoxyxylulose phosphate or mevalonic acid.

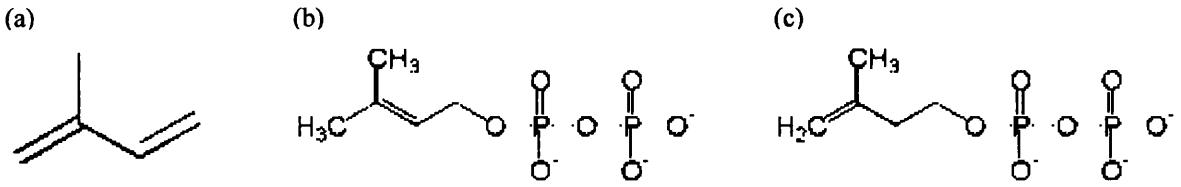

Fig. 1.9. Chemical structure of (a) isoprene, (b) dimethylalyll pyrophosphate and (c) isopentenyl pyrophosphate.

The simplest of terpenes are hemiterpenes (C_5) produced by modification reactions to either IPP or DMAPP and include simple acids such as angelic acid and tiglic acid, which are structural isomers and form esters with many natural products. The complexity of structure then progresses to monoterpenes with 10-carbon skeleton (C_{10}), sesquiterpenes (C_{15}), diterpenes (C_{20}), triterpenes and steroids (C_{30}-derived) and tetraterpenes (C_{40}, also known as carotenoids).

Diterpenes are widely distributed in plant resins and latex, some can be quite toxic. The presence of diterpenes in *Rhododendron sp.* leaves rendered them poisoinous. Diterpenes are formed by the reaction of a 15-carbon chain, farnesyl pyrophosphate (FPP) with IPP, which is the common basic unit of all terpenes with the first step of this reaction yields farnesyl allylic cation. This cation then reacts with IPP causing stereospecific loss of a proton forming geranyl geranyl pyrophosphate (GGPP). Depending on how GGPP cyclise and folds in subsequent reactions, an extraordinarily wide range of diterpenes groups can result as shown in Figure 1.10 which include taxol and ginkgolide B, one of many ginkgolides obtainable from *Ginkgo biloba.*

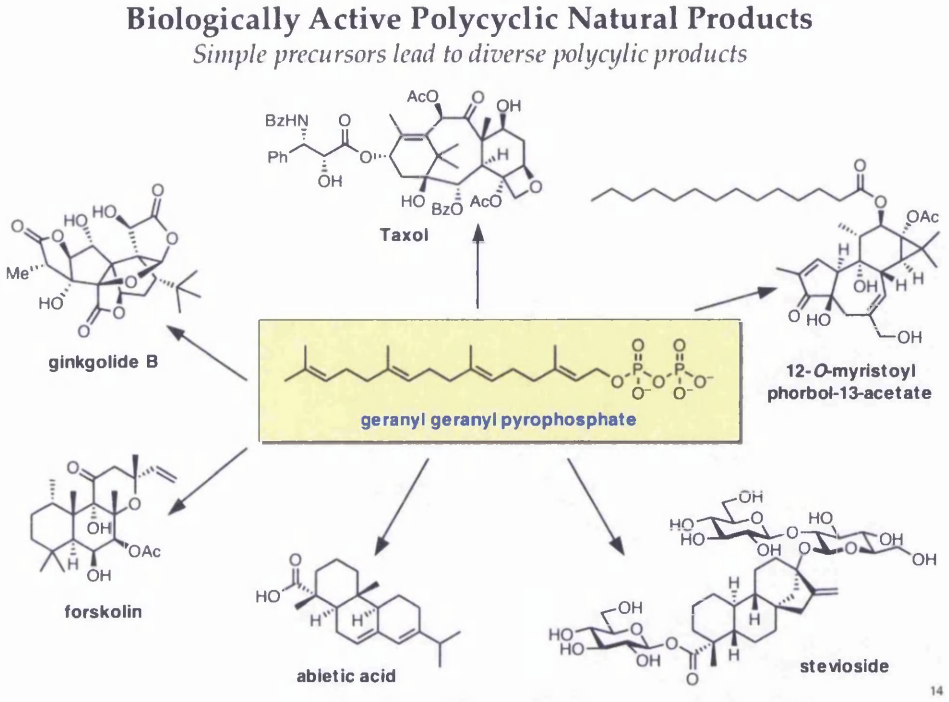

Fig. 1.10. Depending on subsequent reactions, a simple precursor geranyl geranyl pyrophosphate can produce diverse biologically active polycyclic compound. Taxol is a well known anticancer compound, ginkgolide B is an active component from *Ginkgo biloba* and abietic acid is the primary irritant in pine wood and resin of coniferous trees. (Diagram obtained from the Sloan-Kettering Institute official website accessible via www.mskcc.org).

High purity andrographolide which is easily obtained commercially was chosen for this study rather than extract from the plant itself. Furthermore, of all phytochemical components identified from *A. paniculata*, andrographolide was shown to be the most active (Kumar *et al.*, 2004; Nanduri *et al.*, 2004)

It is estimated that 40% of plants extracts lack reproducibility of activity (Cordell, 2000) and this is one of the primary obstacles in incorporating flora in pharmaceutical discovery process, despite the diversity of phytochemicals available. The data generated often do not replicate when sampling and extraction procedures were repeated. Different locations, climates, micro-environments, chemical stimuli and physical stresses, known as elicitors, will affect the content of phytochemicals in quantitative and qualitative manner since the biochemical pathways involved in the biosynthesis of these bioactive compounds are highly inducible. This is especially true for terpenoids, where levels usually increase up to three orders of magnitude following elicitation (Turlings & Tumlinson, 1992; Trapp & Croteau, 2001). Recently, Bhan *et al.* (2006) showed the production of andrographolide, neo-andrographolide and 14-deoxy andrographolide from 10 different accessions was susceptible

to intrinsic factors such as genotype and ontogeny as well as external factors (elicitors), which supported previous finding by Pholphana *et al.* (2004). Other compounds that often exhibit the same propensity are phenylpropanoids and alkaloids. Furthermore, the presence of polyphenols and pigments in complex plant extracts can interfere with the activity of bioactive compounds.

Another important factor is the lack of rapid and efficient methods in isolating and characterising phytochemicals, particularly if they are only present in trace amounts. It usually requires almost 6 months isolating and characterising compounds from a plant extract. This does not include the production of standardised extracts. Cultivation and harvesting times will also affect total yield of andrographolide (Polphana *et al.*, 2004; Bhan *et al.*, 2006) and the fact that *A. paniculata* is an annual herb must also be taken into account. Furthermore, only a standardised extract is ideal for experiments. Thus, employing extracts for experiments within the time limit for this PhD was not feasible.

Other argument that can be put forward is that by studying one potentially beneficial phytochemical at a time, in this case andrographolide, more understanding can be gained on many aspects of that particular bioactive compound, in contrast to working with standardised extract where the level of qualitative understanding can be limited. Taxol (paclitaxel), an important diterpene isolated from *Taxus* (*T. bacata* and *T. brevifolia*) which exhibited anti-tumour activity, is a good example. The main impediment to its wide clinical use is the sourcing of the compound. To obtain 2.5kg of taxol, approximately 12,000 of *T. brevifolia* must be cut down (Wall & Wani, 1996). Thus, an alternative source must be sought, either from hemi-synthetic production or an analogue from other *Taxus* species. This task would be both scientifically inappropriate and economically unfeasible if the whole extract is examined rather than potentially beneficial individual compounds.

On the other side of the coin, isolating an active compound may exclude other pharmacologically relevant phytochemicals. This is particularly true when pharmacological activity is a result of pharmacokinetic influences and/or pharmacodynamic synergism of more than one bioactive compound. Ginkgolides A, B, C, and M from *Ginkgo biloba* is a good example.

1.10 Genotoxicity Information on *A. paniculata* extracts and Andrographolide

Realising the medical potential of *A. paniculata*, particularly androrapholide which is the major active compound, genotoxicity testing is crucial. There are no existing genotoxicity studies published, to the best of the author's knowledge at the time of study, especially recommended tests for genotoxic potential such as *in vitro* cytokinesis block micronucleus assay (CBMA). Furthermore, the toxic effects of this plant are not well known.

However, Liu *et al.* (1990) suggested that the extract of the aerial parts are not mutagenic *in vitro*. This suggestion is questionable since water extract was used instead of alcohol-based extract. Most of the experimental pharmacological studies mentioned previously utilised either alcohol-based or dried extract of the aerial parts or purified andrographolide. Gupta *et al.* (1990,1993) demonstrated that the aqueous extract of the aerial parts was not active in exerting anti-diarrhoeal activity. Yin *et al.* (1991) tested the aqueous extract of *A. paniculata* with the Ames test utilising *Salmonella typhimurium* strains TA98 and TA100 as well as chromosomal aberration assays in mice did not find a positive result on genotoxicity. However, it must be pointed out that even with plant extracts that yielded positive results, there was noticeable discrepancy in results obtained from the mammalian chromosomal aberration and micronucleus assay with those from the Ames test. Usually, the results obtained from mammalian *in vivo* tests will outweigh those derived from bacterial test system *in vitro*. In the study conducted, the coherence between the two was low (Yin *et al.*, 2001). Furthermore, Yin *et al.* (1991) justified the extraction method employed in the study as to simulate the traditional practice conducted in preparing extract for oral medication. As has been pointed earlier, aqueous extract of *A. paniculata* are not ideal for experiment because the diterpene lactones such as andrographolide, are sparingly soluble in water compared to methanol or chloroform (O'Neil *et al.*, 2001) therefore reducing the bioavailability of the compound to the target in this case DNA. Thus, aqueous extract of andrographolide is unable to provide an accurate picture of genotoxicity. Another important aspect that needs to be considered is the suitability of using bacterial test system such as the Ames test, since the extract of *A. paniculata* appeared to have antibacterial activity (Singha *et al.*, 2003).

A standardised dried extract of *A. paniculata* did not produce reproductive toxicity in male Sprague-Dawley rats. There was no sign of testicular toxicity with the treatment of 20, 200

and 1000mg/kg body weight for 60 days as evaluated by testicular histology, testosterone levels, reproductive organ weight and ultrastructural analysis of Leydig cells (Burgos *et al.*, 1997). However, the paper mainly concentrated on histological evaluation and no observation was made on the possibilities of genotoxicological effects of the compound examined. Furthermore, it is known that testicular histology is subjective and not quantitative in testicular toxicity evaluation. Akbarsha and Murugaian (2000) demonstrated that the treatment of andrographolide to male Wistar albino rats at 25mg and 50mg/kg body weight for 48 days resulted in decreased sperm counts, immotile spermatozoa with several of them possessing abnormalities, limited number of fully differentiated spermatozoa, the disruption of the seminiferous tubules and seminiferous epithelium as well as vacuolated Sertoli cells. The Leydig cells did not show any pathological change and supported the finding made by Burgos *et al.* (1997) but there were spermatotoxic effects observed and possible disruption(s) to spermatogenesis.

Andrographolide extract did not cause significant reduction in progesterone concentration in pregnant rats and at therapeutic dose, is incapable of inducing progesterone-mediated termination of pregnancy (Panossian *et al.*, 1999). However, the extract of *A. paniculata* should not be used during pregnancy or lactation due to potential antagonism with endogenous progesterone (Panossian *et al.*, 1999). To the best of the author's knowledge, the teratogenicity effect of the herb has not been evaluated to this date.

As a brief summary, Figure 1.11 overleaf illustrated the factors that are involved in the revival of interest in phytomedicines and the imperative needs for more information on their safety and efficacy.

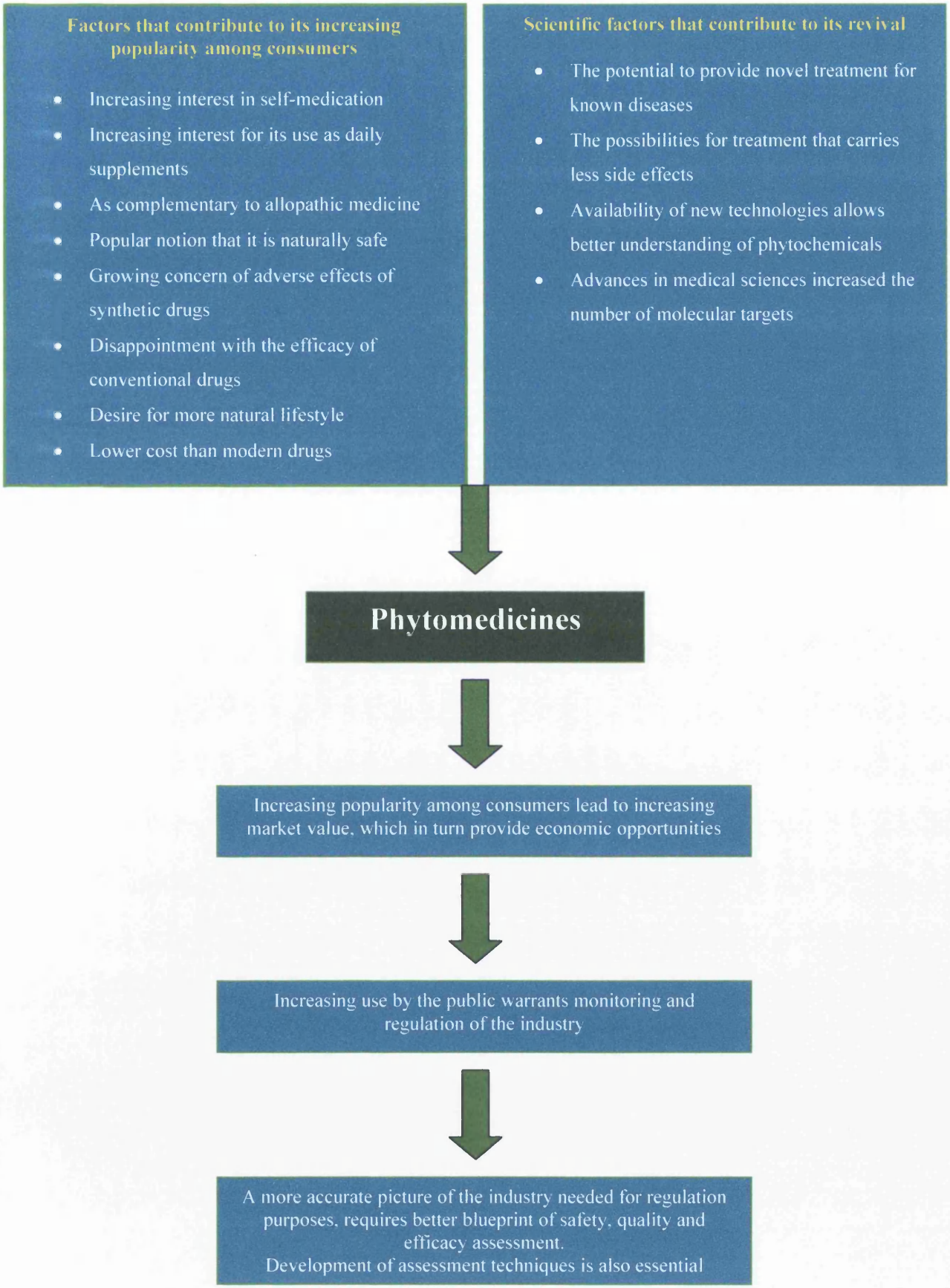

Fig. 1.11 Shows the factors involved in phytomedicines' revival and the need for more information on safety.

CHAPTER 1

PART 2: INTRODUCTION TO THE GENETIC TOXICOLOGY IN MAMMALIAN CELLS AND ITS IMPORTANCE

1.11 Brief Introduction to Genetic Toxicology

Paracelsus first described the 'wasting disease of miners' in 1567 based on his observations in Austrian and other several European mines in the Middle Ages. He later suggested that the exposure to realgar (arsenic sulphide) and other natural ores might have been the culprit in causing this condition, which is today known as cancer. Although this type of cancer was eventually attributed to radioactivity emitted from decay products of radon gas rather than arsenic, Paracelsus was among the first to consider chemical compounds as potential carcinogens.

The study of chemical mutagenesis began in the early 1940s when Charlotte Auerbach and colleagues discovered that mustard gas, a chemical warfare agent used against soldiers in trenches during the First World War was capable of causing genetic mutation in fruit fly, *Drosophila* (reviewed by Beale, 1993). Since then and for the next three decades, most experiments were performed on mice or flies to study chemically-induced mutation. Eventually, better test systems based on yeast and bacteria were developed where data can be obtained cheaper and quicker than using flies or mice. Furthermore, the inclusion of liver extracts and cofactors allowed the detection of more mutagenic agents and highlight the importance of biotransformation in mutagenesis studies. Then, in 1973 Bruce Ames successfully showed that various chemical carcinogens induced mutation in the genetically-engineered *Salmonella typhimurium* bacteria (Ames *et al.*, 1973), known today as the Ames test which has been widely used to screen potential cancer-causing agents.

Genotoxic agents are rather ubiquitous in the environment whether they are man-made products or found naturally. Many synthetic chemicals employed in manufacturing industry, X-rays developed for medical diagnosis and carcinogenic hydrocarbons in coal tar or smelters are examples of genotoxic compounds of man-made in origin. Even the way of how

food is being prepared such as grilling red meat at high temperatures are known to yield potent mutagens. Naturally occurring agents include aflatoxin produced by *Aspergillus flavus* that grows on nuts and isothiocyanates, the mutagenic phytochemicals found in cruciferous vegetables. Reactive oxygen species and free radicals that are endogenously produced as a result of cellular metabolism are also known to be genotoxic. Figure 1.12 shows the mechanisms of actions of DNA and non-DNA reactive genotoxicants.

Genetic toxicology is a broader term than chemical mutagenesis, dedicated to the study of genetic damage, the physical and chemical agents that are responsible, the mechanism involved for it as well as the cellular and organisms' responses to this injury. Since the potential consequences of genetic damage include birth defects and cancer, the elucidation of novel substances' potential to elicit DNA damage and genome instability is an important step in the development of new medicines and other products intended for human use. Various endpoints can be employed in assessing genotoxic damage and they are shown in Figure 1.13.

1.12 Biotransformation of Xenobiotics

All organisms are constantly exposed to foreign chemicals and these can be man-made (drugs, industrial chemicals) or naturally occurring compounds from the environment. Uptake is usually via ingestion, however inhalation and transdermal routes are also possible. Due to the lipophilicity of many chemicals that facilitate their uptake via these routes, organisms have evolved mechanisms to increase their hydrophilicity for rapid excretion via bile and urine. Otherwise, the accumulation of these xenobiotics will overwhelm defense mechanisms and disrupt systemic homeostasis. This process is known as biotransformation and is catalysed by various enzymes primarily in the liver of higher organisms but are also present in other organs such as the gut, kidneys and lungs.

Plants have been known to be one of the reasons for the evolution of biotransformation in animals. Most animals are plant-eaters and customarily being bombarded by various secondary metabolites which play a role in plants' defence mechanisms. However, many chemicals can also be transformed into more reactive metabolites. In pharmacology for example, the metabolites of some parent drugs impose the desired therapeutic effect but in

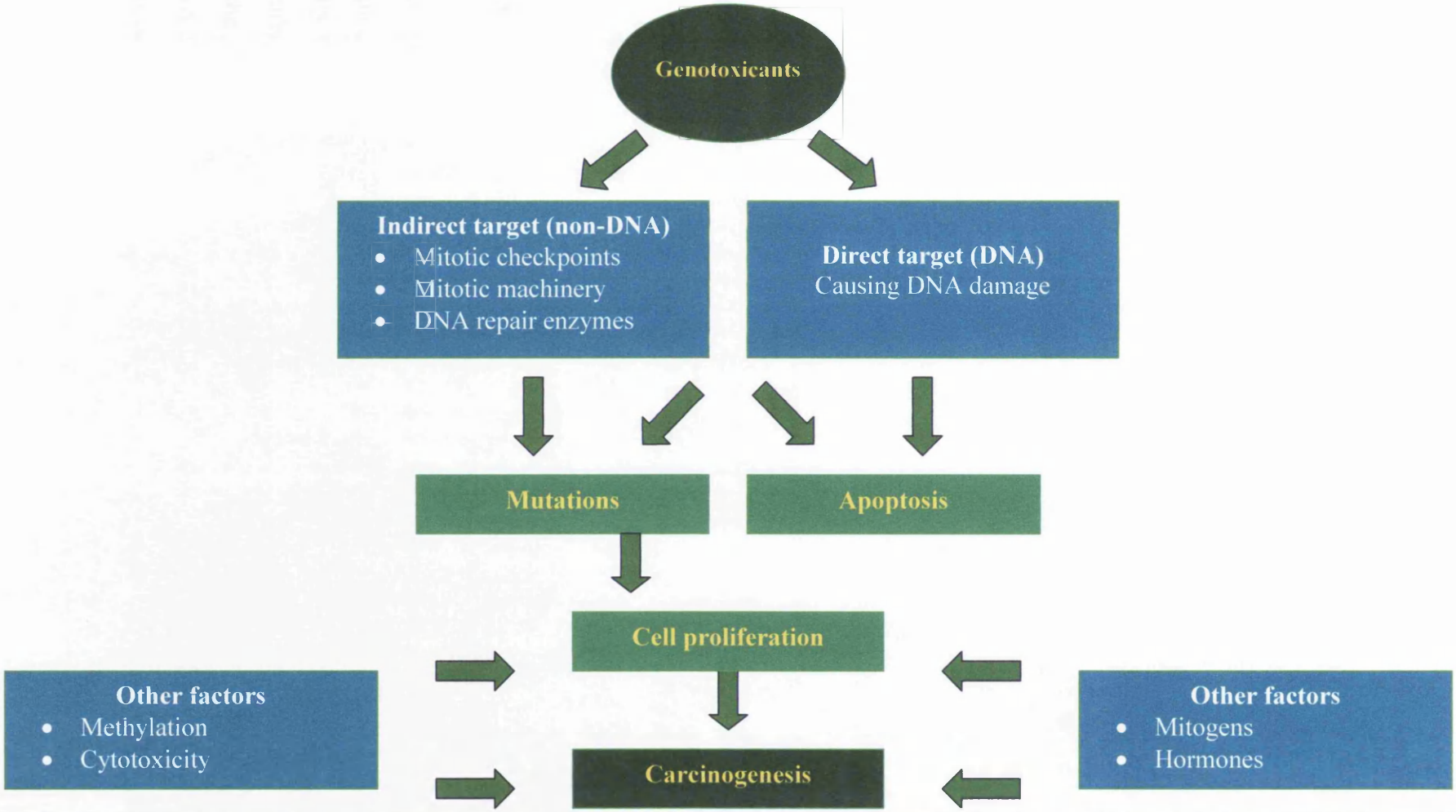

Fig. 1.12. Mechanisms of action of DNA and non-DNA targeting genotoxicants. Genotoxicants can affect DNA either directly or indirectly, by binding to proteins crucial to the maintenance of genome integrity. Non-genotoxic factors or agents such as mitogens are also capable of inducing cancer by increasing cell proliferation rate. Others can cause cytotoxicity or changing the DNA methylation status. Cell proliferation can be a main effect of the carcinogen or as a result of cell toxicity. Many types of genotoxicants can induce apoptosis. Disproportionate elimination of cells by apoptosis can elicit compensatory cell proliferation to restore homeostasis. Thus, carcinogenesis is the consequence of the interplay between mutations, epigenetic changes, cell proliferation and cell death. Page 34.

the case of polycyclic aromatic hydrocarbons (PAHs), that can be subjected to epoxidation resulting in the production of eletrophile that is damaging to DNA and proteins.

Xenobiotic metabolism occurs in two stages namely Phase I and Phase II. Different compounds will possess varying effects due to the length of time they remain in the organism. A compound that is toxicologically very active but is extremely hydrophilic will be easily excreted from the body without the possibility of inducing severe damage in contrast to relatively low activity compound that is hydrophobic but lingers longer in the body and could potentially be more harmful. Biotransformation will be discussed in greater length in Part 2 of the second Chapter in this thesis.

Various pro-mutagenic and pro-carcinogenic compounds require metabolic activation before they can exert their effect and typical cell culture techniques do not often maintain the metabolic capacity of the liver. Accordingly, the addition of S9-fraction of liver homogenate into cell cultures *in vitro* was intended to provide an external metabolic capability. The creation of cell lines for genotoxicology applications, which have been genetically engineered to be metabolically competent such as AHH-1 and MCL-5 serve as an alternative to the addition of S9-fraction, thus permitting the assessment of xenobiotics that need bioactivation.

1.13 The Cycle of Cell Division

Cells proliferate in response to extracellular growth factors, passing through a repeated sequence of events known as the cell cycle. This has four major phases: G_1, then S, G_2 and lastly the mitotic or M-phase. This is followed by division of the cytoplasm and plasma membrane to produce two daughter cells. G_1, S and G_2 together constitute interphase, which is the majority of the cell cycle. During interphase, the cytoplasm increase in volume, the DNA is uncoiled then diffuse within the nucleus and is a stage of general growth where ribosomes, mitochondria and other cellular proteins are synthesise. The chromosomes are replicated during the DNA synthetic or S-phase. Most somatic cells in the body are not actively dividing and are arrested at G_0 within G_1. Figure 1.14 shows the assorted phases of the cell cycle.

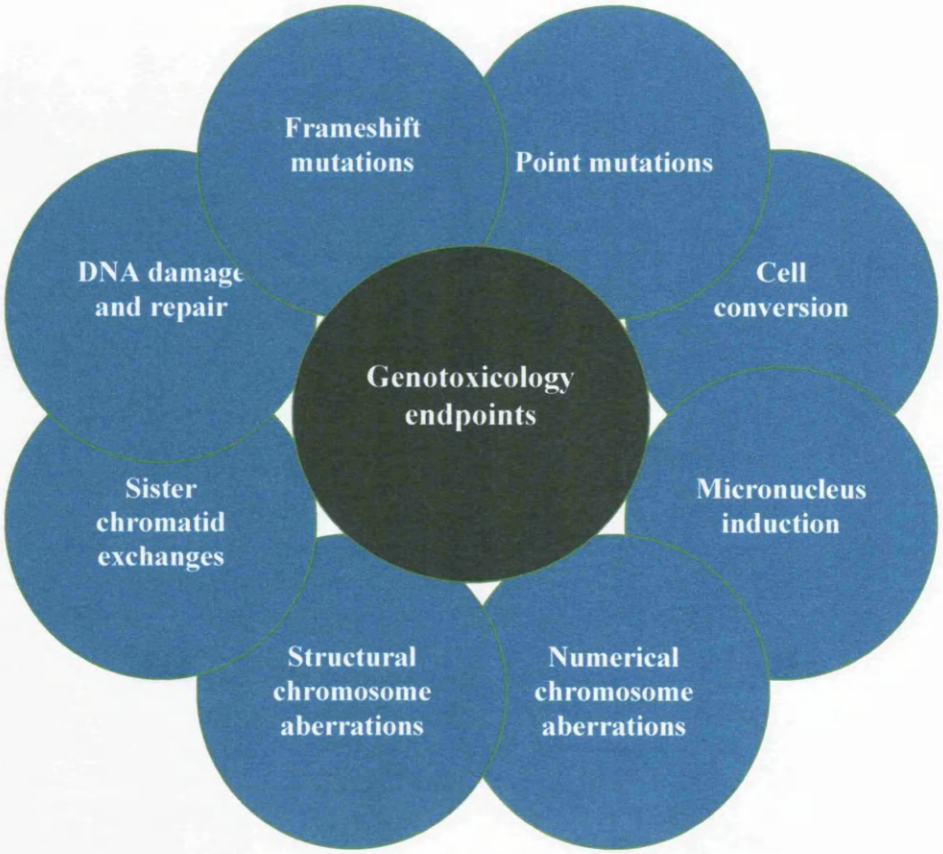

Fig. 1.13. Various endpoints employed in genotoxicity measurement. Point and frameshift mutations involve changes in a single DNA base and the subtraction/addition of one or few bases respectively. Exchange of DNA strands between two chromatids in a single chromosome is referred to as sister chromatid exchanges (SCE). Chromosomal aberrations can arise either in structural or numerical form and can both can be observed microscopically. Structural aberrations include chromosome breaks, intrachanges and interchanges between chromosomes whereas aneuploidy, or numerical abnormalities involve changes in chromosome number. Cell conversion involves the transformation of the cells' physiology and morphology for example, from normal to malignant form. Page 36.

Mammalian cells will proliferate only if stimulated by extracellular growth factors secreted by other cells. These operate within the cell through the proto-oncogene signal transduction cascade. If deprived of such signals during G_1, the cell diverts from the cell cycle and enters the so-called G_0 state. Cells can remain in G_0 for years before recommencing division.

The G_0 block is imposed by mitosis-suppressor proteins such as the retinoblastoma (Rb) protein encoded by the normal allele of the retinoblastoma gene. These bind to specific regulatory proteins preventing them from stimulating the transcription of genes required for cell proliferation. Extracellular growth factors destroy this by activating G_1-specific cyclin-CDK complexes, which phosphorylate the Rb protein, altering its conformation and causing it to release its bound regulatory proteins. The latter are then free to activate transcription of their target genes and cell proliferation ensues (reviewed by Lodish et al., 1995).

The cell cycle is driven by alternating activation and de-activation of key enzymes known as cyclin-dependent protein kinases (CDKs), and their cofactors called cyclins. This is performed by phosphorylation and de-phosphorylation by other phosphokinases and phosphatases, specific cyclin-CDK complexes triggering specific phases of the cycle. At appropriate stages, the same classes of proteins cause the chromosomes to condense, the nuclear envelope to break down and the microtubules of the cytoskeleton to re-organise to form the mitotic spindle.

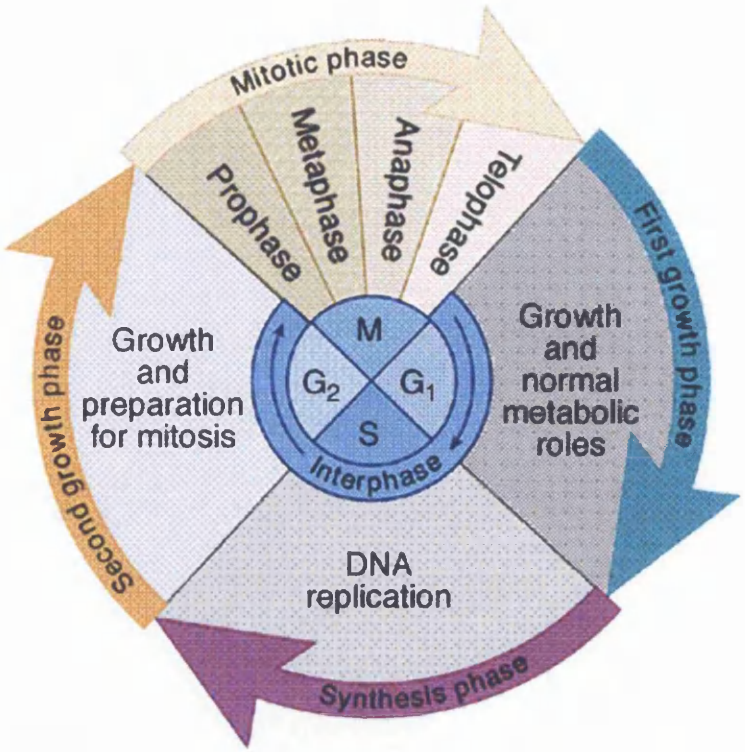

Fig. 1.14. Shows the main stages of the cell cycle divided into two main parts, the interphase and the mitotic phase. Interphase consists of G_1, S and G_2 phases whereas the mitotic (M) phase can be further sub-divided into prophase, metaphase, anaphase and telophase. Cytokinesis marks the end of the cell cycle and produced two genetically identical daughter cells. (Diagram obtained from http://bhs.smuhsd.org).

1.14 Cell Cycle Checkpoints and the Integrity of the Genome

Directly after mitosis, in G_1 phase the cell increases in size and initiates necessary RNA synthesis (transcription) and proteins (translation). In subsequent S phase, nuclear DNA is replicated to produce an exact copy of the genome for the ensuing daughter cells. During G_2, the cells will grow and produce extra proteins to ensure that two viable daughter cells can be formed. The process of RNA and protein syntheses that began in the G_1 phase are extended during the S and G_2 phases. Finally, during M phase, the chromosomes are organised so that two genetically identical progeny cells can be configured, after which the entire cycle can begin again. Cells can also stop dividing to remain in G_0 and may stay in this state for a considerable amount of time before starting to divide again or remain in G_0 permanently until the organism dies (reviewed by Lodish *et al.*, 1995; Purves *et al.*, 1998).

In a normal cell cycle, the passage from one phase to another is strictly governed. Although still being debated, genetic evidence that proteins involved in the orderly progression through the cell cycle are also involved in the checkpoint response to DNA damage is accumulating.

This connotes that in all cells, these cell cycle checkpoint pathways are active in basal state but they are up-regulated in response to DNA damage. The term checkpoint is defined more upon the transition between phases that is being inhibited by DNA damage at the G_1/S, intra-S and G_2/M checkpoints. Although these checkpoints are temporally distinct, they all response to DNA damage and share many proteins (reviewed by Klug and Cummings, 2005).

The DNA damage responses during any phase of the cell cycle possess the same pattern. After the detection of DNA damage by sensor proteins, signal transducer proteins transmit the signal to effector proteins, which in turn launch a cascade of events that cause cell cycle arrest, DNA repairs, apoptosis and/or activation of damage-induced transcription programs.

1.14.1 The G_1/S checkpoint

The G_1/S transition is promoted by non-phosphorylated CDC25A protein. The type of DNA damage encountered determines the response pathway of cell cycle arrest. DNA double strand breaks lead to phosphorylation of ATM which in turn phosphorylates Chk2. Single-strand gaps cause the activation of the ATR, Rad17-RFC and the 9-1-1 complex, resulting in the phosphorylation of Chk1. Thus the phosphorylation of CDC25A by Chk1 or Chk2 causes inactivation of this protein by nuclear exclusion and ubiquitin-mediated proteolytic degradation, leading to G_1 arrest. ATM and ATR also phosphorylates p53, which leads to stabilisation and accumulation of p53 protein as well as the promotion of p53 transcription factor activity. The target of the transcription factor p53 is p21, whose role is to inhibit CDK2 activity causing the maintenance of cell cycle arrest. For this reason, p53 is known affectionately as 'the guardian of the genome'.

1.14.2 The Intra-S-phase checkpoint

There are two pathways mediating this checkpoint. The first pathway, the ATM/ATR-Chk2/Chk1-CDC25A-CDK2 is almost similar to G_1/S checkpoint and is responsible for postponing DNA replication by inhibiting the loading of CDC45 onto chromatin. As a consequent, DNA polymerase-α attach to the pre-replication complexes and prolonging the DNA replication period thus permitting DNA repair to occur.

The second pathway involves NBS1 (NBS stands for Nijmegen breakage syndrome, referring to a human disorder characterised by cancer predisposition, chromosomal instability, immunodeficiency, hypersensitivity to ionising radiation and growth impediment) that is phosphorylated by ATM together with Chk2. This activation leads to a cascade involving

Rad50- and Mre11-like initial DSB recognition that is not only required in cell cycle arrest but also in repair processes activation.

1.14.3 The G_2/M checkpoint

When cells confront DNA damage in G_2, the G_2/M checkpoint halts the cell cycle in order to restrain the cell from entering mitosis. As in the G_1/S checkpoint, the type of DNA damage dictates the cellular response route; the ATR-Chk1-CDC25 for DNA lesions such as those caused by UV light and ATM-Chk2-CDC25 for double-strand breaks. Apart from down-regulating CDC25A, both Chk1 and Chk2 up-regulate WEE1 via phosphorylation, which together manage CDC2/CyclinB activity. This latter complex augments G_2/M transition under normal circumstances and inactivation blocks the cell cycle when damage occurs in G_2. The maintenance of this arrest seems to be partly independent of p53/p21, unlike in the G_1/S checkpoint, whereas tumour cells lacking functional p53 still tend to accumulate in G_2 after the induction of DNA damage (reviewed by Klug and Cummings, 2005).

As the cell cycle checkpoint pathways are predominantly evolved to prevent transferring DNA damage to daughter cells, it is obvious that defects in checkpoint responses can result in genomic instability leading to transformation of normal cells into cancer cells. Indeed, the absence of p53 or ATM causes syndromes featuring cancer susceptibility. In addition, other genes involved in cell cycle checkpoints are related to cancer, most of them also having function in DNA repair. This combination probably makes mutations or deletions more severe where there is less repair and less control.

After the successful completion of interphase, mitosis which is the second major stage of the cell cycle will commence. The replicated chromosomes must become condensed to be able to migrate to the opposite poles, which ultimately will become two separate daughter cells. The sequence of events in mitosis is described below with the aid of Figure 1.15 that shows the delicate dance of chromosomes during mitosis.

Prophase.

Prophase begins immediately after interphase. The chromosomes each consisting of two identical sister chromatids, begin to contract and become visibly condensed within the nucleus. The nucleoli gradually disperse. The centrosomes begin to duplicate, split and subsequently migrate to the opposite sides of the cell and forming the spindle poles

(microtubule organising centres, MTOCs). The spindle apparatus of tubulin fibres begins to assemble around the two centrosomes at opposite poles of the cell.

Pro-metaphase (late prophase).

The nuclear membrane dematerialises and kinetochores develop around the centromeres of the chromosomes. Tubulin fibres enter the nucleus and assemble, radiating out from the kinetochores and linking up with those radiating from the centrosomes.

Metaphase.

Tension in the spindle fibres causes the chromosomes to align midway between the spindle poles thus creating the metaphase plate. This alignment facilitates the separation of chromatids.

Anaphase.

When the chromatids of each chromosome begin to separate, the cells enter anaphase and this is the shortest part of mitosis. The centromeric DNA shared by sister chromatids is duplicated, they separate and are drawn towards the spindle poles. All of the chromosomes begin to separate at the same time.

Telophase.

This is the final stage of mitosis and is essentially the reverse of prophase. The separated sister chromatids (now considered to be chromosomes) reach the spindle poles and a nuclear membrane reforms around each group. New nuclear membranes are produced by the endoplasmic reticulum. The spindle fibers depolymerise, condensed chromatin uncoil then diffuses and nucleoli re-appear. Telophase ends when the nuclei of the two resultant daughter cells appear to be in interphase.

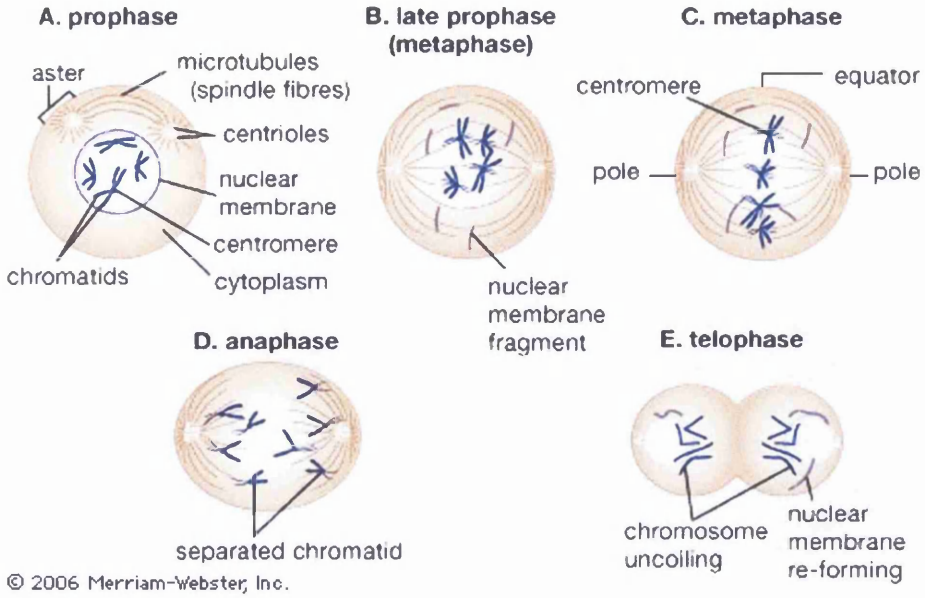

Fig. 1.15. The delicate dance of chromosomes during mitosis can be sub-divided into four main stages. Centrioles are crucial element in centrosome which act as spindle poles pulling sister chromatids in opposite direction. (Diagram obtained from www.britannica.com).

Cytokinesis.

After a successful completion of karyokinesis, cytokinesis or the physical separation of one cell into two daughter cells marks the end of the cell cycle. This process requires a synchronious operation of the membrane systems, the cytoskeleton and the cell cycle mechanism, which are spatially and temporally controlled in a precise manner. One must point out that cytokinesis actually begins in late anaphase where microtubules have elongated and contact the cortex. The rearrangement also created a region of bundled microtubules between the chromosomes termed the midzone. In early telophase, the cleavage furrow ingresses and as cytokinesis progresses, the cleavage furrow has fully ingressed constricting the midzone effectively forming an intercellular bridge containing a microtubule midbody. When the intercellular bridge is resolved and eventually separates the two daughter cells, cytokinesis and ultimately the cell cycle is completed. Figure 1.16 highlights the progressive part of the cytokinesis process.

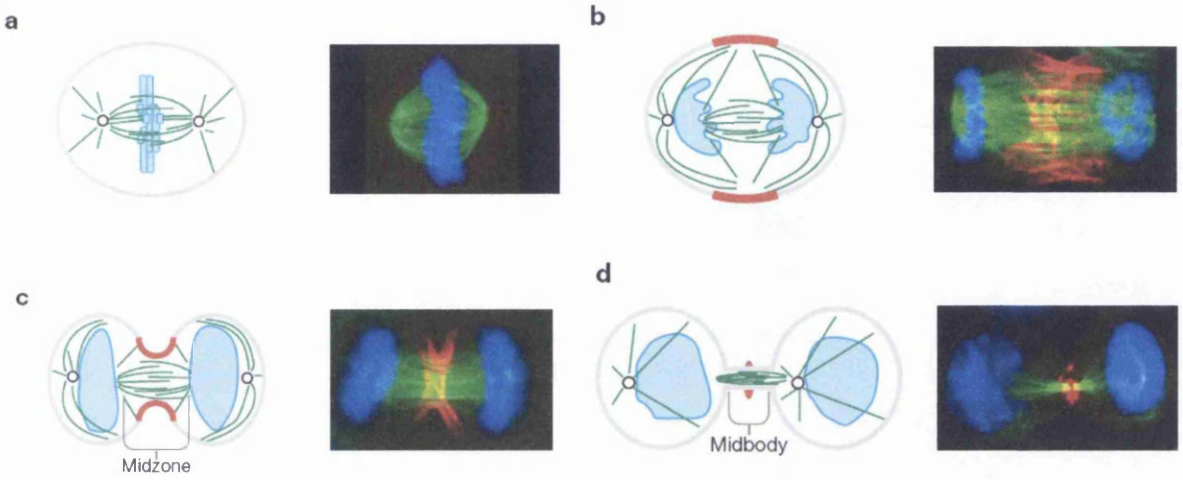

Fig. 1.16. Different stages of cytokinesis shown in a progressive manner by schematic and immunoflurescence illustrations. (a) Cell is in a metaphase stage where chromosomes are aligned at the equator (metaphase plate) by the microtubules of the mitotic spindle. (b) Microtubules have extended and contract the cortex, a region of bundled microtubules between chromosomes known as the midzone was created after microtubule rearrangement. The cell is in late anaphase and the cleavage furrow components (red) have rallied at the equator. (c) Cell is in early telophase and cleavage furrow continues to ingress. (d) In late telophase, the cleavage furrow has completely ingressed and compacted the midzone producing an intercellular bridge consisting of microtubule midbody. Cytokinesis is completed when the intercellular bridge is resolved giving rise to two genetically identical daughter cells. (Eggert *et al.*, 2006)

1.15 The Centrosome Cycle

At G_1 the pair of centrioles associated with each centrosome separate. During S-phase and G_2 a new daughter centriole grows at right angles to each old one. The centrosome then splits the beginning of M-phase and the two daughter centrosomes move to opposite spindle poles. This cycle will be discussed in further details in Chapter 4 of this thesis.

1.16 DNA Damage Repair Mechanisms

There are two processes that enable a cell to cope with the severity of DNA damage it sustains. If the damage is extensive, the cell can initiate apoptosis. However, if the damage is less serious, cells have developed a range of repair processes that restore the DNA to its undamaged state (error-free repair) or to an improved but still altered state (error-prone repair).

DNA damage checkpoints can only prevent the transfer of mutations to daughter cells in the presence of an efficient DNA damage repair machinery. Different types of DNA repair pathways have evolved to counter various categories of lesions possible. Important pathways in mammalian cells include base excision repair (BER), nucleotide excision repair (NER), mismatch repair (MMR) and double-strand break (DSB) repair.

1.17 Genotoxicants and Mutations

When xenobiotics are internalised by cells, most of them are metabolised and the resultant metabolites are either retained or excreted. Inside the cell, genotoxicants or their metabolites are capable of directly or indirectly affect the regulation and expression of genes that are crucial in DNA repair, cell cycle oversight, cell differentiation and/or apoptosis. Some genotoxicants act directly by forming DNA adducts or inducing chromosomal abnormalities such as chromosome fusion, breakage, deletion, non-disjunction and missegregation. For example, arsenic and nickel are known to cause numerical and structural chromosome abnormalities (Hughes, 2002; Kasprzak *et al.*, 2003). Other genotoxicants may act via non-genotoxic routes such as causing inflammation, formation of reactive oxygen species, immunosuppression, epigenetic silencing as well as receptor activation such as oestrogen receptor or arylhydrocarbon receptor. Cumulatively, these genotoxic and non-genotoxic mechanisms can change signal-transduction pathways resulting in hypermutability, genomic instability, failure in cell proliferation control and resistance to apoptosis, which are some of the hallmark of cancer cells (reviewed by Hanahan & Weinberg, 2000). Figure 1.17 overleaf provides an overview of genotoxic and non-genotoxic action routes of genotoxicants.

A mutation is an alteration that occurs to the structure or quality of the genetic material that could lead to a change in phenotype. Mutations can involve modifications of the nucleotide sequence of a single gene, block of genes or whole chromosomes. Changes in: (1) single genes are the consequence of a point mutation, (2) blocks of genes are generally due to strand breaks; and (3) whole chromosomes are due to aneuploidy.

Mutations are permanent changes to nuclear DNA and can be inheritable if germ cells are involved. During cell division, replication errors may arise from damaged bases (e.g. Alkyl-Guanine) resulting in mutation which potentially capable of altering the gene product. The

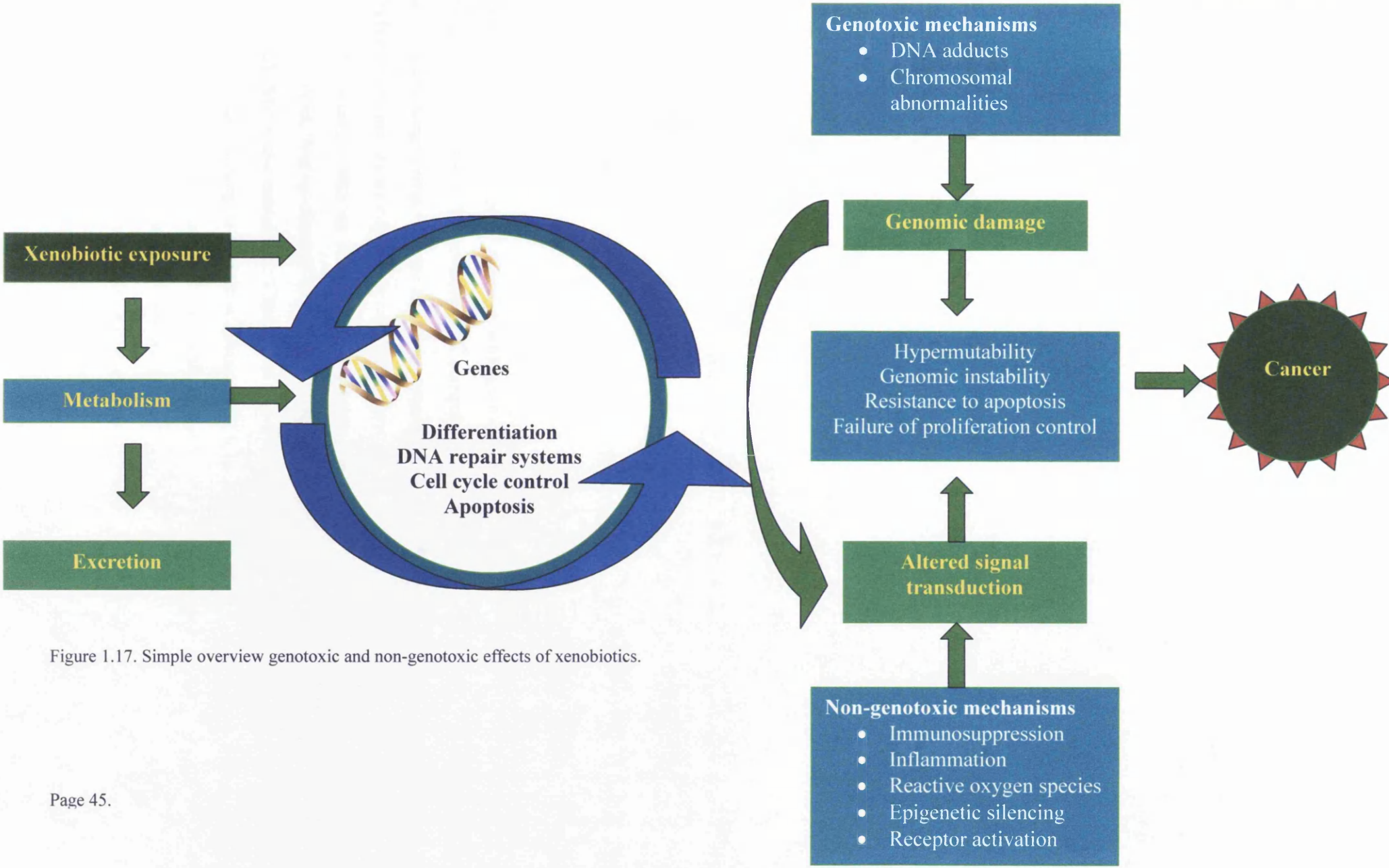

Figure 1.17. Simple overview genotoxic and non-genotoxic effects of xenobiotics.

occurrence of such errors during replication are usually due to exposure to viruses, chemicals, radiation or even internally during normal biological processes such as meiosis and hypermutation (reviewed by Griffiths *et al.*, 2004). Although mutations can have undesirable effects, they are valuable currency in evolution. Deleterious and unfavourable mutations will be removed from the gene pool via natural selection and those that confer advantageous adaptation to a species will accumulate in the population. There are also neutral mutations that accumulate with time but are not deleterious in nature (reviewed by Griffiths *et al.*, 2004).

Mutations can be categorised into somatic mutations that result in neoplasia (cancer) or cell death and germline mutations, which are inheritable and in some cases such as familial adenomatous polyposis (FAP) involving colorectal cancer is attributed to the *APC* gene mutation, capable of causing somatic mutations in the progeny (reviewed by Klug and Cummings, 2005)

Mutations may be genetically sub-divided into different order and those that occur at nucleotide level are micro-mutations whereas those that cause changes at chromosomal level are macro-mutations.

1.17.1 Micro-mutations

a) Point mutations:

Transitions are exchanges of a purine with another purine (i.e. A↔G) or a pyrimidine for a pyrimidine (i.e. C↔T). Transversions in comparison are less common where a pyrimidine has been exchanged with a purine and vice-versa (e.g. A/G↔C/T). There are essentially three kinds of point mutations depending on what the erroneous codon codes for:

1) Silent mutations: Changes to the amino sequence but code for the same amino acid, thus no changes in biological homeostasis.
2) Mis-sense mutations: Changes to the DNA are manifested by changes in amino acid resulting in protein sequence alteration that have no impact, can be lethal or in some rare occasion lead to gain of function.
3) Non-sense mutations: Code for a stop codon that shorten the protein, which may have no effect, leading to a loss or gain of function.

b) Insertions:

One or more nucleotides added into the DNA that normally formed by transposable elements or errors during replication of repeating components (e.g. tandem repeats). Insertions are well known to cause frameshift mutations and modified mRNA splicing, which can both alter the gene product.

c) Deletions:

As the name implies, are removal of a single or multiple nucleotides from DNA that can result in frameshifts. Unlike point mutations and insertions, deletions are irreversible damage to the DNA (Brown, 2002).

1.17.2 Macro-mutations

As stated before, these types of mutations occur at the physically observable chromosomal level and can be categorised as below.

a) Duplications:

Duplication is the presence of two adjoining copies of a chromosomal segment and can be either 'direct' or 'inverted'. Duplications may originate by unequal crossing-over in a previous meiosis or as a result of translocation, inversion or presence of an iso-chromosome in a parent. Generally, duplications are more common and cause higher levels of gene dosage but are less detrimental than deletions.

b) Deletions:

Deletion can arise from two breaks, followed by faulty repair, from unequal crossing-over in a previous meiosis or as a consequence of a translocation in a parent. Deletions of chromosomal regions can be interstitial or terminal. Cri-du-chat syndrome is caused by terminal deletion of the short arm of chromosome 5 and is so-called because the malformed larynxes in the affected babies made them to cry like cats. Sufferers have profound learning disability, low birth weight, low-set ears, epicanthal folds and hypertelorism (widely spaced eyes).

c) Inversions:

Arise from two chromosomal breaks with end-to-end switching of the intervening segment. If this includes the centromere it is pericentric; if not the inversion is paracentric. The medical significance of inversions lies in their ability to cause chromosomally imbalanced gametes following crossing-over.

d) Translocations:

A translocation involves exchange of chromosomal material between chromosomes and three types are recognised namely centric fusion (Robertsonian translocation), insertional and reciprocal. Approximately 4% of Down syndrome cases are due to Robertsonian translocation between the long arms of chromosome 21 and any other acrocentric, normally chromosome 14. Sometimes, one parent has a balanced version of the same translocation.

e) Isochromosomes:

An isochromosome has a deletion of one arm but duplication of the other. In live births, the most prevalent involves the long arm of chromosome X, causing Turner syndrome due to short arm monosomy and long arm trisomy. Most incidents of isochromosomes lead to spontaneous abortion.

f) Loss of heterozygosity:

A locus (or even loci) where a deletion or other process has converted the locus from heterozygosity to homozygosity. This event can lead to cancers due to loss of tumour suppressor genes (Griffiths *et al.*, 2004).

1.18 Aneuploidy

Aneuploid cells have chromosome numbers that differ from the normal number for the species. In aneuploidy, the deviation is due to one or a small number of chromosomes. For example, in humans where the diploid (2n) number of chromosomes is 46, cells with 45 or 47 would be referred to as aneuploid. Cells can give rise to aneuploidy by: (1) the failure of homologous chromosomes to separate properly (non-disjunction) in meiosis I or mitosis or sister chromatids in meiosis II (Dellarco *et al.*, 1985); or (2) the chromosome(s) do not bind to the spindle during division so that the chromosome(s) is lost to either nucleus. The result

of non-disjunction is that one pole receives both homologous chromosomes or chromatids. Assuming only one chromosome or one pair of chromosomes is involved, the daughter nuclei will have one chromosome too many or one too few ($2n \pm 1$). Unlike direct mutagenesis, there are many potential targets for aneuploidy.

Aneuploidy may arise either on a spontaneous basis or chemically-induced during cell division in somatic and germ cells. Aneugens are chemicals that are capable of inducing aneuploidy or polyploidy. There are many possible targets for aneugens including molecules:

- that are crucial part of DNA-containing structures such as centromeres and telomeres.
- essential in chromatid attachment and separation including chromatin glue proteins and kinetochores.
- that are part of the spindle apparatus for example centrioles and tubulins.
- that are part of the anaphase promoting complex (APC) or involved in cell cycle control such as cyclins and p53.
- indirectly involved in the cell cycle such as calmodulin.

Any abnormal putsch to the cellular division by disrupting one or more of its crucial components can be detrimental to chromosome segregation fidelity. There are two classical processes that lead to aneuploidy namely chromosome non-disjunction and chromosome loss. Chromosome non-disjunction occurs when a metaphase chromosome unable to disassociate and both sister chromatids migrate to one of the daughter nuclei (Kirsch-Volders et al., 2002) resulting in one daughter cell gaining a chromosome (e.g. trisomic 2N+1) and the other loses a chromosome (e.g. monosomic 2N-1). Chromosome loss arise due to chromosome lagging during anaphase for example involving the failure of spindle fibres to attach to a chromosome. Lagging chromosomes are displaced chromosome that usually forms a micronucleus and thus are not part of the daughter nuclei at the end of mitosis. Consequently, one or both of these daughter nuclei are hypoploid, where the chromosome number is less than the normal euploid configuration. Micronuclei formed can be detected cytogenetically.

Centrosome amplification may also contribute to aneuploidy where the presence of multipolar microtubule organising centres (MTOCs) pulled chromosomes in different directions resulting in aneuploid progeny with either single, multiple nuclei or even

micronuclei (Pihan & Doxsey 1999; Brinkley, 2001) as shown in Figure 1.18 below. Alternatively, aberrant MTOCs may form pseudo-bipolar spindle poles to mute the supernumerary effect but still incapable of maintaining normal chromosome segregation resulting in unequal chromosome numbers and lagging chromosomes, which would later form a micronucleus (Pihan & Doxsey 1999; Brinkley, 2001). The amplified centrosomes will also be transferred to daughter cells and may be involved in further rounds of abnormal mitoses.

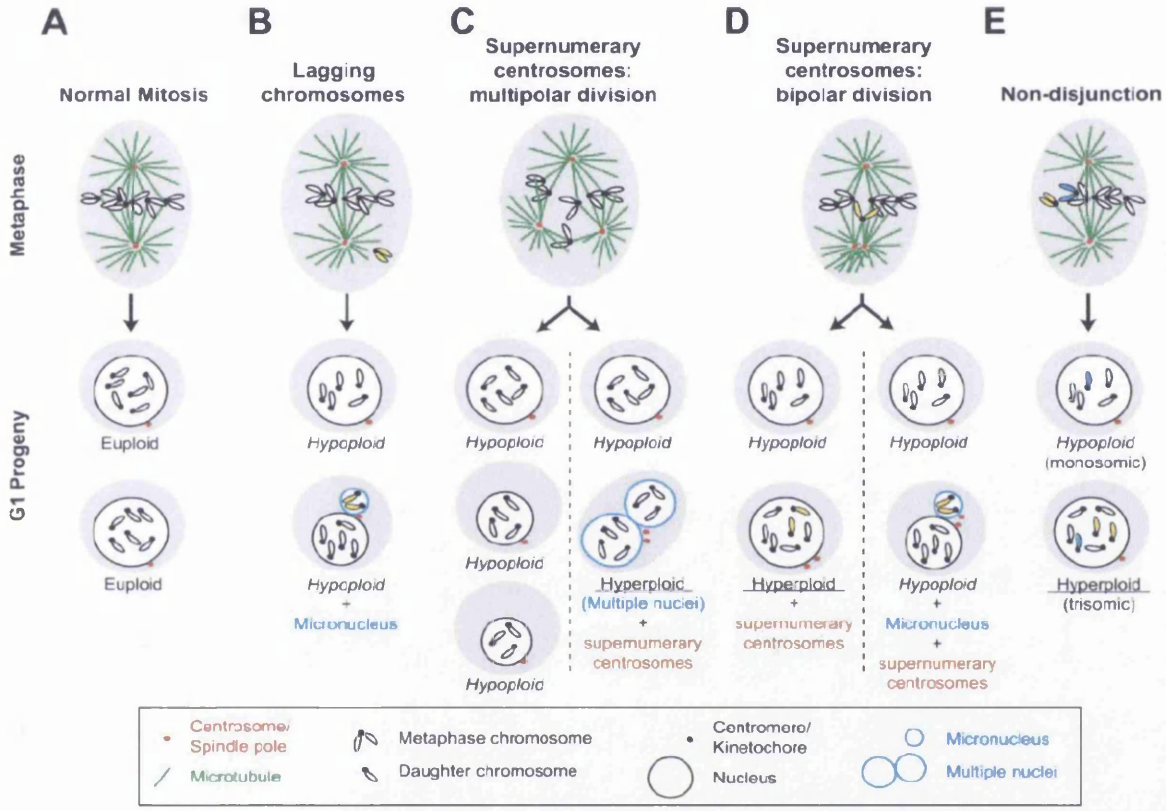

Fig. 1.18. Frequent factors contributing to chromosomal segregation infidelity that leads to aneuploidy. In (A), chromosomes aligned at the metaphase plate and migrate equally to opposite spindle poles producing two euploid daughter cells. (B) shows the outcome of mitosis in the presence of a lagging chromosome which gives rise to a micronucleus. In (C) and (D), anomalous centrosome number presents a segregational putsch to the normal chromosome distribution mechanism causing uneven configuration in daughter cells. In (E), chromosomal non-disjunction generates a hypoploid and hyperploid daughter cells. (Adopted from Yang *et al.*, 2003).

Apart from the two classical processes stated, aneuploidy may also arise via other pathways such as defective centromere division, chromosome replication errors during meiosis and non-conjunction, which is the inability of the homologous chromosomes to achieve a paired state. Some compounds presence in certain concentrations may interact physico-chemically such as lipophilic interaction and in effect disrupt cellular components or processes such as cytokinesis and spindle synthesis. Furthermore, at higher concentrations, cytotoxicity can also induce physico-chemical interactions that may cause non-specific modifications to

cellular division mechanism (Parry *et al.*, 1996). Figure 1.19 also illustrates various routes leading to aneuploidy.

Aneuploidy induction through the inhibition of spindle function for example, does not occur via direct interaction between the suspected compound or its active metabolite with DNA but acting on its target receptor(s) such as tubulin in a characteristic dose-dependent manner that may include a threshold level (Aardema *et al.*, 1998). The existence of thresholds for the initiation of chromosome loss and chromosome non-disjunction by spindle inhibitors such as carbendazim, colchicine, mebendazole and nocodazole has been reported (Kirsch-Volders, *et al.*, 2003).

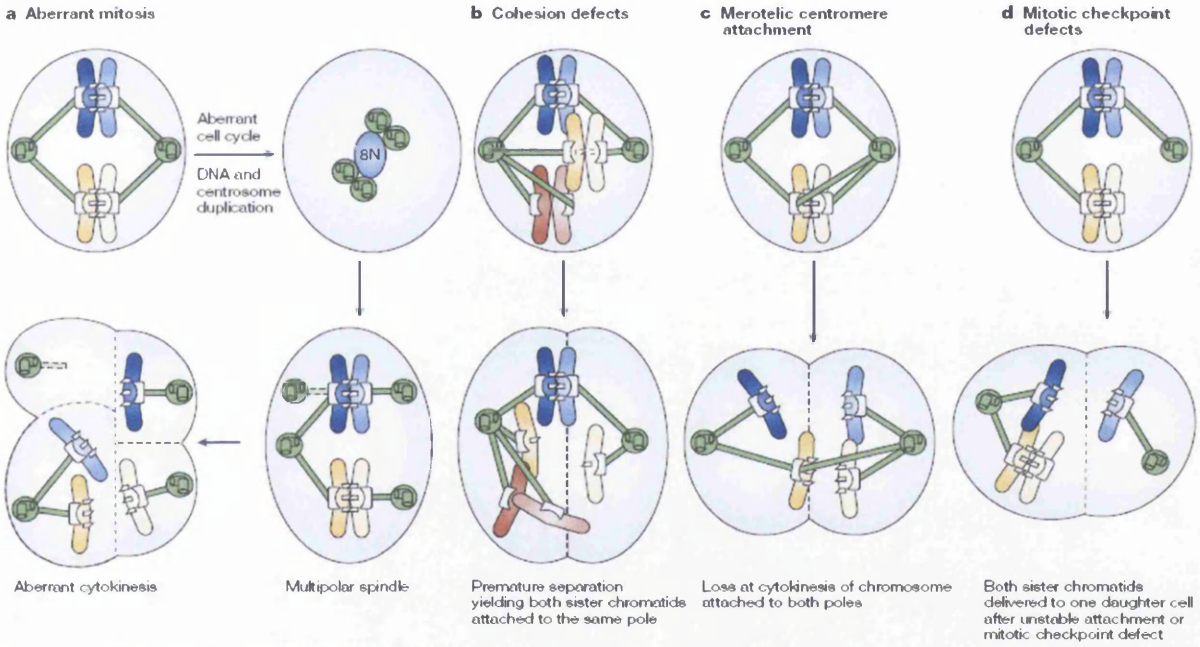

Fig. 1.19. Shows various other routes to aneuploidy. Gains and losses of chromosomes can occur in several ways as displayed. Aberrant mitosis can be caused by abnormal centrosome number due to centrosome amplification resulting in polyploidisation, centrosome duplication errors and ultimately aberrant cytokinesis. Cohesion deficiency and merotelic attachment, where a kinetochore is attached to microtubules from both poles can also cause chromosome loss. Finally in (d), defects in the mitotic checkpoint where weakened mitotic checkpoint signalling by one or more unattached kinetochores does not produce enough signal level for the 'wait anaphase', preventing anaphase advancement in the presence of unattached kinetochores. (Adopted from Kops *et al.*, 2005).

Polyploidy on the other hand corresponds to an exact multiple of the haploid number of chromosomes (N), for example 3N and are caused by the absence of a functional mitotic spindle and the consequent failure of chromatid migration to the opposite poles. This mitotic slippage or the inability to migrate to spindle poles produced cells that possess 4N and 4C

with C denoting to the haploid DNA contents (Elhajouji *et al*, 1998). Cytokinesis failure and nuclear fusion in binucleated cells can also lead to polyploidy (Kirsch-Volders *et al*., 1998).

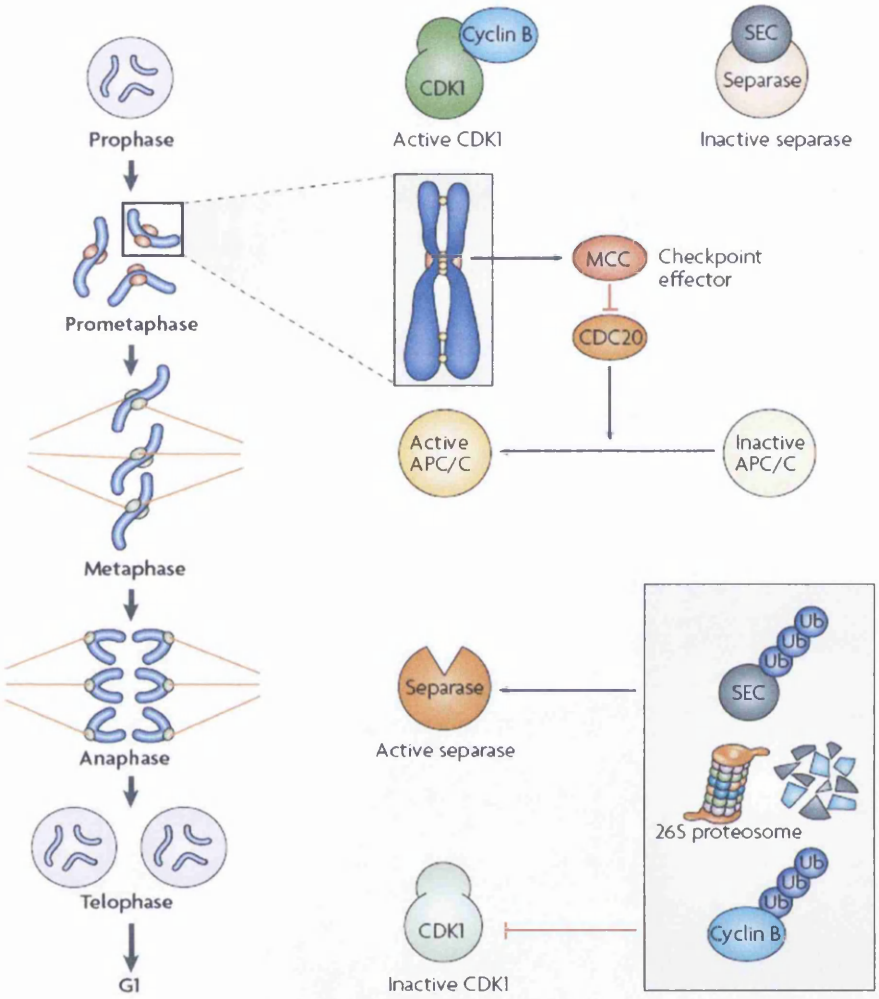

Fig. 1.20. Shows the relation between the mitotic checkpoint with different stages of the cell cycle beginning with prophase and ending with telophase and cytokinesis producing two identical daughter cells. To initiate mitosis, the cell needs the master mitotic kinase, the cyclin-dependent kinase-1 (CDK1) activity that depends on the binding of cyclin B to CDK1. Separase is a protease that is required to abolish sister-chromatid cohesion at the metaphase-anaphase transition. This enzyme is kept inactive by another protein known as securin (SEC) prior to anaphase. Cohesins which hold sister chromatid together are shown as yellow spheres in the expanded view of the chromosome. Unattached kinetochores trigger the formation of the mitotic checkpoint complex (MCC) which prevents CDC20 to activate the anaphase promoting complex/cyclosome (APC/C). The attachment of all sister chromatid pairs to kinetochore mirotubules and their bi-orientation generates congression to the metaphase plate and negatively regulates the mitotic checkpoint signal. Concomitantly, CDC20 is released followed by APC/C activation and leads to polyubiquitination of anaphase substrates such as securin and cyclin B that is subsequently eliminated by the proteasome. Securin destruction activates separase, which immediately separates the sister chromatids by targeting the cohesion rings that are holding them together. The elimination of cyclin B also inactivates the master mitotic kinase CDK1-cyclin B, initiating cytokinesis and the mitotic-exit programme. (Adopted from Musacchio & Salmon, 2007).

The spindle assembly checkpoint or also known as the mitotic checkpoint prevents chromosome missegregation and aneuploidy by repressing anaphase commencement until all

of the replicated chromosomes are successfully connected to spindle microtubules. Figure 1.20 highlights the relationship between the mitotic checkpoint with cell cycle machinery. However, an impaired mitotic checkpoint response or the inability to sustain mitotic checkpoint signalling, has been observed in human tumour cell lines challenged with microtubule poisons as observed by a decreased percentage of cells in mitosis and/or a reduced length of metaphase arrest.

1.18.1 Aneuploidy and Cancer.

As mentioned previously, aneuploidy may arise spontaneously or due to chemical induction of chromosome gain or loss during cell division in somatic and germ cells. Aardema *et al.* (1998) reported that the environment does not possess a major influence on aneuploidy induction based on the similarity of aneuploidy incidence levels found at birth in various evaluations of newborns in different geographical localities. Although various compounds have been examined for their potential aneugenic effects on germ cells, information on carcinogenicity is rather limited for aneugens compared to clastogens and gene mutation inducers (Aardema *et al.*, 1998).

Aneuploidy induction may alter the distribution of oncogenes and tumour suppressor genes (Deusberg *et al.*, 2004) where chromosomes containing genes involve in the mitotic process leads to asymmetric segregation of chromosomes, instituting an autocatalytic karyotypic evolution that generates pre-neoplastic and subsequently cancerous cells (Fenech 2002). However, this is currently not a consensus within the scientific community. Some regarded aneuploidy to be immaterial to tumourigenesis (Hahn *et al.*, 1999), whereas others have argued it to be a wholly benign side-effect accompanying transformation (Marx, 2002) and yet another school of thought considered aneuploidy to play a contributing role to tumour progression but not tumour inititation (Zimonjic *et al.*, 2001).

Cancer cells are not polyploid but aneuploid, which means in addition to alterations in the total chromosome number they also harbour various chromosomal abnormalities such as amplifications and deletions. Thus, comparable to Tolstoy's unhappy families, every aneuploid tumour has its own version of aneuploidy, rendering the quest to determine the role of aneuploidy and in identifying common features shared by aneuploid tumour cells, to

be very challenging. This correlation between anueploidy and cancer has been known for decades but the answer as to whether aneuploidy is the contributing factor or just a secondary consequence of transformation still remains an intriguing mystery (Duesberg & Rasnick, 2000; Matzke *et al.*, 2003).

Even though the relative influence of abnormal chromosome numbers and gene mutations in human cancers is still a focal point of intense debate, aneuploidy is regarded to play a role in tumourigenesis (Fenech 2002). The ubiquity of aneuploidy incidence in human cancer cells cannot be disputed and it is the prominent type of chromosome instability observed in solid tumours in general (Lingle *et al.*, 1998). Aneuploidy is reported to be an early event or present at an early stage in human pre-cancerous neoplasias of the throat, oesophagus, lung, skin, gonads, pancreas and acute leukaemia (Duesberg *et al.*, 2004). Aneuploidy has been used as a screening and prognosis marker for several cancers such as for patients with Barrett's oesophagus (Teodori *et al.*, 1998) and individuals with high risk of developing head and neck squamous cell carcinomas (HNSCC) (Barrera *et al.*, 1998; 1999).

Centrosome amplification is almost consistently associated with aneuploidy but is absent in stable diploid cells (Hollander and Fornace, 2002). Numerical centrosome anomaly may be a common cellular response to genotoxic damage or other cellular stress incidents (Sato *et al.*, 2004). The origin of supernumerary centrosomes in response to genotoxic agents such as radiation (Sato *et al.*, 2004) and metals (Holmes *et al.*, 2006) is not known but various possible suspects include temporal disengagement between centrosome duplication and DNA replication cycles combined with the loss of a centrosome-intrinsic mechanism to prevent re-duplication, centrosome fragmentation and failure of cytokinesis associated with polyploidisation. Cells harbouring multiple centrosomes constantly exhibited abnormal nuclear morphology including the presence of micronuclei.

In light of the detrimental consequences caused by aneugenic compounds such as reproductive failure and tumourigenesis, understanding the mechanisms of action as well as routine testing for regulatory purposes is considered to be paramount (Parry *et al.*, 2002) where the development of suitable detection techniques has been a primary drive of research programmes within the European Union (Parry & Sors, 1993; Parry *et al.*, 1996). The *in vitro* micronucleus assay in combination with kinetochore labelling and chromosome specific centromeric/telomeric probes is a recommended method to screen for aneugens by both the

Committee on Mutagenicity of Chemicals in Food, Consumer Products and the Environment (COM) and the European Union Research Group (Parry *et al.*, 2002).

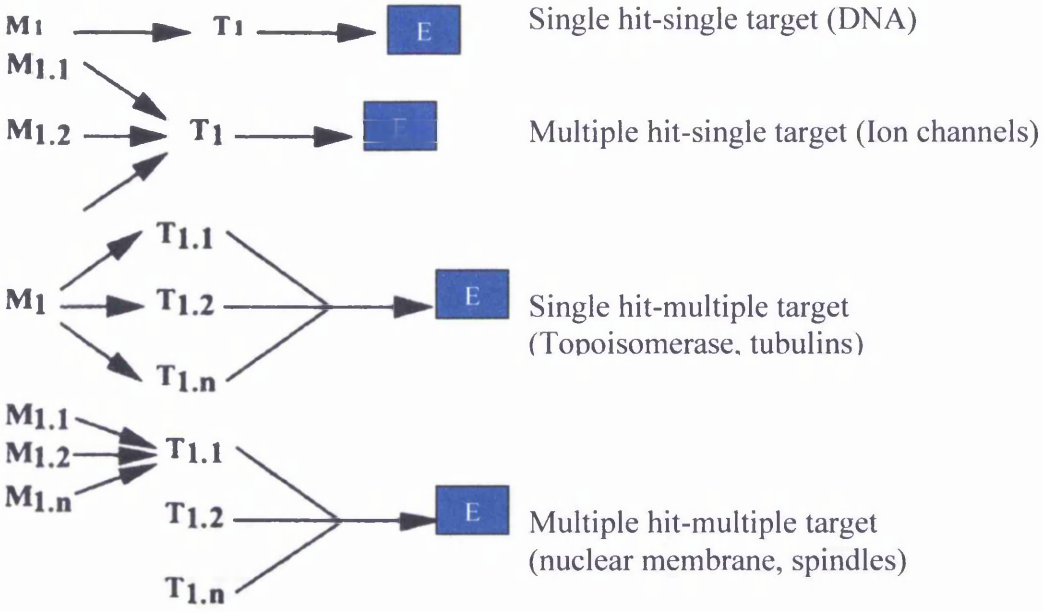

Fig. 1.21. Comparative interactions between mutagen (M), cellular target (T) and the endpoint being measured (E). The identity of possible targets are shown in brackets and different molecules from the same mutagen or different targets are denoted by the numbered subscripts. Diagram adopted from Kirsch-Volders *et al.* (2003).

Indirect mechanisms of genotoxicity is the direct interaction of a genotoxin with non-DNA targets leading to genotoxic effects (Kirsch-Volders *et al.*, 2003). Furthermore, the existence of biologically meaningful threshold dose-response curves for indirect-acting genotoxins such as aneugens is possible since more than one cellular targets need to be overwhelmed before any significant and observable effects are manifested (Parry *et al.*, 1993; Kirsch-Volders *et al.*, 2002). Since the elucidation of possible threshold is beyond the scope of this thesis, it will not be discussed in depth. However, Kirsch-Volders *et al.* (2000; 2003) suggested three important aspects in analysing the basis for the existence of threshold namely the number of targets involved, target identity as well as the sensitivity and type of endpoints measured. As depicted in Figure 1.21, a threshold dose-response curve is considered to be absent from a single hit-single target interaction.

1.19 Testing Strategies for Genotoxicity Detection.

1.19.1 Hazard and Risk Assessments

Since the introduction of the Ames test, various other test systems were developed utilising prokaryotic and eukaryotic cells with each advocated to possess the best ability in detecting carcinogenic agents. Despite this cornucopia of tests, not all of them could singly, reliably differentiate between carcinogenic and non-carcinogenic analogues of similar chemical structure. There was also no or little guidance and consistency in the experiment designs or acceptance criteria. Furthermore, the number and types of studies required for products registration differs widely between regulating agencies worldwide, which in some cases can be viewed as a subtle form of trade barrier rather than scientific requirements.

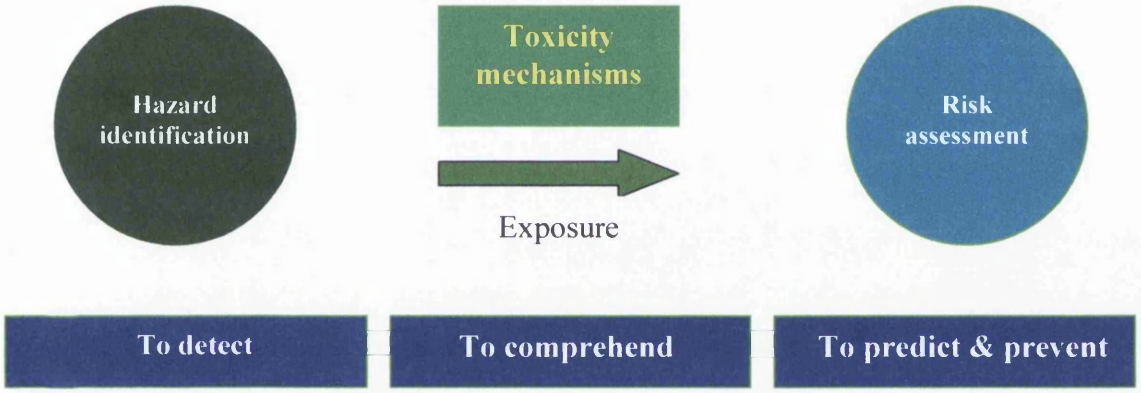

Fig. 1.22. The elucidation of mechanism(s) of toxicity (including genotoxicity) connects hazard detection with risk assessment for human health and permits toxicity prediction and prevention of detrimental exposure.

A plethora of potentially hazardous substances has been detected in the past and the number of new chemicals added to this list is growing steadily. One of the most compelling reasons for improving our detailed comprehension of toxicity mechanisms is that a deeper understanding will allow better data extrapolation and improving risk assessment of potentially genotoxic chemicals for human safety. This does not only apply to pharmacophore in development stage but also chemicals in the work place and in agriculture, pollutants as well as naturally occurring or synthetic hazardous compounds in food or residues in drinking water. The step from the mere detection of a genotoxic hazard (qualitative aspect) to the final assessment of risk in human populations (quantitative aspect) involves a number of assessments, estimations and considerations. For a chemical, it is clearly insufficient to introduce a safety margin based on animal data or cell culture experimentations, instead realistic exposure information has to be taken into account.

Furthermore, information on genotoxicants' mode of actions is useful in calculating more accurately the risk for humans such as exposure to harmful aneugens (Parry *et al.*, 2002; Kirsch-Volders *et al.*, 2003).

As illustrated in Figure 1.22, hazard and risk assessment generally involves three main steps namely hazard identification and characterisation, exposure assessment and risk characterisation. For an agent of interest, firstly the possible hazard such as the compound's inherent properties that may cause adverse health effects upon human exposure are identified. Subsequently, the qualitative and quantitative responses after exposure are determined taking into account the mode of actions as well as type, duration and route of exposure which are normally established through dose-response adverse effects, if there is any. Exposure assessment is the estimation, measurement or prediction of exposure/intake of the agent of interest by the general population, sub-population or individuals in terms of frequency, duration and severity of exposure. Finally, risk characterisation is the integration of information obtained in order to establish a safe level of exposure.

1.19.2 Genotoxicity Testing for Regulatory Purposes

The awareness of this fact prompted the scientific and regulatory communities to pursue the standardisation and harmonisation of protocols and test systems. There are various platforms on which the international experts used to issue guidance such as the International Conference on Harmonisation of Technical Requirements for Registration of Pharmaceuticals for Human Use (ICH) and the International Workshops on Genotoxicity Testing (IWGT) which look into test methods resulting in OECD (Organisation for Economic Co-Operation and Development) guidelines and testing strategies. There are also advisory panels on national level such as the Committee on Mutagenicity of Chemicals in Food, Consumer Products and the Environment (COM) for the UK. Furthermore, Good Laboratory Practice regulations (GLPs) have always been a requirement to guarantee the integrity of non-clinical studies conducted to support regulatory submissions.

Changes or damage to the DNA can be manifested in various forms such as gene mutations or chromosomal aberrations. No single test system is capable of detecting all these changes, thus the concept of using a battery of different tests was conceived.

Testing strategies for mutation detection should include all three levels of mutation with the aim to assess the possibility of gene mutations, aneugens and clastogens. Since the initiation of genotoxicity testing, there has been a steady and continuous development of a wide variety of test systems employing bacterial, yeast and mammalian cell cultures. Most of the test systems have specific endpoints. The Committee on Mutagenicity of Chemicals in Food, Consumer Products and the Environment (COM) is an expert advisory committee responsible in providing advice to the Department of Health and other departments and agencies within Her Majesty's government that possess regulatory roles. The Committee recommends a three-stage testing approach for mutagenic potential. Stage 1 is a battery of *in vitro* screening for potential mutagen involving three test systems. Stage 2 involves *in vivo* tests in somatic cells and the third stage is activity assessment in germ cells (COM, 2000). The COM guidelines (COM, 2000) will be discussed in this thesis unless otherwise stated.

1.19.2.1 *In Vitro* Assays in Somatic Cells in Stage 1

As outlined previously, Stage 1 is the initial screening based on *in vitro* tests and for most chemicals, three tests are recommended where detection for both aneugenicity and clatogenicity is possible at this point (COM, 2000). These three tests are bacterial test for gene mutation, *in vitro* metaphase analysis or *in vitro* micronucleus test and mammalian cell mutation assay. Negative results from these three tests or just two, where small or no human exposure is expected such as industrial intermediates, would provide sufficient data for the assessment of most chemicals. A clearly positive outcome from any of these tests or in cases where equivocal results that cannot be resolved by further *in vitro* tests, warrants *in vivo* assessment in Stage 2. Figure 1.23 shows a flow chart for stage 1 testing procedures.

1.19.2.2 *In Vivo* Assays in Somatic Cells in Stage 2

Stage 2 is a continuation of mutagenicity assessment to elucidate the potential of genotoxic activity seen in Stage 1 to be manifested in somatic cells *in vivo.* A malleable strategy is required for *in vivo* tests taking into consideration the nature of the chemical being investigated, its metabolism information and data obtained in Stage 1. The most suitable test is bone marrow micronucleus assay to measure aneugenicity and clastogenicity unless there is a contradiction to the initial considerations. If the results are negative, further tests

involving other tissue(s) are required to provide clear assurance for the absence of *in vivo* activity for all compounds that was shown to be positive in earlier *in vitro* studies.

Second *in vivo* test(s) that may be appropriate includes the liver UDS (Unscheduled DNA synthesis) assay, comet assay, ^{32}P-postlabelling assay, covalent DNA binding and assays using transgenic animals. The choice of assay in any circumstances should be justified and considered on a case-by-case basis taking into account the available information including data from previous tests. Figure 1.24 shows a flow chart for stage 2 testing procedures.

1.19.2.3 Testing in Germ Cells in Stage 3.

Stage 3 is mutagen assessment in germ cells and requirements for such studies needs careful consideration. Generally, chemicals that have been classified as *in vivo* somatic cell mutagens will be considered to be both potential genotoxic carcinogens and germ cell mutagens, therefore does not warrant further genotoxic testing. However, in some cases germ cell studies may be undertaken to prove otherwise. A number of assays such as micronuclei induction in spermatocytes and the dominant lethal assay, both for clastogenicity and aneugenicity detection, can be used to determine whether the compound of interest is genotoxic in germ cells. Information on DNA lesions induction can be obtained via various Stage I methods discussed previously. Results on mutation types observed in earlier tests will be crucial when considering the most suitable assay in a particular case and none of the assays mentioned is capable of providing definitive data as to the possibility that the mutations are heritable in future generations. The only methods that allow estimates of such risks to be calculated are the mouse specific locus test and the mouse heritable translocation test. However, this route of action is not practical taking into account the very large number of animals required and should only be considered in exceptional circumstances. At the moment there are no routine tests available for elucidating the induction of aneuploidy in progeny of treated animals. Figure 1.25 shows a flow chart for Stage 3 germ cell testing procedure.

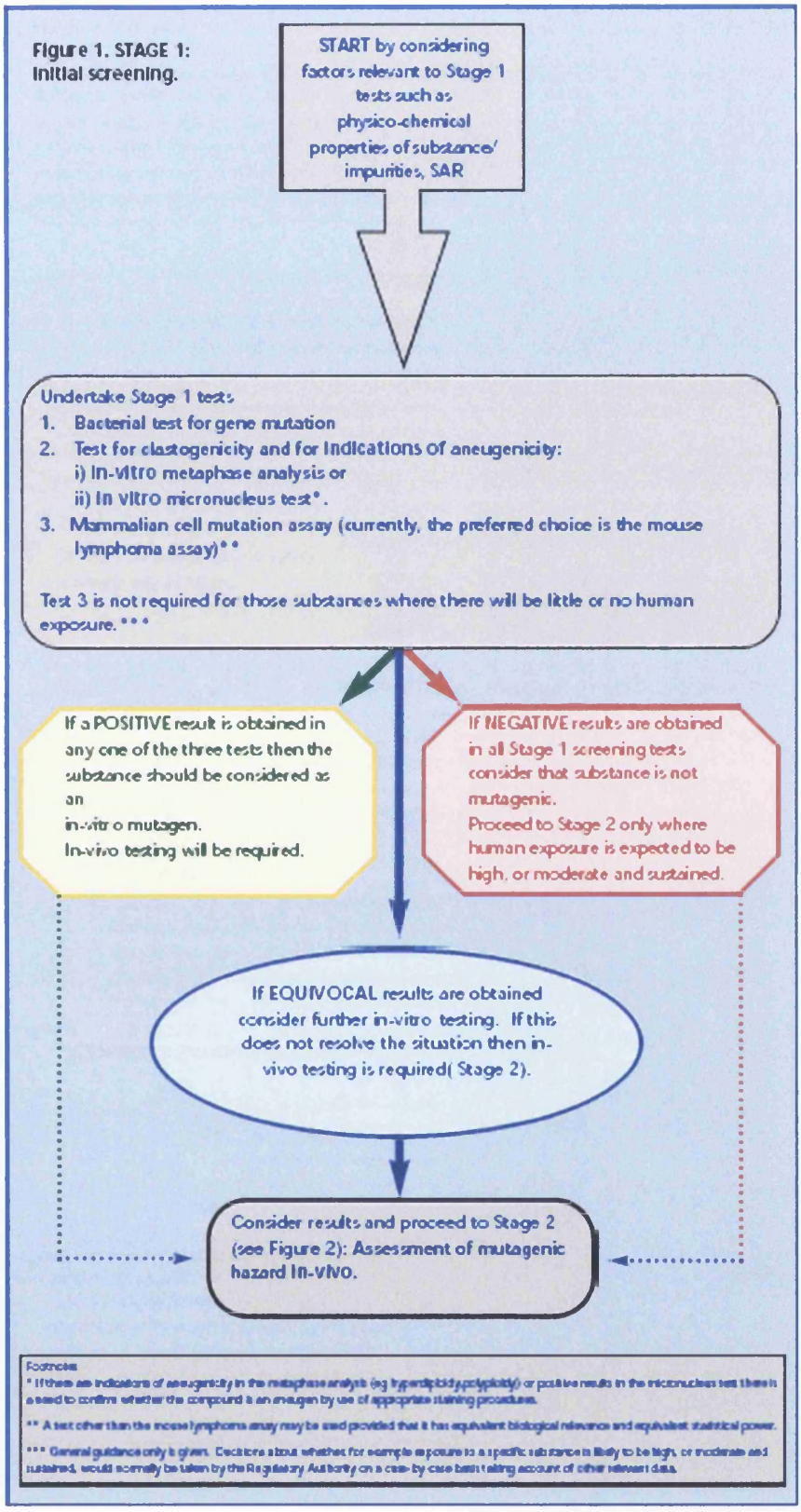

Fig. 1.23. Stage 1 initial screening procedure. Adapted from Guidance on Strategy for Testing of Chemicals for Mutagenicity (COM, 2000).

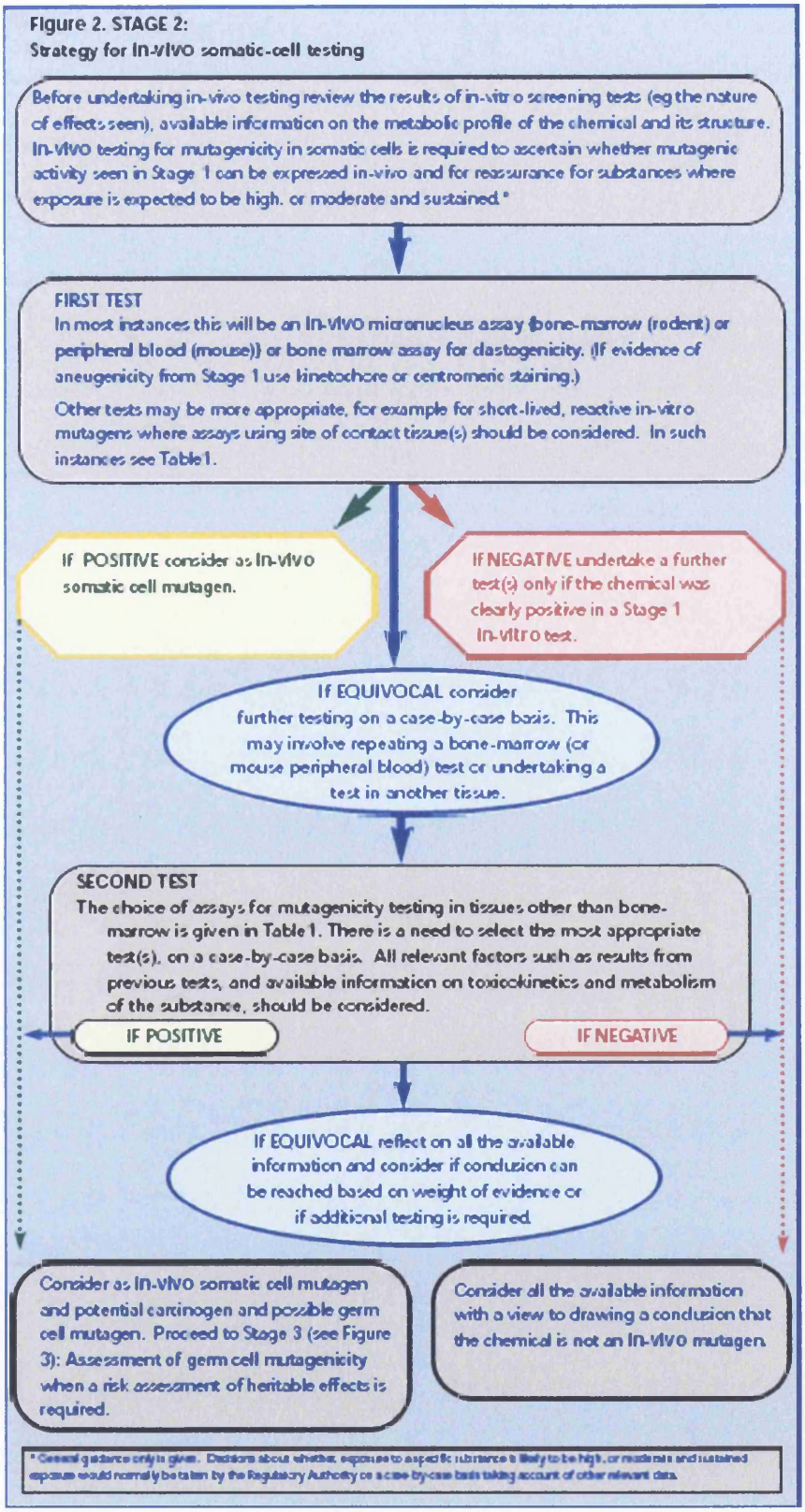

Fig. 1.24. Flow chart for Stage 2 *in vivo* screening procedure. Adapted from Guidance on Strategy for Testing of Chemicals for Mutagenicity (COM, 2000).

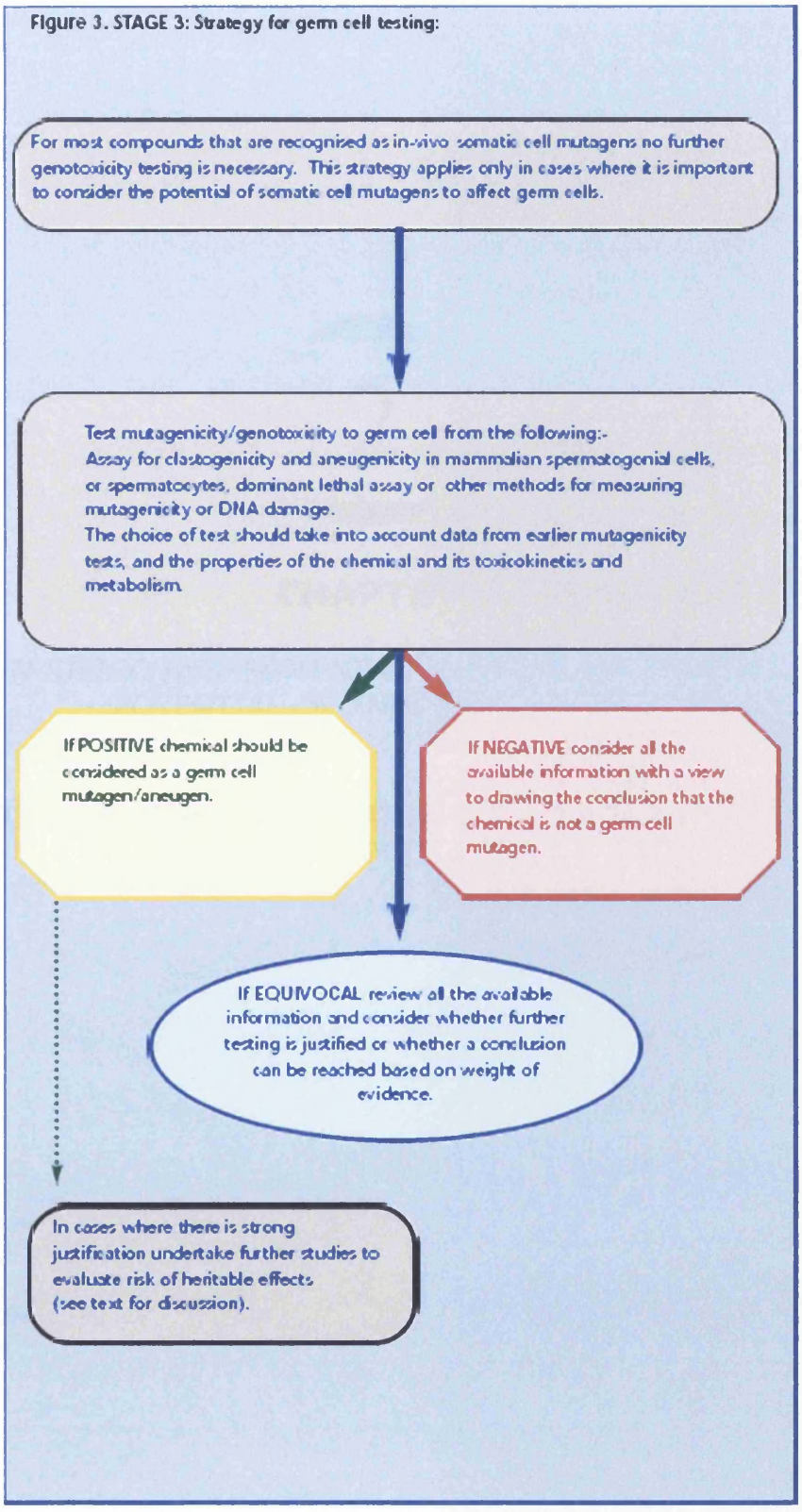

Fig. 1.25. Flow chart for Stage 3 germ cell testing procedure. Adapted from Guidance on Strategy for Testing of Chemicals for Mutagenicity (COM, 2000).

CHAPTER 2

PART 1. *IN SILICO* ASSESSMENT OF GENOTOXICITY AND TOXICITY POTENTIAL OF ANDROGRAPHOLIDE

PART 2. *IN SILICO* PREDICTION OF ANDROGRAPHOLIDE BIOTRANSFORMATION ROUTES

CHAPTER 2

PART 1: *IN SILICO* ASSESSMENT OF GENOTOXICITY AND TOXICITY POTENTIAL OF ANDROGRAPHOLIDE

2.1 General Introduction

There is a general understanding that an in-depth comprehension of all toxicities associated with a new chemical is important to its successful development and marketability. Thus, toxicology in general faces the immensely challenging tasks of conducting safety evaluations in supporting the development of new chemicals prior to human exposures and determining the potential hazard posed by agents whose safety assessments were insufficient.

Currently, genotoxicity is examined through the application of a battery of experimental *in vitro* and *in vivo* test systems that are not always uniformly concordant but applied in a weight-of-evidence approach. However, these tests can be overwhelmed in light of the accelerating pace of chemical discovery and development as well as the economic feasibility of such endeavours, have highlighted the need for efficient prioritisation and toxicity screening approaches in the 'fail-early, fail-safe' context. There is also a requirement to elucidate the genotoxic potential of metabolites, impurities, degradants and in the occupational health aspect, process intermediates. Since exposure to genotoxic chemicals bears the risk of inducing somatic mutations including those leading to cancer as well as germ-line mutations with the possibility of inherited disorders, evaluating genotoxic potential is regarded to be an essential step in the safety assessment of chemicals.

2.2 Chemical Reactivity and Possible Mechanisms of Action

There is quite a large overlap between genotoxicity and carcinogenicity since the initiating step of the carcinogenic process often involves one or more genotoxic insults. A unifying concept has been that genotoxicants and carcinogens act by attacking the DNA, based on their electrophilicity *per se* or after metabolic transformation. Thus, genotoxicity should be

easier to anticipate than other form of toxicities, such as organ-specific toxicities that can be induced by various chemical or pharmacological mechanisms not directly or necessarily related to chemical structure analysis. However, there are indirectly-acting genotoxicants such as aneugens while epigenetic carcinogens do not act through genotoxic mechanisms and the progress in the identification of structural alerts responsible for epigenetic damage has been much slower (Woo, 2003). It is not surprising that chemical genotoxicity has been the focus of various attempts to develop predictive models and among the theoretical models available, the application of structure-activity relationships concepts has emerged to be promising. This concept and with supporting experimental data, has paved the way to several chemical functional groups and substructures identification, which are referred to as structural alerts.

These are capable of causing both mutation and cancer and includes acylating intermediates, aldehydes, carbonium ions (alkyl-, aryl-, benzylic-), epoxides, free radicals, nitrenium ions, oxonium ions, polarized double bonds (α,β-unsaturated carbonyls or carboxylates) and peroxides (Ashby, 1995; Woo et al, 2002). The structural alerts characterisation has been a very important scientific progression because it permitted the possibility of designing safer compounds by avoiding the known structural alerts. In addition, the structural alerts for genotoxicity and carcinogenicity have been incorporated into expert systems for predicting toxicological effects of chemicals (*e.g.* DEREK, MCASE).

2.3 Computer-assisted Structure Activity Relationships (CSAR)

Structure activity relationships (SAR) examine the correlation between the chemical structure of a compound and its biological or pharmacological activity. Compounds are often grouped together because they possess common structural characteristics including topology, stereochemistry, size, arrangement and distribution of functional groups. Other factors contributing to structure-activity relationship include electronic effects, resonance, chemical reactivity and inductive effects. Quantitative structure-activity relationships (QSAR) is a refined attempt to correlate structural or property descriptors of compounds with activities using mathematics and more recently, by computational methods.

MCASE, DEREK and TOPKAT are examples of computer-assisted structure activity relationship (CSAR) systems that are widely used in predicting genotoxicity and carcinogenicity by studying quantitative structure-activity relationships (QSARs). MCASE (www.multicase.com) stands for Multiple Computer Automated Structure Evaluation and it dissociates each input molecule into 2-10 atom fragment (biophore) and statistically examines the strength of the fragments from its database with an associated mutagenicity value that is based on observed mutagenic potency. The database contains information on 3000 compounds and includes *Drosophila* mutation data. Another program, named TOPKAT (Toxicity Prediction by Komputer Assisted Technology) was originally designed by Health Systems Inc. and is now marketed by Accelrys (www.accelrys.com/products/topkat/index.html) is based solely on bacterial mutagenicity data. It applies 'electro-topological' descriptors rather than chemical structures to predict mutagenic reactivity with DNA. The program cannot be customised by the user.

There are also other computer programs that is based on QSAR but built for different purposes. METEOR for example was designed to harness QSAR and expert knowledge in elucidating possible metabolic outcomes of a compound of interest *in silico*.

2.4 Introduction to DEREK

DEREK (Deductive Estimation of Risk from Expert Knowledge) is an expert- knowledge base system that was originally created by Schering Agrochemical Company and was subsequently donated to an independent not-for-profit organisation, Lhasa Limited, UK. Effectively, toxicologists from other organisations are now able to use DEREK and continuously contributing to toxicological data in improving the qualitative structure-activity relationships (QSARs) and expert knowledge rules in the program.

The main difference of an expert knowledge base system such as DEREK and a database is that DEREK is a software that utilises toxicological expert knowledge rules in predicting the toxicity of chemicals, usually in the absence of known toxicological data. Whereas a database is merely a large set of structured data and database management system is a computer software programmed to manage a database. VITIC (Lhasa Ltd.) is an example of a data management system.

DEREK makes semi-quantitative predictions as to whether or not a DNA-reactive moiety is present on the chemical structure of interest and performs a series of key functions based on a substance's chemical structure:

- Acts as a high-throughput screen for genotoxic and mutagenic activities.
- Predicts whether a chemical will be carcinogenic.
- Predicts whether a chemical will be skin sensitiser.
- Highlights potential toxicological hazards covering a spectrum of endpoints from irritancy to hepatotoxicity.

DEREK's learning set was constructed based on bacterial mutagenicity (Ames test) and other available genotoxicity data. Query outputs define the structural alert recognised and the type of genotoxicity attributed to the alert.

How DEREK works.

- Molecular chemical structures are entered into DEREK for Windows by either importing MDL Molfiles or SDF files, or via a chemical editor program such as ISIS/Draw. All the parameters such as species and endpoints were selected. Figures 2.1 and 2.2 shows an example of this step. MDL Molfile is a file format created by Elsevier Molecular Design Limited (MDL) containing information about the atoms, chemical bonds, connectivity and coordinates of a molecule. SDF (structure-data file) file is another file format for holding chemical information especially data on chemical structure.
- Then DEREK will utilise QSARs information and other expert knowledge rules to develop reasonable prediction about the potential toxicity of the chemical in question. Example of this step is shown in Figure 2.3.
- The program also provides supporting evidence for its conclusion that includes literature references, toxicity data and comments. Toxicological data from structurally similar molecules can also be viewed as shown in the example in Figure 2.4.

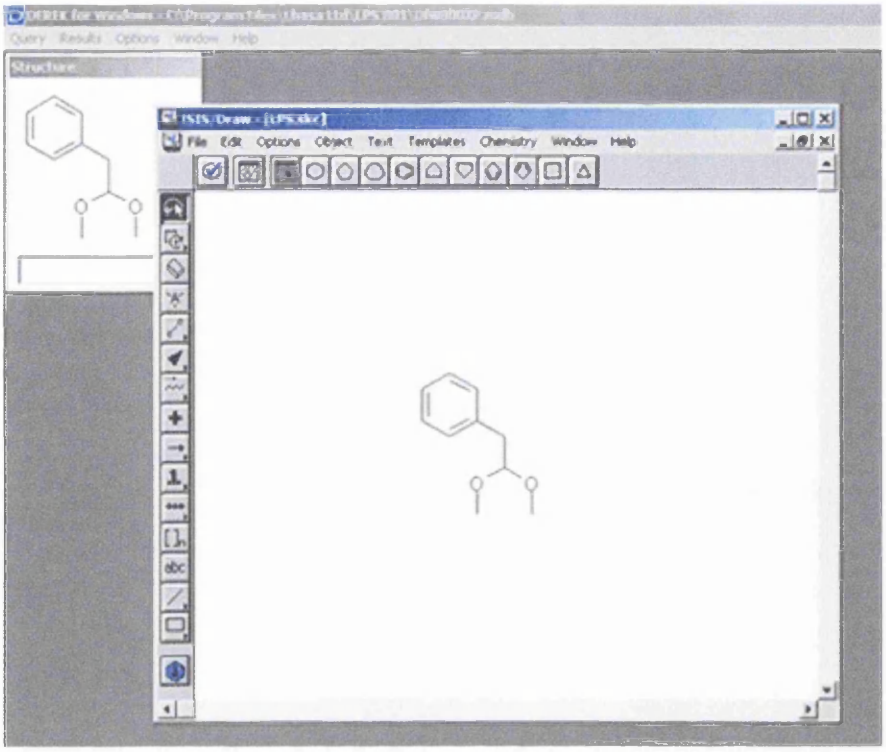

Fig. 2.1. Inserting a chemical structure using ISIS/Draw.

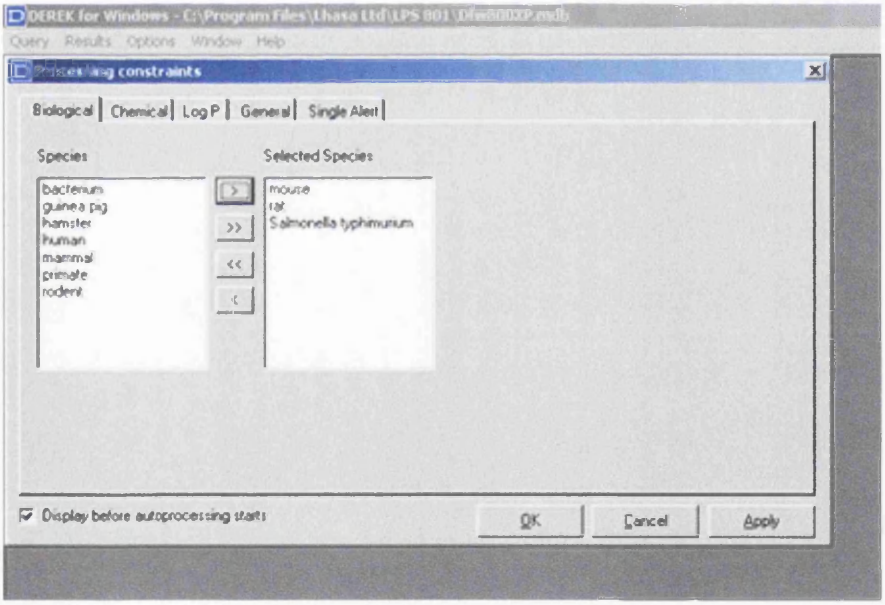

Fig. 2.2. Setting parameters to the query process.

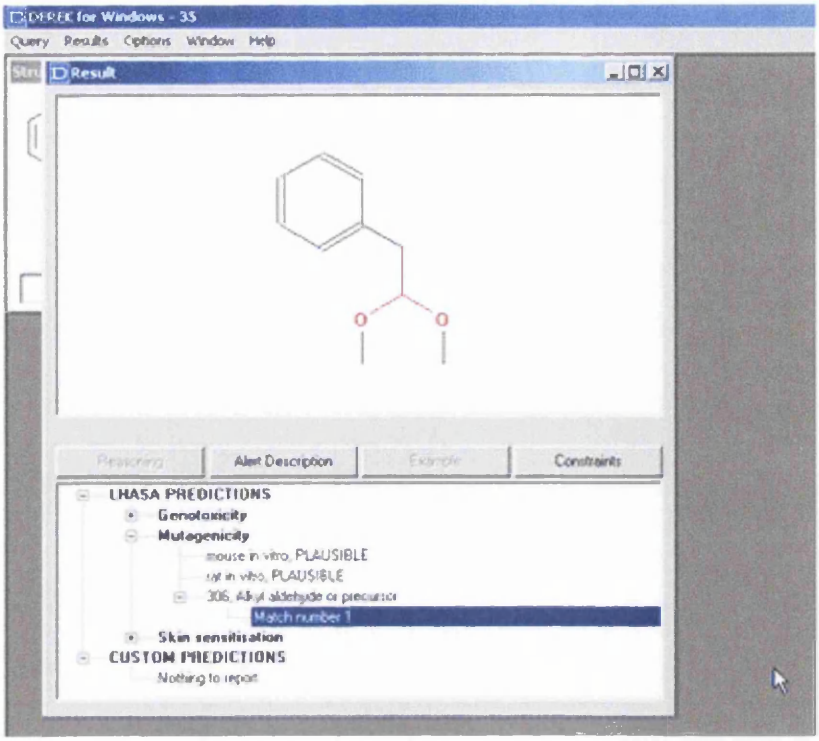

Fig. 2.3. Predictions made by DEREK.

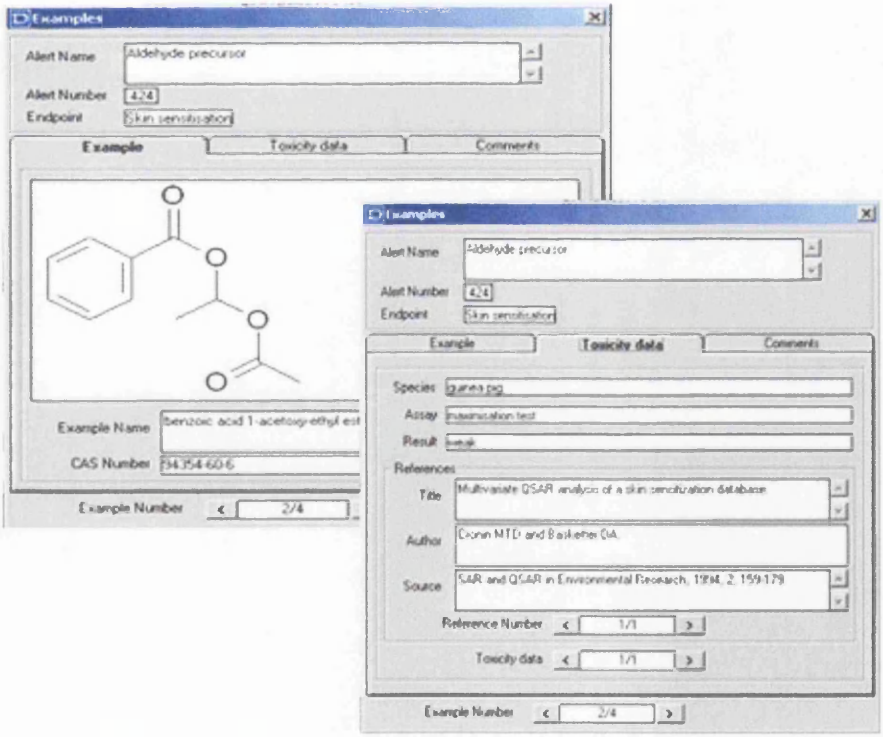

Fig. 2.4. User can compare and contrast the chemical in query with structurally similar compound.

2.5 METHODS

DEREK version 8.0.1 ISIS/Draw was used to draw the chemical structure of andrographolide. The main parameters to the query were set as listed below:

1. Testing against all alerts.
2. Species: bacteria and mammals.
3. Super-Endpoints:
    - Carcinogenicity
    - Genotoxicity
    - Irritation
    - Respiratory sensitisation
    - Skin sensitisation
    - Thyroid toxicity
    - Miscellaneous endpoints
4. Consider tautomers as true.
5. Hydrogen options: perceive implicit and explicit hydrogens.

Full report created by DEREK can be found in the Appendix section. The probability was set to be 'plausible' and above only. Anything less than 'plausible' will not be registered by the program.

2.6 RESULTS

The molecular weight of andrographolide calculated by DEREK is 350.455, a 100% match to the figure supplied by Sigma-Aldrich. Figure 2.5 shows the chemical structure of andrographolide drew using ISIS/Draw. The program made several predictions based on the molecular structure of andrographolide as described below.

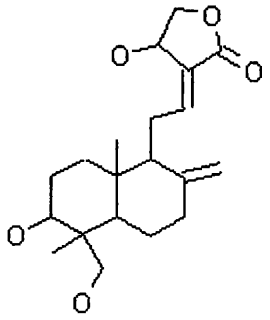

Fig 2.5. Chemical structure of andrographolide.

The ability of andrographolide to induce peroxisome proliferation and α-2-μ globulin nephropathy in mammals is doubted. However, it is plausible for the compound to induce such effect in rat, mouse and other rodents. Figure 2.6 shows all possible locations that can cause peroxisome proliferation and α-2-μ globulin nephropathy in rodents.

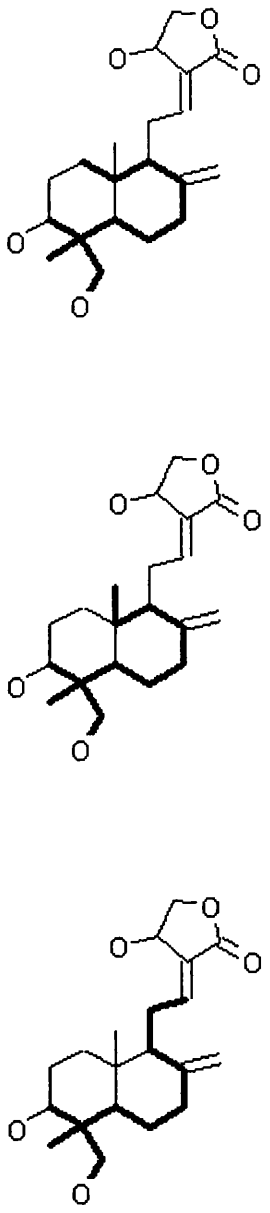

Fig. 2.6. Shows three possible locations where andrographolide may induce nephropathy and peroxisome proliferation in rodents.

Skin sensitisation in mammal is predicted to be plausible. The location of α, β-unsaturated ester (or precursor) within the compound, as shown in Figure 2.7, may cause this effect.

The same location of α, β-unsaturated ester or thioester within the compound can also cause chromosome damage in mammals *in vitro*.

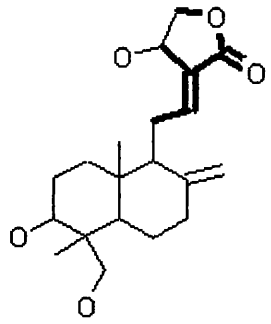

Fig. 2.7. The position within the compound that can cause skin sensitisation and chromosome damage *in vitro* in mammals.

2.7 DISCUSSION

DEREK was utilised to assess the potential mutagenicity, carcinogenicity and toxicity of andrographolide. This computer software utilises toxicological expert knowledge rules in predicting the toxicity of chemicals by identifying the structural alerts that may contribute to its activity. Andrographolide was predicted to be able to cause peroxisome proliferation and nephrotoxicity in rats, mouse and other rodents whereas the α-alkylidene γ-butyrolactone moiety, detected as α, β-unsaturated ester or thioester by DEREK was considered to be able to cause chromosome damage in mammals *in vitro*. Indeed, Nanduri *et al.* (2004) reported that four positions in the andrographolide chemical structure are responsible for its *in vitro* cytotoxic activity. As shown in Figure 2.8, these positions are (1) the intact α-alkylidene γ-butyrolactone moiety, (2) the C-14 hydroxyl or its ester moiety, (3) the $\Delta^{12(13)}$ double bond and (4) the $\Delta^{8(17)}$ double bond or epoxy moiety.

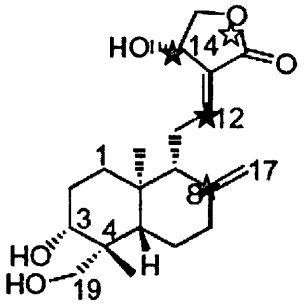

Fig 2.8. The chemical structure of andrographolide with the positions responsible for its cytotoxic activity. Modification was made by the author to the original picture adopted from Nanduri *et al.* (2004) with coloured stars denoting these positions respectively. (Yellow) the intact α-alkylidene γ-butyrolactone moiety, (Red) the C-14 hydroxyl or its ester moiety, (Blue) the $\Delta^{12(13)}$ double bond and (Green) the $\Delta^{8(17)}$ double bond or epoxy moiety.

Whereas the structural alerts define the potential for the chemicals to be carcinogenic or mutagenic, the actual modulation of this potential depends on a series of factors such as molecular weight, chemical reactivity, solubility and possible metabolism which can differ within each individual class of compounds. In fact, chemicals sharing the same structural alert such as aromatic amine for example, can behave in different ways because some are active, to a different degree and some are inactive. Such modulating factors can be estimated by minor, context-dependent structural alerts for example, the alteration in the positions of the skeleton of a chemical with a primary structural alert. However, the qualitative approach based on the recognition of structural alerts is rather limited due to the inability to predict the activity of sub-structures which are not in the list of known structural alerts or those that possess a combination of alerts.

A powerful generalization is provided by the quantitative structure-activity relationship (QSAR) analysis, which is based on a limited number of physical chemical properties with general relevance, and produces a mathematical model for the chemical determinants of the biological activity. The physico-chemical properties of interest for the biological activity of the chemicals are hydrophobic, electronic and stearic effects (Franke & Gruska, 2003). QSARs have been generated for a number of individual chemical classes including aromatic amines, polycyclic aromatic hydrocarbons and lactones (Benigni, 2005). The majority are relative to *in vitro* mutagenicity. However, a number of QSAR models for the animal carcinogenicity exist as well. A great aspect of the QSARs for the individual chemical classes, as performed according to the classical Hansch approach and point to the physico-chemical determinants of the biological activity of the compounds. Therefore, they

have appreciably contributed to the comprehension of the mechanisms of chemical mutagenicity and carcinogenicity. The other important goal of the use of QSAR analyses is the risk assessment of chemicals. Once formulated, the QSARs can be employed for estimating the activity of other chemicals not tested experimentally or those lacking existing experimental data such as andrographolide.

Natural compounds in general are more structurally diverse with greater complexity than synthetic pharmaceuticals and have been shown to be an important source of potential pharmacophores (Rowinsky & Donehower, 1995) and others were found to alter biological function through interaction with cellular macromolecules and affecting xenobiotic metabolism enzymes expression (Chouduri & Valerio, 2005). The fact that natural compounds especially phytochemicals, have a wide spectrum of chemical functional groups where some are known to be structural alerts for toxicologically-based chronic effects such as the induction of carcinogenesis, highlights the need to assess their potential toxicity. However, the predicament is that few phytochemicals have been evaluated for systemic toxicological effects and even less have been subjected to long-term cancer bioassay *in vivo*. In light of the potential human exposure to the high number of synthetic and natural compounds currently in discovery, development or commercialisation phases, there is a practical desideratum for the development and validation for an efficiently reliable and sensitive methods for screening thousands of untested chemicals for toxicity especially crucial endpoints such as genotoxicity. Assessment performed using DEREK supports previous findings on cytotoxicity (Siripong *et al.*, 1992; Nanduri *et al.* 2004; Jada *et al.*, 2007) but as highlighted previously, reliable experimental data on possible induction of genetic damage is absent.

The current accomplishment of CSAR has been moderate but developing steadily, concomitant with their growing importance in compound selection and study duration (Johnson & Rodgers, 2006). These expert-knowledge based systems are not free from limitations such as inability to predict non-positive structures, does not distinguish between target organs for carcinogenicity, inability to predict potential antagonism or synergism of substructures and variability in key data quality (Johnson & Rodgers, 2006). Such systems is also incapable of accounting for mechanistic considerations such as sex- or species specificity and it cannot provide an estimation of dose or time of exposure (acute or chronic) essential for carcinogenesis.

Overall, it can be concluded that predictions for the individual chemicals cannot be taken at face value and cannot replace laboratory experiments, when necessary. Their main role is to complement the information of different nature and from different sources. At the same time, the structure-activity-based methods can have a great role for example in prioritising large numbers of chemicals to be studied or in designing better experiments. In the second part of this Chapter, the metabolism of andrographolide is predicted using METEOR, which is another expert-knowledge rules program and its ability to elicit genomic instability will be examined experimentally by employing genotoxicity tests such as the *in vitro* micronucleus assay and the *HPRT* point mutation assay.

CHAPTER 2

PART 2: *IN SILICO* PREDICTION OF ANDROGRAPHOLIDE BIOTRANSFORMATION

2.8 Biotransformation of Xenobiotics

Biotransformation is the metabolic conversion of endogenous and xenobiotic compounds to more water-soluble derivatives. Generally, the physical properties of a xenobiotic are altered from lipophilicity to hydrophilicity, thereby reducing its absorbability by tissues and favouring its excretion. An exception to this rule is the elimination of volatile compounds by exhalation.

Chemical modification of a xenobiotic via biotransformation may also change its biological effects. Some drugs undergo biotransformation to active metabolites that exert their pharmacodynamic or toxic effect. However, in most instances, biotransformation terminates the pharmacologic effects of a drug and reduces the toxicity of xenobiotics. Enzymes involved in catalysing biotransformation reactions often determine the pharmacokinetics and pharmacodynamics of drugs as well as playing a crucial role in chemical toxicity and chemical tumourigenesis. There are two main phases in xenobiotics biotransformation. Phase I mainly involves functionalisation, which is the introduction or exposure of functional groups on the chemical structure of a compound. This process provides a chemical 'handle' for conjugating agents in Phase II to react with. However, rendering a xenobiotic more chemically reactive to facilitate their excretion also increases the risk of possible interactions with cellular macromolecules such as DNA, ultimately highlighting the existence of a fine balance between producing conjugation reactions and more reactive metabolites. The functional groups can be either nucleophilic such as carboxyl groups or electrophilic in characteristic like the epoxides and these can be injurious to biological systems. Nucleophiles can interact with biological receptors while electrophiles have the potential to covalently react with electron-rich macromolecules such as RNA, DNA and proteins.

There are two groups of enzymes in Phase I, hydrolases and oxidoreductases. Hydrolases are hydrolytic enzymes whose substrates include amides, epoxides, esters and glucuronides. Oxidoreductases introduce an oxygen atom into or expel electrons from their substrates and

cytochrome P450 is the major oxidoreductase enzyme system. Other systems include monoamine oxidases (MAO), flavin-containing monooxygenases (FMO) and cyclooxygenases (COX). These hydrolysis, reduction and oxidation reactions lead to the introduction or exposure of a functional group (-OH, $-NH_2$, -SH or –COOH) which usually cause only a small increase in hydrophilicity.

The second phase of biotransformation involves conjugation, where functional groups from cofactors are utilised by transferases to react with those present or annexed from Phase I on the compound. The resultant conjugates possess increased excretory potential. Although most conjugations result in pharmacological detoxification or inactivation, some may end in bioactivation. Most of the Phase II enzymes are located in the cytosol except UDP-glucuronosyltransferases (UGT) that are microsomal. The consequence of most phase II biotransformation reactions is a large increment in xenobiotic hydrophilicity, thus greatly promote the excretion of xenobiotic compounds. Figure 2.9 summarises the biotransformation process and its main actors.

Phase II reactions are usually faster than Phase I, thus Phase I is the rate-limiting step for biotransformation. Phase II metabolism can deal with all products from Phase I with the exception of glutathione, which requires a chemically reactive conjugating species. The availability of the cofactors during synthesis may have a limiting influence in some Phase II pathways as it affects the formation of sufficient conjugating species necessary for reaction on a substrate or its metabolites. Due to their reactivity, bio-accumulation of these substrates and its metabolites may be harmful.

Various compounds are also capable of causing enzyme induction where they accelerate their own biotransformation and excretion. The opposite effect would be the inhibition of the process. Other factors that change enzyme levels include age, sex and genetic polymorphism. Interspecies differences in biotransformation ability also present a challenge in interpreting animal results to humans.

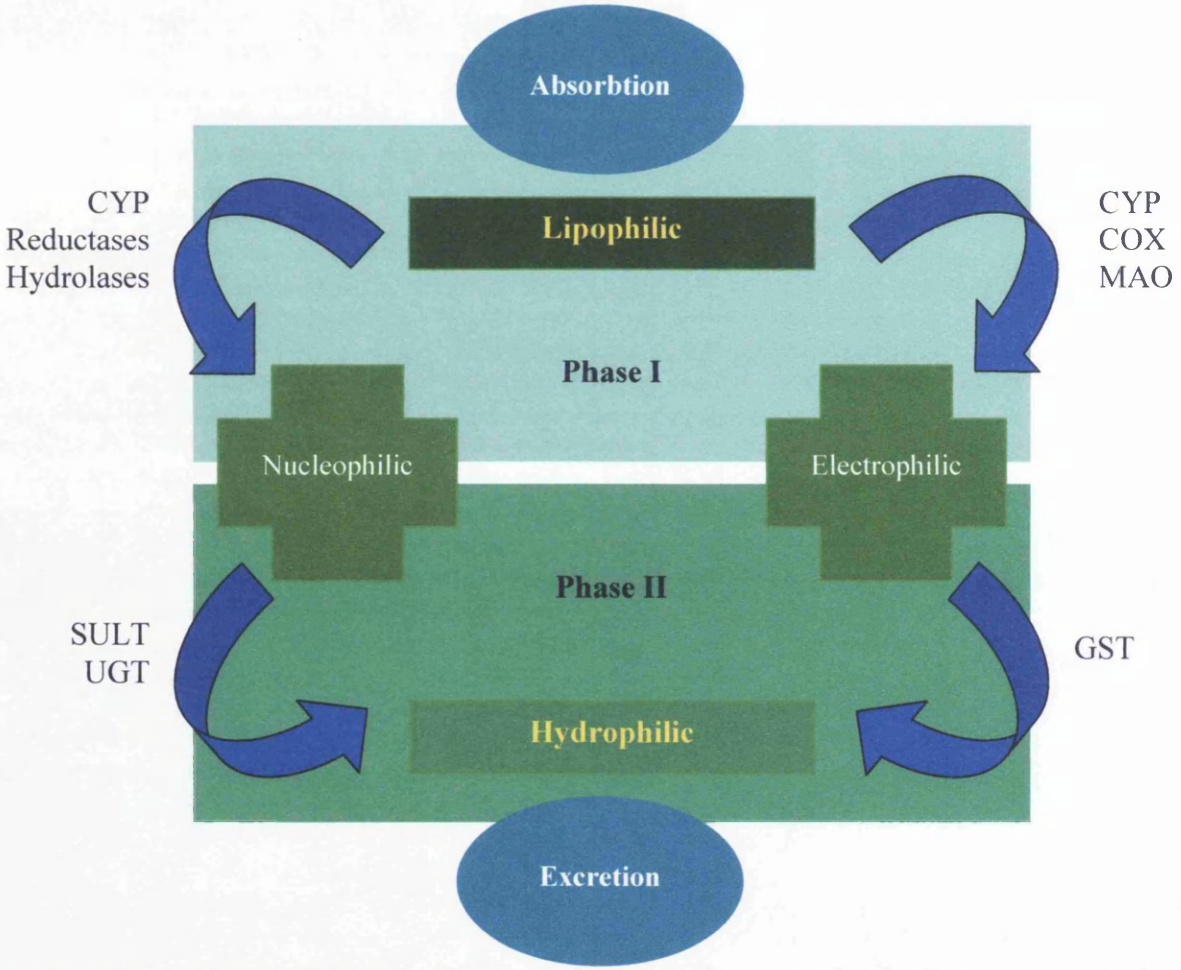

Fig. 2.9. A simplified diagram showing the main actors in Phase I and II biotransformation. The enzymes involved are shown next to the arrows. Examples of nucleophilic species includes carboxylic groups, sulfhyhydryl groups, amino, alcoholic or phenolic hydroxyl groups. Epoxides and unsaturated carbonyl groups are examples of electrophilic species. Abbreviations: CYP:cytochrome P450; COX: cyclooxygenases; MAO: monoamine oxidases; UGT: UDP-glucuronosyltransferases; SULT: sulfotransferases; GST: glutathione S-transferases.

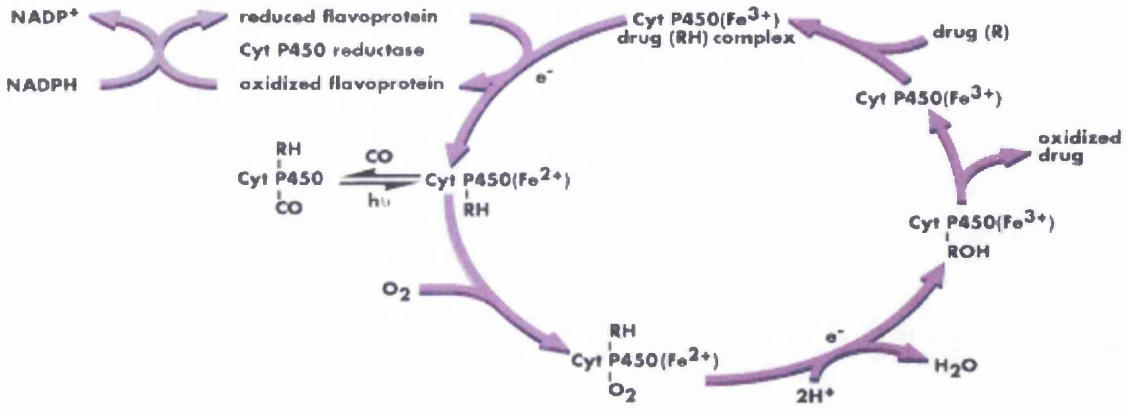

Fig. 2.10. Catalytic cycle of cytochrome P450. Cytochrome P450 and NADPH-cytochrome P450 reductase are located in the phospholipid bilayer of the endoplasmic reticulum. The first part of the cycle involves the activation of oxygen and the final part involves substrate oxidation that entails the abstraction of an electron or a hydrogen atom from the substrate followed by oxygen rebound. (Pratt and Taylor, 1990).

Cytochrome P450 enzymes are ubiquitous in nature. About one quarter of the 57 P450s are typically regarded to be primarily involved in the metabolism of xenobiotics (Guengerich *et al.*, 2005). Unlike P450s that are involved in sterol metabolism which are crucial in normal physiology (Nebert & Russell, 2002), the levels of P450 isoforms involved in xenobiotic metabolism can vary and some individuals may be completely devoid of certain P450 enzymes due to genetics. Figure 2.10 shows the catalytic cycle of cytochrome P450.

The human cytochrome P450 (CYP) superfamily consists of 57 genes (Nelson, 2003) contributing to the metabolism of a variety of xenobiotics including carcinogens and therapeutic drugs. Although the enzymes is crucial in detoxification to facilitate excretion from the body, in some instances xenobiotics are converted to metabolites with greater mutagenicity or cytotoxicity potential and a number of human CYPs including CYP1A1, 1A2, 1B1, 2A6, 2B6 and 3A4 are known to be involved in metabolic activation of pro-carcinogens (Guengerich, 2001).

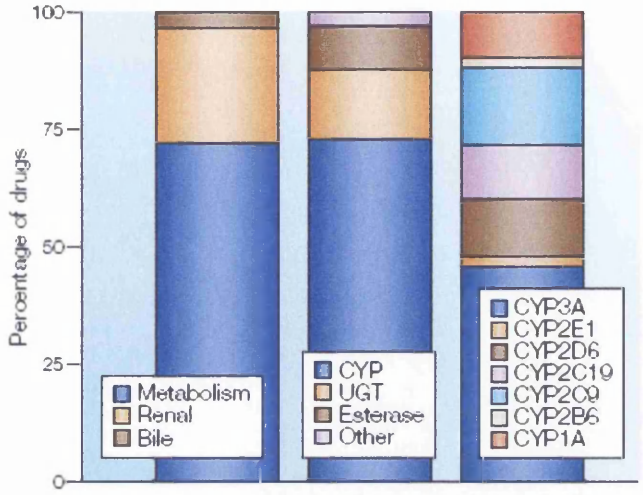

Fig.2.11. Contribution of individual enzyme systems to xenobiotic metabolism. The first bar on the left showed the fate of drugs upon administration, the second bar showed the proportion of enzymes involved in metabolism and the last bar on the right highlights the relative contribution of as cytochrome P450 isoforms. CYP refers to cytochrome P450 and UGT stands for uridine dinucleotide phosphate glucuronosyl transferase (Wienkers & Heath, 2005).

Cytochrome P450 enzymes are probably responsible for more bioactivation processes than other enzymes because several of the reaction products such as epoxides possesses reaction chemistry due to their innate instability and P450s collectively have wider substrate spectrum than any other enzymes, at least on drugs (Guengerich, 2003) as shown in Figure 2.11

In some cases, the same P450 enzyme catalyses both activation and detoxification reactions. For example, CYP3A4 activates aflatoxin B_1 to the tumorigenic and hepatotoxic 8,9-epoxide but it also detoxifies the same compound to aflatoxin Q_1 by 3-hydroxylation (Williams & Aruoma. 2000). This shows that complex factors determine the balance between xenobiotic activation and detoxification.

2.8.1 Induction of Cytochrome P450

Inducers of cytochrome P450 increase the rate of xenobiotic transformation, lowering blood levels and compromising the therapeutic goal of drug therapy but does not cause an exaggerated response to the drug. Thus such reaction can lead to pharmacokinetic tolerance by which larger drug doses must be administered to achieve therapeutic blood levels because of increased drug biotransformation. Induction of cytochrome P450 may increase

the activation of pro-carcinogens to DNA reactive metabolites resulting in increased tumour formation. There is little evidence from either animal experiments or human epidemiologic studies that P450 induction amplify the incidence or multiplicity of tumours caused by known chemical carcinogens. Most available evidence points to a protective role of enzyme induction against chemical-induced damage.

2.8.2 Inhibition of Cytochrome P450

Inhibitory drug interactions generally fall into three categories. The first involves competition between two drugs that are metabolised by the same P450 enzyme. The second is also competitive in nature but the inhibitor is not a substrate for the affected P450 enzyme. The third type of drug interaction results from non-competitive inhibition of the cytochromes by covalent binding to P450.

2.8.3 Phase II Enzyme Reactions

Biotransformation reactions involve in this second phase include acetylation, methylation, glucuronidation, sulfonation, glutathione conjugation (mercapturic acid synthesis) and conjugation with amino acids such as taurine, glycine and glutamic acid.

Acetylation, methylation, sulfonation and glucuronidation involve reactions with activated co-substrates while glutathione or amino acid conjugation concerns reactions with activated xenobiotics.

N-Acetylation is a major course of biotransformation for xenobiotics containing an aromatic amine ($R\text{-}NH_2$) or a hydrazine group ($R\text{-}NH\text{-}NH_2$) that are transformed into aromatic amides ($R\text{-}NH\text{-}COCH_3$) and hydrazides ($R\text{-}NH\text{-}NH\text{-}COCH_3$) respectively. This conversion is catalysed by cytosolic *N*-acetyltransferases and requires the co-substrate acetyl-coenzyme A (acetyl-CoA). N-acetylation masks an amine with non-ionisable group rendering the metabolites less hydrophilic than the parent compound. However, N-acetylation of certain xenobiotics such as isoniazid assists their urinary excretion.

Methylation is a minor route of biotransformation and targeting O-, N- and S-containing functional groups. Like N-acetylation, it generally reduces the water solubility of xenobiotics by shielding functional groups which otherwise might be conjugated by other phase II enzymes. It also requires a co-substrate, which is S-adenosylmethionine that is converted to S-adenosylhomocysteine during the methylation reactions.

Uridine diphosphate-glucuronic acid is a co-substrate essential for glucuronidation, a biotransformation process that targets electron-rich nucleophilic heteroatom (S, O or N) normally present in phenols, aliphatic alcohols, carboxylic acids, primary and secondary aromatic and aliphatic amines as well as free sulfhydryl groups. Bilirubin, thyroid and steroid hormones are examples of endogenous substrates for glucuronidation. These reactions are catalysed by UDP-glucuronosyltransferases and glucuronide conjugates are polar, hydrophilic conjugates. These conjugates are also substrates for β-glucuronidase present in the intestinal microflora and the intestinal enzyme can liberate the aglycone (parent compound or Phase I metabolite) that enters enterohepatic circulation resulting in impediment to the xenobiotic elimination. Whether these conjugates are excreted from the body in urine or bile is subject to the size of the aglycone.

Many xenobiotics and endogenous substrate are conjugated with sulfate, a reaction catalysed by sulfotransferases in the presence of 3′-phosphoadenosine-5′-phosphosulfate (PAPS), generally producing a highly hydrophilic sulphuric acid ester. Sulfonation introduces sulfonate from PAPS to the xenobiotic and these metabolites are excreted mainly in urine. Some sulfate conjugates are subjected to further rounds of biotransformation. Sulfotransferases is a multigene family of cytosolic enzymes and are arranged into gene families (SULT1-SULT5) that share less than 40% amino acid sequence homology. Each family tend to work on a specific functional group. Generally, the addition of sulfonate to an aglycone reduces the pharmacologic and toxicologic acitivity of xenobiotics. However, sulfonation also activates methyl-substituted polycyclic aromatic hydrocarbons, aromatic amines and safrole to mutagenic metabolites.

Conjugation of xenobiotics with glutathione includes a huge number of electrophilic xenobiotics or those that are convertible to electrophiles. Glutathione is a tripeptide consisting of cysteine, glycine and glutamic acid. This reaction is calatysed by a family of glutathione S-transferases that are present in most tissues. The substrates for this enzyme

are compounds that are hydrophobic, containing an electrophilic atom and react non-enzymatically with glutathione at a quantifiable rate. Glutathione S-transferase increases the rate of conjugation via deprotonation of GSH to GS^-. Glutathione conjugates are thioethers, formed by nucleophilic attack of glutathione thiolate anion (GS^-) with an eletrophilic sulfur, carbon, oxygen or nitrogen in the xenobiotic. There are two types of conjugation reactions namely the addition reactions where glutathione is added to an activated double bond or strained ring system, and the displacement reactions in which glutathione replaces an electron-withdrawing group.

The addition of glutathione to a carbon-carbon double bond is facilitated by the presence of a nearby electron withdrawing group, thus the substrate for this reaction normally harbours a double bond attached to –CN, -COR, -COOR or –CHO. The displacement of an electron-withdrawing group usually occurs when the substrate contains halide, phosphate, sulfate, sulfonate or a nitro group attached to benzylic or allylic carbon atom. Glutathione is also capable of conjugating xenobiotics with an electrophilic heteroatom (S, O and N) where the initial conjugate formed between glutathione and the heteroatom is cleaved by a second molecule of glutathione to form oxidised glutathione (GSSG). The initial reactions are catalysed by glutathione S-transferase, whereas the second reaction that leads to GSSG formation typically occurs non-enzymatically.

Last but not least, amino acid conjugation of xenobiotics involves two main pathways and the substrates for conjugation process is limited to certain aromatic, aliphatic, cinnamic, heteroaromatic and arylacetic acids. The ability of xenobiotics to go through amino acid conjugation depends on stearic hindrance around the carboxylic acid group and by substituents on the aliphatic side chain or aromatic ring.

Most Phase II biotransformation enzymes are mainly found in the cytosol and generally progress faster than Phase I reactions. Thus, the rate of elimination of xenobiotics whose excretion hinges on biotransformation by cytochrome P450 followed by Phase II conjugation is generally influenced by the first reaction.

2.9 Introduction to METEOR

METEOR is another computer program developed by Lhasa Ltd. that utilises expert knowledge rules in metabolism to predict the metabolic fate of various chemicals, which can be useful in the absence of experimental data. Prediction is made based on the chemical's molecular structure and physicochemical properties. The program contains a knowledge base of structure-metabolism relationships and each describes a metabolic reaction, characteristic of xenobiotics with a common structural feature. METEOR reasoning rule-base contains 841 rules, 217 mammalian Phase I and II biotranformations allowing the program to evaluate the relative probabilities of various metabolic pathways (Langowski & Long, 2002). Results are accompanied by comments and literature citations as evidence that is specific, making evaluations easier. The strength of METEOR lies in its ability to predict the metabolites that are likely to be generated rather than all possible candidates (Greene *et al.*, 1999).

In certain circumstances, experimental data from metabolism studies discloses empirical formula of metabolites and not their molecular structure, which effectively impair a thorough assessment of the possible chemical properties such as toxicity possess by the metabolites since different molecular structure denotes different activities. The program is capable of recommending the most likely molecular structure and even anticipates different promising structures from the same empirical formula. Figures 2.12, 2.13 and 2.14 highlights the main steps involved in a METEOR search.

METEOR works in the same principle as DEREK and the main steps are outlined as below.

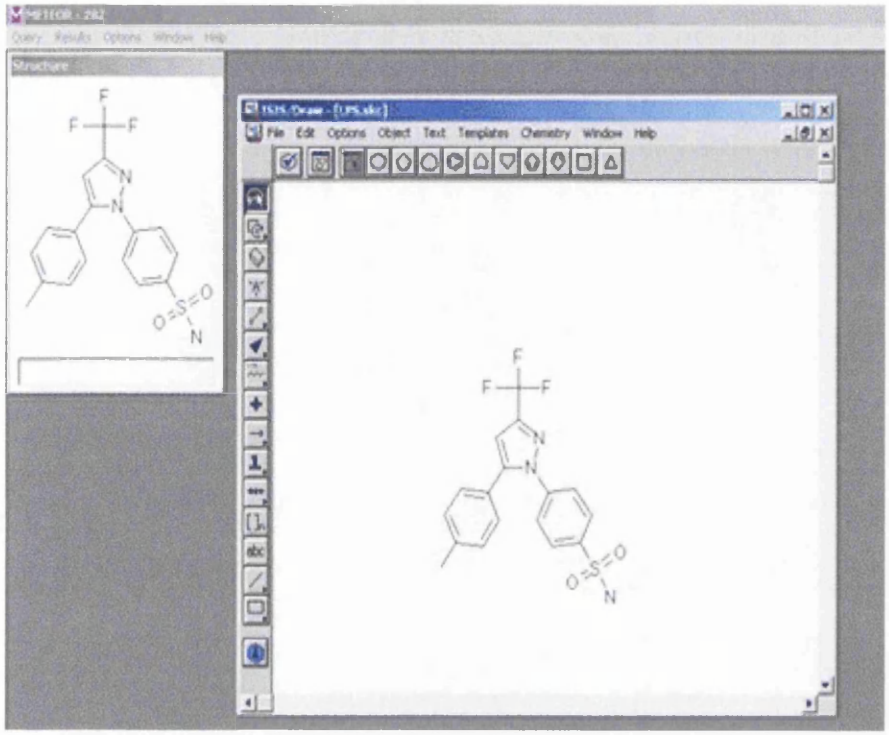

Fig. 2.12. Inserting a chemical structure using ISIS/Draw.

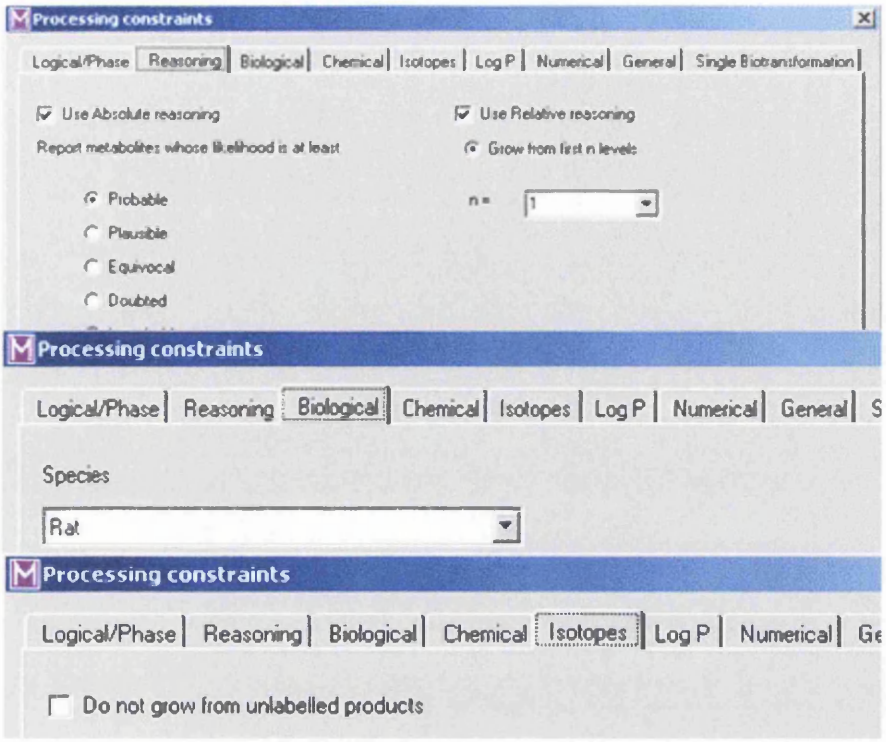

Fig. 2.13. Setting parameters to the query process.

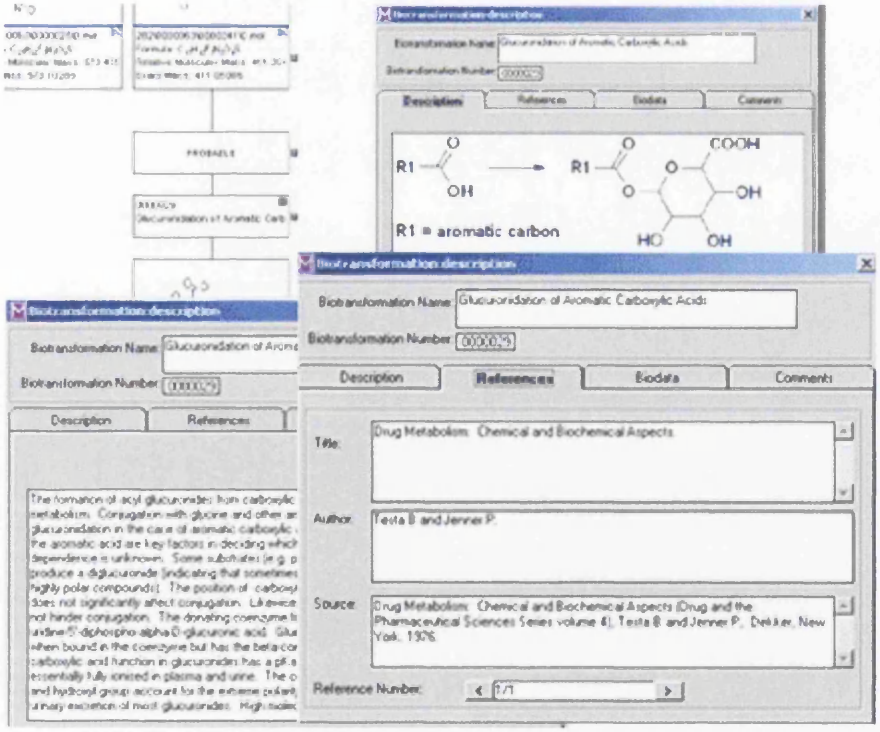

Fig. 2.14. Predictions made by METEOR can be then be examined.

2.10 METHODS

METEOR version 8.0.1 ISIS/Draw was used to draw the chemical structure of andrographolide. Main parameters to the query were set as listed below:

1. Testing against all biotransformations.
2. Absolute reasoning used: True.
3. Phase: Do not grow from phase II products.
4. Species: mammals
5. Likelihood at least: Plausible.
6. Hydrogen options: perceive implicit and explicit hydrogens.

2.11 RESULTS

The METEOR programme predicted plausible andrographolide metabolites in Phase I and II biotransformation and the possible routes are summarised as a metabolic tree in Figure 2.15. The data used for the tree construction were generated by METEOR and various reactions that contributed to this process are also stated. Figure 2.17 is the same metabolic tree but instead of empirical formula, the tree shows molecular weight. As the biotransformation pathway progresses, the molecular weight of the metabolites predicted increased. Another metabolite tree shown as Figure 2.18 is essentially the same as the one depicted in Figure 2.15 but highlighted the Phase II reactions in blue while those that can be achieved by cytochrome P450 are shown in other lighter colours.

Although the empirical formulae of all possible metabolites were shown in Figure 2.15, various different chemical structures can be derived from the same chemical formula, a task METEOR was equipped to handle. Due to the large size of information generated, examples of selected reactions involving the metabolism of andrographolide are shown in Figures 2.16a to 2.16f.

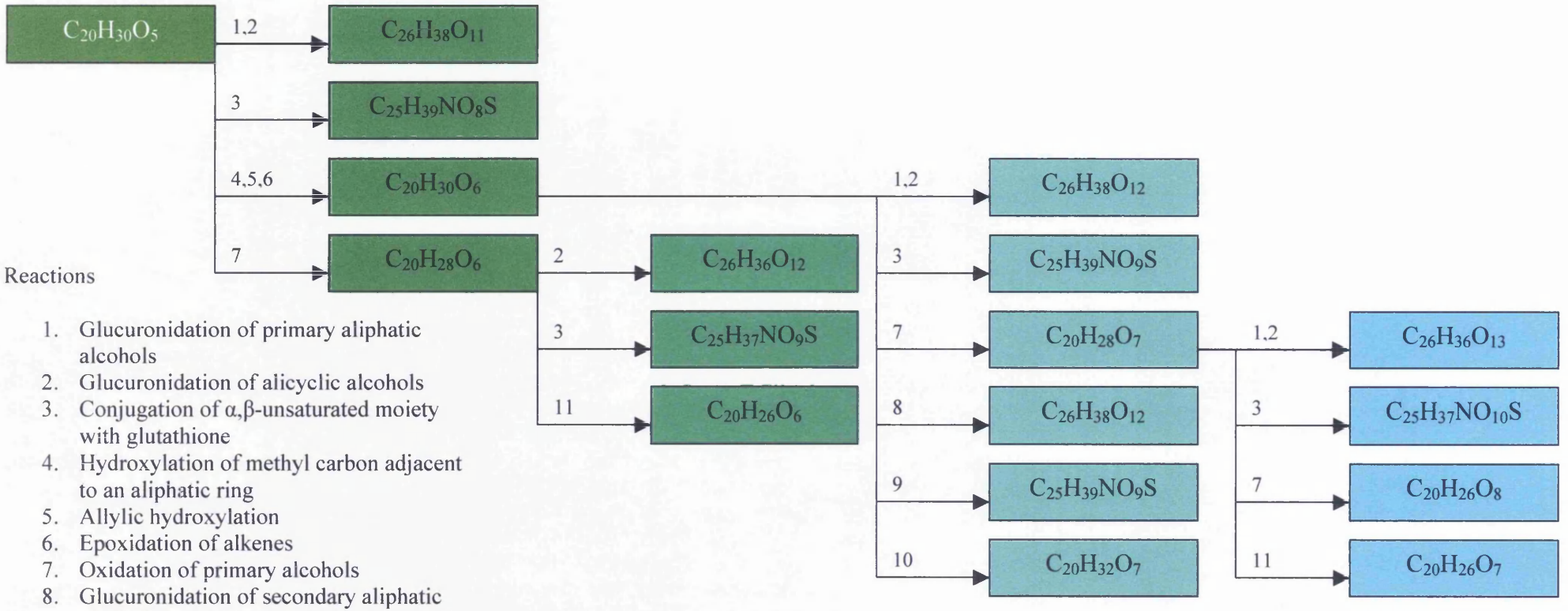

Reactions

1. Glucuronidation of primary aliphatic alcohols
2. Glucuronidation of alicyclic alcohols
3. Conjugation of α,β-unsaturated moiety with glutathione
4. Hydroxylation of methyl carbon adjacent to an aliphatic ring
5. Allylic hydroxylation
6. Epoxidation of alkenes
7. Oxidation of primary alcohols
8. Glucuronidation of secondary aliphatic alcohols
9. Conjugation of epoxides with glutathione
10. Vicinal diols from epoxides
11. Oxidation of secondary alicyclic alcohols

Fig. 2.15. Metabolic tree for the metabolism of andrographolide by Phase I and II reactions. The tree was generated using data produced by METEOR. Page 88.

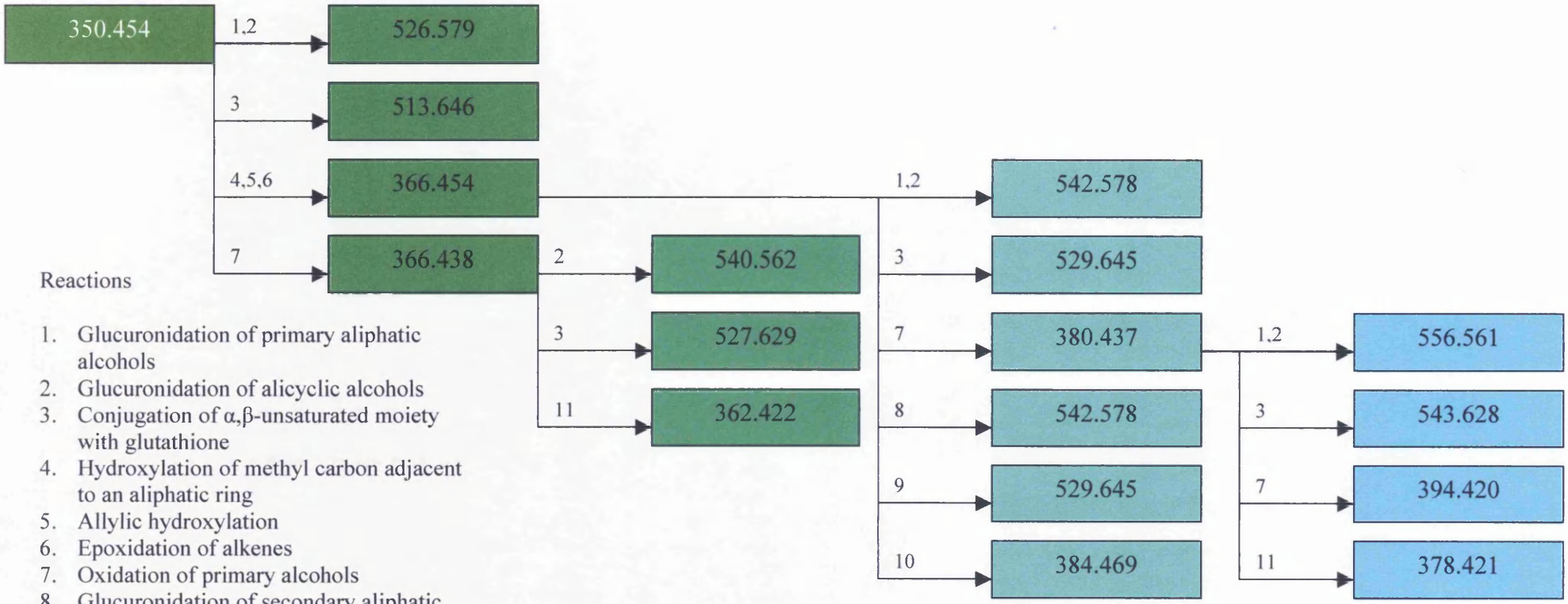

Fig. 2.17. Metabolic tree showing the changes in molecular weight after andrographolide metabolism. The tree was generated using data produced by METEOR.

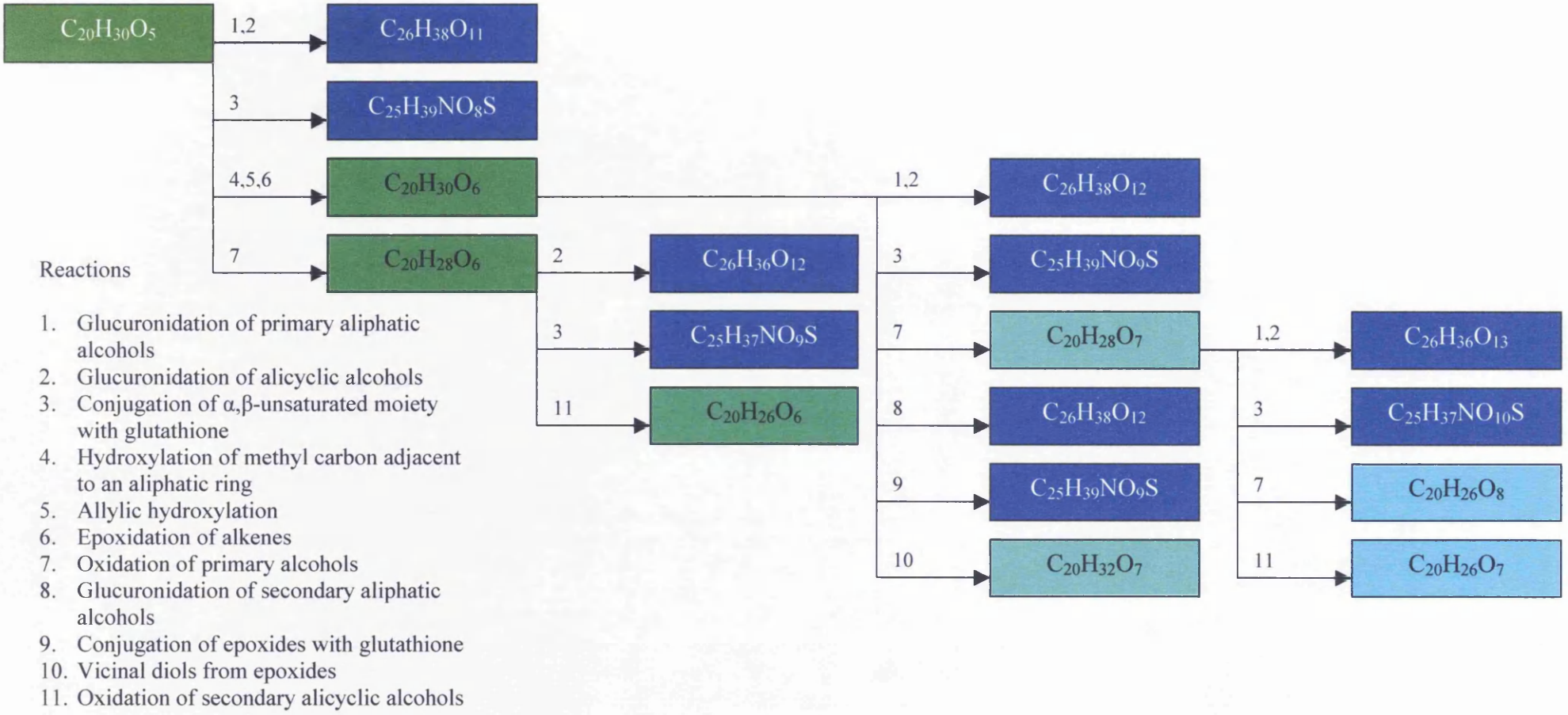

Reactions

1. Glucuronidation of primary aliphatic alcohols
2. Glucuronidation of alicyclic alcohols
3. Conjugation of α,β-unsaturated moiety with glutathione
4. Hydroxylation of methyl carbon adjacent to an aliphatic ring
5. Allylic hydroxylation
6. Epoxidation of alkenes
7. Oxidation of primary alcohols
8. Glucuronidation of secondary aliphatic alcohols
9. Conjugation of epoxides with glutathione
10. Vicinal diols from epoxides
11. Oxidation of secondary alicyclic alcohols

Fig. 2.18. Differentiating Phase I and Phase II biotransformation. Blue boxes are Phase II reactions and other colours are for Phase I reactions. The tree was generated using data produced by METEOR.

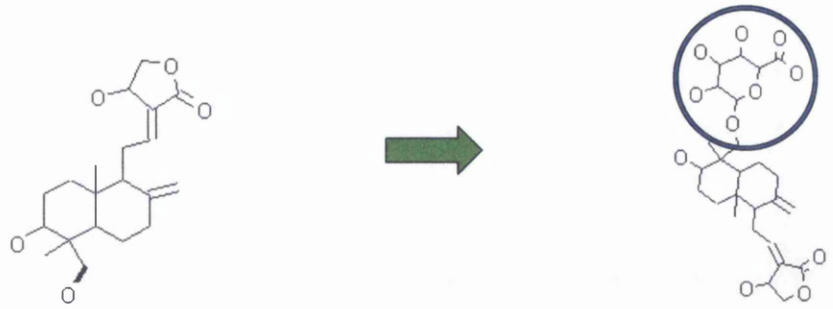

Fig. 2.16a. Glucuronidation of primary aliphatic alcohol. Area in bold print is the reaction substrate whereas the blue ring denotes structural transformation.

Fig. 2.16b. Glucuronidation of alicyclic alcohols. Area in bold print is the reaction substrate whereas the blue ring denotes structural transformation.

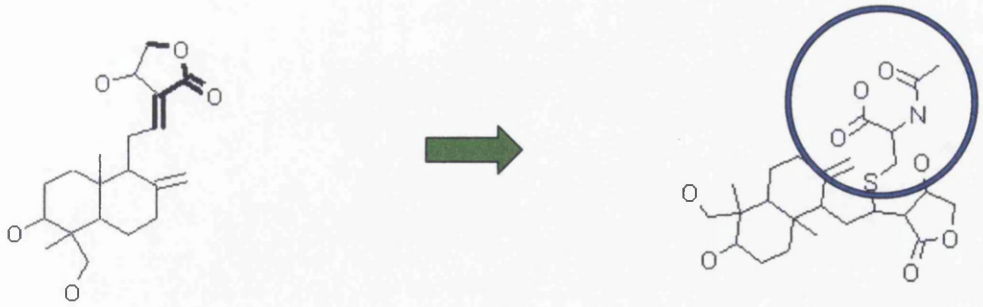

Fig. 2.16c. Conjugation of α,β-unsaturated compounds with glutathione. Area in bold print is the reaction substrate whereas the blue ring denotes structural transformation.

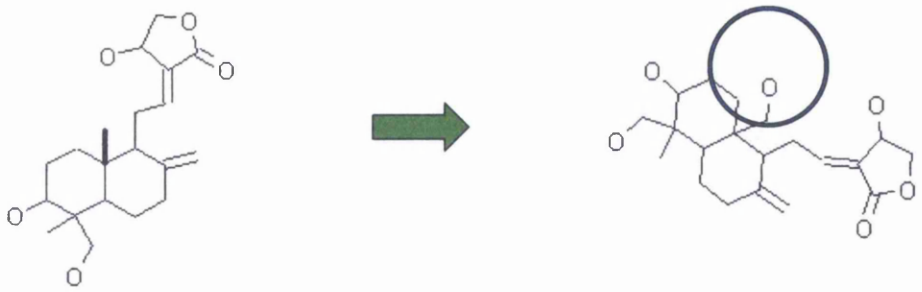

Fig. 2.16d. Hydroxylation of methyl carbon adjacent to an aliphatic ring. Area in bold print is the reaction substrate whereas the blue ring denotes structural transformation.

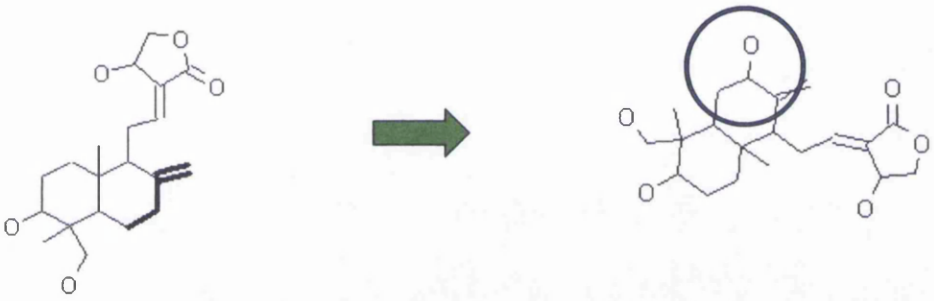

Fig. 2.16e. Allylic hydroxylation. Area in bold print is the reaction substrate whereas the blue ring denotes structural transformation.

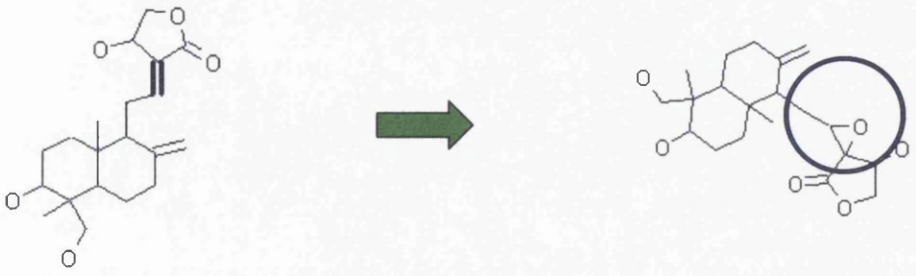

Fig. 2.16f. Epoxidation of alkenes. Area in bold print is the reaction substrate whereas the blue ring denotes structural transformation.

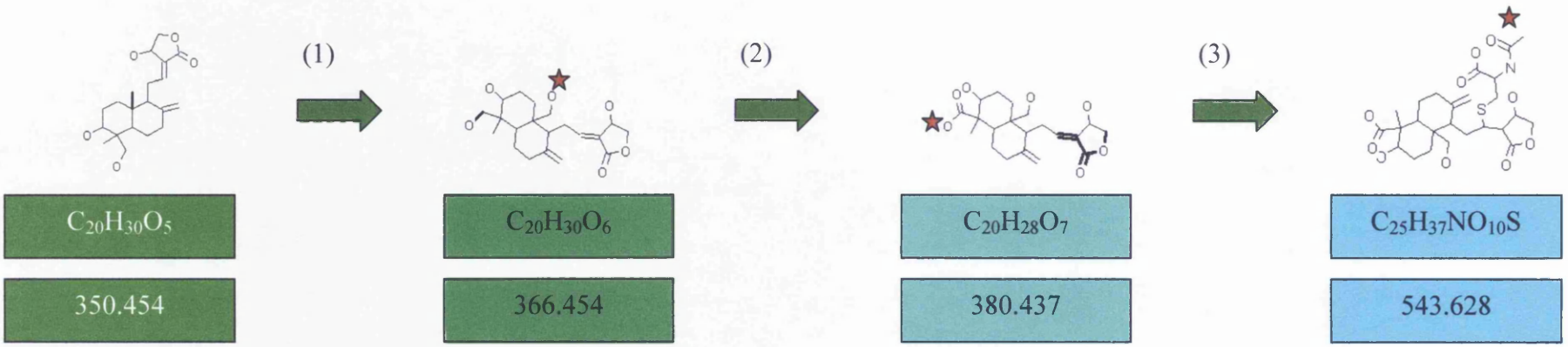

Fig. 2.19. Shows successive metabolism of andrographolide and is one of the reactions in the metabolic tree. Reaction (1) is hydroxylation of methyl carbon adjacent to an aliphatic ring, (2) is oxidation of primary alcohols and (3) is conjugation of α,β-unsaturated compounds with glutathione. The bold print highlights the substrate for the reaction while red star denotes the changes to the chemical structure after the reactions involved respectively. Data generated by METEOR.

2.12 DISCUSSION

The metabolic tree suggested by METEOR is useful in the initial prediction of possible metabolites of andrographolide especially when there is currently a paucity of sufficient data. Figure 2.15 shows all possible metabolites derived from andrographolide, the parent compound. Various functional groups attached to the aglycone provide many possible substrates for Phase I and Phase II enzymes. The progression of the metabolic tree also showed steady increment in molecular weight and polarity of the metabolites by the addition of other groups such as glutathione and glucuronide as shown in Figure 2.17. The resultant metabolites possess higher polarity and hydrophilicity mainly attributed to the high molecular weight of the conjugates, hence facilitates their excretion from the body. As depicted both in Figures 2.17 and 2.18, the molecular size of the metabolites produced by Phase II reactions were higher that those subjected to Phase I metabolism. Indeed, the Phase II biotransformation reactions with the exception of acetylation and methylation, result in a large increase of xenobiotic hydrophilicity (Gibson & Skett, 2001). The extract of *Andrographis paniculata* including andrographolide and its analogues have been shown to affect hepatic biotransformation enzymes such as anilinehydroxylase, N- and O-demethylase (Choudhary & Poddar, 1984), alanine aminotransferase and aspartate aminotransferase (Trivedi & Rawal, 2000) as well as glutathione S-transferase and DT-diaphorase (Phase II biotransformation enzymes) (Singh *et al.*, 2001).

Several metabolites of andrographolide have also been identified in rats and humans. Ten metabolites of andrographolide mainly in the form of sulfonic acid conjugates and sulfate compounds were isolated and identified in urine, feces as well as contents of small intestine after the compound was orally administered to rats (He *et al.*, 2003a, b, c). Cui *et al.* (2004) also reported structural identification of four urinary metabolites of andrographolide from human volunteers, of which three of the metabolites were categorised as 3-O-sulfate conjugates and the remaining one as 3-O-sulfate-12-S-cysteine conjugate. An additional seven Phase II metabolites were isolated from human urine and all were characterised as glucuronide conjugates, where four were found to be two pairs of geometric isomers (Cui *et al.*, 2005). All these findings are in line with the predictions made by METEOR in terms of plausible reactions that might be involved in andrographolide metabolism where different functional groups such as primary aliphatic alcohols and epoxides are being targeted by UDP-glucuronosyltransferases and glutathione S-transferases respectively.

Indeed, assessment of andrographolide structure by DEREK identified the α, β-unsaturated ester position as capable of educing chromosome damage and METEOR also suggested that this position is susceptible to conjugation with glutathione as illustrated in Figure 2.16c. Furthermore, compounds containing the α, β-unsaturated ester has been known to be metabolised via conjugation with glutathione and hydrolysis (Frederick *et al.*, 1992; Greim *et al.*, 1995; McCarthy & Witz, 1997). Glutathione conjugates formed in the liver can be excreted intact in bile or they can be transformed to mercapturic acids in the kidney and excreted in urine. The conversion of glutathione conjugates to mercapturic acids requires sequential cleavage of glycine and glutamic acid from glutathione moiety subsequently followed by N-acetylation of the resulting cysteine conjugate (Gibson & Skett, 2001). Glutathione conjugation of metabolites is an important detoxification step because electrophiles for example, are known to be potentially genotoxic species and can bind to critical nucleophiles such as DNA and proteins leading to genetic mutations and cellular damage. However, in some cases, conjugation with glutathione amplifies the toxicity of a xenobiotic by being inherently toxic or being degraded into a toxic metabolite (Williams & Aruoma. 2000).

As shown in Figure 2.18, andrographolide can be converted into four possible metabolites via 7 different reactions and these metabolites in turn can also be further transformed into various different metabolites. However, cellular conditions and the amounts of cofactors present for Phase II metabolism dictate the direction of biotransformation pathway. Thus, there will be major and minor andrographolide metabolites being produced depending on the circumstances. The cellular concentrations of PAPS for example (approximately 75μM), are significantly lower than those of glutathione (~10mM) and UDP-glucuronic acid (~350μM) and the relatively low concentration of PAPS limits the capacity for xenobiotic sulfonation (Gibson & Skett, 2001). The availability of UDP-glucuronic acid can also limit the rate of glucuronidation of endogenous as well as exogenous compounds especially if they are in high doses and being extensively conjugated such as acetaminophen. Figure 2.19 shows one example of possible routes for andrographolide biotransformation yielding a glutathione-conjugate.

Before the Phase II biotransformation, andrographolide is susceptible to Phase I enzymes as suggested by the metabolic tree (Figure 2.18). Hydroxylation and epoxidation of double

bonds are two main reactions of andrographolide metabolism attributed to cytochrome P450. Even though the aglycone was predicted to be metabolised by these reactions, one cannot really ascertain whether the metabolites are more or less reactive by referring to the metabolic tree. Andrographolide is shown to be susceptible to epoxidation of the double bonds and as shown in Figure 2.16f, this epoxide group resides close to the butyrolactone moiety of the phytochemical. Although, epoxides have been known to be potentially mutagenic (Guengerich, 2003; Benigni, 2005) *per se*, the reactivity of epoxy-andrographolide can only be determined experimentally. Alternatively, another double bond exists within the structure at the $\Delta^{8(17)}$ position as highlighted in Figure 2.8 and is also susceptible to epoxidation according to METEOR assessment. However, the half-lives of relatively simple epoxides are known to be usually on the order of hours in the absence of added nucleophiles. Many of these simple epoxides are carcinogens when administered to rodents at high doses (Dunkelberg, 1979) whereas the evidence for human carcinogenicity such as styrene is probably equivocal at best (Yeowell-O'Connell *et al*, 1998). Functionalisation of epoxides with the addition of certain groups lead to enhanced reactivity such as 2-cyanoethylene oxide that is more reactive than propylene oxide and is mutagenic (Recio *et al.*, 1988; 2001). Butadiene diepoxide is much more reactive and genotoxic than would be expected on the statistical basis of having two epoxides (Cochrane & Skopek, 1994). A comparable example on epoxide generation in herbs is that observed in *Teuchrium chamaedrys* (Germander), which was once promoted as slimming products in the 1990s until hepatotoxicity cases were reported in France. The hepatotoxicity has been attributed to the diterpenoids in *T. chamaedrys* namely teucrin A and teuchamaedryn A. The furan ring of these diterpenoids is susceptible to oxidation by CYP3A4, which has a wide substrate spectrum, to reactive epoxides that react with proteins such epoxide hydrolase and CYP3A (Loeper *et al.*, 1994; Lekehal *et al.*, 1996; Fau *et al.*, 1997; Loeper *et al.*, 2001). The presence of these reactive epoxides led to mitochondrial membrane permeability transition and apoptosis in rat and mouse hepatocytes (Loeper *et al.*, 1994; Lekehal *et al.*, 1996; Fau *et al* 1997). It was revealed that teucrin A binds covalently to hepatocyte proteins and the furano diterpenoid part of the compound increased cytosolic levels of Ca^{2+} but decreased cellular glutathione (GSH) and cytoskeleton-associated protein thiols resulting in the formation of plasma membrane blebs and apoptosis (Lekehal *et al.*, 1996; Fau *et al* 1997).

Futhermore, the epoxide functional group in andrographolide can be further converted into vicinal diols, another functional group that can be mutagenic, which may or may not increase the reactivity of andrographolide and can only be assess in laboratory studies. However, this prediction is made on the probability that these metabolic routes are the one favoured by the cellular or systemic conditions since there were other relatively safer pathways such as glucuronidation. The possibility that these metabolites are produced as minority products cannot be ruled out too. It is also important to note that the unsaturated butyrolactone site of andrographolide was predicted by DEREK as able to cause chromosome damage in mammals and whether structural transformation to this moiety will enhance or reduce the potency of such effect is not deducible without experimental data, which currently is inadequate.

Recently, Jarukamjorn *et al.* (2006) studied the impact of aqueous and alcoholic extracts of *A. paniculata* on mouse hepatic cytochrome P450 enzymes and found the extracts to significantly elevate the activities of ethoxyresorufin O-dealkylase (EROD) and pentoxyresorufin O-dealkylase (PROD) but not methoxyresorufin O-dealkylase (MROD). It was also suggested that CYP1A1 and CYP2B10 were the P450 isoforms responsive to *A. paniculata* extracts (Jarukamjorn *et al.*, 2006). However, the utilisation of crude extracts in the study cannot provide valuable qualitative data on the effects of individual components in the extracts on specific P450 isoforms, especially andrographolide which is a major diterpenoid present (Kleipool, 1952; Siripong *et al.*, 1992). Furthermore, one must take into account that individual substances in the extract, as it is the case with many plant extracts, may act in an antagonistic or synergistic manner in the expression of bioactivation and detoxification pathways. Thus, another study into the effects of andrographolide on cytochrome P450 isoenzymes activities showed that the phytochemical significantly evoked the expression of CYP1A1 and CYP1A2 but not that of CYP1B1 in mouse hepatocytes in a concentration-dependent manner (Jaruchotikamol *et al.*, 2007). The mRNA expression of CYP1A1 induced by andrographolide is higher compared to CYP1A2 but lower than that stimulated with typical CYP1A agonists such as benz(a)anthracene and β-naphthoflavone (Jaruchotikamol *et al.*, 2007). It is known that the mechanisms of transcription regulation differ between CYP1A1, CYP1A2 and CYP1B1 (Guengerich & Shimada, 1998) hence the dissimilarity in the expression levels observed (Jaruchotikamol *et al.*, 2007). However, further studies involving major cytochromes such as CYP3A4 is

needed. This recent study could possibly shed more light into the reported hepatoprotective effect modulated by andrographolide.

Andrographolide has been reported to be the major anti-hepatotoxic compound present in *A. paniculata* extract conferring protection to liver cells against toxicity induced by carbon-tetrachloride, galactosamine and acetaminophen (Handa & Sharma, 1990a; Handa & Sharma, 1990b). Since the mode of action and hence toxicity induced by galactosamine and acetaminophen are different, it was suggested that a non-specific hepatoprotective activity may be attributed to this phytochemical (Handa & Sharma, 1990b). It may be possible that andrographolide is involved in cytochrome P450 activity manipulation, effectively shielding the liver cells from cytotoxicity. After all, cytochromes 1A2, 2E1, 2A6 and 3A4 have been shown to oxidise acetaminophen (paracetamol) into *N*-acetyl-*p*-benzoquinone imine (NAPQI) that in turn is detoxified by glutathione (GSH) resulting in the formation of acetaminophen-GSH conjugate (Patten *et al.*, 1993; Chen *et al.*, 1998)

Although metabolic predictions made by CSAR programme such as METEOR is useful, there are several caveats to this finding. Any predictions made cannot overrule experimental data. Mammals was the chosen parameter for METEOR where no distinction was made between human and animals, thus the metabolic tree generated was not representative of any particular species but mammals in general plus there are inter- and intra-species variability in metabolic capacity. This might explain the absence of sulfonation process from the metabolic tree generated in contrary to experimental findings where sulfate conjugates were isolated (He *et al.*, 2003a, b, c; Cui *et al.* 2004). Secondly, METEOR is able to suggest the most plausible molecular structure of possible metabolites but it cannot exactly determine their reactivity and toxicity, which can only be proven experimentally. This involves extraction and identification of the metabolites using high performance liquid chromatography (HPLC) or gas chromatography-mass spectrometry (GC/MS) to name a few. Subsequently, various genotoxicity studies whether *in vitro* and subsequently followed by *in vivo* if necessary, can be performed on the isolated metabolites to assess its genotoxic potential. For example, butyrylactone moiety of andrographolide was suggested to contribute to its activity but this functional group is susceptible to conjugation with glutathione and one can never be certain whether andrographolide will be more or less reactive. Finally, all of the metabolism studies cited previously merely elucidate the type of metabolites being produced by a rather small sample of healthy male

human volunteers and rats. Although the studies did not report any adverse effects experienced by the human volunteers during the study period, this does not necessarily means that more subtle form of injury such as mutagenesis and cellular damage can be ruled out despite successful extraction of more hydrophilic metabolites. Furthermore, human metabolism studies may produce metabolites from the compound of interest, which may not be observed in *in vitro* or animal studies and therefore may not have been thoroughly assessed for possible risk to humans. In a case where the metabolites were considerably high in humans, additional testing with the metabolites or the pathways involved would be essential to properly evaluate the potential of the compound to cause genotoxicity in humans (US FDA, 2005).

Therefore, METEOR was useful in determining the most plausible routes of biotransformation for a compound based on the application of structure-activity relationships and meant to complement experimental data or assisting in better experimental designs. In this study, many similarities were observed between the results generated via *in silico* assessment of possible andrographolide metabolism pattern using METEOR and *in vitro/in vivo* experiments conducted previously, thereby granting the opportunity to appreciate the strengths and weaknesses of such approach. Furthermore, semi-quantitative information on metabolic fate of this phytochemical along with SAR study conducted using DEREK gave a better picture.

CHAPTER 3

ASSESSMENT OF ANDROGRAPHOLIDE GENOTOXICITY POTENTIAL USING THE *IN VITRO* CYTOKINESIS BLOCK MICRONUCLEUS ASSAY

CHAPTER 3

ASSESSMENT OF ANDROGRAPHOLIDE GENOTOXICITY POTENTIAL USING THE *IN VITRO* CYTOKINESIS BLOCK MICRONUCLEUS ASSAY

3.1 Micronuclei as Genotoxicity Biomarker: A Historical Perspective

The most often used assay in routine genotoxicity testing of xenobiotics *in vitro* is bacterial mutation (Ames test). However, the detection of natural and synthetic carcinogenic substances that act through a non-direct mode of DNA alteration and are negative in bacterial mutation assays requires additional test systems. Another often-used endpoint in routine testing is the induction of chromosomal aberrations in mammalian cells. Alternatively, the *in vitro* micronucleus assay is easier to perform and is suitable to monitor genotoxicity of such compounds in mammalian cells.

Micronuclei were described as "corpuscules intraglobulaires" by Jolly in the late 1800s and early 1900s or known as "fragment of nuclear material" in the cytoplasm of erythrocytes by Howell about a century ago hence these structures are known to hematologists as "Howell-Jolly bodies". Similar intracellular structures were described in other cell types, for example in rat and mouse embryos by Brenneke in 1937 or in *Vicia faba* by Thoday in 1951, and are known as "fragment nuclei" or "micronuclei". These micronuclei were consistently found after radiation exposure of cells and it was assumed that they originated from acentric fragments that were excluded from the two daughter nuclei at the late stages of mitosis. The instrumental application of micronucleus as biomarkers for cytogenetic damage was discovered by Evans *et al.* in 1959, while comparing the efficiency of neutrons to γ-rays in *Vicia faba* roots.

Boller and Schmid's work paved the way for the utilisation of micronuclei as an assay system for elucidating genotoxicity potential and were first to suggest the term "micronucleus". Studies on bone marrow erythrocytes by Heddle also contributed to the

decisive development. Subsequently, Countryman and Heddle introduced lymphocytes as another useful cellular system for detection of chromosomal damage by the determination of micronucleus induction. They also recommended the utilisation of micronuclei as a biomarker in testing schemes.

3.2 The *In Vitro* Cytokinesis Block Micronucleus Assay and Its Application

The simplicity of scoring and wide applicability of the *in vitro* micronucleus test in various cell types makes it an appealing method in cytogenetic abnormality assessment. However, incomplete comprehension of micronuclei induction mechanisms and the absence of sufficient methods to concurrently assess cell proliferation and micronucleus formation, inevitably delayed the validation of the *in vitro* micronucleus test for genotoxicity testing.

Micronuclei are small, membrane bound extranuclear bodies that arise in dividing cells from whole chromosome/chromatids or acentric chromosome/chromatid fragments that lag behind in anaphase and remained outside of the daughter cells' nuclei in telophase. Micronuclei are only formed during cell division regardless of the location of the actual damage that occurred during the cell cycle, either by damage to the DNA or damage to the mitotic apparatus.

In the *in vitro* cytokinesis block micronucleus assay (CBMA) developed by Fenech and Morley (1985), cytochalasin-B is added to the cells in culture. Cytochalasin-B is a metabolite of the fungus *Helminthosporium dematioideum* that blocks cytokinesis but not karyokinesis and results in the formation of binucleated cells from cells that have undergone one nuclear division (Carter, 1967; Ridler & Smith, 1968). Cytochalasin-B prevents cytokinesis by binding to high-molecular-weight complexes in the plasma membrane, which is responsible in inducing actin polymerisation to form microfilaments that governs the cleavage of the dividing cell into two daughter cells. This allowed the identification of once-divided nuclei in binucleated cells and granted an efficient approach to study the mechanism leading to micronuclei formation as illustrated in Figure 3.1. With restriction on micronuclei scoring only in cells that had undergone one cell cycle, the cytokinesis-block micronucleus assay

(CBMA) solved the technical predicament of possible variation in micronucleus frequency caused by modifications in the proportion of dividing cells that may occur either due to sub-optimal culture conditions or exposure to genotoxic agents (Fenech, 2000). Table 3.1 compares the *in vitro* CBMA and chromosomal aberration assay, which is widely used previously to assess genotoxicity.

A micronucleus that contains a whole chromosome mainly results from defects in the chromosome segregation machinery such as failure of the mitotic spindle, kinetochore, or other parts of the mitotic apparatus, deficiencies in the cell cycle governing genes or by damage to chromosomal substructures, mechanical disruption (Albertini *et al.*, 2000) as well as centromeric DNA hypomethylation (Fenech *et al.*, 2005). An acentric or a lagging whole chromosome that is not included into the main nucleus after nuclear membrane reformation, may become enveloped by separate membrane producing a micronucleus due to the inability to migrate towards the opposite microtubule organising centres (MTOCs) (Lynch & Parry, 1993; Schuler *et al.*, 1997; Fenech, 2000). On the other hand, micronuclei harbouring chromosomal fragments may arise from direct double-strand DNA breakage, inhibition of DNA synthesis or conversion of single strand breaks into double strand breaks after cell replication. Misrepair of two chromosome breaks may cause asymmetric chromosome rearrangement generating a dicentric chromosome and an acentric fragment. Usually, the centromeres of the dicentric chromosomes are pulled towards the MTOCs of the cells during anaphase producing a nucleoplasmic bridge (NPB) between the daughter nuclei and an acentric fragment that lags behind to form a micronucleus (Thomas *et al.*, 2003; Fenech, 2005). Micronuclei can also be formed by gene amplification via breakage-fusion-bridge (BFB) cycles when amplified DNA is selectively placed to specific sites at the periphery of the nucleus and extrude via nuclear budding at the S-phase of the cell cycle (Fenech, 2002).

For almost two decades, the *in vitro* CBMA has evolved into a comprehensive technique in assessing cytostasis, chromosome loss, chromosome breakage, non-disjunction, apoptosis and necrosis. New developments also indicated that this assay could be employed to measure nuclear buds, a biomarker for gene amplification and changes in gene dosage as well as the measurement of nucleoplasmic bridges, which is an indicator for dicentric chromosomes

resulting from telomere end-fusions or DNA mis-repair (Haaf *et al.*, 1999; Umegaki & Fenech, 2000). Figure 3.2 shows the possibility of various outcomes in cytokinesis-blocked cells upon exposure to genotoxic and/or cytotoxic agents.

Table 3.1. Comparison of strengths and weaknesses of chromosomal aberration assay and *in vitro* CBMA.

Methods	Advantages	Disadvantages
Chromosomal aberrations assay	• Endpoint: chromosome mutations. • Combined with FISH-painting permits the detection of numerical and structural chromosomal aberrations. • Possible co-detection of mitotic indices. • Able to identify the nature of the clastogenic damage being examined, strand breaks against base damage. • Sensitive method. • Interactive scoring possible but not full automation.	• Labour-intensive and requires *in vitro* cell cultivation. • Requires highly qualified skills and experience.
In vitro CBMA	• Endpoints: chromosome and genome mutations. • Combined with suitable antibodies (e.g. CREST) allows the identification of aneugen and clastogen; detection of chromosome loss and non-disjunction. • Detection of other useful endpoints such as apoptotic, necrotic cells, NPB and NBUD. • Simple and fast. • Economical to perform and the possibility of automation. • Sensitive method with statistical power.	• Requires cell division for micronucleus expression. • Effect of cytochalasin-B on micronucleus frequency. • Not able to detect all chromosomal damage events e.g. symmetrical reciprocal translocations.

N.B. NPB= nucleoplasmic bridges; NBUD= nuclear budding.

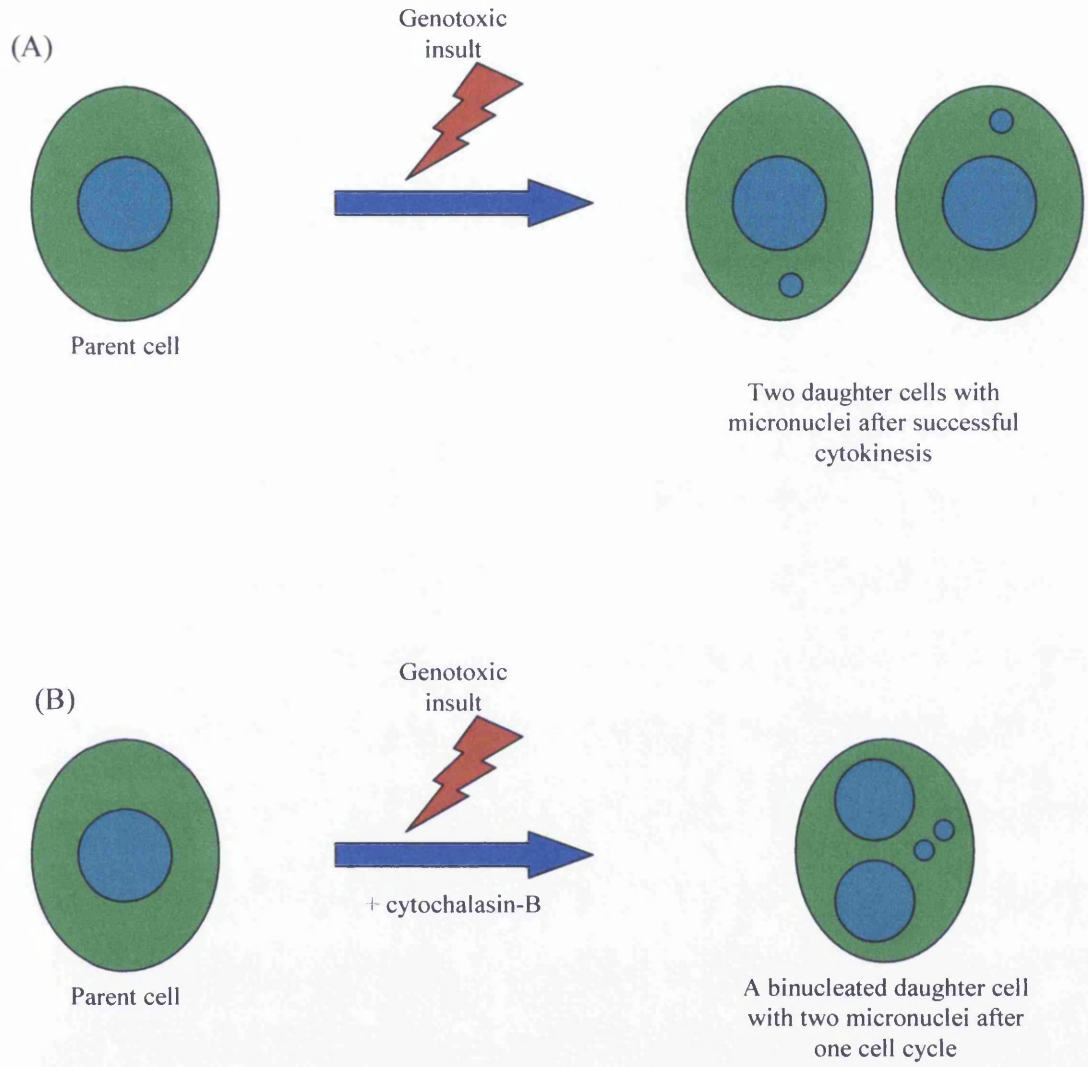

Fig. 3.1. In (A), a cell that has been subjected to a genotoxic insult may produce micronuclei in daughter cells but they are not suitable for scoring as one cannot ascertain whether the cells has gone through only one cell division. However, the addition of cytochalasin-B such as shown in (B) allows micronuclei in a binucleated cell to be quantified since cytokinesis is prevented in a cell that is going through one cell cycle.

One obvious advantage of the *in vitro* CBMA lies in its capability in detecting both aneugenic and clastogenic events, resulting to numerical and structural chromosomal aberrations respectively (Fenech, 2000) making the assay more mechanistically enhanced. Distinguishing the two different events is achievable even at low doses of genotoxin

exposure. For example, the sensitivity of this assay in detecting damage induced by ionising radiation is 0.2Gy for micronuclei (aneugenic and clastogenic events) and 0.1Gy when combined with pan-centromeric FISH (fluorescence *in situ* hybridisation) probes when detecting clastogenic events (Vral *et al.*, 1997; Touil *et al.*, 2002).

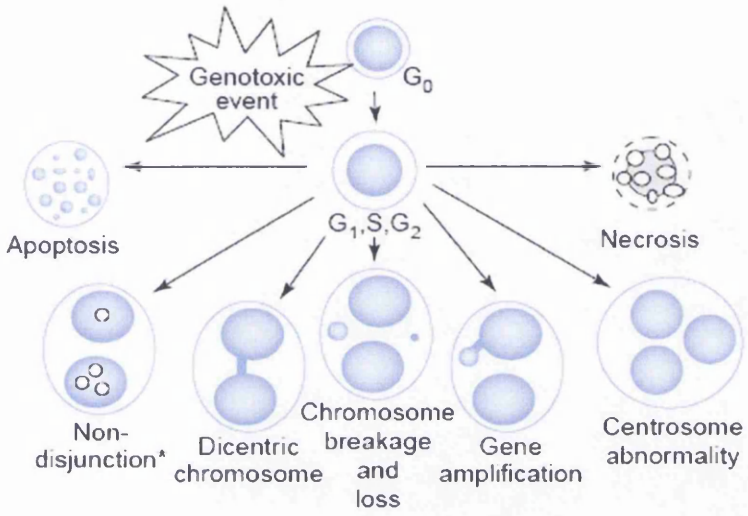

Fig. 3.2. The possibility of various outcomes in cytokinesis-blocked cells upon exposure to genotoxic and/or cytotoxic agents. The application of these biomarkers within the CBMA allows the quantification of chromosome breakage, chromosome loss, gene amplification, chromosome rearrangement and cell death (apoptosis and necrosis). Furthermore, cytostatic effects can be elucidated by the ratio of mono-, bi- and multinucleated cells. The CBMA has not been used previously in measuring centrosome abnormalities incidence but this is possible in theory by quantifying the frequency of tri- and/or tetranucleated cells and confirming that their DNA content is 4N. (Adopted from Fenech, 2002).

3.2.1 CBMA in Combination with Kinetochore Labelling

Auto-antibody present in the sera of patients suffering from a specific type of the autoimmune disease scleroderma, CREST (Calcinosis, Raynaud phenomenon, esophageal dismotility, sclerodactyly and telangiectasia) syndrome, possess a high affinity to kinetochore proteins present at the centromere of chromosomes (Moroi *et al.*, 1980). It was later suggested that the CREST antibody could be utilised in distinguishing between micronuclei that contain fragmented (Kinetochore negative; K-) and whole chromosomes

(Kinetochore positive; K+) (Parry & Parry, 1987). Subsequently, application of the CREST antibody in determining whether structural (clastogenic) or numerical (aneugenic) chromosomal changes was involved in micronuclei induction rapidly ensued (Degrassi & Tanzarella, 1988; Eastmond & Tucker, 1989; Bonassi *et al*, 1992) as illustrated in Figure 3.3 below.

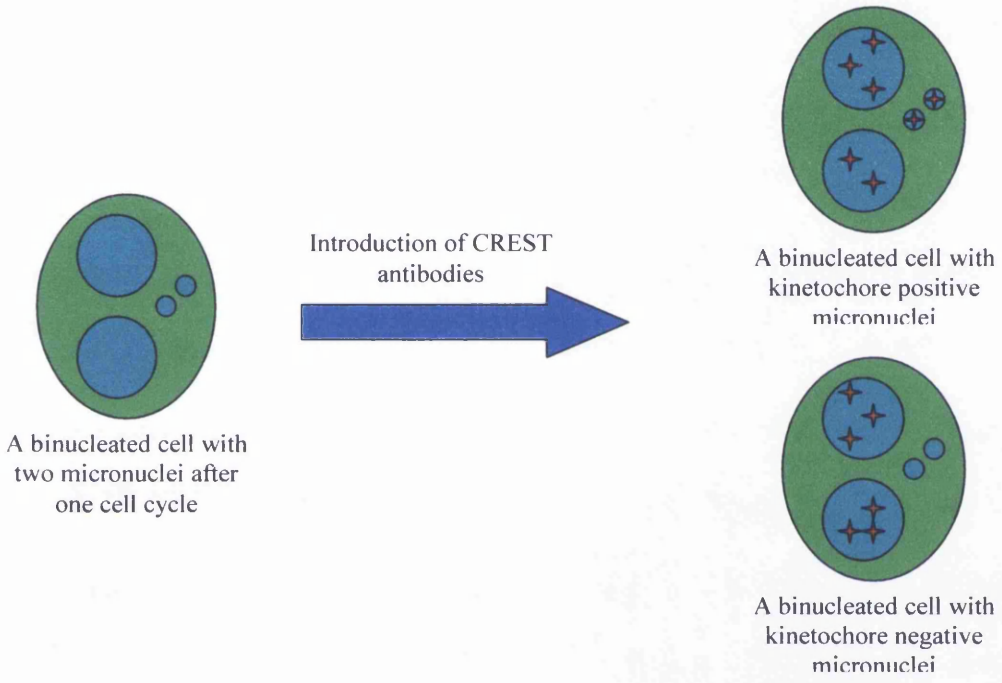

Fig. 3.3. Shows how micronuclei harbouring kinetochore positive and negative can be differentiated by by employing the CREST antibodies against chromosomal kinetochore proteins. Kinetochore positive micronuclei denotes whole chromosome(s) whereas chromosomal fragments detected as kinetochore negative micronuclei.

A micronucleus that harbours a centromeric region arise from whole chromosomes or chromosomal fragments containing a centromere, whereas those that do not contain a centromeric region results from the formation of nuclear membrane around acentric fragments or whole chromosomes that have lost the kinetochore from the centromere. As it is assumed that random kinetochore loss, chromosome breakages and fragments containing centrosomes are not common, regular events, the occurrence of either kinetochore positive or negative micronuclei with 70% frequency or higher indicates aneugenic or clastogenic nature

of the compound tested respectively (Antoccia *et al.*, 1991; Antoccia *et al.*, 1993; Stopper & Muller, 1997).

3.3 Cellular Toxicity in Genotoxicity Assessment

Every genotoxicity tests employed for regulatory submission must be accompanied by relevant cellular toxicity data where the agent must be subjected to the tests involving maximum concentrations (10mmol/l or 5000μg/ml), the highest level permissible by cytotoxicity or the limit of solubility in solvent or growth medium. Thus, the cytotoxicity assessment is not only critical for the elucidation of possible mode of action but also crucial for assay validity.

A toxic compound is capable of initiating two characteristic forms of cell death with clearly distinct biochemical and morphological features namely apoptosis and necrosis (Wyllie *et al.*, 1980). Other forms of cell death include autophagy and senescence. The consequent cell death type hinges heavily on the stimulus and cellular context since every cell death mechanism is a net result of self-propagating signals and others that negate the alternative cell death programs (Clarke, 2002). Typical feature of apoptosis are fragmented nuclei with condensed chromatin, organised DNA degradation (Wyllie *et al.*, 1980; Duke *et al*, 1983) and shrunken cytoplasm within an intact plasma membrane. In contrast, necrosis features severe loss of membrane integrity and leakage of cellular components (Wyllie *et al.*, 1980). The same chemical in different concentrations is capable of triggering both type of cell death due to various factors such as increased physical cellular damage, alterations to cellular biochemical homeostasis or intolerable disruption to cellular repair mechanisms. For example, less than 1μM cadmium chloride would activate apoptotic response but higher concentrations caused necrosis in cells. Therefore, classical apoptotic and necrotic cell death represent only the extreme end of a wide spectrum of possible biochemical and morphological deaths that can occur simultaneously in tissues or cell cultures exposed to the same agent (Nicotera *et al.*, 1999). Apoptosis may also progress to secondary necrosis when dying cells are not removed by heterophagy (Kroemer *et al.*, 1998).

Once a xenobiotic enters the cell, it may directly interact with various receptors and inducing positive or negative effect via signalling pathways manipulation. Alternatively, the xenobiotics are subjected to biotransformation yielding reactive metabolites or become inactive, which is a common fate. However, some of these compounds or their products can have undesired effects. Therapeutic compounds may also possess unrelated effects other than its intended purposes and target sites. For example, an oral fluoroquinolone broad-spectrum antibiotic temafloxacin (Omniflox™) was found to cause allegic reactions in some patients as well as haemolytic anemia, liver and kidney dysfunctions (FDA, 1992) whereas Fansidar™ (pyrimethamine-sulfadoxine) that has been used against malaria and toxoplasmosis was reported to induce micronuclei as well as sister chromatid exchanges (Abou-Eisha & Afifi, 2004). Direct-acting genotoxins will target the DNA causing damage such as adducts formation. where they interact with proteins, other macromolecules such as DNA or small molecules such as glutathione (GSH). Depletion of the oxidative defences can cause changes in cellular redox status resulting in disturbances to regulatory systems affected by redox homeostasis, ultimately leading to cell death via apotosis or necrosis as illustrated in Figure 3.4 overleaf.

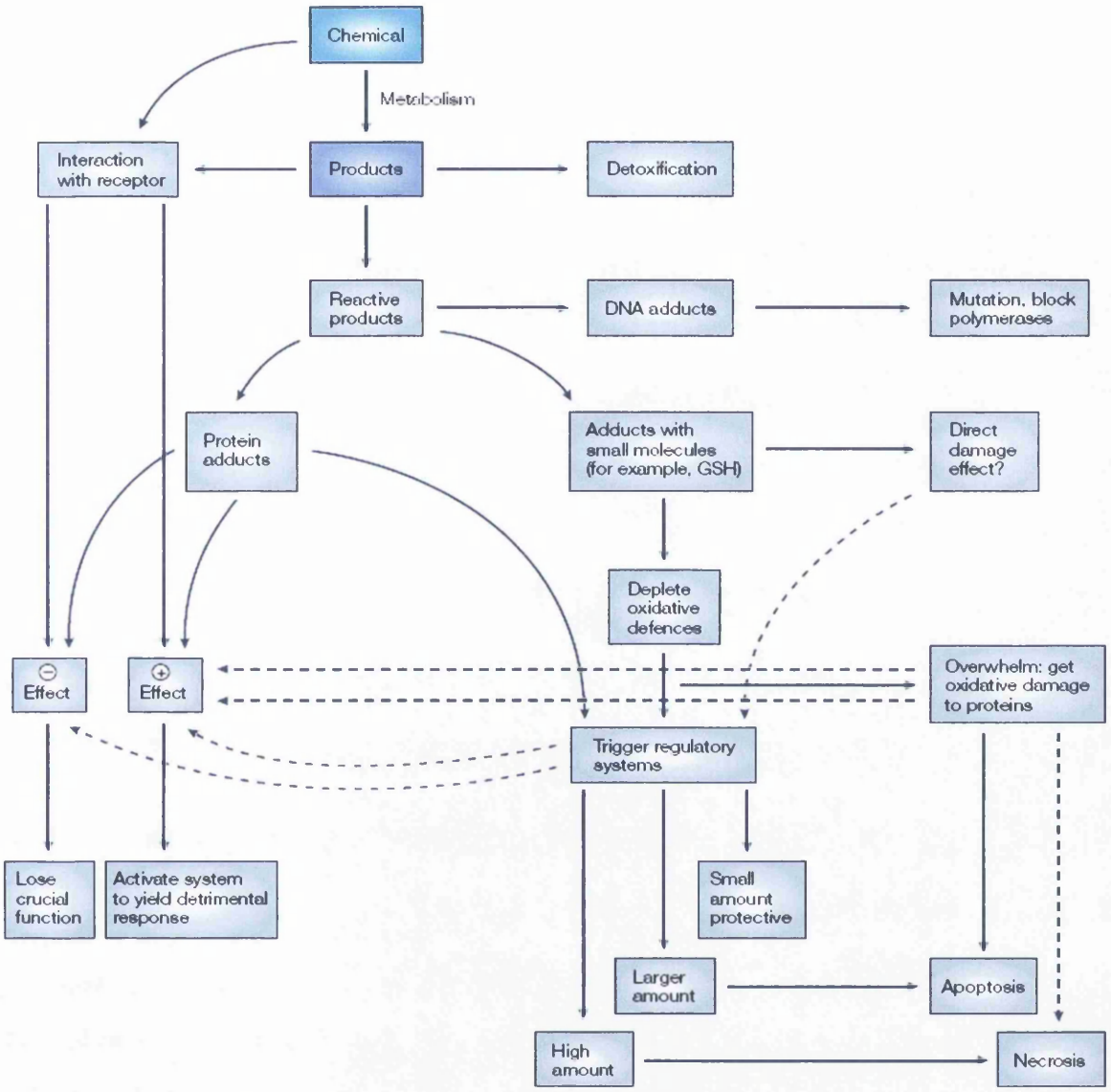

Fig. 3.4. Shows some of the events related to genotoxicity and toxicity of xenobiotics. (Adopted from Liebler & Guengerich, 2005).

3.3.1 Methods in Cytotoxicity Measurement

Various methods as well as measurement endpoints are employed in assessing cytotoxicity exerted by a compound of interest. Thus each of the method employed might differ in the terms of the data generated.

Vital dyes such as trypan blue or fast green are usually excluded from viable cells but can enter through damaged cell membranes to stain the cytoplasm, and they have long been used as indicators of non-viable cells. Trypan blue was used to study the cytotoxicity of anti-tumour drug in a variety of tumours and a good correlation was found between the *in vitro* responsiveness and the *in vivo* chemotherapy results in both animals and humans (Durkin *et al.*, 1979). The limitation of vital dye exclusion tests is that these type of assays measure dead necrotic cells with damaged membranes and may not measure dying or apoptotic cells with intact membranes.

Viable cells can be measured with colourimetric assays utilising a substrate whose colour is modified by living but not dead cells. One example was the development of a rapid colourimetric assay based on the tetrazolium salt 3-(4,5-dimethylthiazol-2-yl)-2,5-diphenyltetrazolium bromide (MTT) (Mosmann, 1983), which is cleaved and converted to a blue formazan by the mitochondrial dehydrogenase in active mitochondria. Thus, cellular metabolic activity is utilised to distinguish between viable and non-viable cells. Good correlation was observed between MTT and clonogenic assays for drug exposures in some cell lines (Carmichael *et al.*, 1987).

Activation of the caspase cascade is an integral event in the apoptotic pathway (Atkinson *et al.*, 1998) and caspase-3 activation is frequently accepted as a reliable marker for apoptosis (Nicholson *et al.*, 1995). Caspase 3 is part of the caspase cascade which initiates the cleavage of various proteins resulting in an ordered breakdown of the cell (Tewari *et al*, 1995).

Determining cell viability is important in assessing mutagenesis, malignant transformation, cellular pathology, toxicity and apoptosis. Furthermore, delineating mechanisms of carcinogenesis would be incomplete without cell viability assessment as tumours may only arise from abnormal living cells. The methods to be employed in cellular toxicity assessment and the advocated levels to be attained are defined in ICH and OECD guidelines (ICH 1995; OECD 1997a; OECD 1997b) that differ between test systems. Cloning efficiency or relative total growth (RTG) are required to be reduced by 80-90% whereas for cytogenetic assays including CBMA, the parameters needed is at least 50% reduction in binucleate index

(Kirsch-Volders *et al.*, 2003) or mitotic index, cell number and confluency (OECD 1997a). Subjecting compound of interest excessively cytotoxic doses may cause artefactual false positive data or difficulties in data interpretation (Kirkland, 1992; Galloway, 2000).

3.4 The Objective of the Study

The objective of this study was to assess the potential of andrographolide to induce genotoxic damage in V-79 as well as metabolically competent cell lines of AHH-1 and MCL-5 using the *in vitro* cytokinesis-block micronucleus assay. This assay was accompanied by kinetochore labelling using the CREST antibodies in order to determine the type of damage induced whether it is clastogenic or aneugenic in nature. Along with other methods of measurement, the cytotoxicity potential of andrographolide was also assessed using trypan blue-exclusion assay.

3.5 MATERIALS AND METHODS

3.5.1 Safety Aspects.

Disposable latex gloves were worn for every laboratory work conducted. Sterile conditions were achieved using Class II Cryomat Pharmaceutical lamina flow hoods which were routinely cleaned with 70% ethanol. Experiments involving toxic and dangerous chemicals were performed with extra gloves in the Class II lamina flow hood. The staining, fixation and mounting of the microscope slides were always conducted inside a flow hood. All items used for the experiments were routinely cleaned with 70% ethanol.

Andrographolide and other toxic compounds in solid form were weighed in the toxic handling room and dangerous substances were carefully disposed of in multi-layered toxic bags destined for incineration. Deionised water used for all experiments was UV-purified and filtered with the Milli-Q PF Ultrapure Water Purification System.

3.5.2 Annual Mycoplasma Testing.

Mycoplasmas are considered as serious contaminants of cell cultures. They are prokaryotes without cellular walls, belonging to the class Mollicutes, order Mycoplasmatules (McGarrity, 1984). They are amongst the smallest of self-replicating prokaryotes, approximately one-sixth the size of an *Escherichia coli* bacterium. They are capable of altering cellular functions like chromosomal arrangements, uptake of nucleic acid precursors, cell responses to mitogens and secretions of interferon by the cells. Mycoplasma may also deplete arginine or glutamine from the culture medium (Kouri *et al.*, 1983). It as been reported that they produce chromosomal and numerical aberrations of cultured cells (Fogh and Fogh, 1965; Paton *et al.*, 1965; Aula and Nichols, 1967) and for a review of the cytogenetic effects see McGarrity *et al.* (1984).

The annual screening of mycoplasma in the laboratory was achieved using MycoAlert® mycoplasma detection based on bioluminescence assay. Basically, the screening experiment was conducted in a two-step process where the reagent containing a substrate for specific enzymes secreted into the culture media by mycoplasma leading to the phosphorylation of

adenosine diphosphate to adenosine triphosphate. The addition of another reagent containing luciferase and luciferin, where the enzyme catalyses a light-generating reaction between ATP, oxygen and luciferin. Initially, 2ml of cell culture was centrifuged at 1500rpm for 5 minutes and 100µl of cleared supernatant was transferred into a sterile 96-well plate. Subsequently, 100µl of MycoAlert® was added to the 96-well plate and left at room temperature for 10 minutes. The luminometer was programmed to take one second integrated reading and the first reading was taken (reading A). Then, 100µl of MycoAlert Substrate solution was added to the same plate and left at room temperature for another 10 minutes before a second reading was taken (reading B). Finally, a ratio between the two readings was calculated and a ratio of less than 1, indicates uninfected cell line as the concentration of ATP in the sample is proportionate to light intensity. None of the cell lines used in the experiments were found to be positive of mycoplasma contamination in the annual screening process.

3.5.3 Introduction to AHH-1 and MCL-5 Cell Lines.

The AHH-1 $TK^{+/-}$ is a human B lymphoblastoid cell line that is derived from the RPMI-1788 cell line isolated from a healthy male donor. This culture was spontaneously transformed probably by the Epstein-Barr virus (Gentest Corporation manual, 1994), and the AHH-1 cell line was subsequently derived. The cell line has stable aryl hydrocarbon hydroxylase (AHH) activity, expressing mixed-function oxygenase (MFO) activity that is essential in oxidative xenobiotic metabolism. Mediated gene transfer of cytochrome P450 (CYP450) genes/cDNAs is a preferred method in the construction of metabolically competent cells (Crespi *et al.*, 1990). AHH-1 is homogenous, clonal derivative designed to be constitutively expressing a relatively high level of CYP1A1 (Crespi & Thilly, 1984) which is an isoform of cytochrome P450 that is involved in the oxidation of polycyclic aromatic hydrocarbons (PAH) hepatically in humans.

The MCL-5 cell line is a derivative of AHH-1 which has been transfected with five cDNAs namely CYP1A1, CYP1A2, CYP2A6, CYP3A4 and CYP2E1 as well as microsomal epoxide hydrolase that are carried on a vector (Crespi *et al.*, 1991). MCL-5 has been demonstrated to be more sensitive than the parent AHH-1 cell line and had been used successfully in

detecting genotoxic properties of many pro-mutagens and pro-carcinogens (Crespi *et al.*, 1991; Doherty *et al.*, 1996).

Human lymphoblastoid cell lines were chosen over rodent cell lines with metabolic activation (S9 liver extract) for several reasons. In comparison to rodent cells, human cells are known to be 1000 times more sensitive to some cytotoxic antibiotics, twice as sensitive to radiation and six times more sensitive to hydrogen peroxide (Cox *et al.*, 1977a; Cox *et al.*, 1977b; Hoffman *et al.*, 1984; Gupta & Prasad, 1992). AHH-1 and MCL-5 cell lines possess genetically enhanced levels of metabolising enzymes as stated before and they are known to be sensitive to chemically active agents and those which require metabolism to manifest their effects.

These cell lines are heterozygous for p53 but undergoes normal DNA repair and apoptotic responses upon genotoxins exposure (Guest & Parry, 1999). Both lymphoblastoid cell line possess a modal chromosome number of 48 with isochromosomes i(3q) and i(9p) (Doepker *et al.*, 1998; Corso & Parry 1999).

Furthermore, both cell lines which were chosen for micronucleus assay are also applicable in forward mutation assays (*HPRT* locus) allowing better data comparisons and illuminating mechanistic information.

3.5.4 Thawing Frozen AHH-1 and MCL-5 Cells.

The cryovial containing the cells were removed from the liquid nitrogen freezer; thawed in a water bath at 37 ± 1^0C for a few minutes and decontaminated by spraying with 70% ethanol. The growth medium used was RPMI-1640 that has been supplemented with 9% horse serum and 1% L-glutamine. The thawed cell suspensions were transferred to two $80cm^2$ plastic tissue culture flasks with 50ml of growth medium, which was pre-warmed at 37 ± 1^0C for 40 minutes. The flasks were then gassed with 5% CO_2 in air and incubated at 37 ± 1^0C. After 24 hours, the flasks were examined under the Nikon TMS phase contrast microscope proceeding from low, then to higher magnification, observing the condition of the cell cultures and any

sign of contamination. Sub-culturing procedure began approximately after four days of growth with 60-75% cell confluency.

The same procedure was employed for MCL-5 cells except 200μg/ml hygromycin-B was added to 50ml of growth medium. Hygromycin-B is an aminoglycosidic antibiotic produced by *Streptomyces hygroscopicus* and the recombinant vectors in MCL-5 are maintained as an extrachromosomal plasmids that confer resistance to hygromycin-B.

3.5.5 Sub-Culturing Procedure for AHH-1 and MCL-5 Cells.

The $80cm^2$ tissue culture flasks were shaken to dissociate loose cell aggregates that were growing exponentially and the cell suspension were dispensed into centrifuge tubes. The cell cultures were centrifuged at 1500rpm for 8 minutes and a Neubauer haemocytometer was used to determine the number of cells. Cell density was maintained at $1.5x10^5$ cells per ml and the cells were cultured for a maximum period of three weeks to ensure a stable karyotype (Doherty *et al.,* 1996). Prior to treatment, the cell cultures were seeded into several $25cm^2$ tissue culture flasks to achieve a final concentration of $1.5x10^5$ cells per ml. The cells were then gassed with 5% CO_2 in air and incubated at 37 ± 1^0C for 24 hours.

The same procedure was employed for MCL-5 cells except 200μg/ml hygromycin-B was added to the growth medium.

3.5.6 Introduction to V-79 Cell Line.

V-79 cells are an immortal cell line derived from male Chinese hamster (*Cricetulus griseus*) lung fibroblasts. It has a long history in its application for mutagenicity assays due to several properties. The cell line possesses a high cloning efficiency at 75-95%, able to grow rapidly from a small inoculum with a doubling time of 12 to 16 hours (Bradley *et al.*, 1981). It also has short lag period. V-79 cells have a relatively stable karyotype with a modal chromosome number of 22±1 that is relatively large, making this cell line suitable for aneuploidy studies (Bradley *et al.*, 1981).

V-79 cells were first grown in $80cm^3$ flasks in a monolayer, with Dulbecco's Modified Eagles Medium (DMEM), supplemented with 10% foetal bovine serum. The cells were gassed with 5% CO_2 in air and incubated at 37±1 °C.

Routine sub-culture of V-79 cells involved re-suspension of cells at $1x10^5$ cells/ml every 2-3 days with fresh growth medium, depending on the culture confluency. Detachment of cells from culture flask surface was achieved using 3ml of 2.5% trypsin-EDTA followed by brief incubation at 37±1 °C for one minute and gentle tapping.

None of the cell lines used were cultured continuously for more than three weeks and cells from new cryovials were used for each replicate of experiments. Cells were sub-cultured routinely but not to exceed 10 passage numbers.

3.5.7 Cell Doubling Time Determination.

The cell doubling times for AHH-1, MCL-5 and V-79 were determined beforehand. Even though the doubling times for these cell lines can be found in the literature, the author conducted a short experiment to determine the cells doubling time. The cells were seeded at the initial concentration of $1.5x10^5$ cells/ml in different $25cm^2$ culture flasks containing the necessary components to suitable growth media as stated previously. Each of the $25cm^2$ culture flasks were labelled to correspond to different time-points between 16 to 24 hours, where the cell number were determined using a Neubauer haemocytometer at the desired time-points. The result for this experiment was then used for subsequent experiments where the cell doubling time for V-79, AHH-1 and MCL-5 were established to be 18, 19 and 23 hours respectively and was considered to be comparable to those described in the literature (Gentest Technical Manual; Crofton-Sleigh *et al.*, 1993). However, a treatment time of 24 hours for all cell lines were adopted instead. The experiments were conducted in three replicates and the raw data can be found in Table A1 of the Appendix.

3.5.8 Treatment with Andrographolide.

Andrographolide (CAS no.5508-58-7; molecular weight 350.45) with 98% purity was stored in cool and dry place. Andrographolide to be used at various concentrations was prepared by dissolving the crystals with DMSO (CAS no.67-68-5, >99.5% purity) as solvent and administered to AHH-1/MCL-5/V-79 cell cultures within two hours of preparation. Fresh stocks were always prepared for each experiment replicates. Flasks containing healthy-looking, evenly distributed cells were selected and labelled according to doses. Less confluent flasks were allocated for negative control and low dose treatments while more confluent flasks were allocated for high dose treatments. After serial dilutions, the labelled $25cm^2$ flasks containing 10ml of cell cultures were treated with increasing doses andrographolide in DMSO to give 10-90μM final concentrations respectively. Two $25cm^2$ flasks were allocated for each dose and at the top dose of 90μM andrographolide, there was 0.9% DMSO. Four $25cm^2$ flasks were assigned as untreated negative control. Subsequently, 40μl of cytochalasin-B in DMSO was added to each flask giving a final concentration of 6μg/ml as suggested by Parry *et al.* (2002). The addition of cytochalasin-B was performed under subdued lighting as the compound is light sensitive. The final concentration of DMSO in the culture medium was less than 1%.

The cell cultures were then gassed with 5% CO_2 in air for approximately 10 seconds and incubated at 37 ± 1^0C for 24 hours. The possibility of andrographolide precipitation occurring in the growth medium pre- and post-incubation was determined earlier and at these concentrations, no precipitations were observed.

Positive control slides were obtained by treating the AHH-1 and MCL-5 cells with 25μg/ml Mitomycin –C (CAS no.50-07-7). Mitomycin-C (MMC) is a known cross-linking agent in the absence of exogenous metabolic activation which had demonstrated to be genotoxic in all *in vivo* and *in vitro* test systems using mammalian cells, including the in vitro micronucleus test (Gupta & Singh, 1982; Ishidate *et al.*, 1988; Mavournin *et al.*, 1990; Sofuni *et al.*, 1996; Matsushima *et al.*, 1999; von der Hude *et al.*, 2000). The Ames test also showed that MMC is a genotoxicant (Quillard *et al.*, 1985) and the compound was proven to be carcinogenic

(Ishidate *et al.*, 1988). DMSO at 90μM final concentration was also use as a second negative control since it was used as a vehicle for andrographolide.

In the initial phase of the study, a dose-setting assay was conducted where AHH-1 cells were treated with andrographolide between 10 and 100μM. However, the number of doses was later reduced.

3.5.9 Cell Harvesting and Slides Preparation.

After 24 hours, the cell suspensions were dispensed into correspondingly labelled 10ml centrifuge tubes and centrifuged at 1500rpm for 8 minutes. The supernatant was safely disposed and the cell pellets were re-suspended into clean and clearly labelled centrifuge tubes containing 3ml PBS (pH 7.4); they were vortexed using a Whorlimixer for one minute to achieve a suspension of single cells. 120μl of the each treated cell suspension were added into the wells of the cytospin and spun at 1000rpm for 5 minutes. Subsequently, slides were fixed in 90% ice-cold methanol for 10 minutes as described by Fenech (2000) and air-dried before storage at -20^0C.

3.5.10 Staining Techniques.

Staining with Giemsa.

The air-dried slides were immersed in 20% Giemsa solution for 8 minutes but the slides were examined after 6-7 minutes to ensure appropriate staining intensity, which is important for the scoring procedure. After 8 minutes, the slides were removed, rinsed twice in PBS (pH 6.8) for 5 minutes and air-dried. Subsequently, the slides were briefly dipped in Xylene (99.99%) and coverslips were immediately but carefully placed over the cells mounted with DPX. Care was taken to avoid the formation of air bubbles underneath the coverslips. Slides were viewed using the Olympus BH-2 light microscope.

Staining with Acridine orange.

Prepared slides were also stained with acridine orange. Fixed slides were placed in coplin jar containing 1.25μg/ml acridine orange for 10 seconds. The slides were then placed in phosphate buffer (pH 6.8) for 10 minutes and then transferred to fresh buffer and left for one

hour. The slides were air-dried in the dark and stored away from light. Olympus BH2-RCF fluorescence microscope with triple band-pass filter was used to view the slides, which involved placing a few drops of PBS (pH 7.4) onto the cytodots of the slides.

3.5.11 Cell Scoring Procedures.

The Giemsa-stained slides were coded and scored at 1000X magnification under oil immersion using an Olympus BH-2 light microscope. The scoring procedure was performed as described by Fenech *et al.* (2003) as shown in Figures 3.5, 3.6 and 3.7 respectively. The cells were categorised into mono-, bi-, tri-, tetra-, and multinucleated cells. In this study, micronuclei were scored in at least 2000 binucleated cells per dose; micronuclei in other cells were not taken into account.

As suggested by Fenech *et al.* (2003), the binucleated cells selected for scoring micronucleus frequency must possess the following characteristics.

1. The cells should be binucleated.
2. The presence of two nuclei with intact nuclear membranes and located within the same cytoplasmic boundary.
3. The two nuclei in a binucleated cell should be approximately equal in size, staining pattern and intensity.
4. The two main nuclei in a binucleated cell may touch but ideally should not overlap each other. A binucleated cell with two overlapping nuclei can only be scored if the nuclear boundaries of each nucleus are distinguishable.
5. The presence of intact cytoplasmic boundary or cell membrane and clearly distinguishable from the membrane of neighbouring cells.

The criteria adopted for classifying micronuclei in binucleated cells were as suggested by Fenech *et al.* (2003):

1. Micronuclei are oval or round in shape.
2. The diameter of micronuclei in human lymphocytes usually varies between $1/16^{th}$ and $1/3^{rd}$ of the mean diameter of the main nuclei which, corresponds to $1/256^{th}$ and $1/9^{th}$ of the area of one of the main nuclei in a binucleated cell respectively.

3. Micronuclei are not linked or connected to the main nuclei.
4. Micronuclei may touch but must not overlap the main nuclei and the micronuclear boundary should be distinguishable from the nuclear boundary.
5. Micronuclei usually have the same staining intensity as the main nuclei but occasionally staining may be more intense.
6. Micronuclei are non-refractile and they can therefore be readily distinguishable from artefacts such as staining particles.

Nucleoplasmic bridges (NPB) are sometimes observed in binucleated cells following exposure to clastogens and are believed to originate from rearranged chromosomes with more than one centromere, e.g. dicentric chromosomes. The criteria used for scoring nucleoplasmic bridges as suggested by Fenech *et al.* (2003):

1. NPB are a continuous nucleoplasmic link between the nuclei in a binucleated cell.
2. The width of a nucleoplasmic bridge may vary considerably but usually does not exceed ¼ of the diameter of the nuclei within the cell.
3. NPB should have the same staining characteristics of the main nuclei.
4. NPB are preferably scored in binucleated cells with clearly separated nuclei because it is usually difficult to observe an NPB when the nuclei are touching or overlapping.
5. A binucleated cell with a nucleoplasmic bridge may or may not contain one or more micronuclei and on rare occasions more than one nucleoplasmic bridge may be observed within one binucleated cell.

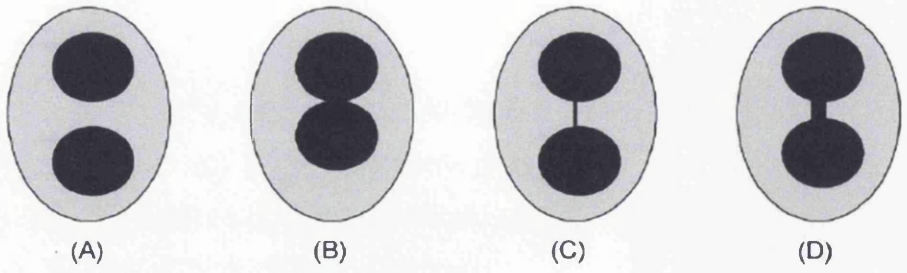

Fig. 3.5. Displays different binucleated cells that can be scored for micronuclei in the cytokinesis-block micronucleus assay. (A) is the ideal binucleated cell to be scored while (B) has a touching daughter nuclei. Nucleoplasmic bridges between the two daughter nuclei, as shown in (C) and (D), with (D) possessing a relatively wider bridge. (Adopted from Fenech *et al.*, 2003).

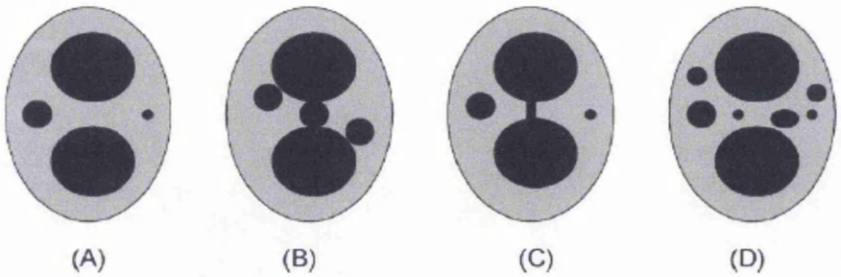

Fig. 3.6. Four examples where micronuclei presence in binucleated cells that are suitable for scoring. The relative sizes of the micronuclei is also shown. In (A), the cell contains two micronuclei with different sizes whereas in (B) the micronuclei touched but did not overlapped with the main nuclei. Nucleoplasmic bridge is observed in (C) and multiple micronuclei is shown in (D), a rare occurrence in cells. (Adopted from Fenech *et al.*, 2003).

The guidelines followed for scoring necrotic and apoptotic cells were as recommended by Fenech *et al.* (2003).

Necrotic cells:

1. Early necrotic cells can be identified by the presence of a pale cytoplasm with numerous vacuoles (mainly in the cytoplasm and some in the nucleus) and damaged cytoplasmic membrane with a fairly intact nucleus.
2. Late necrotic cells exhibit loss of cytoplasm and irregular/damaged nuclear membrane with only a partially intact nuclear structure and often with nuclear material leaking from the nuclear boundary.
3. Staining intensity of the nucleus and cytoplasm is usually less than that observed in viable cells.

Apoptotic cells:

1. Early apoptotic cells can be identified by the presence of chromatin condensation within the nucleus and intact cytoplasmic and nuclear boundaries.
2. Late apoptotic cells exhibit nuclear fragmentation into smaller nuclear bodies within an intact cytoplasm/cytoplasmic membrane.
3. Staining intensity in the nucleus, nuclear fragments and cytoplasm is usually greater than in viable cells.

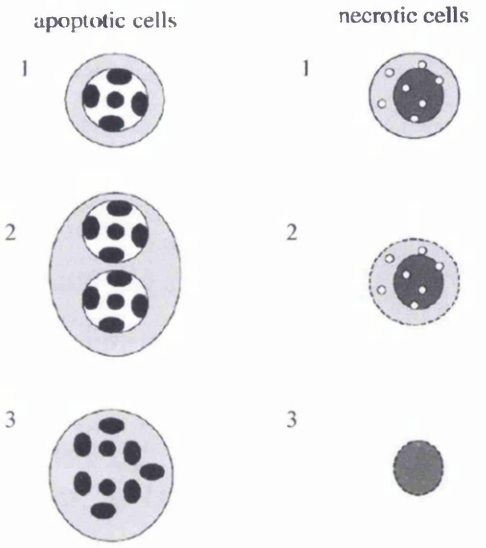

Fig. 3.7. Shows different stages of apoptotic and necrotic cell death. The mono- and binucleated cells shown experienced an early stage of apoptotic response where chromatin condensation occurred without disintegration of the plasma membrane, whereas the third example shows cells in late apoptosis with apoptotic bodies in the absence of nuclear membrane. In comparison, cells suffering from necrotic cell death show the presence of vacuoles, cytoplasmic loss and damage to the cell membrane. The first two examples are mononucleated cells in the early stage of necrosis and the third example is necrotic cell in late stage evident from the absence of cytoplasm and damaged nuclear membrane (Adopted from Fenech *et al.*, 2003).

3.5.12 Replication Index Calculation.

Apart from utilising the frequency of necrotic and apoptotic cells as biomarkers for cytotoxicity, assessment of toxicity was performed by determining cell proliferation in both treated and control cultures using the replication index (RI) values which denotes the relative number of nuclei in cell cultures exposed to test agent compared to negative control cultures as described by Kirsch-Volders *et al.* (2004):

$$RI = \frac{\left(Number\ of\ binucleates + 2 \times number\ of\ multinucleates\right)_T / Total\ number\ of\ cells_T}{\left(Number\ of\ binucleates + 2 \times number\ of\ multinucleates\right)_C / Total\ number\ of\ cells_C} \times 100$$

.....(1)

where T: test agent treatment culture; and C: solvent control culture.

Therefore, the measurement of reduction in treated cultures due to the presence of test agent;

$$Cytotoxicity = 100 - RI. \qquad .....(2)$$

3.5.13 Trypan Blue Exclusion Assay for Cell Viability.

AHH-1, MCL-5 and V-79 cells were grown in 25cm^2 culture flasks as described previously in Section 3.5.5; 3.5.6 and treated with various doses of andrographolide as mentioned in Section 3.5.8 respectively. After 24 hours, the cells were treated with various doses of andrographolide; gassed with 5% CO_2 and incubated for another 37±1^{0}C for 24 hours. Subsequently and as described by the manufacturer, 0.5ml of 0.4% Trypan Blue solution was transferred into centrifuge tubes containing 0.3ml HBSS. Cells that were floating and attached to the flask surface were collected; washed by centrifugation at 1500rpm for 5 minutes and re-suspended in HBSS in correspondingly labelled tubes. Then, 0.2ml of cell suspensions in HBSS that were prepared earlier, were transferred into each of those centrifuge tubes and mixed thoroughly (5 dilution factor). The cell number were counted using Neubauer haemocytometer; the ratios of viable and non-viable cells (blue-stained) in treated and untreated cells were determined.

Cell growth to determine any changes in cell counts was calculated as;

$$Cell\ growth = \frac{(Cell\ number\ in\ treated\ cultures)}{(Cell\ number\ in\ untreated\ cultures)} \times 100$$

3.5.14 Kinetochore labelling.

The indirect immunofluorescent labelling of kinetochore proteins was performed as described by Ellard *et al.* (1991) with some minor modifications. The prepared slides were removed from storage and were rehydrated in PBS at room temperature for one minute. The slides were then dipped in a primulin solution (0.005µg/ml) for 10 seconds in order to stain the cytoplasm. This was subsequently followed by washing and rewashing the slides in PBS and any excess PBS was removed.

CREST antibody was diluted in PBS with a 1:1 ratio and 50µl of the diluted antibody were applied onto the cytodots of each slide. Plastic cover slips were applied and the slides were incubated in humidified chambers at 37°C for 45 minutes.

After the incubation, the cover slips removed; slides were washed three times for 3 minutes in PBS with 1% bovine serum albumin (BSA) followed by washes in PBS for 3 minutes. The slides were left in PBS to prevent drying out while a second antibody was prepared. A second antibody, FITC-conjugated goat anti-human IgG with PBS in 1:100 ratio and 50µl of the diluted antibody were applied onto the cytodots of each slide. Cover slips were added and the slides were incubated for 45 minutes in humidified chambers. Again, the slides were washed twice with PBS+1% BSA followed by a final wash with water to remove salt. The slides were then left to air-dry in the dark and kept at 20°C until needed.

To visualise the signals, 20µl DAPI/Antifade (1µl + 9µl water + 990µl vectashield) solution were added and the slides viewed using Olympus BH-F Fluorescence microscope. The DAPI and fluorochrome signals of the kinetochore can be visualised through the triple band filter.

3.5.15 Statistical Analyses.

The t-test was employed to assess whether the means of two groups examined were statistically different from each other and the 95% ($p<0.05$) confidence limits were adopted. Dunnett's test is a multiple comparison post-hoc test performed after an ANOVA or t-test, which compares all treatment data against the control. A sample size formula was included guaranteeing the possibility of correctly detecting each treatment with mean value. Again, a 95% level of confidence was applied ($p<0.05$ significance) to reject the null hypothesis. The SPSS® statistical analysis software was employed in performing the analyses.

Figure 3.8 shows a flow chart that briefly summarised the materials and methods employed.

Fig. 3.8 The flow chart for materials and methods employed in CBMA.

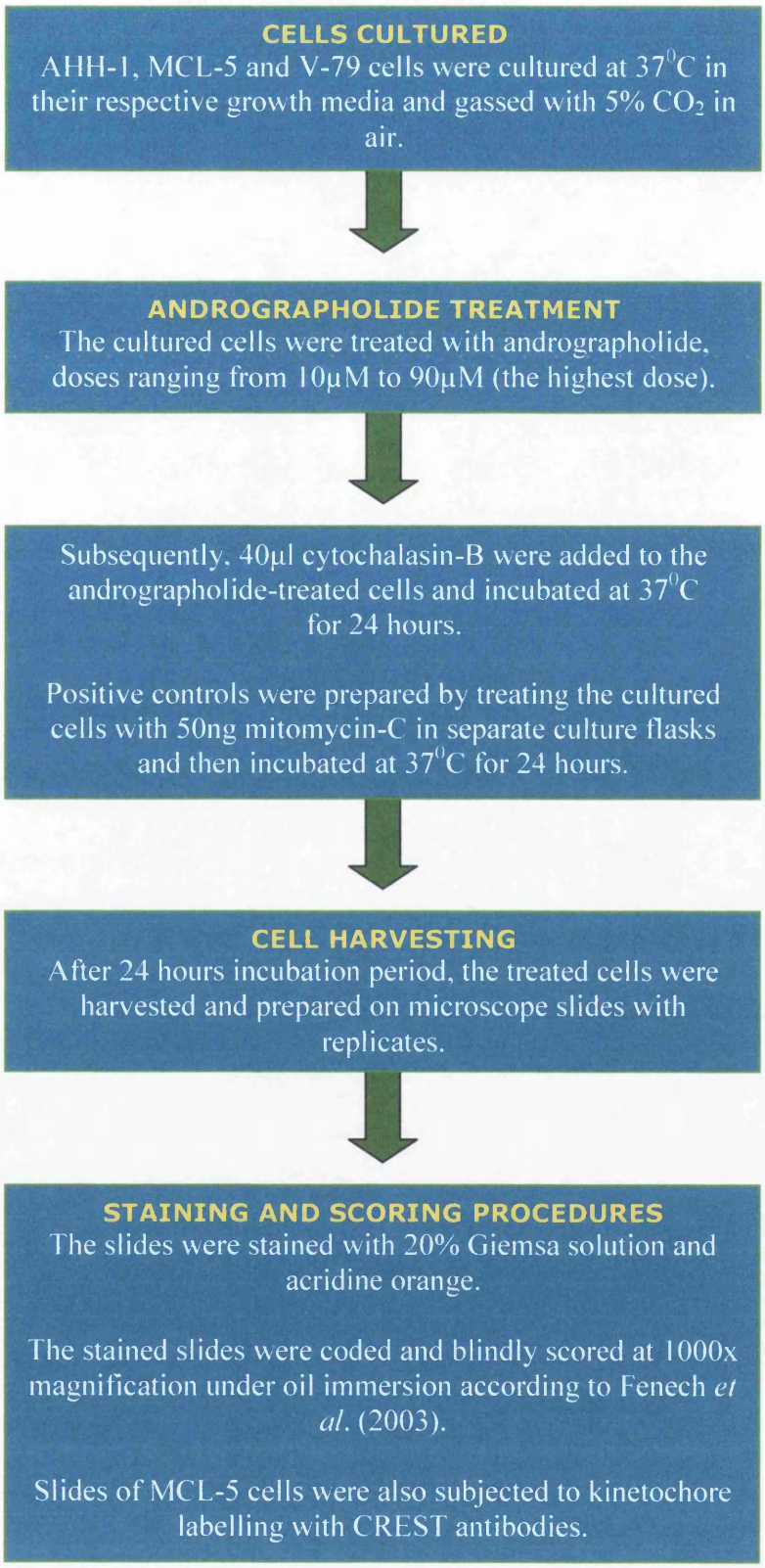

3.6 RESULTS

The dose-setting experiment for *in vitro* CBMA was conducted on AHH-1 cells treated with andrographolide and the results tabulated in Table 3.2. Andrographolide induced micronuclei and cytotoxicity at the concentrations as indicated in Table 3.2. In further experiments, the number of andrographolide doses used was reduced from 10 to 5 since no significant difference was observed between the 10 doses adopted initially. Subsequently, the same dose-range selected for AHH-1 was used in treating V-79 and MCL-5 cell lines respectively.

Table 3.2. A summary of CBMA data on AHH-1 cells treated with andrographolide for dose-setting assay.

Dose (μM)	Mean % Binucleated cells	Mean % Mn/Bi	Mean Relative RI	Mean % Cytotoxicity
0	56.61	0.15	100.00	0.00
10	51.48	0.33*	91.45*	8.55*
20	50.23	0.33*	89.36*	10.64*
30	44.36	0.40*	79.03*	20.97*
40	42.05	0.35*	75.40*	24.60*
50	35.67	0.35*	64.52*	35.48*
60	34.44	0.18	61.84*	38.16*
70	22.00	0.18	38.95*	61.05*
80	21.92	0.13	38.54*	61.46*
90	16.85	0.05*	29.55*	70.45*
100	15.84	0.03*	27.80*	72.20*

Notes: Mn/Bi: Micronuclei in binucleates; RI: Replicative index. *Indicates statistically significant difference against the negative control ($p<0.05$).

V-79, AHH-1 and MCL-5 cells were employed in determining the genotoxicity potential of andrographolide using the *in vitro* cytokinesis block micronucleus assay. The results obtained are tabulated and the raw data are available in the Appendix. As shown in Tables 3.3, 3.4 and 3.5 respectively, the mean percentage of binucleated cells decreased with increasing dose of andrographolide in all three cell lines tested. Figure 3.12 shows an example of a binucleated AHH-1 cell harbouring two micronuclei stained with acridine orange. The frequency of micronuclei in binucleated cells exhibit the same pattern in all three cell lines where the values accrued steadily with dose before beginning to decrease at 70 and 90μM doses respectively. As shown in Tables 3.3 and 3.5, andrographolide was capable of inducing micronuclei in binucleated cells with statistically significant difference to the negative control between the doses of 10 and 50μM in AHH-1 and V-79 cells respectively. In

comparison, 30 to 50μM of the same phytochemical were required to cause the same effect in MCL-5 cells. For both V-79 and AHH-1, 30μM of the compound caused the highest statistically significant induction of micronuclei in binucleated cells. As for MCL-5, which has five cytochrome CYP450 isoforms compared to AHH-1 cells, the highest statistically significant value ($p<0.05$) of micronuclei occurrence was observed at 50μM of andrographolide as tabulated in Table 3.4. Graphs in Figures 3.9, 3.10 and 3.11 each illustrated the steady reduction of binucleated cells and the frequency of micronuclei induced by andrographolide in AHH-1, MCL-5 and V-79 cells during 24 hours treatment period.

Table 3.3. A summary of CBMA data on AHH-1 cells treated with andrographolide.

Dose (μM	Mean % Binucleated cells	Mean % Mn/Bi	Mean Relative RI	Mean % Cytotoxicity
0	57.10	0.16	100.00	0.00
10	51.21	0.30*	90.27*	9.73*
30	44.19	0.40*	78.31*	21.69*
50	35.20	0.33*	62.83*	37.17*
70	22.05	0.18	38.56*	61.44*
90	16.92	0.05*	29.29*	70.71*
MMC	50.16	1.90*	90.47*	9.53*

Notes: Mn/Bi: Micronuclei in binucleates; RI: Replicative index. *Indicates statistically significant difference against the negative control ($p<0.05$). MMC refers to mitomycin-c.

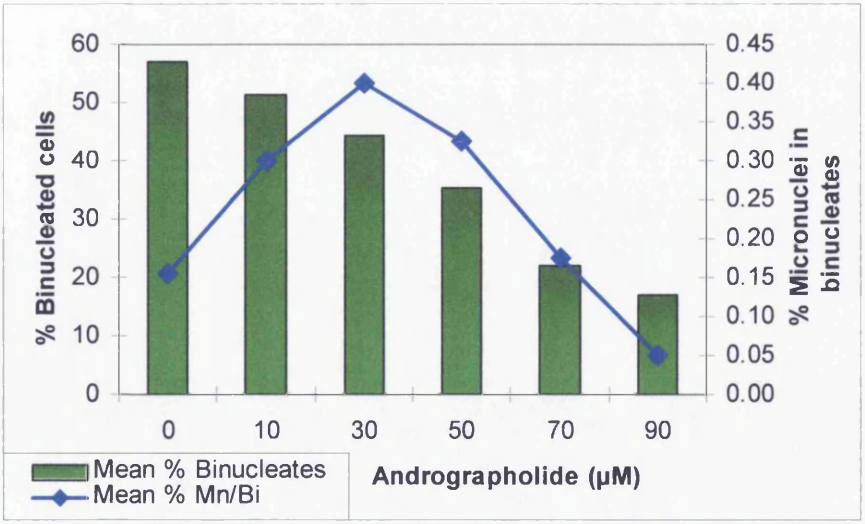

Fig. 3.9 Binucleated cell frequency and the incidence of micronuclei in AHH-1 cells treated with andrographolide for 24 hours.

Table 3.4. A summary of CBMA data on MCL-5 cells treated with andrographolide.

Dose (μM	Mean % Binucleated cells	Mean % Mn/Bi	Mean Relative RI	Mean % Cytotoxicity
0	54.79	0.14	100.00	0.00
10	50.42	0.15	93.95*	6.05*
30	40.53	0.33*	74.78*	25.22*
50	34.82	0.40*	64.57*	35.43*
70	22.34	0.13	40.37*	59.63*
90	18.66	0.08	33.59*	66.41*
MMC	49.74	2.30*	92.91*	7.09*

Notes: Mn/Bi: Micronuclei in binucleates; RI: Replicative index. *Indicates statistically significant difference against the negative control ($p<0.05$). MMC refers to mitomycin-C.

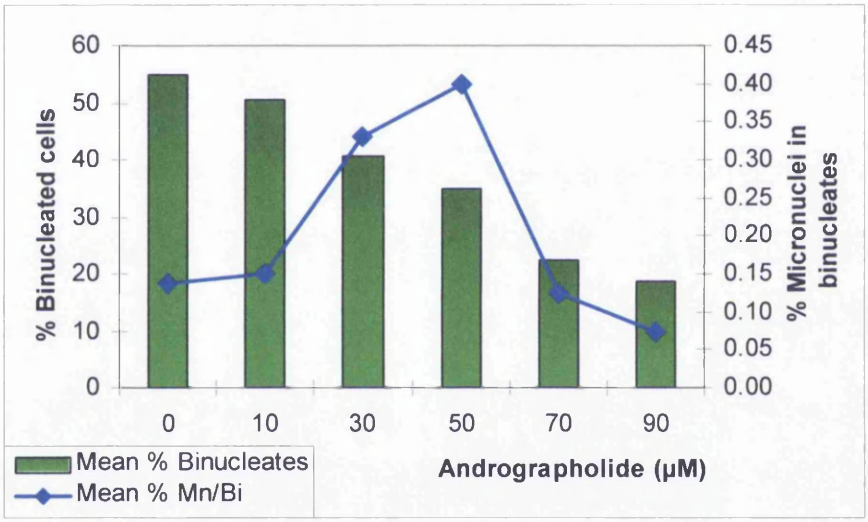

Fig. 3.10 Binucleated cell frequency and the incidence of micronuclei in MCL-5 cells treated with andrographolide for 24 hours.

Table 3.5. A summary of CBMA data on V-79 cells treated with andrographolide.

Dose (μM	Mean % Binucleated cells	Mean % Mn/Bi	Mean Relative RI	Mean % Cytotoxicity
0	45.44	0.14	100.00	0.00
10	41.29	0.33*	92.66*	7.34*
30	38.20	0.50*	83.60*	16.40*
50	28.88	0.43*	66.07*	33.93*
70	19.63	0.15	42.68*	57.32*
90	17.11	0.08	36.92*	63.08*
MMC	41.08	2.20*	91.91*	8.09*

Notes: Mn/Bi: Micronuclei in binucleates; RI: Replicative index. *Indicates statistically significant difference against the negative control ($p<0.05$). MMC refers to mitomycin-c.

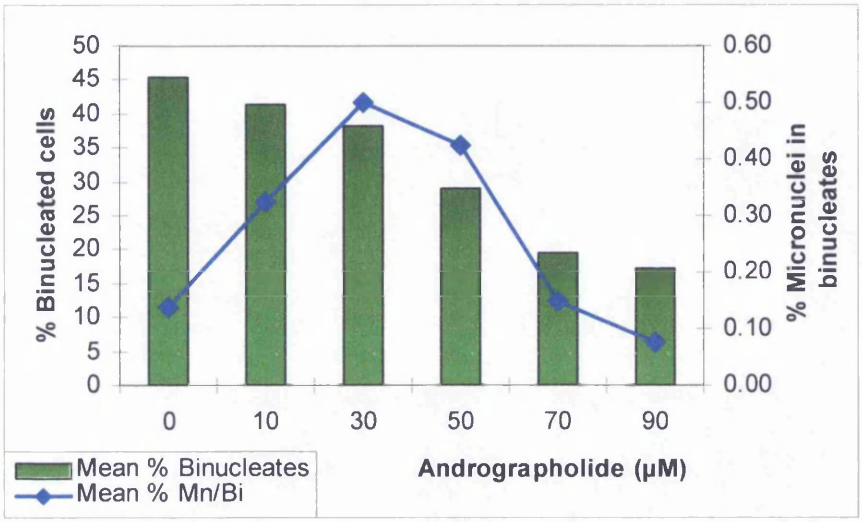

Fig. 3.11 Binucleated cell frequency and the incidence of micronuclei in V-79 cells treated with andrographolide for 24 hours.

Although, the presence of nucleoplasmic bridges in binucleated cells were also examined, there were only random and very rare incidence of this particular endpoint (data not shown). Nucleoplasmic bridge is an indicator for the occurrence of dicentric chromosomes resulting from DNA mis-repair or telomere end-fusions (Haaf *et al.*, 1999; Umegaki & Fenech, 2000). The incidence of micronucleated mononucleate counted in AHH-1 and MCL-5 cells also did not exhibit a statistically significant difference between the doses of andrographolide except at 90μM where the compound was clearly cytotoxic as shown in Table 3.6.

Table 3.6. The frequency of mononucleate AHH-1 and MCL-5 cells harbouring micronuclei after treatment with andrographolide.

Dose (μM)	AHH-1	MCL-5
0	0.10	0.08
10	0.13	0.13
30	0.12	0.12
50	0.11	0.12
70	0.05	0.04
90	0.03*	0.02*

Notes: Mn/Mono: Micronuclei in mononucleates; *Indicates statistically significant difference against the negative control ($p<0.05$).

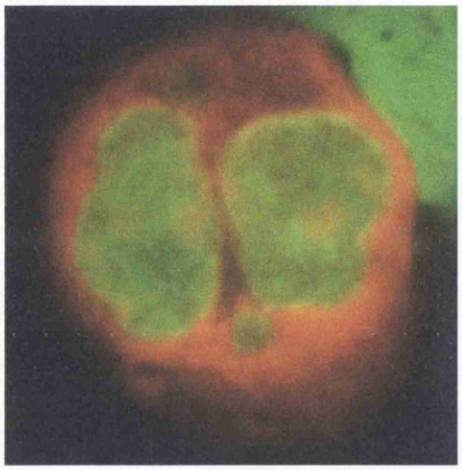

Fig. 3.12 A binucleated AHH-1 cell with two micronuclei stained with acridine orange (1000x magnification)

Table 3.7. Comparison of the incidence of micronuclei in binucleated cells between different cell lines.

Dose (μM	AHH-1 (1)	MCL-5 (2)	V-79 (3)	Difference
0	0.16	0.14	0.14	None
10	0.30*	0.15*	0.33*	1 vs. 2; 2 vs. 3
30	0.40	0.33*	0.50*	2 vs. 3
50	0.33	0.40	0.43	None

Notes: *Indicates statistically significant difference ($p<0.05$) against the mean Mn/Bi values between the cell lines. Each value were tested against each other as shown above and unless stated otherwise, the difference were regarded to be insignificant. The numbers in brackets represent the cell lines.

Linear regression analysis on the incidence of micronuclei revealed that the probability of dose-response relationship for the doses tested to be not significant, thus higher doses of andrographolide may not induce more micronuclei.

The data obtained also demonstrated that these three cell lines exhibited different frequency of micronuclei indicating that the properties of these cell lines may be attributed to such incidence. Table 3.7 compares the micronuclei values for the cell lines tested where andrographolide at 10μM caused significant incremental increases of micronuclei frequency in AHH-1 and V-79, with the values registered for these cell lines were significantly lower than that observed in MCL-5, hence MCL-5 was capable of tolerating the presence of andrographolide at this dose. At 30μM of the phytochemical, there was significant difference between micronuclei induction in MCL-5 and V-79 but not between MCL-5 and AHH-1 nor

those of AHH-1 and V-79. No difference was observed at 50μM of andrographolide. It can be proposed that MCL-5 superior metabolic capacity plays a role in this observation.
The levels of andrographolide cytotoxicity were measured using different methods. Mean cytotoxicity percentages tabulated in Tables 3.3, 3.4 and 3.5 were calculated using the equation (1) that measured cell replicative index (RI) and cytotoxicity values were derived from equation (2) as stated in Section 3.5.9. Andrographolide cytotoxicity in all cell lines tested upon, exhibited a steady increase in tandem with dose where 70 and 90μM of the phytochemical caused cell death and reduced cell viability in more than 50% of cells.

Apart from RI calculations on cytotoxicity, cell death was also measured via microscopical identification of necrotic and apoptotic cells. The results obtained were tabulated and the significant difference ($p<0.05$) against the negative controls for necrotic and apoptotic cells were shown in Tables 3.8, 3.9 and 3.10 respectively. It was found that the trend witnessed in RI cytotoxicity calculations was mirrored in the incidence of necrotic and apoptotic cells in all cell lines. The data also revealed that the cells died primarily via necrosis compared to apoptosis. There was significant dose-dependent accruement of necrotic cells and comparable to the RI cytotoxicity values, the concentration of 70 and 90μM of andrographolide induced more than 50% of cell population to die via necrosis. The percentage of apoptotic cells in all cell lines increased with dose until 30μM but beginning from 50μM to the highest concentration of andrographolide tested, the values started to dwindle. None of the concentrations tested cause apoptosis more than 2% of the cell populations in the cell lines tested. However, 30 and 50μM andrographolide produced higher number of apoptotic response in AHH-1 and MCL-5 cells relative to other concentrations and statistically significant against the negative controls. In V-79 cells, 30μM of andrographolide produced 1.38% of apoptotic cells which is statistically significant compared to negative controls. More than 50% of AHH-1, MCL-5 and V-79 cells died via necrosis compared to less than 0.45% of apoptotic cells at the top doses of 70 and 90μM, a value that was generally less than those observed in negative control. Reduced cell number was also observed on the scored slides as the concentration of andrographolide increased. The dose of andrographolide that caused more than 1% of apoptotic cells were observed to be those that caused micronuclei induction, which were 30 and 50μM respectively.

Table 3.8. A summary of cell death data on AHH-1 cells challenged with andrographolide for 24 hours.

Dose (μM)	Mean % Necrotic cells	Mean % Apoptotic cells
0	8.44	0.41
10	12.20*	0.90*
30	35.85*	1.15*
50	41.93*	1.13*
70	49.65*	0.83*
90	66.05*	0.35

*Indicates statistically significant difference against the negative control ($p<0.05$).

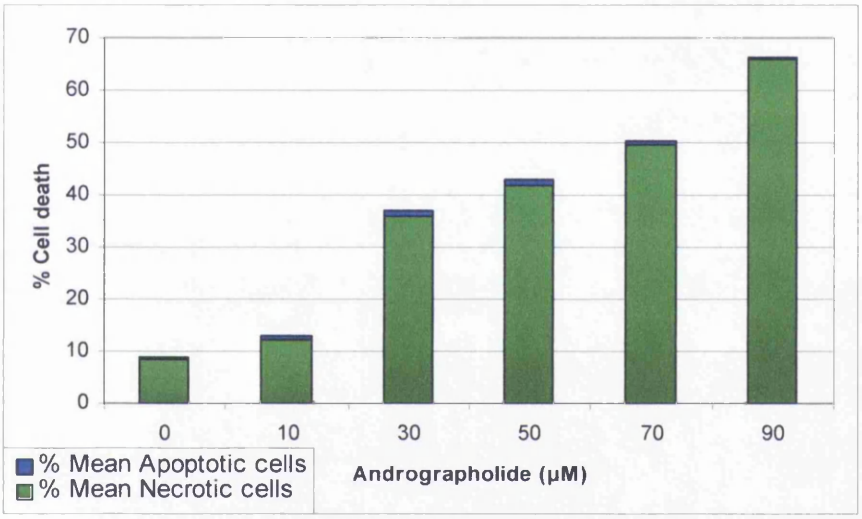

Fig. 3.13. A graph to show the induction of necrotic and apoptotic cell death in AHH-1 cells treated with andrographolide for 24 hours.

Table 3.9. A summary of cell death data on MCL-5 cells challenged with andrographolide for 24 hours.

Dose (μM)	Mean % Necrotic cells	Mean % Apoptotic cells
0	7.75	0.46
10	15.28*	0.75*
30	35.55*	1.27*
50	46.51*	1.02*
70	61.15*	0.83*
90	65.88*	0.45

*Indicates statistically significant difference against the negative control ($p<0.05$).

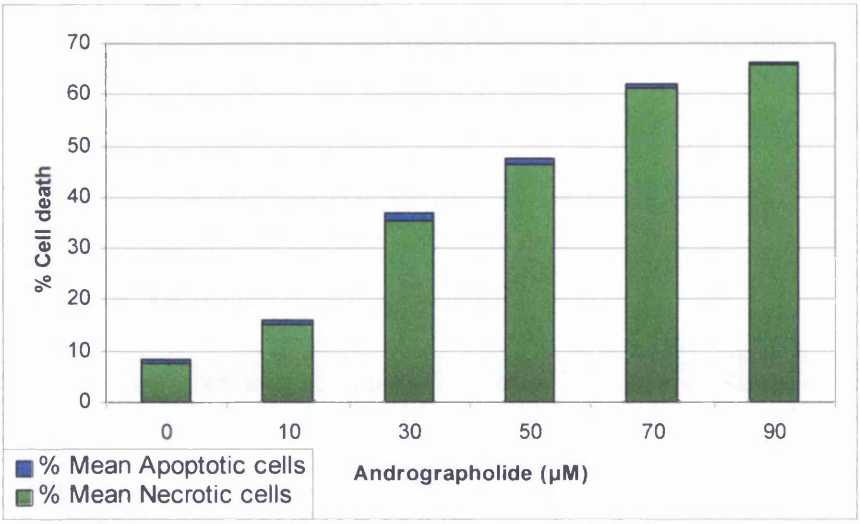

Fig. 3.14. A graph to show the induction of necrotic and apoptotic cell death in MCL-5 cells treated with andrographolide for 24 hours.

Table 3.10. A summary of cell death data on V-79 cells challenged with andrographolide for 24 hours.

Dose (μM)	Mean % Necrotic cells	Mean % Apoptotic cells
0	8.16	0.40
10	15.43*	0.88*
30	24.73*	1.38*
50	41.80*	0.80*
70	50.48*	0.35
90	69.00*	0.30

*Indicates statistically significant difference against the negative control ($p<0.05$).

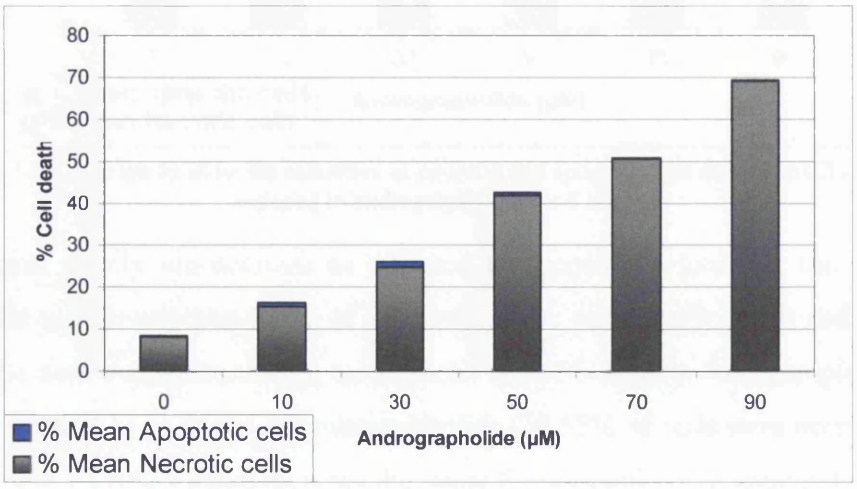

Fig. 3.15. A graph to show the induction of necrotic and apoptotic cell death in V-79 cells treated with andrographolide for 24 hours.

Determination of the influence of treatment duration on andrographolide exposure was also conducted with the aim of determining the prevalent mode of cell death preformed using only MCL-5 cell line. As tabulated below in Table 3.11, MCL-5 cells incubated for 8 hours in the presence of andrographolide showed a similar trend to longer duration treatment of 24 hours. The data were presented graphically in Figure 3.16.

Table 3.11. A summary of cell death data on MCL-5 cells exposed to andrographolide for 8 hours.

Dose (μM)	Mean % Necrotic cells	Mean % Apoptotic cells
0	7.58	0.39
10	10.82	0.83
30	18.08*	1.30*
50	20.35*	1.43*
70	33.70*	0.43*
90	41.40*	0.35*

*Indicates statistically significant difference against the negative control ($p<0.05$).

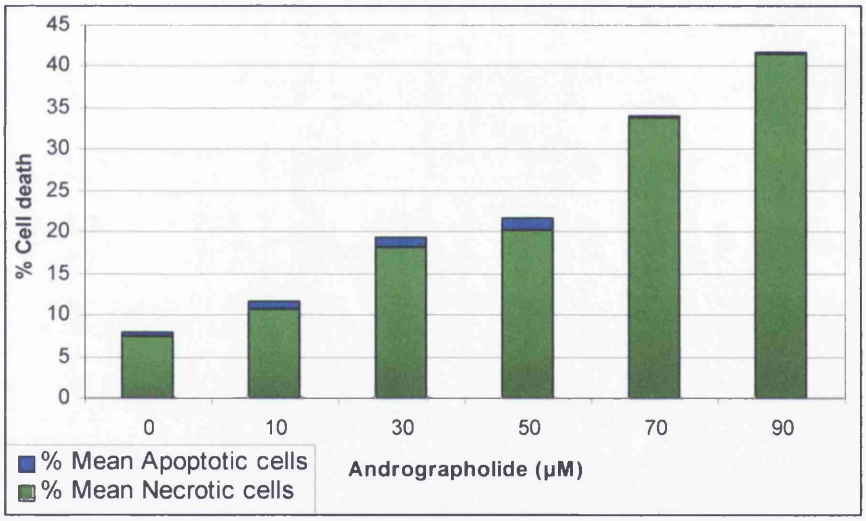

Fig. 3.16. A graph to show the induction of necrotic and apoptotic cell death in MCL-5 cells exposed to andrographolide for 8 hours.

The cells died mainly via necrosis as opposed to apoptosis. However, the percentage of necrotic cells was lower than those of apoptotic cells, particularly at 30 and 50μM which were also the dose that induced high micronuclei in MCL-5 cells. For example, in reference to Tables 3.9 and 3.11 at 30μM of andrographolide, 35.55% of cells were necrotic compared to 18.08% during 8 hours incubation but the value for apoptotic cells were not different from each other at 1.27%(24 hours) and 1.30%(8 hours) respectively. This data demonstrated that

the induction of necrosis in MCL-5 cells was time-dependent apart from relying on the concentration of the compound administered whereas apoptotic response was not. The percentage of apoptotic cells was similar between short and longer treatment periods.

Cellular viability was also assessed using the trypan-blue exclusion assay and three replicate experiments were performed on AHH-1 and MCL-5 cells whilst retaining the same dose range used in CBMA studies. The results are tabulated in Tables 3.12 and 3.13 for the two cell lines respectively. Correspondingly, cell count data revealed that cell growth was also reduced when the dose increased. MCL-5 cells exposed to andrographolide for one cell cycle also exhibited a same trend as observed in AHH-1. There was a reduction in both cell viability and cell growth. Figures 3.17 and 3.18 compares the values of non-viable cells and cell growth inhibition in AHH-1 and MCL-5 cells. Andrographolide seemed to have a relatively more profound effect ($p<0.05$) on MCL-5 cell growth than on AHH-1 cells evident from cell growth inhibition values at the same concentration of the phytochemical due to cytotoxicity as shown in Table 3.14.

Therefore, cumulatively all the data generated on the cytotoxicity of andrographolide using RI calculation, microscopical identification and trypan-blue exclusion assay painted a similar picture where this diterpene lactone phytochemical affects cell growth and caused cell death primarily via necrosis in a dose-dependent manner. However, apoptotic response was observed to be highest at 30 and 50µM, which also elicit high micronuclei formation.

Table 3.12. Cell viability data summary assessed by Trypan-blue on AHH-1 cells treated with andrographolide.

Dose (µM)	Mean % Non-viable cells	Mean % Viable cells	Mean cell growth (% tc negative control)
0	2.55	97.45	100.00
10	6.89*	93.11	98.69
30	21.54*	78.46	97.06
50	31.97*	68.03	91.61
70	54.40*	45.60	68.88
90	66.22*	33.78	53.23

*Indicates statistically significant difference against the negative control ($p<0.05$).

Table 3.13. Cell viability data summary assessed by Trypan-blue on MCL-5 cells treated with andrographolide.

Dose (μM)	Mean % Non-viable cells	Mean % Viable cells	Mean cell growth (% tc negative control)
0	3.10	96.90	100.00
10	5.54	94.46	88.98
30	20.53*	79.47	79.91
50	40.27*	59.73	74.15
70	59.90*	40.10	48.09
90	69.86*	30.14	41.47

*Indicates statistically significant difference against the negative control ($p<0.05$).

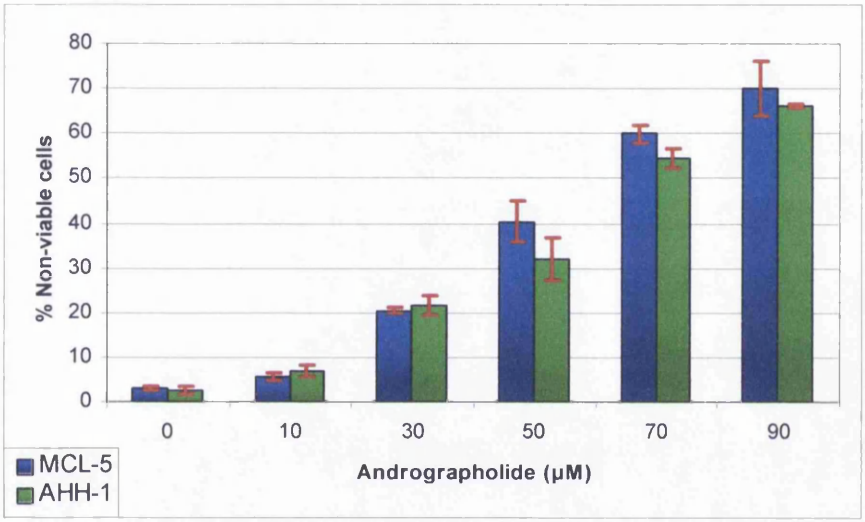

Fig. 3.17. A bar graph comparing the mean percentage of non-viable cells in MCL-5 and AHH-1 cells treated with andrographolide for one 24 hours as measured using the trypan-blue exclusion assay.

Table 3.14. Effect of andrographolide on the growth of MCL-5 and AHH-1 cells.

Dose (μM)	MCL-5	AHH-1
0	100.00	100.00
10	88.98	98.69
30	79.91*	97.06
50	74.15*	91.61
70	48.09*	68.88
90	41.47*	53.23

*Denotes significant difference against the values in AHH-1 cells ($p<0.05$).

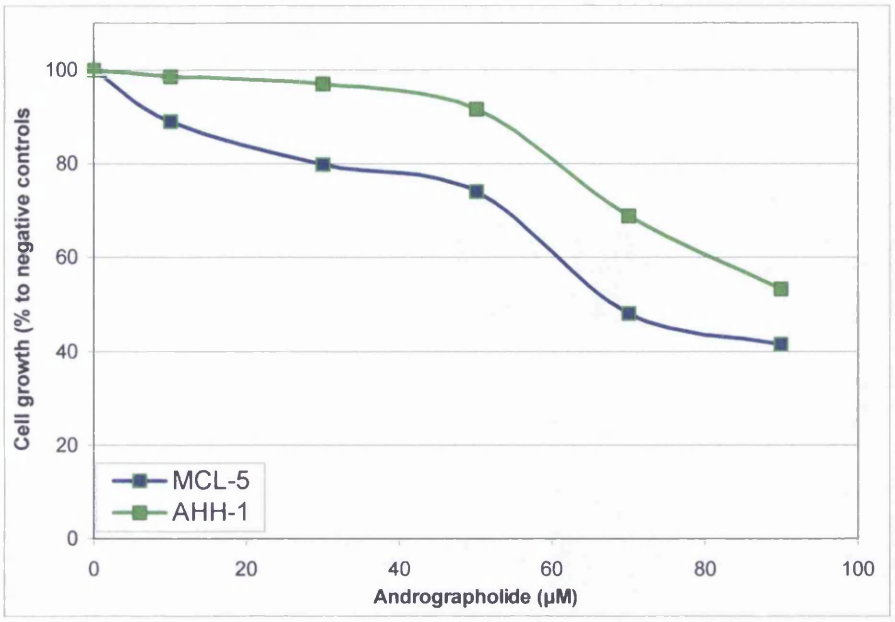

Fig. 3.18. A line graph comparing the effect of increasing concentration of andrographolide at various concentrations on the growth of MCL-5 and AHH-1 cells exposed to the phytochemical for 24 hours.

In order to elucidate the mechanism through which andrographolide induces micronuclei, kinetochore labelling utilising CREST anti-kinetochore antibodies was performed on treated MCL-5 cells. A total of 60 binucleates harbouring micronuclei were scored for the presence or absence of kinetochore within the micronuclei. Three replicates of experiment with new stocks of andrographolide were performed yielding a grand total of 180 micronuclei scored per dose. The data obtained were tabulated and graphically presented in Table 3.15 and Figure 3.19 respectively. Clearly, andrographolide possesses the propensity to cause the loss of whole chromosomes with increasing dose indicated by the increasing frequency of kinetochore positive micronuclei compared to untreated cells. Andrographolide induced 0.40% micronuclei in MCL-5 cells at 50μM, which was the highest value recorded and more than 70% of the micronuclei scored were positive indicating the presence of chromosomes with centromere. Thus, this phytochemical acts in aneugenic manner causing the loss of whole chromosomes that were later manifested as micronuclei. Figure 3.20 overleaf shows images of kinetochore-positive micronuclei and a kinetochore-negative micronucleus observed using the Olympus BH2-RCF fluorescent microscope.

Table 3.15. Data summary showing the mean results of kinetochore labelling in MCL-5 cells treated with andrographolide in cytokinesis-block micronucleus assay.

Andrographolide (μM	Mean % Kinetochore positive	Mean % Kinetochore negative
0	48.33	51.67
10	52.78	47.22
30	63.89	36.11
50	72.22	27.78

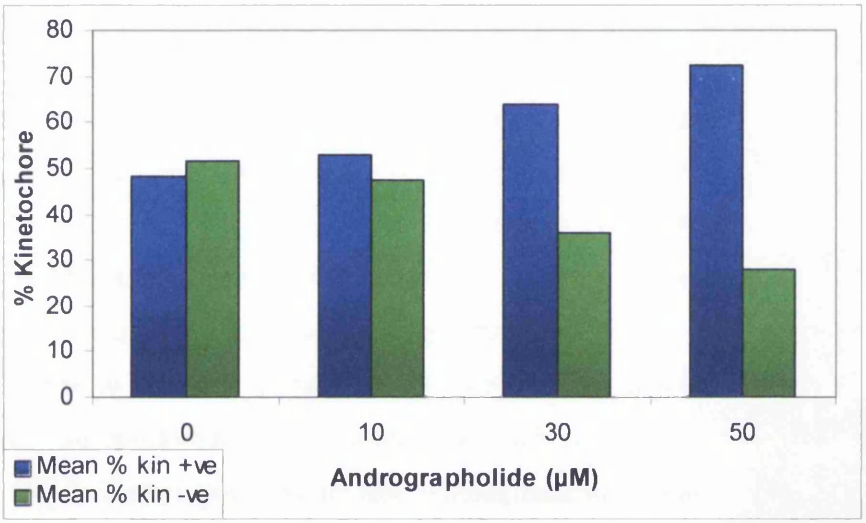

Fig. 3.19 Bar graph comparing the induction of kinetochore positive against kinetochore negative in MCL-5 cells treated with andrographolide in cytokinesis-block micronucleus assay.

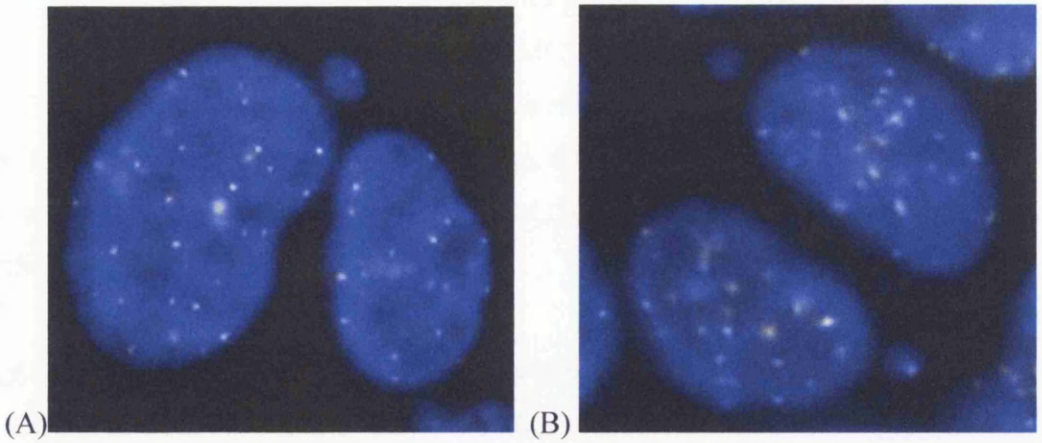

Fig. 3.20 Shows two examples of binucleated cells with micronuclei subjected to kinetochore labelling. In (A), the micronucleus is kinetochore positive whereas in (B) both kinetochore positive and negative micronuclei were detected. (1000x magnification).

3.7 DISCUSSION

Realising the medical potential of *Andrographis paniculata* especially andrographolide based on previous publications and the paucity of genotoxicity information on the compound, determining the genotoxicity potential of the phytochemical was deemed to be imperative.

As discussed previously, *in silico* assessment of a compound of interest utilising CSAR was very useful but insufficient in drawing a reliable conclusion. The author showed that toxicity assessment of andrographolide employing an expert knowledge-based system DEREK, which anticipated the compound to be capable of causing chromosome damage *in vitro* due to the presence of α-alkylidene γ-butyrolactone moiety. Furthermore, the author also employed METEOR, another knowledge-based program harnessing QSAR concept to predict biotranformation routes of andrographolide and its possible metabolites. As elaborated earlier in Chapter 2, andrographolide can be subjected to various Phase I/II reactions and the α-alkylidene γ-butyrolactone moiety of the phytochemical is also a metabolism target. Thus, a genotoxicity test will augment such findings.

The *in vitro* cytokinesis-block micronucleus assay was used to assess the genotoxicity potential of andrographolide on three cell lines namely V-79, AHH-1 and MCL-5 where the latter two are metabolically competent with MCL-5 being more sensitive due to the presence of cDNAs for four human cytochromes plus microsomal epoxide hydrolase (Crespi *et al.*, 1991). To the best of the author's knowledge, this is the first study utilising *in vitro* CBMA, which is a recommended Stage I assay (COM, 2000) in examining the genotoxicity potential of andrographolide.

Andrographolide Induced Aneugenicity *in Vitro.*

The phytochemical caused statistically significant ($p<0.05$) incidence of micronuclei between 10 and 50μM in AHH-1 and V-79 cell lines and the values decreased between 70 and 90μM. In MCL-5 cell line, which is metabolically superior to both AHH-1 and V-79 cells, exposure of the cells to 10μM for one cell cycle did not elicit substantial genotoxic damage.

Statistically significant ($p<0.05$) inductions of micronuclei were only observed in MCL-5 cells challenged with 30 and 50μM but the two top doses tested did not cause increases in micronuclei frequency. The lower incidence of micronuclei witnessed in all cell lines at higher andrographolide concentrations of 70 and 90μM was primarily due to high cytotoxicity exerted by the phytochemical.

The interesting part of the data obtained concerns the difference in micronuclei frequency between the cell lines tested. As summarised in Table 3.7, MCL-5 cells were capable of tolerating 10μM of andrographolide evident in the absence of significant micronuclei frequency unlike in AHH-1 and V-79 cells, where there was significant difference in values between AHH-1 and MCL-5, as well as V-79 against MCL-5. At 30μM, metabolically-deficient hamster lung fibroblast V-79 cells possess the highest percentage of micronuclei recorded which was significant against that observed in MCL-5 but not in AHH-1. All three cell lines harbour significantly different ($p<0.05$) micronuclei frequency at 50μM against untreated cells but there were no difference between them at the 50μM dose. Thus, the metabolic capacity possesses by AHH-1 cell line may be insufficient in reducing the genotoxic activity of andrographolide compared to MCL-5 cells, which boast CYP1A1, CYP1A2, CYP2A6, CYP3A4 and CYP2E1 as well as microsomal epoxide hydrolase activities (Crespi *et al.*, 1991). Furthermore, there were no significant difference observed in the incidence of micronuclei at 10, 30 and 50μM andrographolide between metabolically-deficient V-79 cells and AHH-1 cells that has stable aryl hydrocarbon hydroxylase and CYP1A1 activities. As MCL-5 cells began to exhibit increased incidence of micronuclei at 30μM and upwards, it can be proposed that the intrinsic metabolic capacity was overwhelmed and the cells were no longer able to tolerate the accumulation of andrographolide molecules between 30 and 90μM concentrations. The absence of a statistically significant increase of micronuclei frequency in mononucleated AHH-1 and MCL-5 cells ruled out the possibility of accumulation in mitotic slippage incidences.

Mitomycin-C, a direct-acting clastogen was employed as a positive control in. As shown in Tables 3.3, 3.4 and 3.5 previously, mitomycin-C induced statistically significant micronuclei

against the negative control and these figures are within the range normally used in the laboratory.

As shown in Tables 3.3, 3.4 and 3.5, the number of micronuclei and binucleated cells decreased at higher doses of andrographolide, in agreement with elevated level of cytotoxicity elicited by the phytochemical. It is conceivable that the higher cytotoxicity imposed a greater selective pressure on the cells and cell cycle kinetics where the scored binucleated cells might be the subpopulations that survived.

Apart from disparity in metabolic potential, these cell lines also differ in p53 status. Both AHH-1 and MCL-5 are heterozygous for p53 but able to conduct normal DNA repair (Doherty *et al.*, 1996) whereas V-79 is deficient in p53 (Chaung *et al.*, 1997). p53 has been described to accumulate into micronuclei although its role has not been determined (Granetto *et al.*, 1996; Sablina *et al.*, 1998). Referring to the data generated, there were no indications that p53 may affect cellular response in concordance to previous findings that andrographolide activity is independent of a cell's p53 status (Rajagopal *et al.*, 2003). Clearly, the Phase I biotransformation capacity exhibited by MCL-5 cell line may have played a role in reducing the genotoxic impact of andrographolide at 10μM concentrations. These data provided valuable insights into andrographolide biotransformation in human cell lines that also complement the *in silico* predictions derived from DEREK and METEOR. The incidence of mitotic slippages was absent based on the frequency of micronucleated mononucleate cells that did not change significantly.

MCL-5 cells that were challenged with 10, 30 and 50μM of andrographolide and then labelled with anti-kinetochore CREST antibodies to determine the presence of kinetochores, revealed that the phytochemical induced mainly kinetochore positive micronuclei. This method identifies the presence of kinetochore protein associated with the centromeres of chromosomes or its absence from acentric chromosome fragments (Brinkley *et al.*, 1985). This discovery suggest that andrographolide behaves primarily in an aneugenic manner in which whole chromosomes are lost as opposed to breakage producing chromosomal fragments that were manifested as kinetochore negative micronuclei. The ratio of kinetochore

positive/kinetochore negative micronuclei in MCL-5 cell line was within the range normally observed in the laboratory and comparable to those observed in the literature (Parry *et al.*, 2002; Kayani & Parry, 2008) as well as the percentage of kinetochore positive/negative induced by andrographolide against known clastogen and aneugen reported in Parry *et al.*, (2002).

The induction of damage by aneugenic compounds may involved the chromosomes and various other cellular components crucial for cell division including the signal transduction pathways which ensure the fidelity of the whole process (Parry & Parry 1989), hence the rise of aneuploidy may not always be attributed to direct chromosome aberration or gene mutation, both of which have DNA as primary target for chemical action. Since indirect mechanisms of a genotoxin involve interactions with non-DNA targets leading to a genotoxic effect (Kirsch-Volders *et al.*, 2003), various cellular targets would have to be damage before any manifestation of scorable biological effects can be observed. Therefore, aneugens exhibit threshold concentration-effect response curve (Aardema *et al.*, 1998; Kirsch-Volders *et al.*, 2003). Potential thresholds have been elucidated for aneugens which are spindle inhibitors such as benzonitrile, nitrobenzene (Bonacker *et al.*, 2004) benomyl and its active metabolite carbendazim (Bentlery *et al.*, 2000), colchicine, mebendazole and nocodazole (Elhajouji *et al.*, 1995; 1997; 1998) using the *in vitro* micronucleus assay in combination with kinetochore labelling and fluorescence *in situ* hybridisation (FISH).

Andrographolide Primarily Evoked Necrotic Cell Death *in vitro.*

Genotoxicity assessment would be incomplete without the cytotoxicity level determination. Cytotoxicity of andrographolide was determined using replicative index calculation, microscopical identification of cell death and trypan-blue exclusion assay. Replicative index (RI) measures the relative number of nuclei in cells exposed to andrographolide compared to negative control cultures and the mean relative RI values for all cell lines significantly ($p<0.05$) decreased with dose, concomitant with a consistent increase in cytotoxicity values where the top two doses caused more than 50% cytotoxicity. It transpired that 10μM of

andrographolide was sufficient to significantly affect the replicative index but the caveat to this was the assumption that untreated cells possess 100% viability.

The same trend was also observed in the incidence of necrotic cells where 10μM of the phytochemical initiated statitistically significant and unfluctuating increases with the top two doses caused more than 50% necrotic death in the cell population, close to the 60% cytotoxicity mark. This was in stark contrast to apoptotic cells where the highest percentage of occurrence was lower than 2% of the cell population in all cell lines where 30 and 50μM of the phytochemical always induced the highest frequency of apoptosis in AHH-1 and MCL-5 cell lines. However, these figures were still low in comparison to population of cells that were primarily greeted by necrosis. The generally low frequency of apoptotic response at the two top doses compared to other treatment concentrations was due to profound damage to the cells and possibly the apoptotic machinery. Furthermore, andrographolide was found to trigger necrosis in a time- and dose-dependent manner, the longer duration of incubation from 8 to 24 hours increased necrotic cell frequencies but not apoptotic cells. The incidence of apoptosis in MCL-5 cell population remained almost constant between those exposed for 8 and 24 hours respectively, where less than 2% of cells experienced apoptosis. The dose of 30 and 50μM of andrographolide that induced high and significantly different apoptotic cells against negative controls also elicit significant micronuclei induction indicating possible correlation between the two. However, the prevalence of apoptosis amongst cells was low to affect micronuclei induction and cells mostly died via necrosis.

Therefore, all cell lines treated with andrographolide exhibited one common trait in terms of cell death despite their differences in metabolic capacity and p53 status, that the cells died primarily via necrosis in a dose-dependent fashion as compared to programmed cell death. Furthermore, cell viability assessment performed using the trypan-blue exclusion method, which primarily measures cellular membrane integrity shows that the majority of cells died in a dose-related fashion. Since only cells with damaged membrane would be susceptible to the dye, it can be safely assumed that the dead cell population measured by this method experienced necrosis because apoptotic cells normally possess intact cellular membrane. Even though the dye itself is toxic, the exposure time for all samples were limited to 9

minutes, well below the maximum 15 minutes limit recommended by the manufacturer. The replicative index, the necrotic and apoptotic cells frequency determination as well as trypan-blue exclusion assay indicated the same trend of dose-dependent cytotoxicity exerted by andrographolide. Furthermore, trypan-blue exclusion assay and cellular replicative index measure different cytotoxicity endpoints, the cumulative effects are additive where andrographolide reduced the population of viable cells and caused inhibited cellular proliferation of the surviving cell population. The adoption of either measurement on its own negates accurate assessment of cytotoxicity.

Exposure of HepG2 cells to andrographolide was reported to lead to the collapse of mitochondrial membrane potential (MMP) (Li *et al.*, 2007). The damage caused to the glutathione (GSH) system in the mitochondria by andrographolide was found to be in a dose-dependent fashion with corresponding depletion of glutathione. Glutathione plays a crucial role in the maintenance of cellular function and defence against oxygen free radicals. The presence of andrographolide changed the normal intracellular redox status and the collapse of mitochondrial membrane potential but failed to elicit a potent apoptotic response in HepG2 cells (Li *et al.*, 2007). As mentioned previously in the second Chapter, teucrin A was considered a comparable example since it is a diterpene-containing phytochemical and in the presence of CYP3A4, formed reactive epoxides that interacts with proteins and also caused mitochondrial membrane permeability and caspase activation. Teucrin A was also shown to reduced cytoskeleton-associated protein thiols, cellular glutathione levels but increased cytosolic concentration of Ca^{2+}. Indeed, moderate accumulation of Ca^{2+} concentration leads to caspase activation and increase FasL expression that would initiate apoptosis. In contrast, higher levels of cytosolic Ca^{2+} can activate calpains, endonucleases and phospholipase A_2, all of which have been implicated in necrotic cell death (Trump & Berezesky, 1995; Kass & Orrenius, 1999; Berridge *et al.*, 2000). The chemical structure of teucrin A in comparison to andrographolide is shown in Figure 3.21. The MCL-5 cell line carries CYP3A4 cDNA, amongst other P450 cytochromes and CYP3A is known to possess wide substrate spectrum (Wienkers & Heath, 2005) as well as epoxide hydrolase. It can be proposed that andrographolide may behave in the same manner. Furthermore, predictions by METEOR demonstrated that andrographolide is capable of forming epoxides.

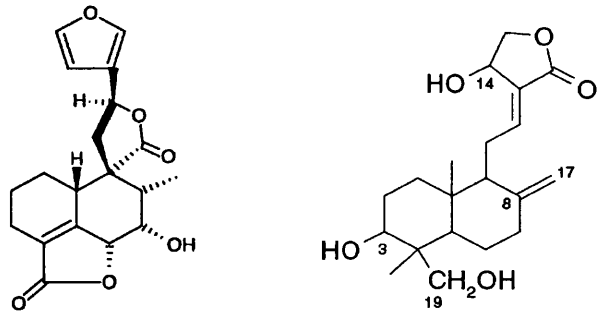

Teucrin A Andrographolide

Fig. 3.21. Chemical structure comparison between teucrin A and andrographolide. Both phytochemicals contain bicyclic diterpene.

Glutathione is a ubiquitous tripeptide consisting of glycine, cysteine and glutamate. One of the prediction made by METEOR was the conjugation of glutathione with andrographolide at the α,β-unsaturated moiety, where the cysteine part of GSH directly attached to andrographolide abolishing the $\Delta^{12(13)}$ double bond as shown in Figure 2.16c. Furthermore, Cui *et al.* (2004) reported the presence of 3-O-sulfate conjugates and 3-O-sulfate-12-S-cysteine conjugate metabolites in human urine, that were not within the list of possible metabolites suggested by METEOR. It may be possible that andrographolide is capable of reacting to cellular proteins that contains the thiol group. Its ability to attenuate inflammation was suggested via the inhibition of NF-κB activation by forming a molecular adduct with reduced cysteine[62] of p50, hence blocking the binding of NF-κB oligonucleotide to nuclear proteins (Xia *et al.*, 2004). Andrographolide was demonstrated to reduce cyclooxygenase-2 (COX-2) expression, which is an example of pro-inflammatory proteins also via binding to NF-κB (Hidalgo *et al.*, 2005). Thus, it can be speculated that higher concentrations of andrographolide caused depletion of cellular proteins with thiol group such as GSH, changing redox status.

These results might explain the observation made by Akbarsha & Murugaian (2000), where Sertoli cells in rats treated with andrographolide were highly vacuolated, indicating cell death. Indeed the presence of vacuoles within the cytoplasm is a mark of necrotic cell death. The seminiferous epithelium was also thoroughly distorted and disorganised with the epithelium and/or lumen contained multinucleated giant cells with several nuclei harbouring

marginalised chromatin in rats subjected to andrographolide treatment (Akbarsha & Murugaian, 2000). These anomalies were observed to be more profound in rats given higher doses of andrographolide (Akbarsha & Murugaian, 2000). Sperms were also found to possess no or little motility with tail abnormalities (Akbarsha & Murugaian, 2000). Furthermore, all the female rats mated with control males delivered litters, whereas none of the females mated with andrographolide-treated males delivered any offspring. Whether this is due to abnormal sperms itself or development deficit at conceptus level are not entirely clear but aneuploidy is known to cause reproductive failure. Andrographolide it seemed affects cell growth by causing chromosome malsegregation, disrupting the mitotic machinery and caused necrotic cell death in a dose-dependent fashion.

Thus, necrosis was a prevalent mode of cell death after andrographolide exposure, which was a surprise considering aneugens are known to primarily elicit programmed cell death (Decordier *et al.*, 2002). Necrosis has long been considered as a consequence of physico-chemical stress and thus as accidental and uncontrolled event. There are increasing number of evidence supporting the existence of caspase-independent cell death pathways responsible in a well-controlled cell death induction as observed in apoptosis (Zong & Thompson, 2006) and providing an alternative suicide mechanism in the event of apoptotic machinery failure (Fiers *et al.*, 1999; Leist & Jaattela, 2001). For example, *Salmonella* and *Shigella* can cause necrosis of infected neutrophils and macrophages (Brennan & Cookson, 2000; Francois *et al.*, 2000) as well as $CD4^+$ T lymphocyte destruction by HIV-1 (Borthwick *et al*, 1999; Plymale *et al.*, 1999; Lenardo *et al*, 2002). Caspase-independent death is also implicated in myocardial infarction, ischemia-reperfusion injury after cerebral ischemia, glutamate excitotoxicity (Eliasson *et al.*, 1997; Cipriani *et al.*, 2005; Schwabe & Brenner, 2006), diseases such as Alzheimer's (Akiyama *et al.*, 2000), epilepsy (Fujikawa, 2000) and other inflammatory injuries (Kaplowitz, 2000) also involves necrosis.

Ménage-à-Trois: Micronuclei Induction by Andrographolide and Possible Connections to Apoptosis and Caspase-3 Activity

The effect of andrographolide on apoptosis is still debatable. It was reported to protect human endothelial cells from growth factor deprivation-induced apoptosis via the activation of phosphatidyl inositol-3-kinase/Akt pathway (Chen *et al.*, 2004). Apoptosis induced using hydrocortisone and phorbol 12-myristate 13-acetate in thymocytes were also shown to be attenuated by andrographolide (Burgos *et al.*, 2004). However, a relatively high concentration between 40 to 100μM of the phytochemical could induce apoptotic cell death in human leukaemic HL-60 cells (Cheung *et al.*, 2005) and human prostatic adenocarcinoma PC-3 cells (Kim & Milner, 2005) where in both cases, the activation of the caspase cascade was proposed. In contrast, Li *et al.* (2007) recently suggested apoptosis only occur late in HepG2 cells and did not require the caspase cascade. Caspase-3 activity was significantly up-regulated in andrographolide-treated cells between 24 and 48-hours of *in vitro* exposure with the absence of potent apoptotic response despite diminishing cell growth and viability (Li *et al.*, 2007). Furthermore, cell death cannot be prevented using neither the caspase-3 specific inhibitor, Ac-DEVD-CHO nor vZAD-fmk which is a pan-caspase inhibitor, indicating that cell death elicited by andrographolide was not relying on cellular caspases activities (Li *et al.*, 2007) and as shown here, necrotic cell death which does not require caspases was the prevalent mode of cell demise.

It is still to be ascertained whether the caspase cascade was not initiated or andrographolide is directly inhibiting the apoptotic machinery despite caspase-3 activation. Thus, it is still not clear whether andrographolide is an anti- or pro-apoptotic agent and the detailed molecular mechanism(s) is still largely uncharted. Even if it does promotes programmed cell death in cells, it is still not known whether such an induction is a direct effect of the phytochemical on cellular apoptotic machinery or indirectly via other pathways and/or as a consequence of other events such as severe damage to mitotic apparatus. It was demonstrated that different treatment times with andrographolide, namely for 8 and 24 hours did not show any difference in apoptotic cells induction even though necrosis incidence was lower in shorter treatment duration. Hence, the possibility that apoptosis might be provoked earlier than 24 hours can be ruled out and even at 8 hours, apoptotic response was still lower than the incidence of

necrosis. As andrographolide exerts its influence primarily as an aneugen, which suggest the possibility of perturbations on the mitotic machinery, the absence of significant apoptotic response relative to necrosis is intriguing. Furthermore, the revelation that the majority of cell death occurs via necrosis begs the question whether cells adopt this mode of cell death because of disruptions to apoptotic components or other factors. The percentage of apoptotic cells in V-79, AHH-1 and MCL-5 were significantly higher at 30 and 50μM respectively and as pointed out earlier, these concentrations also caused micronuclei induction. Disruption to the mitotic apparatus might have a stake in apoptosis induction.

Aneugens are known to be good micronuclei inducer and also possess high propensity to initiate programmed cell death. It was demonstrated that spindle poisons such as carbendazim and nocodazole induced both apoptosis as well as micronuclei, which were later preferentially eradicated via apoptotic cell death (Decordier *et al.*, 2002). The occurrence of apoptosis can eradicate micronucleated cells and leads to the alteration of micronuclei frequency, ultimately negate an accurate damage assessment due to genotoxins exposure that can also act as apoptogens. Thus, the inhibition of apoptosis may increase micronucleated cells ratio in cytokinesis-block micronucleus assay (Kirsch-Volders *et al.*, 2003). Quite recently, it was demonstrated that the inhibition of apical caspases-8 and -9 caused increases in the frequency of nocodazole-induced micronuclei but remarkably, caspase-3 which is regarded to be an effector caspase for apoptosis execution was not involved in the elimination of micronucleated cells (Decordier *et al.*, 2005). Instead, caspase-3 activity was hypothesised to play a direct role in micronuclei formation (Decordier *et al.*, 2005). In this study, the highest incidences of micronuclei were observed to occur at the same concentrations where andrographolide also induced significant apoptotic response in the cell lines tested. Furthermore, the micronuclei scored within the binucleated cells were primarily one micronucleus per binucleated cells and since the cells were examined using both Giemsa and acridine orange, the possibility of mistakenly identifying these cells as containing apoptotic bodies were reduced. Apoptotic cells harbouring apoptotic bodies also possess other features such as visible chromatin condensation within the nucleus as described by Fenech *et al.* (2003).

Caspase-3 has been suggested to be involved in cell cycle control and cell growth modulation. For example in proliferating lymphoid cells, caspase-mediated cleavage of the cyclin-dependent kinase (CDK) inhibitor $p27^{KIP1}$ contributes to the induction of cell cycle progression (Frost *et al.*, 2001) whereas Carlile *et al.* (2004) reported the involvement of caspase-3 in normal erythroid differentiation. Yan *et al.* (2001) showed the presence of active caspase-3 in the nuclei of dividing cells within the proliferative regions of rat forebrain and it was also reported to be involved in embryonic keratinocytes differentiation (Okuyama *et al.*, 2004). However, caspase-3 is also known to inhibit B-cell proliferation (Woo *et al.*, 2003), hence this caspase can mediate a paradoxical proliferative or pro-apoptotic roles. Since apoptosis regulation is closely affiliated to cell cycle and cell division fidelity, where the proteolysis of different substrates is crucial for a spectrum of processes in both non-apoptotic and apoptotic conditions. The exact mechanism(s) of caspase involvement in micronucleation is yet to be elucidated but lamin B may be involved, a nuclear membrane component that has been demonstrated to be associated with micronuclei formation due to DNA replication impairment (Tanaka & Shimizu, 2000; Kottke *et al.*, 2002) and other possible nuclear-mitotic apparatus proteins that are required in mitotic assembly as well as nuclei formation after mitotic completion (Hirata *et al.*, 1998; Decordier *et al.*, 2005).

As will be discussed in the following Chapter, andrographolide is capable of inducing microtubule organisation centres (MTOCs) aberration that can lead both to micronuclei formation and/or multinucleated cells.

4

CHAPTER 4

INDUCTION OF CENTROSOME AMPLIFICATION AND ITS CONSEQUENCES IN CELLS CHALLENGED WITH ANDROGRAPHOLIDE

CHAPTER 4

INDUCTION OF CENTROSOME AMPLIFICATION AND ITS CONSEQUENCES IN CELLS CHALLENGED WITH ANDROGRAPHOLIDE

4.1 Introduction to Microtubules

Many important cellular processes in higher eukaryotic cells including motility, intracellular organelle trafficking, cell growth and division rely on the cytoskeleton which is a complicated network of protein filaments. The functional diversity of the cytoskeleton depend on three kinds of protein filaments namely:

- Microfilaments that are also known as actin filaments, dictate cell shape and topography. They are also crucial for cell motility and polarity as well as for being indispensable during cytokinesis.
- Intermediate filaments that grant mechanical strength and resistance to physical stress.
- Microtubules that manage intracellular trafficking of proteins and organelles, and involve in chromosome segregation during mitosis.

Despite their differences in dynamic and mechanical properties, these protein filaments possess some identical fundamental characteristics, especially the fact that they exist as polymers consisting of helical assemblies of specific protein subunits which self-associate through side-to-side or end-to-end non-covalent interactions and their dynamic nature to disassembly/reassembly. The functions of these cytoskeletal filaments hinge on various accessory proteins.

Therefore, polymerised microtubules remain in a dynamic steady state, alternating between a phase of growth and recession in a situation known as dynamic instability (Mitchison & Kirschner, 1984; Erickson & O'Brien, 1992).

Microtubules consist of 13 parallel protofilaments. The subunit of each protofilament is a tubulin heterodimer constructed from a very tightly linked pair of alternating α-tubulin and β-tubulin monomers arranged along the longitudinal axis of the microtubule. There are 6 isotypes of each α- and β-tubulin in human cells, possessing cell- and tissue-specific patterns of expression as well as differences in drug binding abilities (Khan *et al.*, 2000; Hallworth & Luduena, 2000; Burkhart *et al.*, 2001). Microtubules also possess polarity with distinct 'plus' and 'minus' ends.

Even though both microtubule ends alternately lengthen and shorten, it is known that net growing occurs at the 'plus' end, which are often free in the cytoplasm or situated near the plasma membrane, whereas net shortening occurs at the 'minus' ends. The 'minus' ends of the microtubules are frequently associated with the microtubule organising centres (MTOCs) or centrosomes, the specific site in the cytoplasm from which microtubules are nucleated.

The protein γ-tubulin, is the main component of the MTOC and possesses a 28-35% homology with α- and β-tubulins but are being expressed at lower values than these latter isoforms (Moudjou *et al.*, 1996)

4.2 Introduction to Centrosomes and Its Functions

The centrosome is a small non-membraneous organelle, approximately 1-2μm in diameter and is normally located at the periphery of the nucleus. It contains at least 150 proteins (Andersen *et al.*, 2003) that change in abundance through the cell cycle, essential to its main function in nucleating microtubules to determine the spatial organisation of the microtubule network, hence it is often referred to as a major microtubule organising centres (MTOCs). During interphase, the network involves in a number of crucial cellular processes, such as cell growth and division, cell shape determination, polarity, intracellular organelle trafficking and the ability to interact with the environment. The function of the centrosome is equally important during the interphase as well as in mitotic cell.

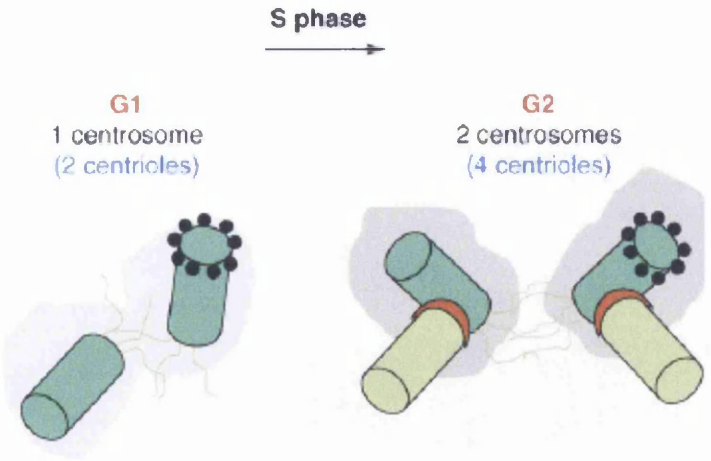

Fig. 4.1. In G_1-phase of the cell cycle a single centrosome consisting of two structurally-distinct centrioles, where the mother centriole possesses appendages (denoted in black) that are crucial in microtubule anchoring. Both centrioles are situated inside an electron-dense matrix known as the pericentriolar material, PCM (grey). Subsequently in S-phase, both centrioles produced a progeny and by G_2-phase of the cycle, the cell contains two centrosomes with each consisting of two closely associated centrioles. Also in late G_2, the pericentriolar material achieved maturation (dark grey) in a phosphorylation-dependent process. This augments γ-TuRC recruitment and permits increased microtubule anchoring activity essential for spindle formation. (Adopted from Nigg, 2007).

The centrosome consists of three major domains with the most prominent being the centriolar and pericentriolar areas with an average diameter of approximately 1μm in most animal cells. The centriolar domain defines the centre of centrosome and contains either a single centriole or a pair of centrioles, depending on the stage of the cell cycle and each centrioles are composed of characteristic nine parallel triplets of microtubules. The pair of centrioles structurally differ from each other where one with a set of appendages at the distal ends (maternal centriole) and one without appendages (daughter centriole). The daughter centriole acquires these appendages, which appear to be essential for anchoring microtubules, in late G_2 phase of the cell cycle. Figure 4.1 shows the changes that occur during normal centrosome duplication between G_1 and G_2 phases of the cell cycle.

The pericentriolar domain encircles the centriole as a cloud of protein meshwork known as pericentriolar material (PCM) containing a large number of coiled-coil proteins and functions as the site for microtubule polymerisation (Bornens, 2002). This matrix provides a scaffold for proteins that are important for regulating centrosome duplication and function, containing the basic unit for microtubule nucleation, the γ-tubulin ring complex (γ-TuRC) (Moritz *et al.*, 1995a; 1995b), a complex of six proteins in humans that includes γ-tubulin and GCP2-6 (Fava *et al.*, 1999; Murphy *et al.*, 2001). The γ-tubulin is a

conserved, ring-shaped multi-protein complex of all microtubule organising centres that apparently serve as a template for microtubule polymerisation from the closely-associated α- and β-tubulins (Moritz *et al.*, 1995a). The centrosome extends out of the pericentriolar domain by integrating with the surrounding organelles and cytoplasm through microtubules and microfilaments as depicted in Figure 4.2 below. These outer extensions of the centrosome are called the outer centrosomal domain.

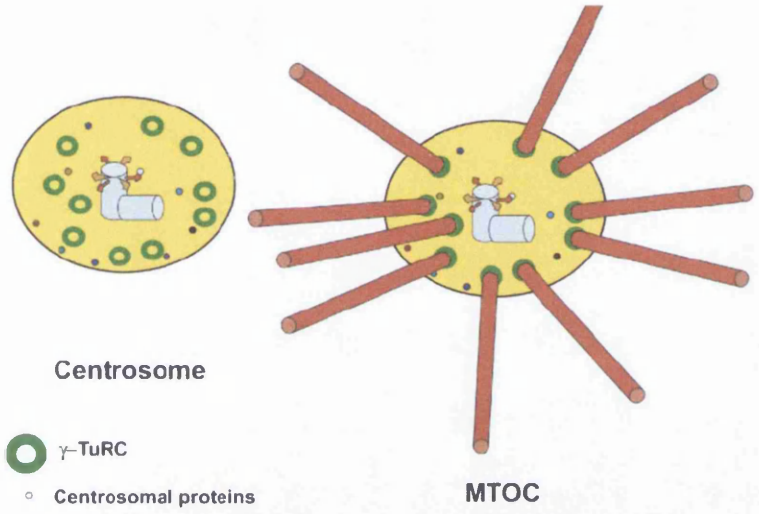

Fig. 4.2. The centrosome is crucial in nucleating microtubules. The γ-TuRC (shown as green circles) initiates the polymerisation of α- and β-tubulin promoters into microtubules (depicted as red rods). Maturation of the centrosome in G_2 controls the γ-TuRC content in the pericentriolar material. (Adopted from Sankaran & Parvin, 2006).

During mitosis as well as meiosis, centrosomes are the primary organising centre for microtubule in most eukaryotic cells, become the core structures of spindle poles and dictate the formation of mitotic spindles. Each of the daughter cell inherits only one centrosome upon cytokinesis, hence the centrosome must duplicate once prior to the next cell division. Therefore, at any particular time of the cell cycle, cells possess either one unduplicated or two duplicated centrosomes. Since DNA and centrosome are the only organelles that undergo semi-conservative duplication once every single cell cycle, animal cells are equipped with a mechanism that coordinates these two events, ensuring only one duplication step takes place at any one time.

In late G_1-phase, the centrosome triggers duplication via physical separation of the paired centrioles and losing their orthogonal orientation with respect to each other but remained attached via a fiber. Tsou and Stearns (2006) proposed that this disorientation step permits

the following duplication steps. In early S-phase, pro-centrioles (daughter centrioles) formed close to the proximal end of each centriole, perpendicular to each pre-existing mother centriole. Pro-centrioles can appear anywhere in the cytoplasm but a regulatory mechanism which is not well understood limits the sites of synthesis to the base of mother centrioles (reviewed in Hagan & Palazzo, 2006). The nascent pro-centrioles elongate through S and G_2 phase of the cell cycle and two centrosomes continue to mature by recruiting pericentriolar material.

At the G_2/M-phase, the centrosomes undergo a dramatic increase in size due to accumulation of several proteins including γ-TuRC and the influx of γ-TuRC into the pericentriolar material is associated with a higher level of centrosomal microtubule nucleation activity (Khodjakov & Rieder, 1999). The new mother centriole also matures via the binding of specific proteins and in M-phase both centrosomes have acquired the maximal amount of pericentriolar material.

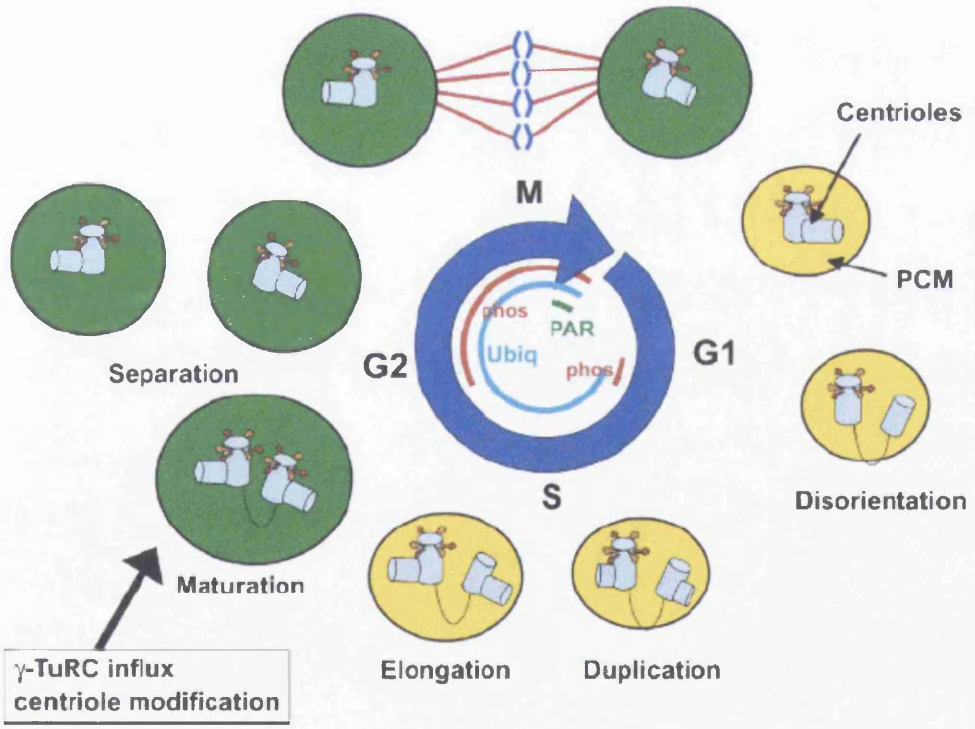

Fig. 4.3. The centrosome cycle. Centrosomes consisting of paired centrioles (depicted as light blue cylinders) surrounded by pericentriolar material (yellow in G_1/S-phases and green, upon maturation in G_2/M-phases). Appendages of the mother centrioles are also shown (red and orange). Different stages of the centrosome cycle are shown corresponding to the cell cycle and with temporal scale of activity for kinases (red arcs), ubiquitin ligases (blue arc) and poly-(ADP)-ribosylation or PAR (green arc) that are known to influence centrosome duplication and maturation. Finally, in mitosis the two pairs of centrioles split off the centrosome and migrate to the opposite poles of the nucleus. (Adopted from Sankaran & Parvin, 2006).

Subsequently, the two mature centrosomes move to the opposite poles of the nucleus to form the mitotic spindle regulated by a slew of kinases. It has become increasingly clear that other protein modifications, including ubiquitination and ADP-ribosylation, regulate this process and Figure 4.3 illustrated the centrosome duplication cycle in relation to different phases of the cell cycle.

The centrosomes have three important roles. It nucleates the polymerisation of tubulin subunits into long microtubule polymers, it manages nucleated microtubules into functional arrays and it duplicates once per cell cycle, hence legitimising cell cycle progression from G_1 into S phase, including exit from cytokinesis. After nucleation in the pericentriolar material by γ-TuRC, microtubules are liberated from their nucleating sites and translocated to the anchoring sites situated at the sub-distal appendages of the maternal centrosomes that contain centriolin and ninein as anchor proteins but lack microtubule-nucleating proteins (Doxsey *et al.*, 2001).

Centrosomes play a pivotal role in bipolar spindle formation during mitosis and therefore exert a strong influence on karyokinesis and cytokinesis. Cells of higher plants and eggs of many animal species are capable of forming bipolar spindles through centrosome-independent mechanisms (Heald *et al.*, 1996; Schmit 2002, Basto *et al.*, 2006). However in their presence, centrosomes usually adopt a domineering role in determining the orientation and bipolarity of the mitotic spindle (Brinkley, 2001). The presence of two MTOCs during mitosis is critical for the formation of bipolar mitotic spindles because chromosomes are pulled in opposite direction towards each spindle pole and this bipolarity is essential for accurate chromosome segregation into two daughter cells during cytokinesis, hence they are vital for both the fidelity of chromosome segregation and the positioning of the cleavage plane during cell division. Thus, numerical homeostasis of centrosomes is a highly controlled process and abrogation of this control leads to abnormal amplification of centrosomes, which in turn increases the frequency of aberrant mitoses and chromosome segregation errors.

4.3 Centrosome Abnormalities

Centrosome abnormalities can be classified in two, namely structural and numerical aberrations. Although these aberrations often occur together, their origins as well as their

consequences may differ. Both type of centrosomal anomalies have been considered to present diagnostic and/or prognostic values (Deusberg, 2001).

Structural centrosome anomalies are most likely to arise from deregulated expression of genes coding for centrosomal proteins or alteration in post-translational modifications, such as phosphorylation defects of the corresponding proteins. Consequently, altered or imbalanced protein levels caused the centrosomal structural modification, for example in size due to PCM accumulation around the centrioles. Furthermore, centrosomal coiled coil proteins have the tendency to form intracellular assemblies and this can be manifested as centrosome-related bodies at ectopic sites (Fry *et al.*, 1998, Casenghi *et al.*, 2003). The exact protein compositions of the structurally altered MTOCs and centrosome-related bodies have an impact on function, for example the recruitment of γ-TuRCs may be either reduced or enhanced and microtubule nucleation is either suppressed or stimulated (Lingle & Salisbury, 2001; Lingle *et al.*, 2002), which in turn influence the polarity, shape and motility of cells.

Numerical centrosome abnormalities are usually linked to genome instability and loss of tissue differentiation (Ghadimi *et al.*, 2000; Lingle *et al.*, 2002,). There are several mechanisms that lead to centrosome amplification. Firstly, centrosomes replicate more than once in a single cell cycle and may not always undergo re-duplication process, hence the final centrosome number can be either odd or even. Cytokinesis failure, resulting in genome and centrosome doubling in even numbers is the second well-known mechanism. There has been a debate as to whether centrosome multiplication is a cause or consequence of chromosome instability and most incidence of centrosome amplification involves deregulated replication and cytokinesis failure. Consequently, the existence of abnormal centrosome number abrogates centrosomal numerical homeostasis, disrupts normal mitotic process and increases the frequency of aberrant mitoses and chromosome segregation errors. Other mechanisms that can cause centrosome multiplication but less frequent than those described previously includes improper splitting of the paired centrioles, *de novo* formation of acentriolar centrosomes and cell fusion via fusogenic viruses as illustrated in Figure 4.4 overleaf.

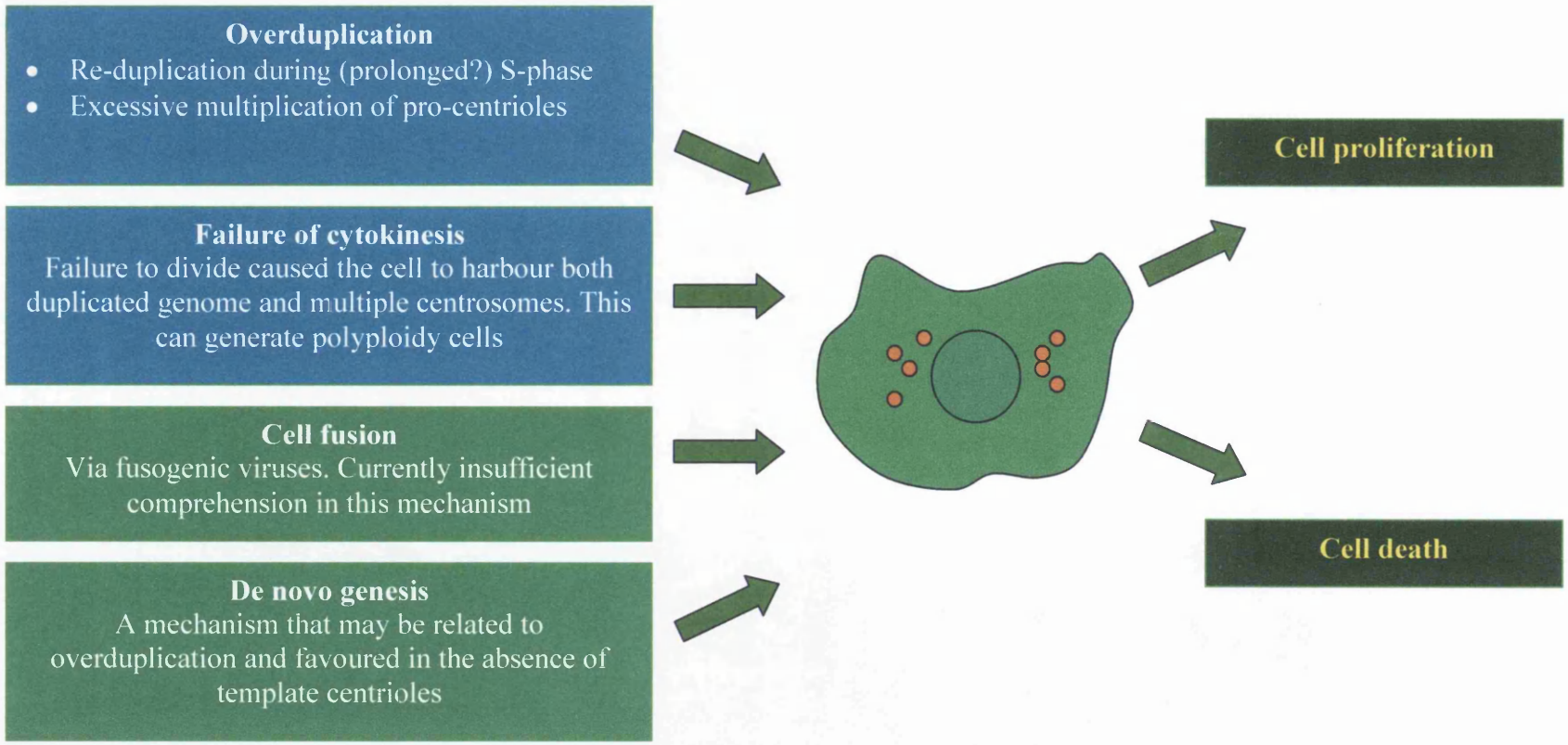

Figure 4.3. Different mechanisms resulting in numeral centrosome amplification. Out of the four mechanisms shown, overduplication and division failure are known to be the most common route of supernumerary centrosomes induction.

4.4 Centrosome Amplification, Aneuploidy and Cancer

Centrosome defects are observed in many types of carcinomas including gall bladder, breast (Lingle et al., 1998), pancreas (Sato *et al.*, 1999), colorectal (Ghadimi *et al.*, 2000), prostate (Pihan *et al.*, 2001), head and neck cancers (Doxsey, 2001; Carroll *et al*, 2000). For example, almost 80% of invasive breast tumour cells possess amplified centrosome numbers (Lingle *et al.*, 2002) and centrosomal changes are strongly associated with aneuploidy and chromosomal instability in various studies (Lingle *et al.*, 1998; Pihan *et al.*, 2001; Ghadimi *et al.*, 2000; Pihan *et al.*, 2003). Furthermore, MTOCs defects are known to increase in severity during tumour development (Doxsey, 2001; Pihan *et al.*, 2001; Pihan *et al.*, 2003). The prevalence of centrosomal multiplication in cervical carcinoma cells for instance, progressively accrued to approximately 20% of the cell population in grade 1 tumours to nearly 70% in grade 3 tumours (Pihan *et al.*, 2003) and genetically unstable aneuploid breast tumours exhibit around 6.8 centrosomes per cell compared to 1.5 in normal tissues (Lingle *et al.*, 2002).

Due to karyotypic shuffling, aneuploidy could disrupt global transcription process resulting in down-regulation of genes involved in growth control and up-regulation of growth promoting genes. Indeed, previous finding suggests that aneuploidy due to the addition of one single chromosome lead to misregulation of 100-200 genes and only 5-20% of misregulated genes were contained on the trisomic chromosome (Upender *et al.*, 2004)

Figure 4.5 shows the effects of abnormal MTOCs on chromosome segregation fidelity and the scenarios resulting from such amplification. Most cells harbouring amplified MTOCs will be primarily ushered towards programmed cell death due to deleterious chromosome missegregation. However, some cells may survive after gaining favourable chromosome complement that permits further growth and propagation, usually leading to neoplasms propelled by autocatalytic karyotype shuffling.

Most centrosome abnormalities can be allocated into three groups namely abnormal centrosome number, aberrant microtubule nucleation and inability to correctly segregate during mitosis. Centrosomes of tumour cells display different structural alterations including an increase in centrosome number and volume, supernumerary centrioles,

accumulation of excess pericentriolar material and inappropriate phosphorylation of centrosome proteins (Pihan *et al.*, 1998; Lingle *et al.*, 1998). Furthermore, centrosomes in tumour cells exhibit functional abnormalities characterised by increased microtubule nucleation activity (Lingle *et al.*, 1998; Salisbury *et al.*, 1999). There can be at least two detrimental consequences of centrosome defects that may contribute to neoplastic transformation and tumour progression. First, centrosome duplication anomaly may severely affect maintenance of cell polarity in interphase cells due to disorganisation in cytoplasmic architecture and directional vesicular trafficking in a cell with multiple MTOCs. Second, centrosome defects may intensify the incidence of multipolar mitoses leading to chromosomal segregation abnormalities and aneuploidy.

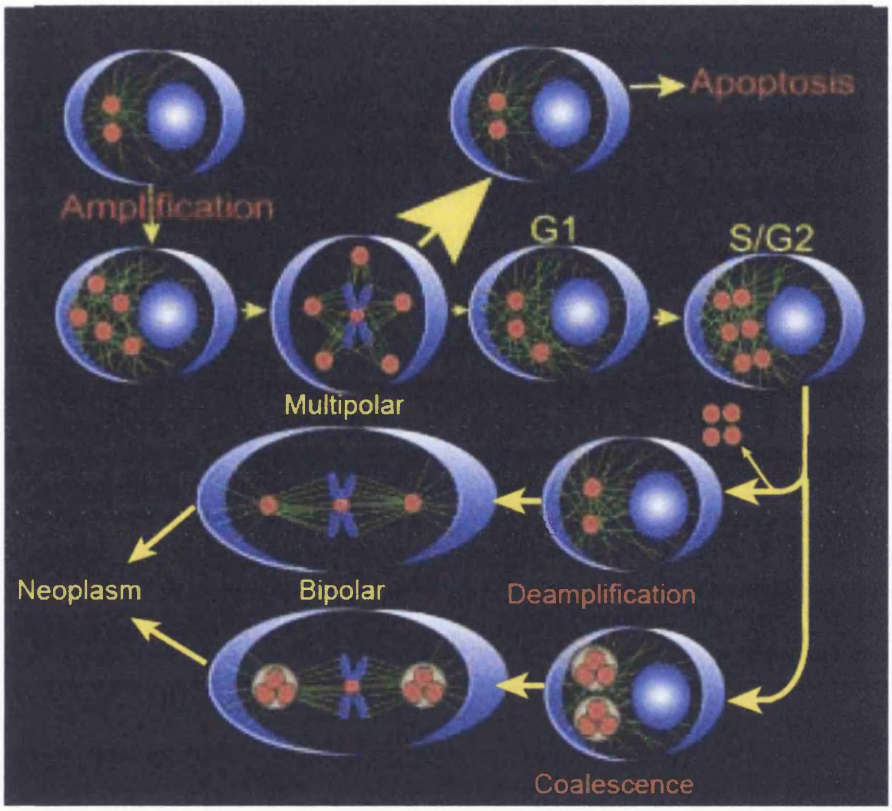

Fig. 4.5. The presence of supernumerary centrosomes bears different tidings to the cells affected depending on the circumstances. Abnormal MTOCs (red dots) numbers lead to multipolar division where the MTOCs nucleate abnormal number of microtubule (green lines), consequently the chromosomes are pulled to different poles. Chromosomes missegregation caused genomic instability that primarily courts apoptotic response. Sometimes, daughter cells might gain a chromosome complement favourable to survival. In deamplification scenario, all but two dominant centrosomes are eliminated or deactivated thus reverting to a more manageable ability in nucleating microtubule. Alternatively, in coalescence, the amplified MTOCs formed a pseudo-bipolar segregation. Both routes lead to neoplastic growth. (Adopted from Brinkley, 2001).

The observation that centrosome abnormalities are very common in tumour cells considering supernumerary centrosomes rendered a clear disadvantage to the affected cells' ability to proliferate is currently a bewildering paradox especially when the definitive long-term data on the cellular fate is limited. Only a sub-population of tumour cells observed to possessing multiple MTOCs and tumour-derived cell lines usually contains around 5-25% of cells with the same feature when cultured *in vitro* (Lingle *et al.*, 2002; Pihan *et al.*, 2003). Notably, this population seemed to remain roughly constant as the culture is propagated and it is conceivable that cells with aberrant MTOCs number were generated *de novo* through any of the mechanisms mentioned previously and the majority subsequently died due to chromosomal instability, although some will survive. Therefore, the population size of cells with multiple MTOCs is determined by the generation, elimination and survival rates of these cells.

4.5 The Objective of the Studies

This study was initiated to elucidate the influence of andrographolide on MTOCs, microtubules, mitotic index and cell fate upon removal of the compound in V-79 cells *in vitro*. Mitotic machinery aberrations have been shown to lead to aneuploidy and multipolar mitosis is known to be a mechanism for micronuclei induction (Parry *et al.*, 2002). The determination of possible mechanism of action for micronuclei induction by andrographolide does not require a high statistical power since only mechanistic information is needed. The cell fate study was intended to complement the MTOCs studies in determining the outcome of mitoses in the presence of abnormal MTOCs number. The fate of cells after pro-longed exposure to the phytochemical was also examined and intended to determine the frequency of daughter cells with more than one nucleus. The cell recovery study was necessary to assess whether V-79 and MCL-5 cells are capable of recovering from exposure to andrographolide at various concentrations since threshold level of damage is suspected and to determine if damage to mitotic machinery will affect subsequent mitoses.

4.6 MATERIALS AND METHODS

4.6.1 Introduction to V-79 cell line.

As stated in section 3.5.6 in Chapter 3.

4.6.2 Sub-culturing V-79 cells for treatment.

The cells were seeded at $8x10^4$ cells/ml onto sterile glass microscope slides. The slides were placed in Petri dishes with a total volume of 12ml medium in each Petri dish and incubated at 37 ± 1^0C for 24 hours with circulated 5% CO_2 in air prior to treatment.

4.6.3 Treatment of cells with andrographolide.

Andrographolide with 98% purity was stored at room temperature. Andrographolide to be used at various concentrations was always freshly prepared by dissolving the crystals with DMSO as solvent and administered to V-79 cell cultures within two hours of preparation. The cells were then incubated for another 24 hours at 37 ± 1^0C in the presence of andrographolide inside the incubator with circulating 5% CO_2 in air.

The experiments were accompanied by negative and positive controls. The negative control preparations were essential for monitoring spontaneous incidence of aberrations in the cell culture and to validate DMSO, the solvent used in formulating andrographolide, was not itself affecting the cells and hence the outcome of the experiments. Colchicine (CAS no. 64-86-8) was chosen as positive control in this study at 0.5pg/ml as used in the laboratory. It possesses the typical profile of a non-carcinogenic aneugen and was shown to be positive in the *in vitro* and *in vivo* micronucleus tests (Heddle *et al.*, 1977; Mavournian *et al.*, 1990; Miller *et al.*, 1998; Matsushima *et al.*, 1999) but negative in gene mutation assays (Heddle *et al.*, 1977; Honma *et al.*, 1999a) except for the mouse lymphoma assay when a 24-hour treatment was adopted (Honma 1999b). Colchicine is known to cause numerical aberrations due to metaphase-blockage by the inhibition of tubulin polymerisation (Galloway *et al*, 1987; Miller *et al*, 1998) and have been tested positive for aneuploidy induction in a number of test systems (Liang & Brinkley, 1985), including somatic cells *in vivo* (Miller & Adler 1989) and mammalian germ cells (Mailhes & Zhin, 1987; Russo & Pachierotti, 1988).

For each set of experiment, different andrographolide stock solutions were used and a total of three sets of replicate experiments were conducted for this study.

4.6.4 Harvesting the slides.

After 24 hours, the growth medium removed and the slides gently washed with cold PBS twice. Subsequently, the slides were fixed in two different fixatives depending on the staining purposes as stated below.

4.6.5 Spindle staining using conventional dyes.

The slides were fixed in methanol and acetic acid with 3:1 ratio in the presence of $MgCl_2$ and $CaCl_2$ for three washes; 14 minutes for each wash. The additions of magnesium ions were to enhanced protein staining while calcium ions were to decrease spindle solubility, resulting in irreversibly stabilised spindles and prevented their possible shrinkage. The slides were air-dried thoroughly and placed in 5% perchloric acid at 4^0C for 24 hours for RNA removal. This was followed by washing the slides thoroughly in distilled water for three times; 4 minutes for each wash. Subsequently, the slides were stained with 0.5% Brilliant blue and 0.5% Safranin O in 15% acetic acid for 12 hours at room temperature. Brilliant blue stains the spindle fibres blue while Safranin O stains the chromosomes red in colour. Finally, the slides were gently washed with distilled water; air-dried and mounted in DPX. The spindle staining procedure was originally described by Wissinger *et al.* (1981).

4.6.6 β- and γ-tubulin immuno-fluorescence staining.

The prepared slides were fixed in ice-cold 90% methanol and air-dried (alternatively, they can be stored at –20^{O}C until needed). The slides were then washed once in ice-cold phosphate-buffered saline (PBS), then fixed in 90% methanol at –20°C for 30 minutes, followed by 20 seconds in acetone at –20°C. The slides were then rinsed in PBT (PBS plus 0.1% Tween 20). Subsequently, the cells were incubated with a diluted 1:200 mouse monoclonal anti-γ-tubulin (T6557) in a humidified chamber at 37±1^{0}C for two hours. Then they were rinsed again in PBT followed by incubation with diluted 1:32 anti-mouse IgG Fab specific TRITC conjugate (T7782) in a humidified chamber at 37±1^{0}C for two hours. After another rinse in PBT, the slides were later incubated with diluted 1:100 monoclonal anti-α-tubulin conjugate (F2168) in a humidified chamber at

37±1^{0}C for one hour. After another extensive rinsing in PBT, DNA was counter-stained with diluted DAPI.

4.6.7 Slides Scoring Criteria.

Mitotic index.

For mitotic index measurement, slides were coded and 1000 cells per slide were scored to obtain the interphase:mitotic cells ratio according to the formula;

$$\text{Mitotic index (M.I.)} = \left[\frac{\text{number of mitotic cells}}{\text{number of interphase cells}} \right] \times 100$$

Scoring was performed under 1000X magnification with oil immersion using Olympus BH-2 light microscope.

Cell division aberrations (fluorescent microscopy).

The immunofluorescence-stained slides were also coded and scored at 1000X magnification under oil immersion using an Olympus BH2-RCF fluorescence microscope. 100 cells per slide were analysed for α- and γ-tubulin alterations. γ-tubulin is a centrosome protein and involves in microtubule nucleation whereas α-tubulin is a microtubule monomer.

- α-tubulin (microtubules) stained green.
- γ-tubulin (centrosomes) stained red.
- chromosomes stained blue.

Characteristics employed for identification:

- Bipolar: cells with normal metaphase and bipolar microtubule organising centre (MTOC) division.
- Tripolar: cells exhibiting abnormal metaphase with three MTOCs.
- Tetrapolar: cells with abnormal metaphase due to four MTOCs and relatively more extensive aberrations.
- Multipolar: More than four MTOCs present in a cell at the metaphase stage.

- Abnormal mitotit cells were scored as lagging chromosome (attached to microtubules), telophase bridge, multipolar whereas condensed chromatin were considered as dead cells.

Figure 4.6 shows a flow chart highlighting all the necessary steps involved in elucidating the effects of andrographolide exposure on MTOCs and chromosomal aberrations in V-79 cells.

4.6.8 Trypan Blue exclusion assay for cell viability.

The assay was conducted as described in Section 3.5.13 in Chapter 3.

4.6.9 Studies on Mitotic Fate and Cell Recovery

4.6.9.1 MCL-5 cells

Culturing and treatment procedures employed for MCL-5 in these cell fate and cell recovery studies were the same as those described in Sections 3.5.4 and 3.5.6 but without the addition of cytochalasin-B. The cells were grown in carefully labelled, 25cm^2 flasks and subjected to andrographolide treatment for 24 or 48 hours. After the treatment phase, cells intended for cell fate assessment were promptly harvested as described in Section 3.5.7 and on the other hand for cell recovery experiments, the cells were harvested via centrifugation at 1500rpm for 5 minutes.

For the continuous treatment of MCL-5 cells with andrographolide, the cells were left in the presence of andrographolide for 5 cell cycles (120 hours) before being harvested as conducted previously.

4.6.9.2 V-79 cells

For V-79 cells, the same culture and treatment procedures were followed as described in Sections 4.6.1 and 4.6.3. After exposure to andrographolide for 24 hours, the cells were harvested according to the aim of the experiments. For assessing aberrations in MTOCs and chromosomes, the slides that were grown in Petri dishes were carefully and gently washed twice with pre-warmed PBS in a sterile Petri dish. Autoclaved forceps was used when handling the slides and the tips of the forceps were briefly dipped into 90% ethanol

then dried before the next slides are handled. New Petri dishes were used for each slide. Washed slides were promptly placed in new Petri dishes with fresh growth medium and incubated at 37 ± 1^0C with 5% CO_2 in air for another 24 and 48 hours respectively. After these recovery periods, the slides were harvested as described in 4.6.4. Staining procedures were the same as those stated in Sections 4.6.5 and 4.6.6.

For cell fate study involving V-79 cells, the cells were grown in $25cm^2$ flasks rather than Petri dishes as described in Section 3.5.5 and treatment was performed as in Section 3.5.6 in the absence of cytochalasin-B. The method employed was similar to that of MCL-5 as described previously but both floating and cells that were attached to the flasks were collected for harvesting using the cytospin as described in Section 3.5.7.

Three replicate experiments were conducted for each study. Figure 4.7 displays the important steps employed in studies for cell fate, cell recovery and continuous treatment with andrographolide.

4.6.10 Statistical analysis

The Fisher's Exact test was used for the analysis of cell division aberrations and 95% confidence limits were accepted as the measure of significant difference unless otherwise stated. Analysis was performed via the Simple Interactive Statistical Analysis website accessible via http://home.clara.net/sisa/

Fig 4.6 Flow chart for important steps involved in assessing MTOCs, mitotic index and chromosome aberrations in V79 cells.

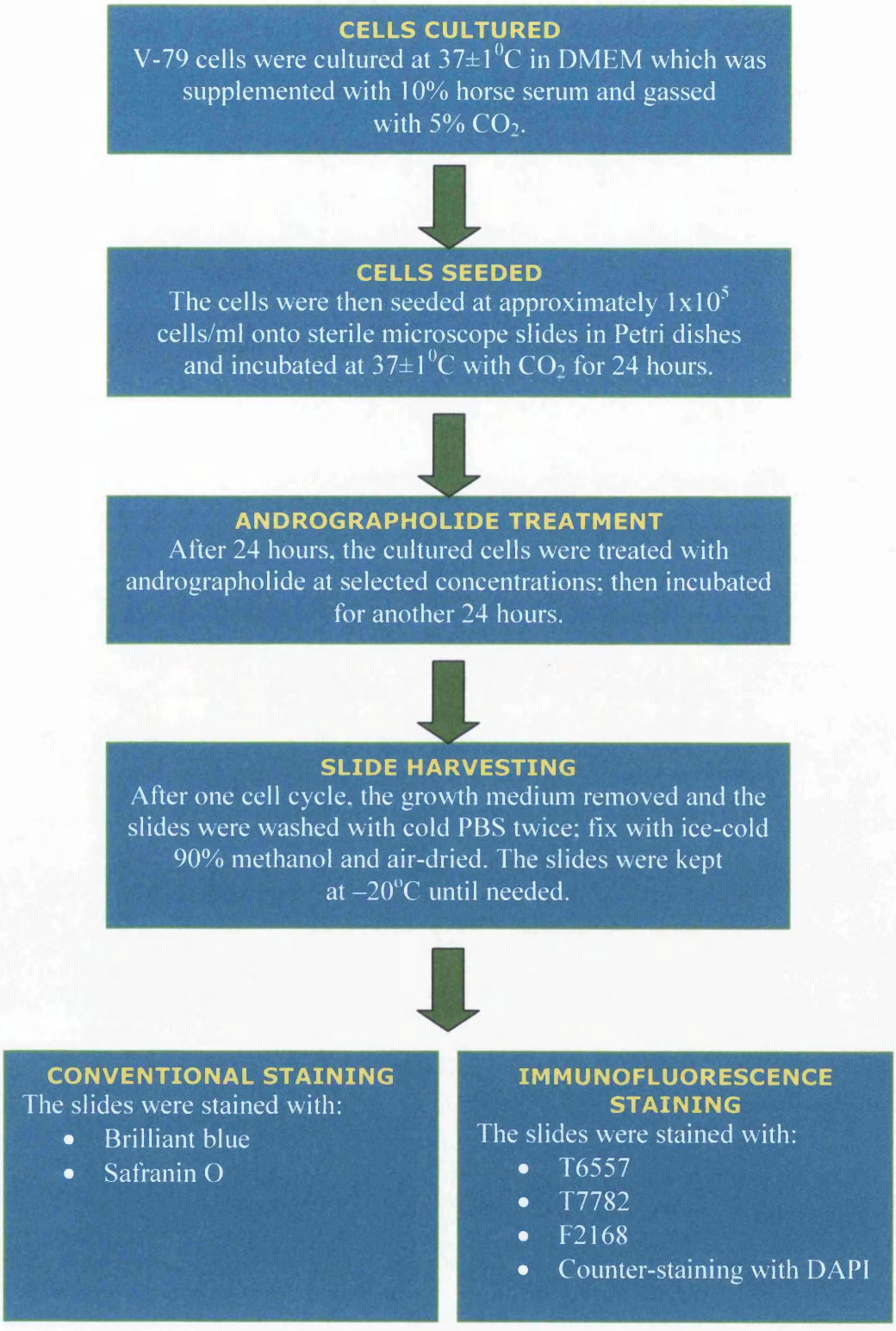

4.7 RESULTS

Cell division aberrations due to andrographolide exposure were investigated in Chinese hamster lung fibroblasts V-79 cell line. The mitotic spindle fibres and chromosomes were stained with Brilliant blue and Safranin O respectively; visualised using light microscopy to assess cell cycle irregularity and shifts in mitotic index value. Abnormalities in microtubule organising centres (MTOCs) were qualitatively evaluated using fluorescent microscopy for better accuracy against using conventional dyes. The effect of andrographolide on MTOCs integrity in interphase and mitotic cells were investigated using immunofluorescence of γ-tubulin, a centrosomal protein whereas microtubule organisation was examined by means of α-tubulin immunofluorescence. Quantification of multiple MTOCs actuation was performed by establishing the relationship between the number of tubulin signals with different concentrations of andrographolide.

In untreated interphase cells the microtubule network was constructed all over the cells and centrosomes were detected as a one-spot signal of γ-tubulin as shown in Figure 4.8. In untreated mitotic cells, two spots of γ-tubulin signals co-localised with spindle poles. Incubation of the cells with andrographolide for 24 hours induced abnormal tripolar, tetrapolar and multipolar spindles that co-localised with three, four and multi-spots of γ-tubulin signals respectively. In contrast, the presence of andrographolide did not influence the microtubule architecture and the number of γ-tubulin signals in interphase cells. Data as shown in Table 4.1 revealed a pattern of steady and significant ($p<0.05$) dose-dependent accruement in multiple MTOCs with tripolar mitosis being the most prominent. Tetrapolar and multipolar mitoses also increased significantly with reduction in normal bipolar spindle ratio in scored mitotic cells respectively. Concomitantly, mean percentage mitotic index also accrued in a dose-dependent fashion. Figures 4.9 and 4.10 shows examples of a bipolar, tripolar, tetrapolar and multipolar V-79 cells.

(A) (B)

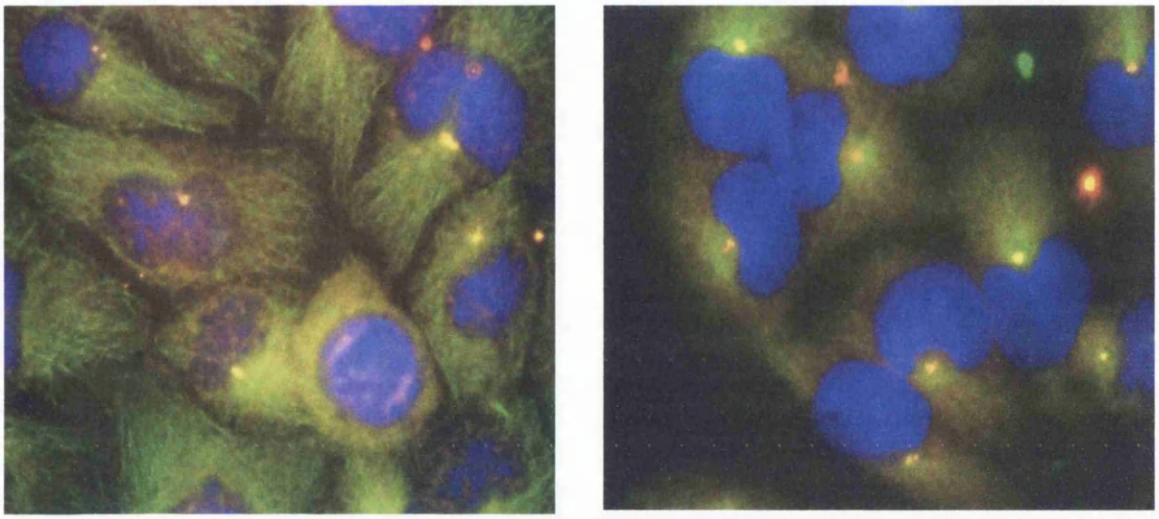

Fig. 4.8. Showing untreated interphase V-79 cells stained with immunofluorescence probes. Chromosome was stained blue with DAPI, γ-tubulin observed as orange/yellow spots whereas α-tubulin, a microtubule monomer clearly visible in green. In (A), the microtubule network was clearly constructed all over in the resting cells. In (B), the γ-tubulin spots are observed in one position within the cells. (1000x magnification)

(A) (B)

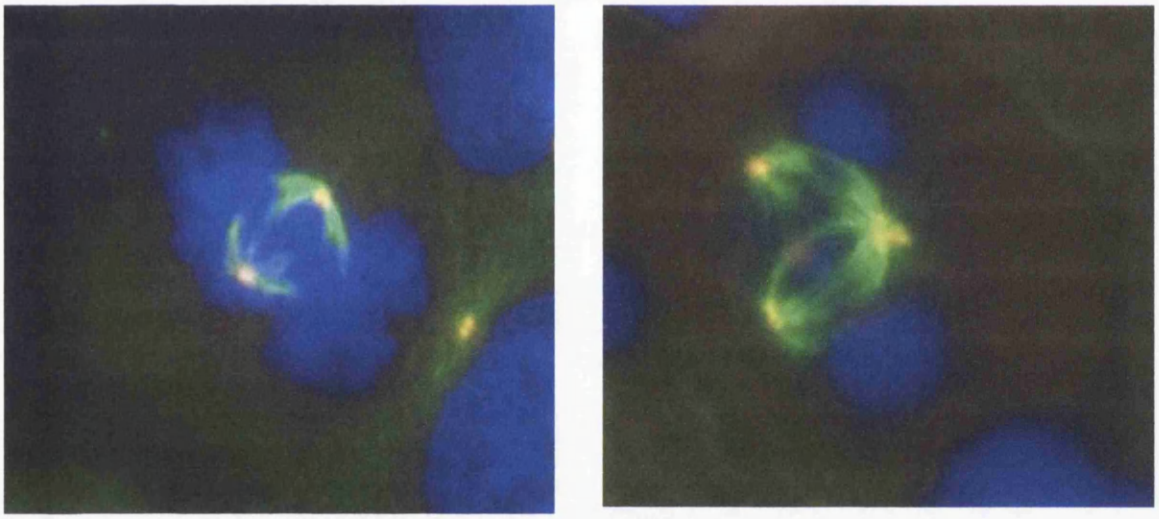

Fig. 4.9. Shows different number and MTOCs polarity in V-79 cells. (A) A bipolar cell and (B) a tripolar cell. Centrosome observed as orange/yellow spots, microtubule is green and chromosome in blue. (1000x magnification).

(A) (B)

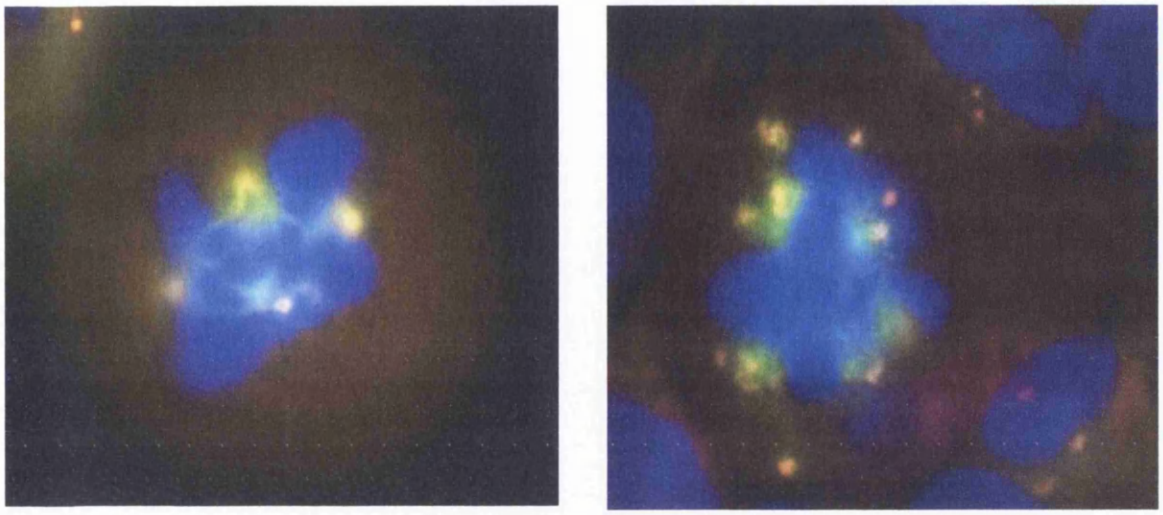

Fig. 4.10 Shows different number and MTOCs polarity in V-79 cells. (A) A Tetrapolar cell and (B) a multipolar cell. Centrosome observed as orange/yellow spots, microtubule is green and chromosome in blue (1000x magnification).

(A) (B)

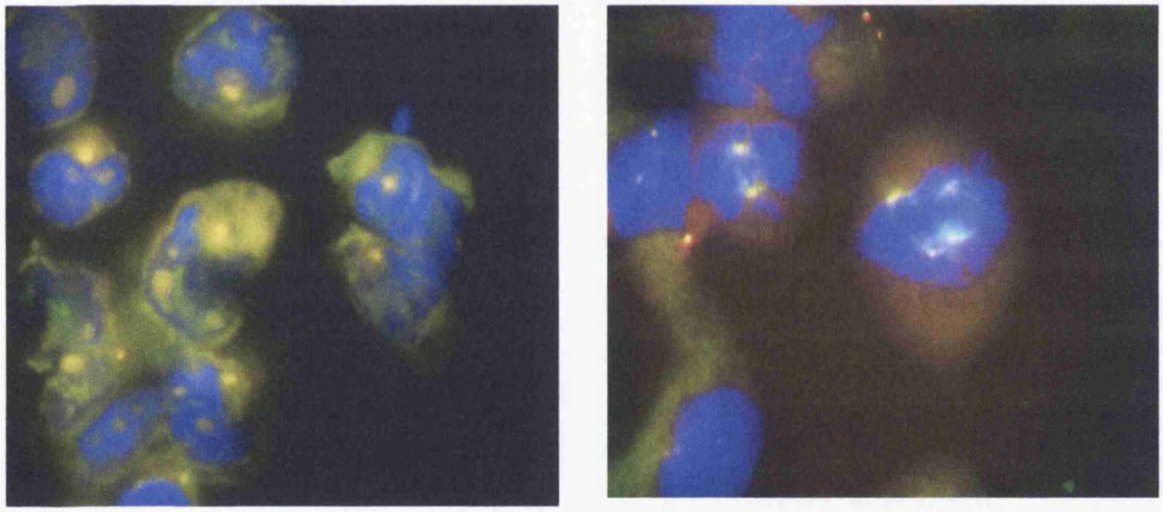

Fig. 4.11. (A) Shows dead V-79 cells challenged with high doses of andrographolide where evaluating centrosomal integrity was not possible due to the absence of endpoints. (B) Compares a two cells. The smaller one on the left hand side is a V-79 cell that is bipolar whereas the one on the right hand side possesses two pairs of spindle poles. This particular type was considered to be pseudo-bipolar.

Table 4.1. Induction of centrosome and mitotic spindle abnormalities in V79 cells after 24 hours of continuous exposure to andrographolide.

Dose (μM	Mean % bipolar	Mean % tripolar	Mean % tetrapolar	Mean % multipolar	Mean % mitotic index
0	95.86	3.02	0.86	0.27	4.65
10	93.33	4.67	1.00	1.00	5.71
30	82.44	11.00	3.67	2.89	6.36
50	76.33	13.89	5.78	4.00	5.52
Colchicine	53.56	31.33	9.67	5.44	6.98

Figure 4.12 shows the incremental increases in tripolar, tetrapolar and multipolar centrosomes whereas Figure 4.13 compares the reduction of normal bipolar spindle poles ratio with multiplications in MTOCs and increases in mitotic index after 24 hours exposure to andrographolide. All cells were observed to possess direct association between spindle poles (γ-tubulin) and microtubule (α-tubulin) as shown in Figures 4.9 and 4.10. There were no visible disruptions to the microtubule network. An increase in mitotic index was observed at 10μM, continued at 30 before beginning to decrease again at 50μM. Between 10μM and 30μM of andrographolide, the increased mitotic index value indicated aberrant MTOCs was affecting cellular division and causing mitotic arrest that can be followed by cell death. Although, higher MTOCs were observed at 50μM, the mitotic index began to decrease steadily in tandem with reduced cell viability frequency observed at 70 and 90μM of the compound. As shown in Figure 4.11(A), dead cells were not scorable for centrosome integrity. The data on the positive control, colchicine was also shown in comparison to andrographolide with expected outcome.

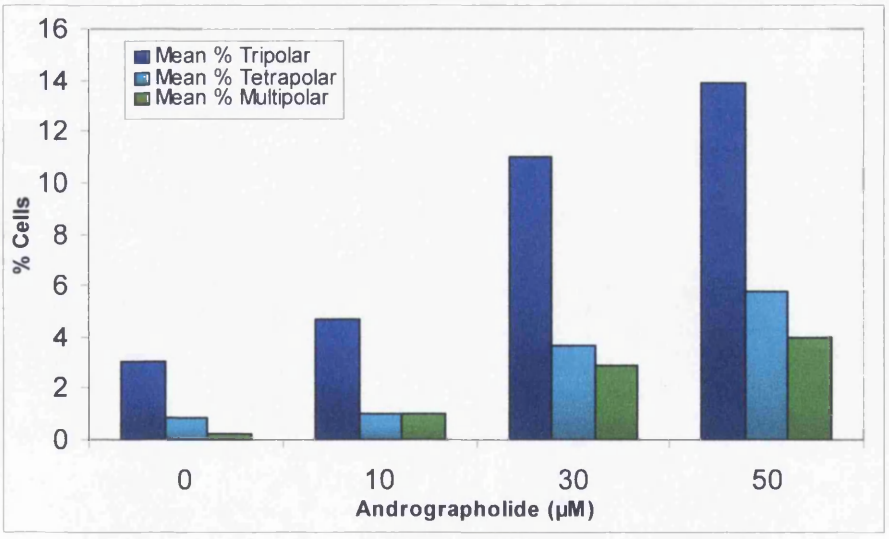

Fig. 4.12 Graph showing the induction of aberrations in mitotic spindle and centrosome organisation in V-79 cells after 24 hours continuous exposure to andrographolide.

The cells seemed more able to tolerate the presence of tripolar MTOCs where 3.02% of untreated V-79 cell populations possessed this feature as compared to less than one percent of cells with tetrapolar and multipolar centrosomes respectively, illustrating that higher number of MTOCs are not sustainable and cells are less likely to survive the next rounds of mitoses. Furthermore, prior to harvesting, the number of floating and unhealthy-looking cells inside the petri dishes was observed to be higher than viable cells attached to the slides in a dose-dependent manner, where higher andrographolide concentration was affecting cell number.

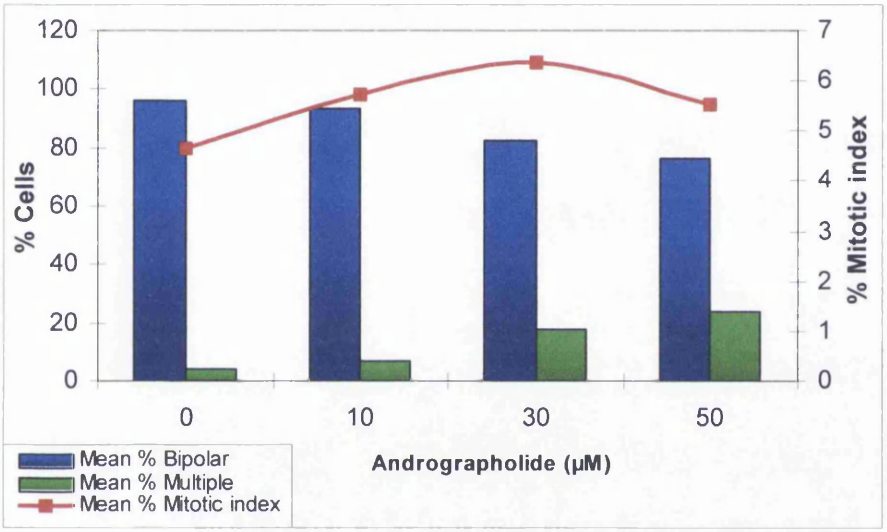

Fig. 4.13 Graph to compare and contrast the reduction in normal bipolarity with increases in multiple centrosomes (tripolar, tetrapolar and multipolar) and mitotic index accruement.

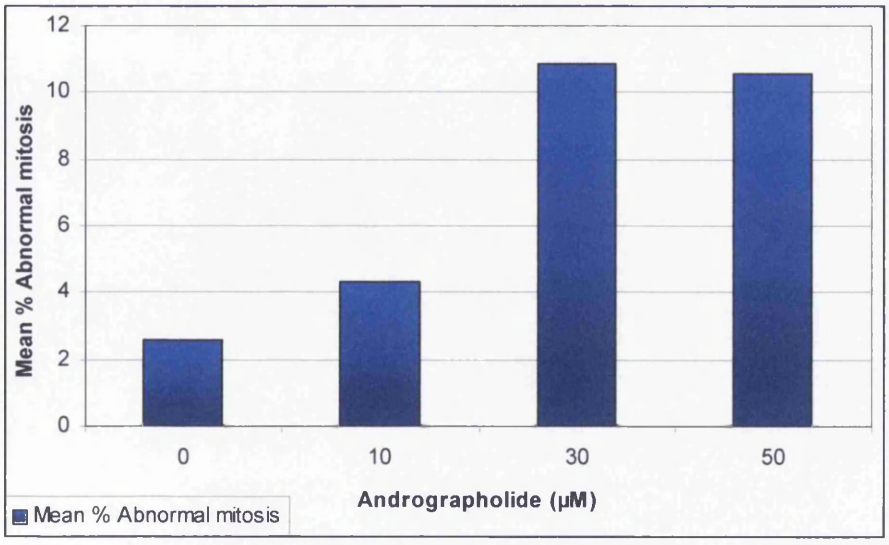

Fig. 4.14 Shows the incidence of abnormal mitosis in V-79 cells exposed to andrographolide for 24 hours.

The incidence of abnormal mitosis was also determined and as shown in Figure 4.14 and the data in Table 4.2 the frequency of aberrant mitoses increased in relation to andrographolide concentration. The presence of more than two spindle poles affected normal chromosome segregation process.

Table 4.2. Mean % incidence of aberrant mitosis in V-79 cells treated with andrographolide for 24 hours.

Dose (μM)	Mean % abnormal mitosis
0	2.56
10	4.33*
30	10.89*
50	10.56*

*Statistically significant values ($p<0.05$) against the negative controls.

Cell viability assessment using Trypan-blue exclusion assay revealed the number of viable cells as well as scorable centrosomal aberrations decreased beginning from 50μM to 90μM, which was the highest concentration of andrographolide tested on V79 cells. The cells were exposed to andrographolide for 24 as well as 48 hours, evidently the frequency of non-viable cells increased steadily with dose, in agreement with cell growth reduction. The duration of andrographolide treatment also affected V-79 cell viability as shown in Table 4.3 and Figures 4.15 respectively. Thus, andrographolide cytotoxicity is dose- and time-dependent in V-79 cells. Figure 4.16 shows the effect of different concentrations of andrographolide with different treatment time on V-79 cell growth.

Table 4.3 Mean percentage of non-viable V-79 cells treated with andrographolide for 24 and 48 hours with corresponding cell growth values (percentage to negative controls).

Dose (μM)	Mean % non-viable cells		Mean Cell growth (% to 0)	
	24 hours	48 hours	24 hours	48 hours
0	6.83	26.50	100.00	100.00
10	7.08	44.98	85.64	69.82*2
30	14.45*	81.41*2	59.12*	26.89*2
50	38.25*	91.08*2	58.39*	15.48*2
70	61.10*	94.91*2	21.90*	8.34*2
90	75.76*	94.88*2	14.11*	5.66*2

*Statistically significant values ($p<0.05$) against the negative controls. 2 denotes significant difference ($p<0.05$) between 24 and 48-hours treatment.

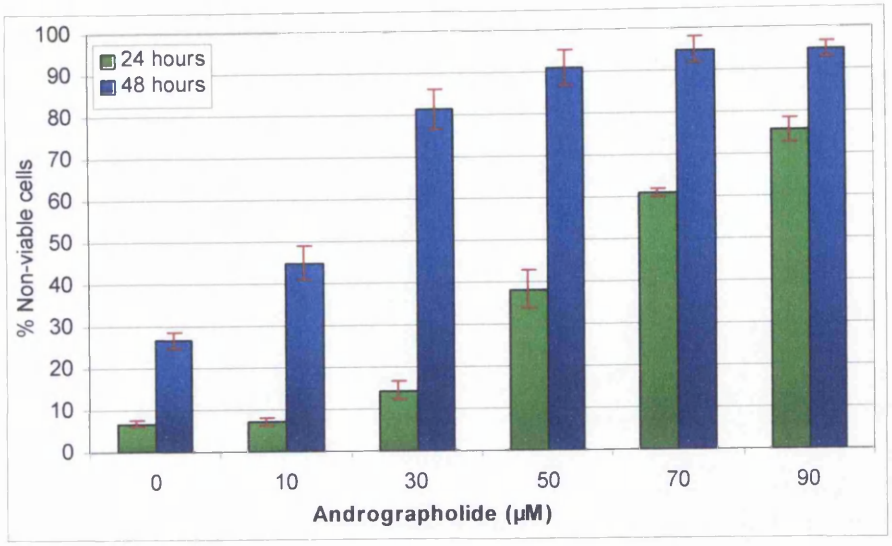

Fig. 4.15 A comparison of non-viable cell frequency between 24- and 48-hour treatment of V-79 cells with different concentrations of andrographolide. Longer treatment reduced cell viability.

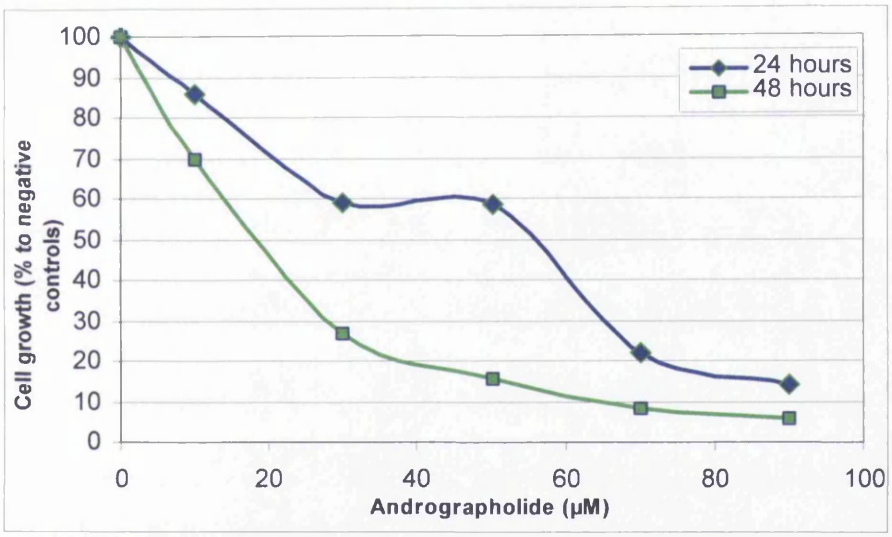

Fig. 4.16 The effect of different concentrations of andrographolide on V-79 cell growth during 24- and 48-hour treatment period. Longer treatment significantly reduced cell growth.

In order to determine whether the presence of abnormal centrosome numbers after treatment would be continued in subsequent cell divisions in the absence of andrographolide, V-79 cells that were exposed to various concentrations of the compound were washed with pre-warmed PBS and allowed to grow in fresh medium for a further one and two cell cycles.

Table 4.4 and Figure 4.17 shows the data on MTOCs abnormality in V-79 cells growing for 24 hours post-treatment whereas Table 4.5 and Figure 4.18 shows the aberrations observed after two cell cycles (48 hours) after andrographolide removal respectively.

Table 4.4 Induction of centrosome and mitotic spindle abnormalities in V79 cells 24 hours after the removal of andrographolide.

Dose (μM)	Mean % bipolar	Mean % tripolar	Mean % tetrapolar	Mean % multipolar	Mean % mitotic index
0	94.38	4.25	0.88	0.50	5.21
10	91.75	5.75	1.25	1.25	5.75
30	84.50	11.00	3.25	2.50	6.31
50	81.75	11.25	3.75	3.25	6.08

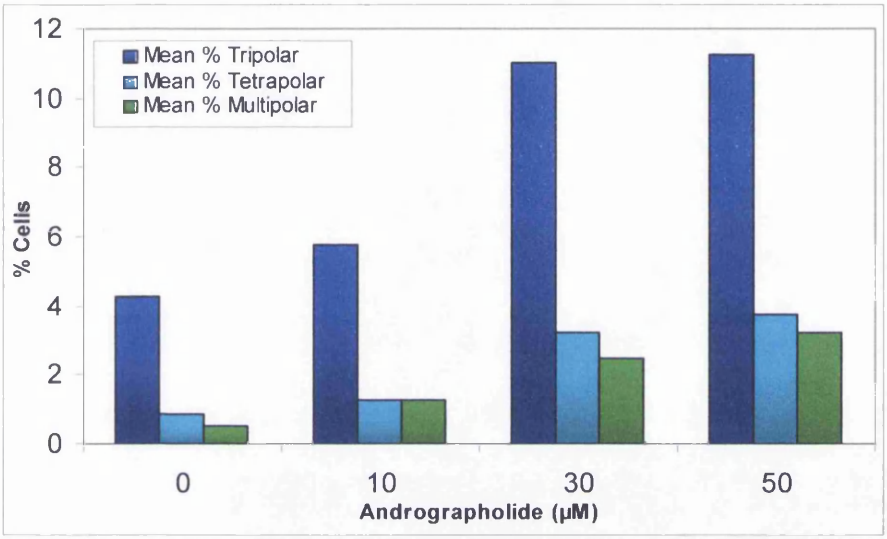

Fig. 4.17 Graph showing the induction of aberrations in mitotic spindle and centrosome organisation in V-79 cells 24 hours after the removal of andrographolide.

Based on both sets of data, MTOCs tripolarity constituted the most prevalent type of aberrant multiplication even after andrographolide was removed from the growth medium. Tetrapolar and multipolar division also registered an increase against negative control but were less than 6% and 4% respectively. It is interesting to note that of the MTOCs aberrations induced, tripolarity in particular can be as high as those observed in continuous treatment with andrographolide. Figure 4.19 compares the induction of MTOCs aberration between the three treatment sets. However, one must also take into account that the occurrence of multiple MTOCs (i.e. tripolar, tetrapolar and multipolar) were higher in untreated cells for these sets of experiments as compared to negative controls in cells subjected to continuous 24-hour treatment.

Table 4.5 Induction of centrosome and mitotic spindle abnormalities in V-79 cells 48 hours after the removal of andrographolide.

Dose (μM)	Mean % bipolar	Mean % tripolar	Mean % tetrapolar	Mean % multipolar	Mean % mitotic index
0	93.13	4.88	1.00	0.50	5.66
10	89.50	7.25	2.25	1.00	6.88
30	81.25	12.25	3.75	2.75	7.30
50	77.50	14.00	5.25	3.25	8.03

As aberrant centrosome multiplication increased with dose, so did the mitotic index values. This value was higher in cells treated with various doses of andrographolide and allowed to recover for a further two cell cycles as shown in Figure 4.20.

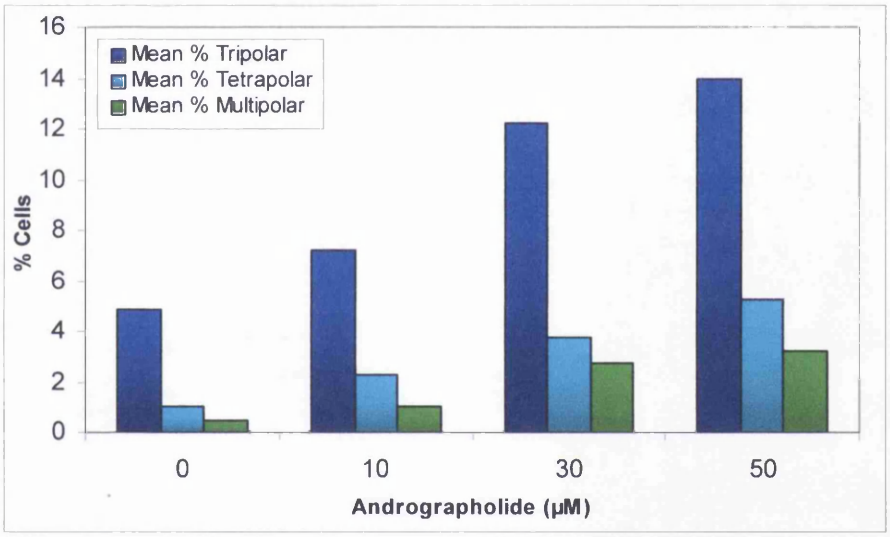

Fig. 4.18 Graph showing the induction of aberrations in mitotic spindle and centrosome organisation in V-79 cells 48 hours after the removal of andrographolide.

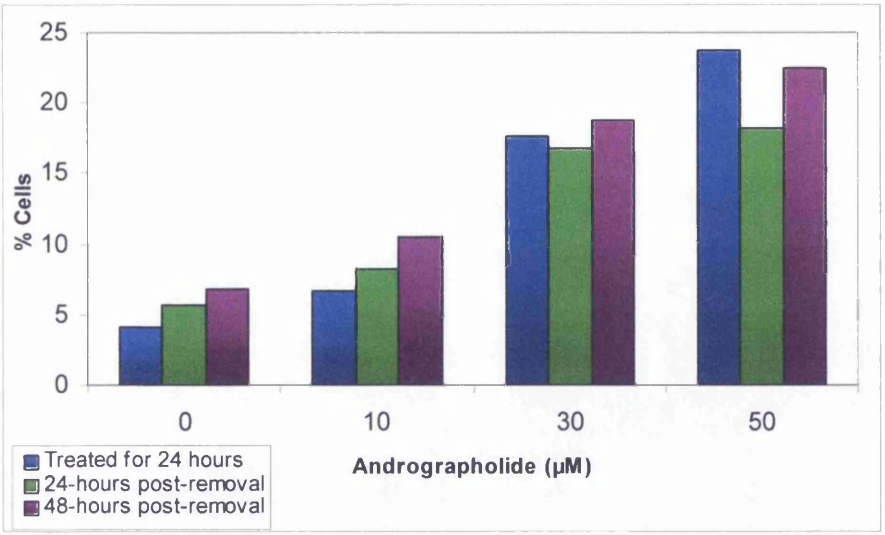

Fig. 4.19 Graph to compare and contrast the frequency of microtubule organising centres (MTOCs) aberrations (tripolar, tetrapolar and multipolar) between V-79 cells that were treated continuously for 24 hours and those that were allowed to recover one and two cell cycles post-treatment. Tripolarity was the most common form of centrosome multiplication observed.

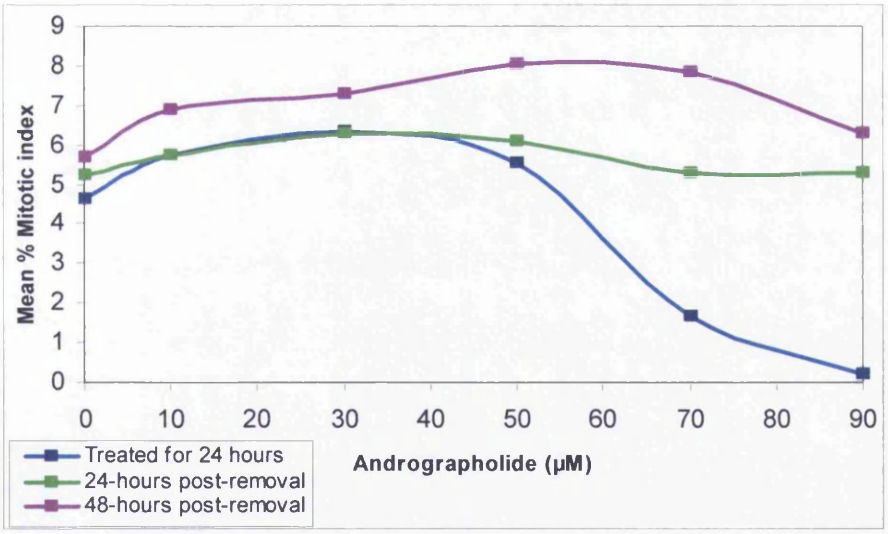

Fig. 4.20 A line graph to compare and contrast the levels of mitotic index observed between V-79 cells that were treated continuously for 24 hours and those that were allowed to recover one and two cell cycles post-treatment. The mitotic index for cells treated continuously fell in the presence of andrographolide due to cytotoxicity.

When comparing the data presented in tables 4.1, 4.4 and 4.5, the percentage of cells with more than two spindle poles in the negative control remained mostly constant in value, although slight increase were observed, they were not statistically significant. There were dose-related increases between 10-50µM even after andrographolide removal but these were mostly tripolar in nature. Remarkably, the percentage of cells with tripolar MTOCs

remained similar even in the absence of andrographolide, post-treatment. The same can be said about tetra- and multipolar MTOCs values although there was a decrease of tetrapolar cells before it increased again when allowed to progress for another one cell cycle. The mitotic index values also changed with the values were higher for cells that were permitted to proceed through subsequent cell cycles after 24-hour andrographolide challenge. Cells that completed two cell cycles (48 hours) post-treatment showed the highest mitotic index value.

Table 4.6 The mean percentage incidence of condensed chromatin in V-79 cells treated with andrographolide for 24 hours and those that were allowed to recover 24 hours post-treatment.

Dose (μM)	24-hours treatment	24-hours post removal
0	0.10	0.12
10	0.16	0.18
30	0.60*	0.69*
50	1.82*	2.07*
70	3.62*	4.38*
90	5.33*	5.29*

*Statistically significant values ($p<0.05$) against the negative controls.

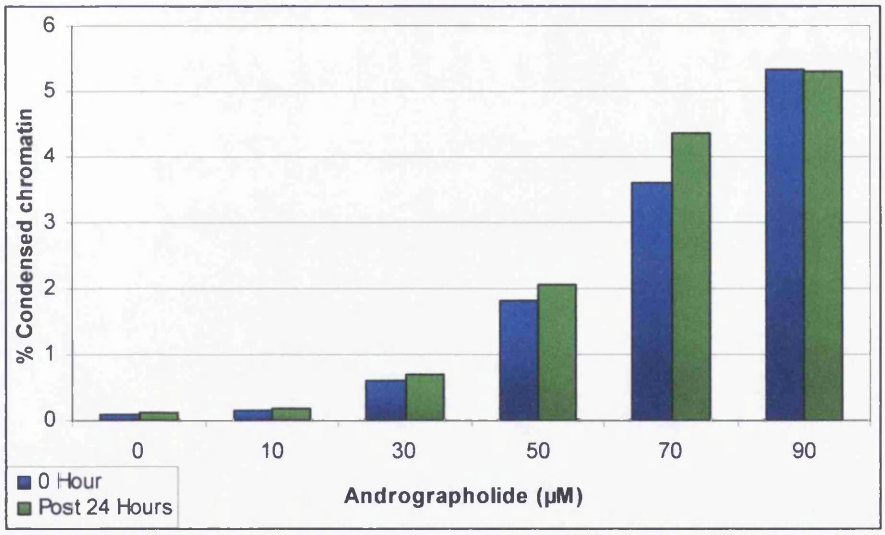

Fig. 4.21 A graphic comparison in the mean percentage incidence of condensed chromatin observed between V-79 cells that were treated continuously for 24 hours and those that were allowed to recover 24 hours after andrographolide insult. The presence of condensed chromatin indicates dead cells.

The incidence of condensed chromatin, which indicates cell death was also quantified and andrographolide elicited condensed chromatin frequency in a dose-related fashion as presented in Table 4.6 and Figure 4.21. There were no significant difference in condensed

chromatin frequency between V-79 exposed to andrographolide for 24 hours and those that were permitted to grow for another 24 hours period in the absence of the phytochemical.

As the induction of multiple MTOCs was observed in a dose-dependent manner between 10-50μM of continuous exposure to andrographolide, discovering how it affects cell fate was deemed an interesting venture. Table 4.7 shows the data of V-79 cells exposed to andrographolide in the same concentration range and the data displayed graphically as shown in Figure 4.22. Generally, the pattern of the data is supporting the trend observed as shown in Table 4.1 earlier. Abnormal centrosome number promoted aberrant mitoses and the percentage of cells containing more than one nucleus and failed to complete cytokinesis, increased in a dose-dependent fashion with 30μM of the phytochemical. 13.28% and 13.73% of the cell population remained as binucleates whereas 1.55% and 1.35% of cells were trinucleates, upon treatment with 30 and 50μM of andrographolide respectively. Statistically significant values ($p<0.05$) for difference against the negative controls were as shown in Table 4.7. Even though the percentage of tri-, tetra- and multipolar cells generated were lower than the percentage of cells that were shown to have tripolar, tetrapolar and multipolar MTOCs when treated with the same dose of andrographolide, the presence of more than two spindle poles forced anomalous chromosome migration in different directions manifested by trinucleated, tetranucleated and multinucleated cells. Whereas, the effects observed at higher doses were closely linked to cell viability since most cells challenged with 70 and 90μM of the compound died due to necrosis. As demonstrated in the Chapter 3, V-79 cells exposed to andrographolide for 24 hours experienced reduced cell viability with most cells died primarily via necrosis in a dose-dependent manner.

Table 4.7 Cell fate of V-79 cells after 24-hour treatment with different doses of andrographolide.

Dose (μM)	Mean % Binucleate	Mean % Trinucleate	Mean % Tetranucleate	Mean % Multinucleate
0	3.39	0.24	0.13	0.06
10	6.85*	0.30	0.25	0.15*
30	13.28*	1.55*	0.85*	0.28*
50	13.73*	1.35*	0.55*	0.35*
70	9.93*	0.70*	0.35*	0.58*
90	4.45	0.38	0.08	0.18*

*Statistically significant values ($p<0.05$) against the negative controls.

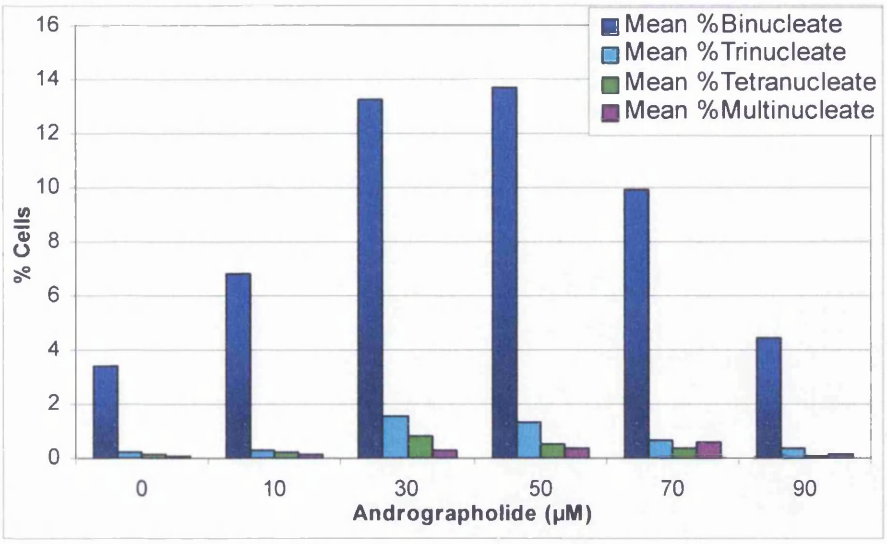

Fig. 4.22 Graph showing the cellular division stage of V-79 cells after 24-hour continuous treatment with different doses of andrographolide.

The ability of V-79 cells to recover after andrographolide insult for 24 hours was also investigated and the data were presented as Table 4.8 and Figure 4.23 respectively. It turned out that there was still significant presence ($p<0.05$) of cells harbouring more than one nucleus in concordance with the MTOCs abnormality data as demonstrated in Tables 4.4 and 4.5. Trinucleated cells frequency was prominent so did tetra- and multinucleated cells. Thus, the presence of abnormal MTOCs polarity promoted multinucleation of V-79 cells even after andrographolide removal.

Table 4.8 Cell fate of V-79 cells after 24-hour treatment with different doses of andrographolide and subsequently allowed to recover for another 24 hours in the absence of the phytochemical.

Dose (µM)	Mean % Binucleate	Mean % Trinucleate	Mean % Tetranucleate	Mean % Multinucleate
0	2.55	0.33	0.03	0.04
10	3.08	0.98*	0.20*	0.10*
30	6.13*	1.58*	0.50*	0.15*
50	7.03*	1.78*	0.63*	0.33*
70	3.53*	0.50	0.30*	0.13*
90	2.23	0.38	0.10	0.05

*Statistically significant values ($p<0.05$) against the negative controls.

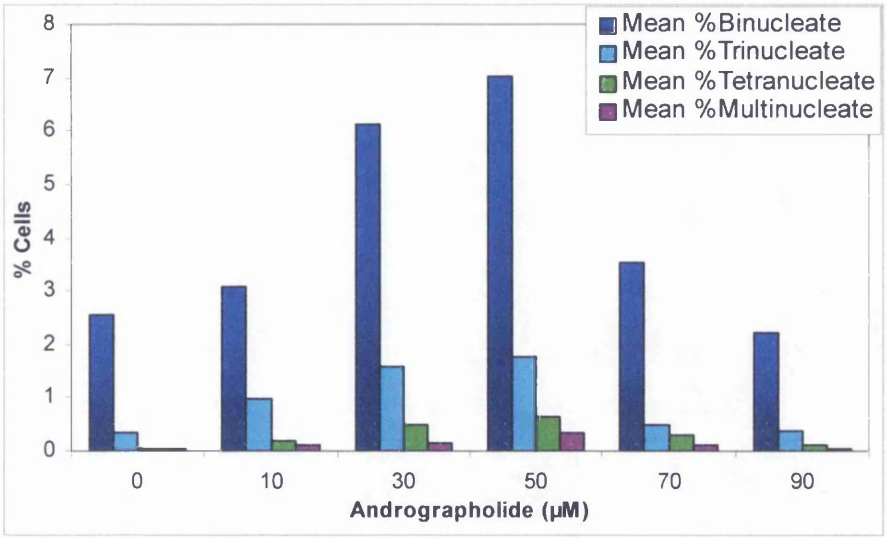

Fig.4.23 Cell fate of V-79 cells after 24-hour treatment with different doses of andrographolide and subsequently allowed to recover for another 24 hours in the absence of the phytochemical.

Since the V-79 cell line is p53-deficient, another cell line, MCL-5 that is metabolically-competent and capable of normal DNA repair was also subjected to the same treatment for one and two cell cycles. As shown in Tables 4.9 and 4.10 respectively, MCL-5 cells were observed to generally experienced less effects of andrographolide challenge evident from the percentage of cells harbouring more than one nuclei, especially trinucleates. Figures 4.24 and 4.25 graphically displayed the data obtained. There was a steady accruement of cells containing more than one nucleus in the order of binucleates > trinucleates > tetranucleates > multinucleates, where binucleated cells were statistically significant between 10-50μM of andrographolide against negative control as observed after 24 hours treatment. The presence of cells with more than two nuclei (tri-, tetra- and multinucleated) were less than 1% of the cell population in all doses tested and again 30μM of the phytochemical induced the highest number whereas 50μM was required to attain statistically significant percentage of multinucleated cells. This suggests that MCL-5 may be more able to withstand andrographolide challenge than V-79 cells.

Table 4.9 Cell fate of MCL-5 cells after 24-hour treatment with different doses of andrographolide.

Dose (μM)	Mean % Binucleate	Mean % Trinucleate	Mean % Tetranucleate	Mean % Multinucleate
0	5.90	0.43	0.37	0.09
10	10.32*	0.65*	0.25	0.13
30	13.38*	0.90*	0.60*	0.18*
50	10.45*	0.65*	0.50*	0.30*
70	6.23	0.30	0.15*	0.15
90	3.90	0.30	0.20	0.15

*Statistically significant values ($p<0.05$) against the negative controls.

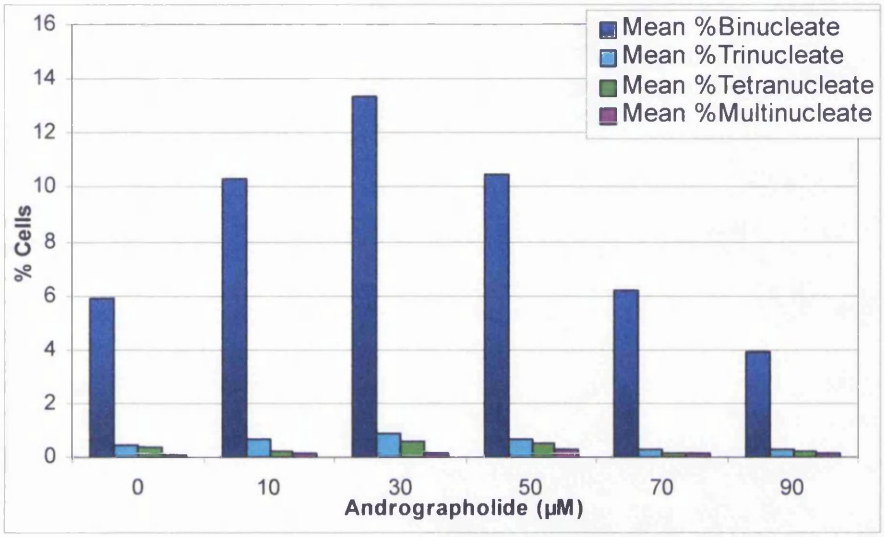

Fig. 4.24 Graph showing the cellular division stage of MCL-5 cells after 24-hour continuous treatment with different doses of andrographolide.

MCL-5 cells that were subjected to 48 hours (two cell cycles) continuous exposure also showed that 30μM of andrographolide remained the optimum concentration in arresting cells as bi-, tri- and tetranucleates but only at a higher concentration of 50μM that multinucleated cells were of significant value, the same trend as observed with 24 hours exposure demonstrated earlier in Table 4.9

Table 4.10 Cell fate of MCL-5 cells after 48-hour treatment with different doses of andrographolide.

Dose (μM)	Mean % Binucleate	Mean % Trinucleate	Mean % Tetranucleate	Mean % Multinucleate
0	3.25	0.21	0.10	0.09
10	7.00*	0.30	0.20*	0.05
30	10.18*	0.50*	0.43*	0.13*
50	9.93*	0.45*	0.23*	0.25*
70	8.88*	0.48*	0.23*	0.05
90	7.83*	0.10	0.10	0.05

*Statistically significant values ($p<0.05$) against the negative controls.

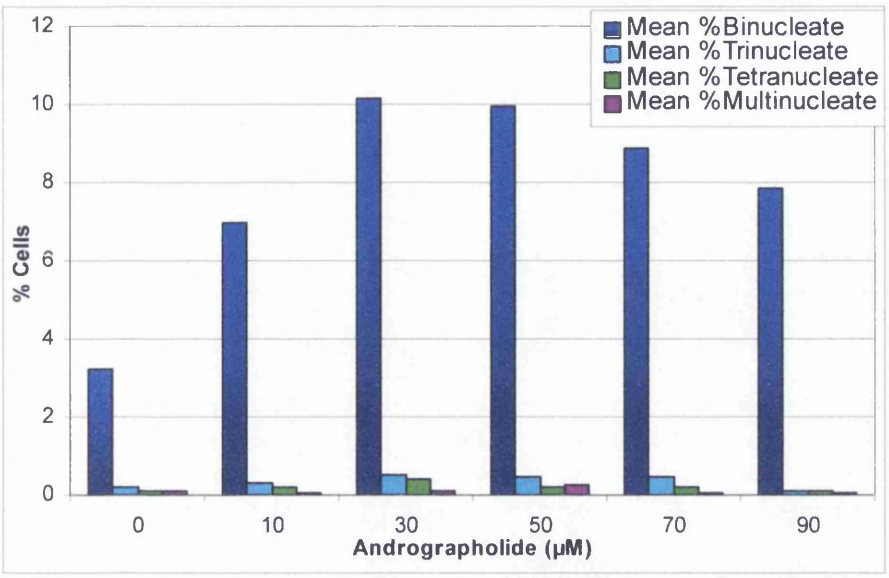

Fig. 4.25 Graph showing the cellular division stage of MCL-5 cells after 48-hour continuous treatment with different doses of andrographolide.

This data sets highlight the fact that even though the treatment time was prolonged by another one cell cycle, direct doubling of effects measurable by the percentage of non-mononucleated cells, in this case the most obvious would be binucleated cells, was not observed. In fact, simple direct comparison between data in Tables 4.9 and 4.10 showed a slight decrease rather than an expected increment, observed between doses 10 to 50μM. Interestingly, the percentage of binucleated cells at 70 and 90μM were higher compared to the cells exposed to the same concentrations but at shorter treatment period. However, these figures should not be interpreted as a direct effect of andrographolide but merely changes to the number of scorable cells since many cells died due to necrosis.

MCL-5 cells were also exposed to a similar concentration range of andrographolide up to 50μM but with a longer treatment period of 120 hours (5 continuous cell cycles) and a similar result emerged. Referring to Table 4.11 and Figure 4.26, shows the percentages of cells arrested with different mitotic outcomes.

Table 4.11 Cell fate of MCL-5 cells after continuous exposure for five cell cycles to different concentrations of andrographolide.

Dose (μM)	Mean % Binucleate	Mean % Trinucleate	Mean % Tetranucleate	Mean % Multinucleate
0	7.05	0.43	0.48	0.03
10	12.18*	0.93*	0.65*	0.30*
30	11.25*	1.84*	1.03*	0.53*
50	10.05*	1.89*	0.91*	0.50*

*Statistically significant values ($p<0.05$) against the negative controls.

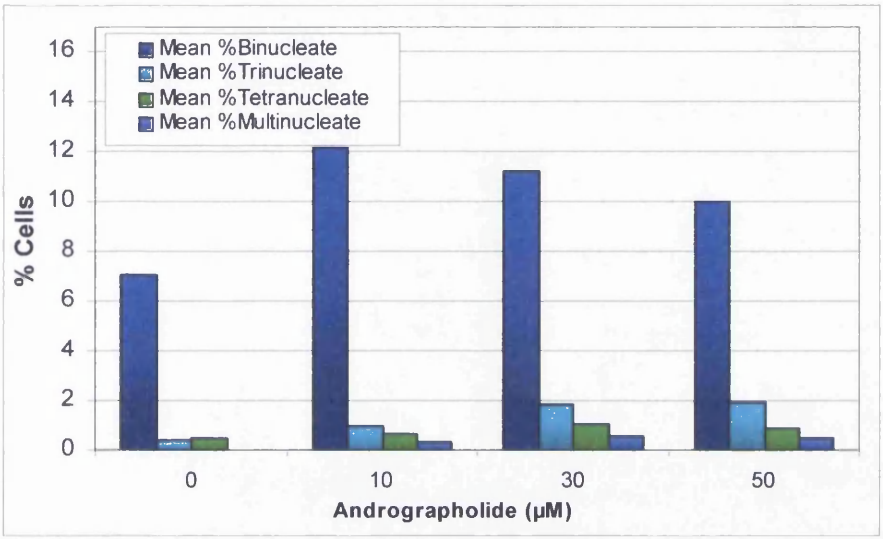

Fig. 4.26 Graph showing MCL-5 cells at various stages after continuous exposure to andrographolide for five cell cycles (120 hours).

Although, generally the numbers were slightly higher when compared to 24- and 48-hour exposure, the percentage of binucleated cells in untreated cultures were also higher possibly due to stress during the culture period. The percentages of trinucleated cells were almost 2% and tetranucleated cells were almost 1% between 30 and 50μM whereas the percentage of multinucleated cells was still less than 1% of the cell population. Again at these concentrations, andrographolide induced a statistically significant number of binucleated cells more than 10% of 4000 cells scored.

Table 4.12 Frequency of necrosis and apoptosis in MCL-5 cells treated for five cell cycles to different concentration of andrographolide.

Dose (μM)	Mean % Necrotic cells	Mean % Apoptotic cells
0	13.05	0.73
10	24.45	1.00
30	33.15*	1.45*
50	50.95*	1.30*

*Denotes statistically significant difference against the negative controls.

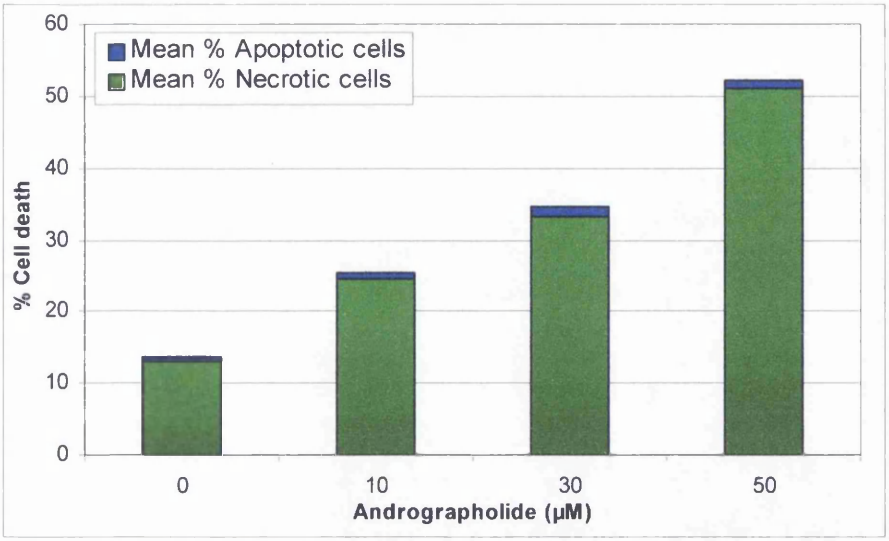

Fig. 4.27 The incidence of necrosis and apoptosis in MCL-5 cells exposed to andrographolide for five cell cycles (120 hours).

Again, MCL-5 cells exposed to the longer treatment period of 120 hours (five cell cycles) reproduced the same trend observed previously where andrographolide mainly incited necrotic cell death in a dose-dependent manner, rather than apoptotic response. In all concentrations tested more than 1% of the cells were apoptotic as demonstrated in Table 4.12 and Figure 4.27. Thus, subjecting the cells to longer treatment period did not increase the incidence of cell death. This can be attributed to the dynamics of cell growth and demise, where the values were for the cells scored at that time. Cellular debris and remnants were observed on the microscope slides indicating the presence of cells that died earlier. It is also to be stated the frequency of necrotic and apoptotic cells in the negative control may be related to cell culture stress.

4.8 DISCUSSION

Chromosomes are segregated by attachment to the highly organised microtubule spindle that only forms during mitosis, replacing the long monoastral array present in the interphase stage. In normally dividing cell, microtubule organising centres (MTOCs) or centrosomes exist in mirror symmetry at the opposite poles connected by microtubules from each spindle pole. To this highly symmetrical structure, the duplicated chromatids attached, then are diametric and equally apportioned during anaphase to each daughter cell. Disruption to any actors during this mitotic theatre can lead to dire consequences. Indeed, abnormalities of centrosome integrity and mitotic spindle apparatus may have a role in the initiation of neoplasia (Yuen *et al.*, 2005).

The exposure of V-79 cells to andrographolide at various concentrations induced aberrant mitotic division in a dose-response manner and this is the first study, to the best of the author's knowledge, which provided evidence for the propensity of andrographolide to disrupt microtubule organising centres function hence contributing to chromosome segregation abnormalities such as those manifested as micronuclei. The data suggested a direct correlation between aberrant MTOCs number, cell division and mitotic index upon andrographolide challenge, with such an insult inflicted damages that can still be observed even after the removal of the phytochemical.

Centrosomes can be indispensable for microtubule polymerisation (Heald *et al.*, 1996; Khodjakov *et al.*, 2000) but are crucial for spindle nucleation and thus affect chromosome segregation process. Centrosomes also influence other key roles governing cell division including cytokinesis initiation and the entry into S-phase of the cell cycle (Khodjakov *et al.*, 2000; Hinchcliffe *et al.*, 2001; Piel *et al.*, 2001). In the absence of the centrosome, microtubule polymerisation and chromosome segregation can still occur but cell division is usually accompanied by defects in cytokinesis and cell cycle progression (Khodjakov & Rieder, 2001). For accurate chromosome separation process, each daughter cell must receive only a single centrosome and this centrosome must replicate only once per cell cycle.

Andrographolide caused significant numerical centrosomal abnormality manifested by the presence of the γ-tubulin signal in tri-, tetra- and multipolar MTOCs, in a descending

order of prominence especially between 30 and 50μM doses, with corresponding significant increases in the mitotic index value. This anomalous number of spindle poles affects normal chromosome segregation process due to the presence of multipolar mitotic spindles. Unequal chromosome segregation leads to aneupoidy and higher doses of andrographolide increased the proportion of not only cells with tripolar MTOCs but also cells with higher number of centrosomes, suggesting a worse disruption to the centrosome numeral homeostasis and carries more risks to cellular division process. It is possible for disruption to normal levels of proteins involved in centriole duplication to cause numeral amplification within one cell cycle consistent with increases in pseudo-bipolar and multipolar mitoses frequencies (Duensing *et al.*, 2007).

Indeed, centrosomal anomaly in cultured mammalian cells is associated with the induction of multipolar spindles, multipolar division and micronucleation (Ochi 2002). Diazepam for example was shown to induce abnormal anaphases consisted primarily of multipolar spindles and a high frequency of kinetochore-positive micronuclei in binucleated cells (Izzo *et al.*, 1998). A study on centrosome integrity using a mouse model of human breast cancer revealed that 25% of the cells contained micronuclei and approximately 60% harbouring aberrant centrosome numbers (Montagna *et al.*, 2002). Furthermore, the presence of micronuclei was detected only in 7% of cells with normal bipolar MTOCs in contrast to 18% in cells with amplified centrosome numbers (Montagna *et al.*, 2002). The statistically significant dose-dependent elevation in aberrant MTOCs number in V-79 cells subjected to andrographolide for 24 hours is in concordance with the micronuclei frequency induced in AHH-1, MCL-5 and V-79 cell lines as discussed in the previous chapter and assists in the elucidation of possible mechanism involved in micronuclei induction by this phytochemical. The presence of more than two MTOCs affected normal chromosome migration towards opposite spindle poles since the frequency of aberrant mitotic cells accrued with increased andrographolide concentrations. The immunofluorescence staining technique employed not only assisted in centrosome numerical aberration assessment but also revealed a direct connection between MTOCs represented by γ-tubulin antibody (red in colour) and microtubules (α-tubulin antibody, green in colour), hence lend credence to the notion that andrographolide caused centrosome multiplication as opposed to microtubule disruption and disassociation with the MTOCs.

Centrosome duplication is controlled by members of the Aurora/IpII, CDK, NIMA and Polo-like families of cell cycle kinases (Fry *et al.*, 1998; Mayor *et al.*, 1999; Hinchcliffe *et al.*, 1999; Lacey *et al.* 1999; Mussman *et al.*, 2000; Meraldi & Nigg, 2001). CDK2 bound to cyclins E or A and involves in stabilising the centrosomal kinase hMps1 permitting its maintained association with the centrosome in mice (Fisk *et al.*, 2001) while phosphorylating and dissociating nucleophosmin/B23 (Okuda *et al.*, 2000). During G_2, various additional proteins are recruited including members of CDK1 kinases, Aurora and Polo-like families, presumably involves in centrosome maturation (Bailly *et al.*, 1989; Pockwinse *et al.*, 1997; Jackman *et al.*, 2003). In M-phase, nucleophosmin is again present at the spindle poles and associates with the centrosomal organising protein NuMA (Zatsepina *et al.*, 2003). Also at this stage, the tumour suppressor proteins p53, BRCA1 and TACC are present at the centrosomes (Raff, 2002; Fisk *et al.*, 2002).

Cells with abnormal centrosome number customarily produce multiple MTOCs such as tri-, tetra- and multipolar spindles (Fukasawa, 2005). Tripolar MTOCs seems to be more tolerable and frequent in occurrence as shown by the results and they are able to complete cytokinesis with some daughter cells from this mitosis are viable but aneuploid in status whereas others may not survive due to ruinous karyotypic modifications (Fukasawa, 2005). Cells containing more than three spindle poles frequently fail to undergo cytokinesis, subsequently generating either binucleated or arrested as mono-nucleated cells. The results generated showed that the presence of multiple centrosomes were translated into cells with multiple nuclei. V-79 cells challenged with andrographolide for 24 hours exhibited significant frequency of bi-, tri-, tetra- and multinucleated cells between 30 and 70μM doses, which suggest chromosome segregation fidelity was affected in the presence of andrographolide.

Furthermore, abnormal centrosome number was maintained in the absence of andrographolide, after the initial 24-hours exposure period as illustrated in Figure 4.19. The values remained almost similar and it was expected that should the cells were able to recover, the frequency of cells with abnormal MTOCs would be reduced by cell death but this was not supported by the data obtained and the mechanism(s) involved is not entirely clear. Consequently, the presence of multiple MTOCs lead to abnormal mitoses observed in V-79 cells even after the compound was removed from the growth medium and cells

were subsequently allowed to grow for a further 24 and 48 hours after exposure. Anomalous centrosome number can be transferred to daughter cells after division.

After andrographolide removal, the frequency of tri-, tetra- and multinucleated cells were still above the untreated samples. At 10μM of the phytochemical, in comparison to cells subjected to continuous 24-hours treatment (Table 4.7), the percentage of binucleated cells was lower whereas trinucleated cells increased (Table 4.8). The percentages of binucleated cells were also lower than those observed in Table 4.8 but were still significant against the negative controls. This shows that centrosome amplification induced by andrographolide were maintained if not accrued and also affected subsequent cell divisions. However, it is also not distinguishable whether such incidence corresponds to new daughter cells or existing cells that were not able to divide.

Evidently, the presence of tripolar MTOCs within a cell is more tolerable than those with four or more centrosomes, hence the frequencies of trinucleated cells were higher than those of tetra- and multinucleated cells. When cells attempt cytokinesis in the presence of abnormal MTOCs number, only one cleavage furrow may prevail due to insufficient new surface area to complete more than one and constantly resulting in two daughter cells containing different chromosome complement (Duesberg & Li, 2003). Division involving three or more daughter cells are produced by multiple cleavage furrows and aneuploid progeny are generated. When comparisons were made between V-79 and MCL-5, the incidence of trinucleated cells were higher in the former than the latter as shown in Tables 4.7 and 4.9 respectively. This explained previous findings that male rats subjected to andrographolide treatment for 48 days exhibited reduced sperm counts, caused necrotic death amongst Sertoli cells and the seminiferous epithelium as well as lumen are consisted of multinucleated cells (Akbarsha & Murugaian, 2000). Mating of andrographolide-treated rats with untreated females counterparts did not produced any offspring (Akbarsha & Murugaian, 2000).

The statistically significant increase of mitotic index value connotes an increase of metaphase arrest suggesting a build-up of dividing cells unable to complete mitosis. There is a correlation between DNA repair and the maintenance of normal MTOCs number. Centrosome amplification has been shown to occur during prolonged G2-arrest in Rad51-deficient cells due to G_2-M checkpoint activation by DNA damage (Dodson *et*

al., 2004). Therefore, DNA damages that are usually repaired, will accrued in the presence of defective repair system or genomic injury induced by the detrimental agent that essentially overwhelmed the DNA repair mechanisms, consequently triggering the G_2-M transition checkpoint activation leading to mitotic arrest.

Previous studies showed that andrographolide caused cell cycle arrest at the G_0-G_1 phase of the cell cycle concomitant with decrement of cell populations at the G_2-M phase in human cancer cells (Rajagopal *et al.*, 2003; Satyanarayana *et al.*, 2004). It was further revealed that there was significant elevation of $p27^{Kip1}$ and reduction in CDK4 protein expression levels (Rajagopal *et al.*, 2003; Satyanarayana *et al.*, 2004). However, no changes were recorded in cyclins D1 and B1 levels (Satyanarayana *et al.*, 2004). However, another recent study reported andrographolide induced G_2-M arrest with treated HepG2 cells possessing a low level $p34^{cdc2}$, which is a key cyclin-dependent kinase for G_2-M transition (Li *et al.*, 2007). Both the G_2 and the mitotic checkpoints possess a restricted capacity in maintaining arrest following cytoskeletal disruptions and DNA damage respectively, which means after a period of time in arrest, cells might progress to the next stage of the cell cycle in an aberrant manner. Adaptation of the G_2 and mitotic checkpoints can lead to genomic instability. However, there was no clear pattern in andrographolide effects on cell cycle arrests since different cell lines including cancer cells studied in previous works exhibited a non-specific cell cycle arrest.

Centrosome duplication can become temporally detached from the cell cycle allowing multiple centrosomes to materialise in a single cell. Over-duplication is connected with decreased activity of the p53 tumour suppressor pathway, commonly via mutational inactivation of the *TP53* gene (Fukasawa *et al.*, 1996; Carroll *et al.*, 1999). Reduced p53 activity can also be due to over-expression of the p53 inactivating protein MDM2 (Carroll *et al.*, 1999) or reduced activity of p53 downstream targets, Gadd45 (Hollander *et al.*, 1999; Wang *et al.*, 1999) and $p21^{Cip1/waf1}$ (Mantel *et al.*, 1999; Tarapore *et al.*, 2001a), all of which correlated with centrosome multiplication. The p53 protein localises to centrosomes before and after duplication. It is capable of regulating centrosome replication independent of its role as transcription regulator (Tarapore *et al.*, 2001b) then dissociates from the centrosomes to be stabilised in cytoplasm of cells with mitotic defects leading to G_1 arrest in the next cell cycle. Whereas, no mitotic arrest occurred in cells without p53 (Fisk *et al.*, 2002; Raff *et al.*, 2002). Andrographolide was shown to

exert its effects independent of a cell's p53 status (Rajagopal *et al.*, 2003). The V-79 cell line used in this study is p53-deficient (Chaung *et al.*, 1997) hence, cells that can escape mitotic arrest, customarily generates tetraploid cells (Lanni & Jacks, 1998).

Loss of normal p53 activity has been shown to permit polyploid cells to proliferate instead of apoptose (Casenghi *et al.*, 1999; Andreassen *et al.*, 2001). It has been suggested that p53 is responsible in coordinating the initiation of centrosome duplication with DNA replication in addition to its role in preventing centrosome over-duplication. In response to DNA damage, p53 should activates its target genes including for p21, which in turn binds to and inhibit the CDK2-cyclin E complex. CDK2-cyclin E complex is needed for centrosome duplication but the paradox is centrosome hyperamplification is still observed in p53 positive cells in which p21 would be induced and CDK2-cyclin E activity would be inhibited. Thus, p53 status alone may not significantly influence normal centrosome presence since abnormal centrosome number can be seen in tumours with persistent p53 activity (Lingle *et al.*, 2002; D'Assoro *et al.*, 2002; Pihan *et al.*, 2003) suggesting that actors other than the 'guardian of the genome' might be involved.

The major cell cycle control mechanism that acts during mitosis is the spindle assembly checkpoint, also known as the mitotic checkpoint which prevents chromosome malsegregation and aneuploidy via inhibition of cell cycle progression into anaphase, until all of the replicated chromosomes have attached to spindle microtubules. Mitotic checkpoint proteins are recruited to kinetochores of unattached chromosomes leading to the generation of an at least partially diffusible signal inhibiting the anaphase promoting complex/cyclosome (APC/C). The APC/C is an E3 ubiquitin ligase that ubiquitinates substrates whose degradation is essential for anaphase inception (securin) and mitotic exit (cyclin B). Abolition of securin post-ubiquitination releases its binding partner separase, whereas simultaneous depletion of cyclin B-dependent CDK1 kinase activity resulting in separase dephosphorylation. Both events cause separase activation, which then cleaves the cohesins that hold replicated chromosomes together and initiates anaphase. Even a single unattached kinetochore can be sufficient to delay anaphase onset (Rieder *et al.*, 1994; Rieder *et al.*, 1995). A weakened mitotic checkpoint where inability to maintain checkpoint signalling process can lead to chromosome loss or non-disjunction concordant with decrease length of arrest. Complete absence of the mitotic checkpoint on the other hand, results in rapid cell-autonamous lethality due to extensive chromosome

missegregation and the cells die within six divisions (Michel *et al.*, 2004; Kops *et al.*, 2004). Chromosome segregation errors due to microtubules nucleated by multipolar MTOCs cannot be prevented by the mitotic checkpoint if the kinetochores made productive attachment to the spindles.

A large number of gene products are involved in the mitotic checkpoint response including but not limited to MAD2, BUB1, BUBR1 and Aurora B. Direct mutation in any of the essential genes could compromise the checkpoint response. Alterations to the expression levels of these genes, which apparently occur more frequently in comparison to direct mutations, can also jeopardise the mitotic checkpoint. Lower expression of the crucial proteins would result in aneuploidy and chromosome instability, at least in proteins whose accumulation was rate-limiting for checkpoint signalling at individual kinetochores. Indeed, this was shown to be the case for MAD2 and BUBR1 (Michel *et al.*, 2001; Baker *et al.*, 2004). The mechanism by which overexpression of individual checkpoint proteins can elicit aneuploidy is not fully understood yet but has been observed in various human cancers. For example, BUB3 was found to be upregulated in breast (Yuan et al., 2006), gastric (Grabsch *et al.*, 2003) and lung (Miura *et al.*, 2002) cancers respectively. It is not known whether andrographolide is capable of affecting the expression levels of crucial genes involved in checkpoints.

Surprisingly, there is no known checkpoint that terminates mitosis in response to abnormal MTOCs accumulation (Sluder *et al.*, 1997). Cells can compensate for having multiple MTOCs by clustering them together to bipolar division with equal or almost equal chromosome segregation (Ring *et al.*, 1982; Brinkley, 2001; Quintyne *et al.*, 2005). Some V-79 cells were observed to possess an ability to form a pseudo-bipolar MTOCs by clustering or aligning multiple centrosomes by a mechanism still to be understood which structurally mimics the normal bipolar spindle poles and is suspected to segregate chromosomes equally, at least for that particular division. Figure 4.11(B) shows an example of a pseudo-bipolar V-79 cell in comparison to a normal bipolar cell. It is also conceivable that some multipolar spindles can transform to pseudo-bipolar spindles during mitosis but are not devoid of chromosome segregation errors. Centrosomes spatial proximity at the beginning of mitosis may determine the possibility and extent of centrosome clustering, where amplified centrosomes close to each other will be grouped and those widely apart will nucleate microtubules independently. The centrosome

clustering dimension in turn may determine whether chromosome separation process is equal or almost equal. Centrosomal clustering requires the microtubule motor cytoplasmic dynein. In some tumours, it has been speculated that multipolarity is correlated to the overexpression of the spindle protein NuMa and that NuMa interferes with dynein localisation to the spindles (Quintyne *et al.*, 2005). Whether these factors contribute to the multipolar spindles observed after DNA damage remains to be established. The size of cells with multinucleated MTOCs were also bigger compared to normal cells as shown in Figure 4.10, or even those possessing abnormal censtrosome numbers such as tri- and tetrapolar cells as animal cells do not proliferate exponentially and thus would not necessitate the evolution of a cell-size checkpoint (Brooks & Shields, 1985).

An increase in cell number always stems from the balance between cell proliferation and cell death, cell viability assessment performed using trypan-blue exclusion assay revealed that andrographolide caused cellular toxicity in a dose- and time-dependent manner, in agreement with data obtained earlier. There were statistically significant difference in the frequency of non-viable cells between 24- and 48- hour exposure with the latter possess higher percentage of dead cells as shown in Figure 4.3. Furthermore, the frequency of condensed chromatin, which also indicates cell death, accrued with andrographolide concentration and remained similar in the absence of andrographolide 24 hours after the initial insult (Figure 4.21). This observation indicates that cells challenged with andrographolide may not be able to recover from the damage inflicted.

Regardless of whether abnormal centrosome number arise due to overduplication, cytokinesis failure or any other mechanism, they are unlikely to behave merely as an audience to the mitotic dance. A frequent but not inevitable short-term effect of MTOCs multiplication is the formation of multipolar spindle, which can be superseded by a multipolar division producing more than two daughter cells. Undoubtedly, cells that were generated from multipolar division are destined to die due to the lack of essential genes. Thus, in reference to their proliferative potential, cells harbouring multiple MTOCs are expected to be at disadvantage when compared to cells with normal centrosome numbers.

On the other hand, multipolar cell divisions are capable of inducing chromosomal instability especially chromosome combination where such occurrence are not only

compatible with life, it also confers a selective advantage to the surviving but genetically abnormal cell.

In the studies conducted, andrographolide was shown to promote centrosome amplification, MTOCs multipolarity and aberrant mitotic cells leading to mitotic aberration. These effects along with cytotoxicity occurred in a dose-dependent manner and may shed more lights into the formation of micronuclei. Hence, andrographolide cellular target(s) may include the mitotic machinery. The presence of aberrant centrosome number might be transferred to daughter cells after division and can affect subsequent mitoses.

CHAPTER 5

ASSESSMENT OF ANDROGRAPHOLIDE'S MUTAGENIC POTENTIAL USING THE *HPRT* FORWARD MUTATION ASSAY

CHAPTER 5

ASSESSMENT OF ANDROGRAPHOLIDE'S MUTAGENIC POTENTIAL UTILISING THE HPRT FORWARD MUTATION ASSAY

5.1 Introduction

A reliable and robust assay that is sensitive in detecting mutations in the low dose region of exposure is needed for both the qualitative and quantitative analysis of the dose response relationship of genotoxicants.

Usually mutations are detected using mammalian cell test systems with high efficiency. In similarity to the microbial-based test systems, testing on mammalian cells are also rapid and can be conducted at a relatively low cost. The most common assays for gene mutation assessment in mammalian cells depend upon forward mutations that confer resistance to a toxic chemical, in contrast to the Ames test which is based on a reverse mutation principle. Thymidine kinase (TK) and hypoxanthine phosphoribosyl transferase (HPRT) mutation assays are two examples where forward mutations cause the inactivation of a wild type gene at heterozygous loci ($TK^{+/-}$) and sex-linked loci ($HPRT^{+}$). The mammalian forward mutation assays are capable of responding to a wide spectrum of mutagens because any mutation interfering with gene expression confers resistance to the toxic chemical (McGregor *et al.*, 1989; Morris *et al.*, 1994; Domon *et al.*, 2001; Doak *et al.*, 2007).

The HPRT forward mutation assay employs hemizygous mammalian *HPRT* gene to elucidate genetic damage that is manifested as a loss of phenotypic characteristic. In this case it is the loss of cell proliferation in the presence of the lethal analogue 6-thioguanine which is cytotoxic to $HPRT^{+}$ but not to $HPRT^{-}$ mutants. In humans, mutations in the *HPRT* gene leads to a neurological condition known as Lesch-Nyan and partial loss leading to gouty arthritis (Gibbs *et al.*, 1990).

Three appealing features of the mammalian *HPRT* gene mutation assay that contributed to it being widely used are;

- The HPRT gene is encoded on the mammalian X-chromosome thus making it easier to select for loss of function in mutants in cells derived from males, which in mammals are heterogametic. On the other hand, in cells from females it could be due to inactivation of one of the X-chromosome.
- Mutations in the same HPRT gene can be compared among cell lines, experimental animals and humans (Chen *et al.*, 2002).
- The biochemical selection systems for loss of function for cells that survive in the presence of 6-thioguanine and/or 8-azoguanine are effectively simple (Caskey & Kruh, 1979).

As large losses in the X-chromosome lead to lethality, detection of small changes such as point mutations in the *HPRT* gene provided valuable insights into possible mechanism of action involved.

Further multiple events are required to transform DNA changes into selectable phenotypes after a chemical insult and these are fixation of the mutation and reduction of the pre-existing enzyme to a level with no biological activity. Fixation of a mutation needs the initial lesion in the DNA such as strand break or damage to DNA-dependent protein, to be translated into change(s) to the DNA sequence such as point mutation or deletion. In the case of point mutation, the mutated strand must be separated from the wild type strand by cell division resulting in one of the progeny cells no longer able to synthesise active mRNA and/or protein. Point mutations can only occur after the completion of the cell cycle as the lesion affecting the base may be removed or repaired by DNA repair mechanisms and thus such mutation is only relevant in these assays after its incorporation into both strands. For selection, the existing enzyme or mRNA must be reduced either by cell division or degradation to non-functional levels, so that the original phenotype can no longer be identified. Figure 5.1 shows the principle of the *HPRT* point mutation assay.

5.2 Objective of This Study

In this study, the potential of andrographolide to induce point mutations in mammalian cells will be examined and determining whether such mutations can occur at concentrations used previously in this thesis as well as other published works. The author employed the *HPRT* mutation assay in this study because the method was routinely used in the laboratory (Barber *et al.* 2006, Doak *et al.*, 2007) as compared to the Ames test.

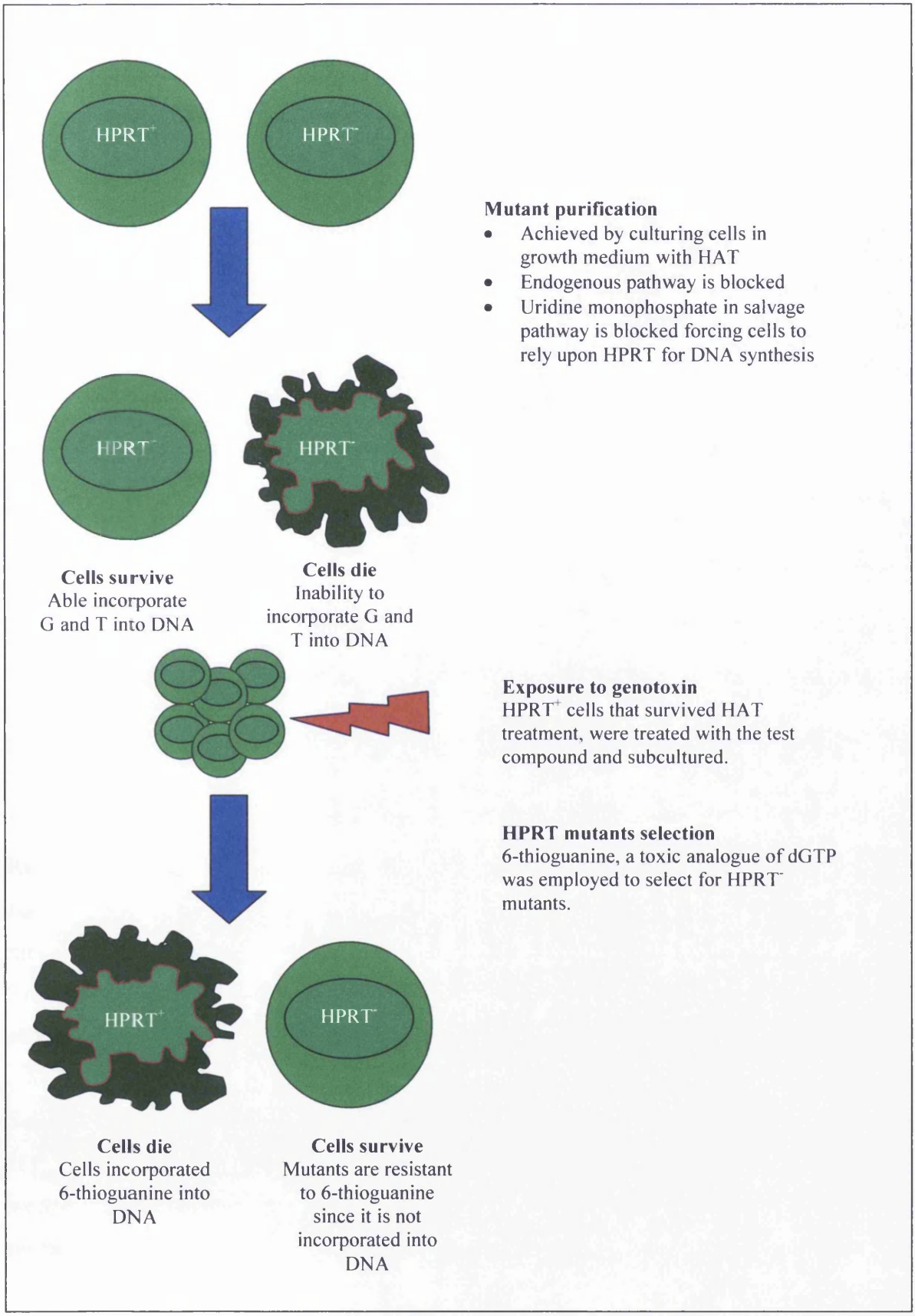

Fig. 5.1 Shows the main concept of HPRT point mutation assay.

5.3 MATERIALS AND METHODS

5.3.1 Thawing Frozen AHH-1 Cells.

This procedure was performed as described in Section 3.5.4 of Chapter 3.

5.3.2 Sub-culturing Procedure for AHH-1 Cells.

This procedure was performed as described in Section 3.5.5 of Chapter 3.

5.3.3 *HPRT* Forward Mutation in Cultured AHH-1 Cells.

5.3.3.1 *HPRT* mutant purification.

The main working principle of mammalian forward mutation assays is the quantification of mutant cells using selective media. Thus the number of mutant cells for each gene such as $TK^{-/-}$ and $HPRT^{-}$ were reduced to decrease the background mutation frequency (MF) by utilising selective growth media that inhibits the endogenous pathway without affecting the salvage pathway, which produces the required dNTP for DNA replication. Cells that are incapable of undergoing the replication process through the salvage pathway (i.e. $TK^{-/-}$ or $HPRT^{-}$) will ultimately die. Figures 5.2 and 5.3 illustrate the endogenous and salvage pathways.

Initially, during the mutant purification procedure, mutant cells (*HPRT*$^{-}$) were reduced in RPMI 1640 growth medium supplemented with 9% horse serum and 1% L-glutamine. HAT (Hypoxanthine-aminopterin-thymidine) at 50-times strength was added to the growth medium at 1:50 ratio (1 HAT: 50 medium); gassed with 5% CO_2 in air and incubated at 37 ± 1^0C for three consecutive days. Thus endogenous pathway was blocked and only allowing DNA synthesis via the salvage pathway during this step.

Subsequently, cells were grown at $5x10^5$ cells per ml for 24 hours in growth medium with HT solution (HAT without aminopterin) added, also at 1:50 ratio. After 24 hours, the cells were washed once by centrifugation at 1500rpm for 8 minutes and grown in normal growth medium for 3-4 days in order to obtain optimum cell numbers suitable for treatment.

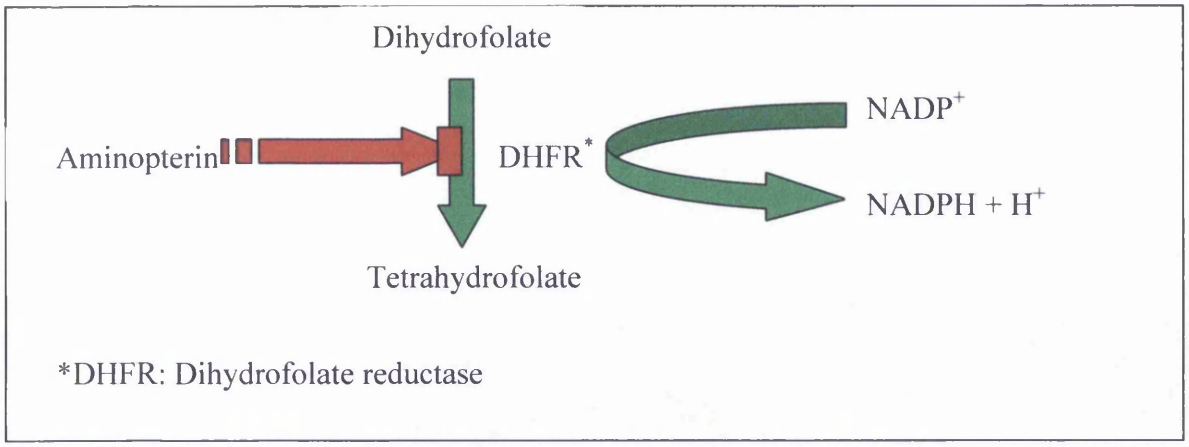

Fig. 5.2 Endogenous pathway-direct synthesis of nucleotides.

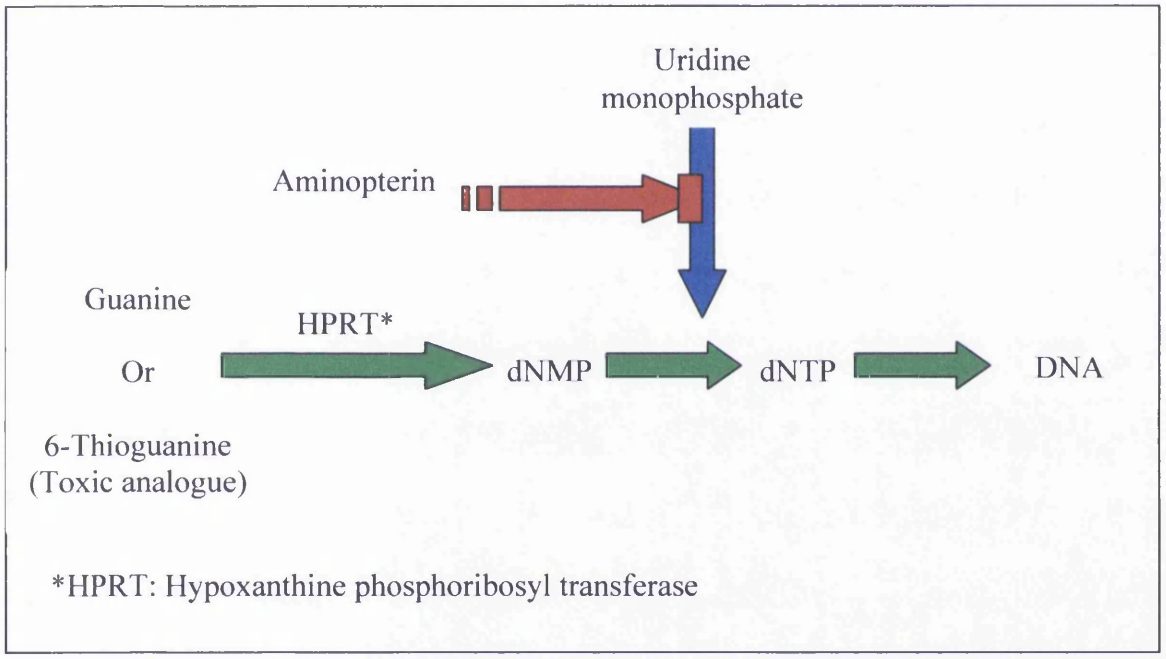

Fig. 5.3 Salvage pathway-synthesis from free purines and pyrimidines.

5.3.3.2 Treatment procedures.

Andrographolide with 98% purity to be used at various concentrations was prepared by dissolving the crystals with DMSO as solvent and administered to AHH-1 cell cultures within two hours of preparation. Fresh stocks were always prepared for each experiment replicates. Flasks containing healthy-looking, evenly distributed cells were selected and labelled according to doses. Less confluent flasks were allocated for negative control and low dose treatments while more confluent flasks were allocated for high dose treatments. Cells seeded at $5x10^6$ cells per ml in 10ml medium were challenged with andrographolide

at the specified concentrations and cultured for 24 hours at 37±1^{0}C. Unlike previous studies, the concentrations of andrographolide used in this particular study were slightly different where the higher concentrations of 70 and 90μM were replaced with lower doses of 1 and 5μM of the compound respectively.

Methylmethanesulfonate (MMS) is a known insecticide and chemotherapeutic agent (Fishbein, 1970) with a high Swain-Scott constant (s>0.83). It is an alkylating agent that is often used a model genotoxin and functions via an S_N2 mechanism targeting adduct generation at the nucleophilic centres such as N-7 of guanine and to a lesser extent the N-3 of adenine, both of which are not mutagenic but caused breaks in DNA (Lawley, 1979; Sega, 1984; Friedberg *et al.*, 1995; IARC 1999). MMS was employed as the positive control for this study and administered to the cells at 4μM final concentration, which was used previously in the laboratory.

Following andrographolide exposure, the cells were washed twice by centrifugation at 1200rpm for 5 minutes and re-suspended in fresh growth medium for mutant expression. The phenotypic expression phase for HPRT mutation assay was 14 days incubation, to allow fixation of possible mutations and the degradation of the already expressed HPRT proteins. During the expression phase, the cell concentrations were routinely diluted to 1.00x10^5 cells per ml with dilutions carried out on 1,3,5,7,9 and 11th days respectively, involving centrifugation and re-suspension in fresh growth medium.

Mutant frequency determination followed the phenotypic expression phase where the cells were added to 96-well plates at the concentration of 4x10^4 cells per well in fresh growth medium. A toxic analogue of guanine, 6-thioguanine at the final concentrations of 0.6 μg/ml was employed as a selection agent.

For the plating efficiency determination, 20 cells per well were plated at each dose in the absence of the selecting agent. Plates were scored for colony formation after 14 days of incubation at 37±1^{0}C in humidified incubator with circulating 5% CO_2 in air.

5.3.3.3 Scoring Procedures.

After 14 days, the plates were scored using Nikon TMS phase contrast inverted microscope under 100X magnification where colonies with a diameter consisting of more than 20 cells were scored as viable colonies and ensuring that separate colonies were clearly apart, thereby accounting for clonal expansion. The cloning efficiencies and mutant frequencies were estimated as described by Furth *et al.* (1981). Figure 5.4 highlights all the procedures followed when conducting this study.

5.3.3.4 Mutation Frequency and Plating Efficiency Calculations

Plating efficiency, cell viability and mutation frequency were calculated using the formulae shown below.

Plating Efficiency % (PE) = $-\text{Ln}\,(X_o/N_o) \times 100$ ....(1)

Cell Viability

$$\text{Cell viability \%} = \frac{\text{PE}}{\text{PE of control}} \times 100 \quad \text{....(2)}$$

Mutant Fraction

$$\text{Mutation frequency (MF)} = \frac{-\text{Ln}\,(X_s/N_s)}{-\text{Ln}\,(X_o/N_o)} \times \text{dilution factor} \quad \text{....(3)}$$

$$\text{Dilution factor} = \left[\frac{\text{(No. of initial cells per well) Non-selective conditions}}{\text{(No. of initial cells per well) Selective conditions}}\right]$$

X_s= Number of wells without colonies
N_s = Total number of wells
} Selective conditions

X_o= Number of wells without colonies
N_o = Total number of wells
} Non-selective conditions

Worked examples:

HPRT⁻ mutation frequency (MF) calculation for untreated cells.

$$\text{MF} = \left[\frac{-\text{Ln}\,(296/300)}{-\text{Ln}\,(2/300)}\right] \times \frac{20}{40000} = 0.01342302 / 5.01063529 * 0.0005$$

$=1.339 \times 10^{-6}$

HPRT⁻ mutation frequency (MF) calculation for cells treated with 30μM andrographolide

$$\text{MF} = \left[\frac{-\text{Ln}\,(236/300)}{-\text{Ln}\,(10/300)}\right] \times \frac{20}{40000} = 0.23995067 / 3.40119738 * 0.0005$$

$=3.527 \times 10^{-5}$

5.3.3.5 Statistical Analyses

Dunnetts and 2-sample t-test.

Dunnetts is a specialised multiple comparison post-hoc test performed after an ANOVA or a t-test by comparing all treatment data against the negative control. A samples size formula is proposed that guarantees the probability of correctly detecting each treatment with mean value sufficiently different from the control mean value (Liu 1997). Dunnetts alongside t-test statistical analysis provides sufficient confidence in analysing the significance of the results. The 2 sample t-test is more subjective as it compares each sample mean to the control separately, which is why both tests were required.

Fig. 5.4 Flow chart for necessary steps in the methods employed for HPRT mutation assessment in AHH-1 cells treated with andrographolide.

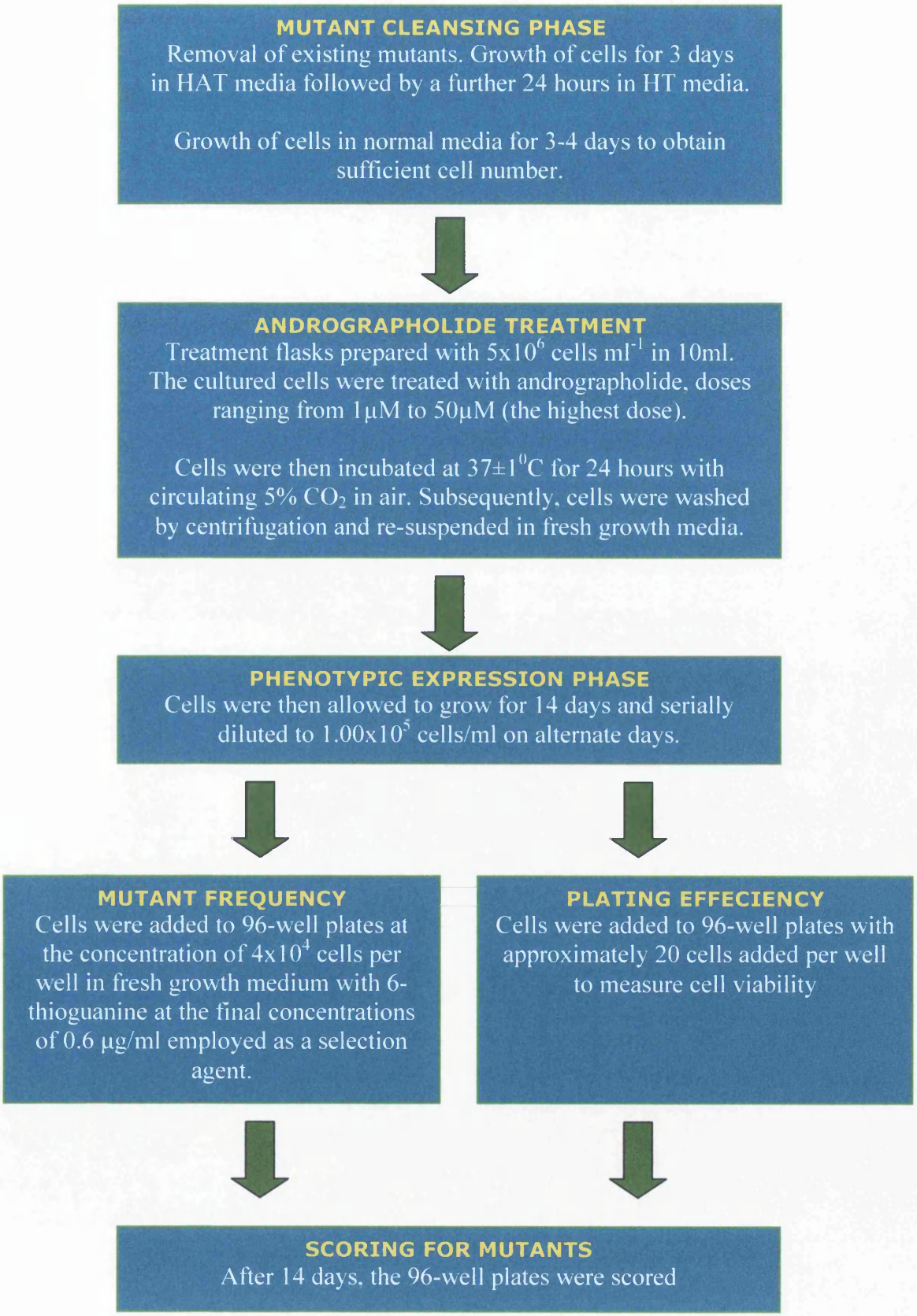

5.4 RESULTS

The data generated for mutation at the *HPRT* locus in AHH-1 cells treated with andrographolide are tabulated in Table 5.1 below. Four sets of experiment replicates using freshly prepared new stocks of andrographolide were used with five plates per dose in order for suitable statistical analysis to be performed. Only 60 out of 96 wells were examined for colony formations as the periphery wells around the 96-well plates were not suitable for scoring. The concentrations of andrographolide used in this study were changed and are slightly different where the higher doses of 70 and 90μM of the phytochemical were discarded because of previous cell viability studies demonstrated that more than 50% of the cells subjected to these doses died primarily due to necrosis. Instead, 1 and 5μM of andrographolide were used to examine the effect of the compound at lower concentrations while retaining other doses used previously.

Table 5.1. Data summary for mutation frequency ($x10^{-6}$) of andrographolide-treated AHH-1 cells with 6-thioguanine selection for *HPRT* mutant detection.

Dose (μM)	Set A	Set B	Set C	Set D
0.00	1.45	0.41	1.43	0.39
1.00	3.37	0.85	0.43	1.23
5.00	2.88*	2.32*	3.37*	5.80*
10.00	4.83*	3.97*	5.80*	8.56*
30.00	35.27*	46.93*	47.46*	59.50*
50.00	4.90*	9.62*	7.36*	7.15*
MMS	63.18*	68.93*	71.24*	69.71*

Each set of experiment replicates involves 5 plates of 96-well plates per dose and 60 wells scored per plate. *Denotes significant ($p<0.05$) difference between sample means obtained using the two-tailed two-sample t-test and Dunnetts. *HPRT* = Hypoxanthine phosphoribosyl transferase. MMS =methyl methane sulfonate.

Data are presented as presence of viable colonies in a series of 96 well plates and mutation frequency values were calculated using formula (3) as described in section 5.2.3.4 previously incorporating colonies observed both with and without 6-thioguanine selection. As shown in Table 5.1, there were statistically significant increases ($p<0.05$) in the frequency of *HPRT*$^-$ mutants induced in a dose-response manner between 5 and 10μM of andrographolide. Although the incidence of mutant colonies formation was abruptly reduced at 50 μM of the compound, the values were still significantly different ($p<0.05$) against the negative control of untreated AHH-1 cells. The statistical analyses were conducted using t-test and Dunnetts test where the values were as shown in Table 5.2 respectively. This finding suggests that andrographolide is mutagenic to the mammalian

cells AHH-1 *in vitro* at a concentration as low as 5μM with the maximum induction of *HPRT*⁻ mutants was observed at 30μM of the phytochemical as graphically presented in Figure 5.5.

Table 5.2. Two-tailed two sample t-test and Dunnetts test performed on AHH-1 *HPRT* data.

Dose (μM)	Standard deviation ($x10^{-6}$)	T-test probability	Dunnetts probability
0.00	0.707	Not applicable	Not applicable
1.00	1.307	0.351	0.891
5.00	1.535	0.002*	0.012*
10.00	1.991	0.000*	0.000*
30.00	9.892	0.000*	0.000*
50.00	1.928	0.000*	0.000*
MMS	3.525	0.000*	0.000*

*Denotes significant ($p<0.05$) difference between sample means obtained using the two-tailed two-sample t-test and Dunnetts.

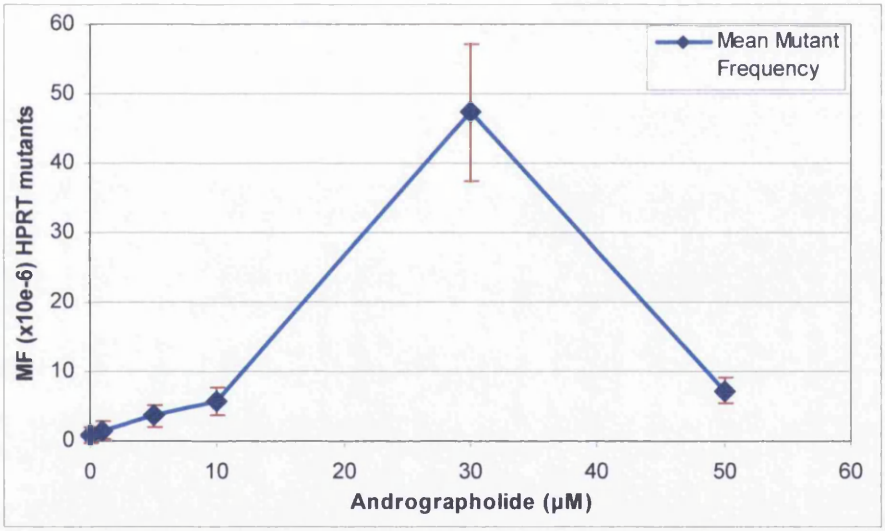

Fig. 5.5. Mutation frequency (MF) of AHH-1 *HPRT*⁻ mutant cells after treatment with various concentrations of andrographolide. Data points derived from mean of four experiment replicates.

Plating efficiency (P.E.) is a cell viability count in plates without 6-thioguanine selection and viable colonies are regarded as mutants after selection. AHH-1 cell viability after andrographolide insult at different doses was calculated using the formulae (1) and (2) that were described in section 5.2.3.4 previously with all data values compared to negative control of untreated cells as 100% cell viability. The data are tabulated in Table 5.3 and graphically displayed in Figure 5.6. Statistical analyses performed using Dunnetts and two-tailed two-sample t-test revealed that 5μM of andrographolide was sufficient to induce statistically significant difference in AHH-1 cell viability against the negative control. Thus, andrographolide caused cell death in a dose-dependent manner and it can be

speculated that such trend would be continued if the cells were challenged with 70 and 90μM of the compound as in other previous studies.

Table 5.3. Data summary of cell viability (%) of andrographolide-treated AHH-1 cells with 6-thioguanine selection for *HPRT* mutant detection.

Dose (μM)	Set A	Set B	Set C	Set D	Mean
0.00	100.00	100.00	100.00	100.00	100.00
1.00	76.14	97.82	95.55	94.83	91.09
5.00	76.14	90.63	85.64	74.55	81.74*
10.00	76.14	85.05	78.62	69.39	77.30*
30.00	73.86	76.64	66.14	59.49	69.03*
50.00	59.92	62.14	56.24	54.93	58.31*
MMS	84.95	87.69	88.52	83.95	86.27

Each set of experiment involves 5 replicates of 96-well plates. *HPRT* = Hypoxanthine phosphoribosyl transferase. MMS= methyl methane sulfonate.

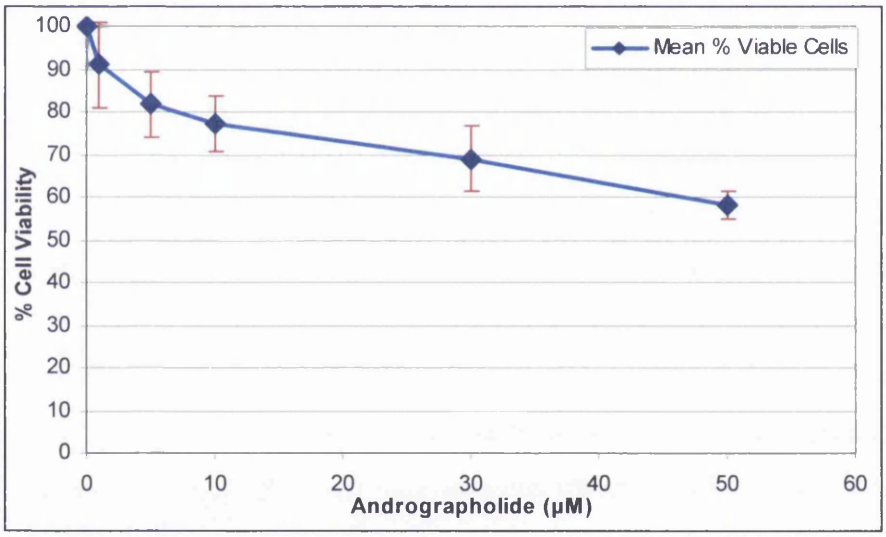

Fig. 5.6 Shows the reduction in AHH-1 cell viability after treatment with andrographolide. Graph was derived using plating efficiency (PE) data. Data points derived from mean of four experiment replicates.

5.5 DISCUSSION

The *HPRT* mammalian forward mutation assay was employed to examine the potential mutagenicity of andrographolide, a phytochemical derived from the annual herb *Andrographis paniculata*. To the best of the author's knowledge, there were no previous publications to this date that attempted to elucidating the phytochemical's ability to elicit point mutations using mammalian cell line.

The AHH-1 cell line was chosen for this assay due to a proven track-record in its utilisation in genotoxicity testing. This lymphoblastoid cell line was chosen over rodent cell lines since human cells are known to be 1000 times more sensitive to some cytotoxic antibiotics at least six times more sensitive to hydrogen peroxide and twice as sensitive to radiation (Cox *et al.*, 1977a; Cox *et al.*, 1977b; Hoffman *et al.*, 1984; Gupta & Prasad, 1992). The *HPRT* forward mutation assay had been used successfully in the past in evaluating genotoxic potencies of mutagens (Crespi *et al.*, 1985; Furth *et al.*, 1981; Doak *et al.*, 2007).

The extract of the aerial parts of *Andrographis paniculata* with high andrographolide content was reported to be not mutagenic *in vitro* using the Ames test (Liu *et al.*, 1990). As mentioned previously in the section 1.10 of Chapter 1, the use of aqueous extract of *A. paniculata* may hamper the bioavailability of the compound to cellular targets (Gupta *et al.*, 1990; 1993; O'Neil *et al.*, 2001) and the anti-bacterial property of andrographolide (Singha *et al.*, 2003) may affect the *Salmonella typhimurium* bacteria used for the Ames test.

The data generated from this study contradicted the findings made by Liu *et al.* (1990) since andrographolide was shown to be capable of inducing mutation of the *HPRT* locus in AHH-1 cells *in vitro*. Andrographolide caused statistically significant ($p<0.05$) increases of *HPRT* mutations in a dose-related fashion between 5 to 30μM followed by the reduction in *HPRT*$^-$ mutants frequency at the top dose of 50μM, where the value is still significantly ($p<0.05$) different against untreated cells. This mutagenic potential exerted by andrographolide on AHH-1 cells *in vitro* supported the DEREK report that this phytochemical can cause chromosome damage in mammals *in vitro*. The highest incidence of *HPRT*$^-$ mutants was observed at 30μM of andrographolide and as demonstrated earlier, the highest frequency of micronuclei was also registered at this particular concentration in AHH-1 cells.

Although andrographolide was found to be mutagenic to AHH-1 cells *in vitro*, it also caused a consistent decrement in cell viability. Apart from the lowest dose tested which was 1μM, all other doses exhibited significant ($p<0.05$) reduction in cell viability against the negative controls. At the top dose tested, the phytochemical caused almost 50% reduction of viable cells, which was close to the 60% cytotoxicity mark.

Earlier, andrographolide was demonstrated to cause cytotoxicity in a dose- and time-dependent manner in V-79, AHH-1 and MCL-5 using different methods of assessment. There were concerns that the measurements of cell viability immediately after exposure to toxic agents may underestimate or generate inaccurate cellular toxicity data (Greenwood *et al.*, 2004; Fellows & O'Donovan, 2007). In this study, andrographolide-treated AHH-1 cells were subsequently allowed to grow for the next 14 days in the absence of the phytochemical and selective agent during the mutant expression period, registered a steady and statistically significant ($p<0.05$) reduction in cell viability, measured as cloning efficiency. This finding provided additional support to the results obtained earlier that andrographolide caused a dose- and time-dependent cytotoxicity. Furthermore, it is now clear that this phytochemical might have a delayed effect on cytotoxicity even after its removal from the growth medium as demonstrated previously.

Even though this is the first finding to exhibit the potential mutagenicity of this phytochemical, the mutagenic mode of action is not really known due to the paucity of data in the literature. It cannot be ascertain whether andrographolide is acting directly or indirectly in causing mutations. Furthermore, as the treatment dose increased, so did cell viability. Hence, mutations may not be passed efficiently since many of the cells will die. The author believes that further studies, including independent verification are warranted to elucidate the biological significance of this mutagenic potential and whether this *in vitro* effect can be translated *in vivo*. Data derived from *in silico* predictions using DEREK and this assay employing AHH-1 cell line did not take into account the influence of a more profound metabolic process *in vivo*. MCL-5 cell line that has superior metabolic ability than AHH-1 was found to be able to withstand andrographolide at 10μM and high micronuclei incidence was observed at 50μM compared to 30μM in AHH-1. Attempts to use MCL-5 cell line in this assay were not successful due to inconsistencies in plating efficiency values.

MCL-5 cell line only has limited Phase I biotransformation capacity and predictions made using METEOR with concordance to previous published studies, revealed various biotransformation routes. Currently, the pharmacokinetic and pharmacodynamic data on andrographolide is still lacking and the serum concentration has not been determined. As a conclusion, andrographolide was shown to educe mutations in AHH-1 cells *in vitro* and further study is needed to determine the biological significance of this finding. However, the absence of initial experiments to determine the optimum expression period meant that AHH-1 cells harbouring larger intragenic mutations might have been lost before scoring can be performed, since andrographolide was shown to elicit chromosome damage. The 14-days incubation period was adopted because it was the routine procedure performed previously in the laboratory (Barber *et al.* 2006, Doak *et al.*, 2007).

Even though the cell viability in this study was performed using equation (2), where viability was measured as part of the plating efficiency after 14-days, other methods can also be employed and the Relative Total Growth (RTG) calculation is one example. The RTG calculation depends on cell number. As stated previously, during the 14-day phenotypic expression period the cells were sub-cultured routinely on alternate days but the author inadvertently did not record the figures, since sub-culturing was performed primarily to maintain a low cell number and cell viability will be determined after another 14-days (equation 2). However, based on visual observation made by the author, the cell number showed a dose-response relationship between sub-culturing procedures and the author believes that should the Relative Total Growth were calculated for cytotoxicity, the outcome would have be the same as that observed in Figure 5.6, where the phytochemical exerted a increasing cytotoxicity with increasing concentrations. Thus, the author recommends the inclusion of Relative Total Growth (RTG) calculation as part of cytotoxicity assessment in this assay for a more accurate measurement since cell death during the long expression period was excluded in the cell viability calculation. This may lead to underestimation of cytotoxicity.

This study showed that andrographolide is able to elicit point mutations in mammalian AHH-1 cells *in vitro* at a concentration as low as 5μM with the highest frequency of mutants recorded at 30μM. The biological significance of this finding remains to be seen.

CHAPTER 6

GENERAL DISCUSSION

CHAPTER 6

GENERAL DISCUSSION

6.1. The Objectives of the Studies

The studies discussed in this thesis were performed to investigate the potential genotoxicity and toxicity of andrographolide, an active phytochemical found in various parts of the annual herb *Andrographis paniculata.*

Herbal products containing phytochemicals have long been an important part and parcel of traditional medicines, that were handed down from one generation of practitioners to another over hundreds of years. The plants to be used and its applications were carefully described in various older traditional healthcare systems such in China and Ayurveda in India, which are philosophically-based and regarded to be holistic in principle, which aim to treat the patient as a whole rather than singling the disease suffered by the patient. They have much in common with traditional medical herbalism as it was and still is practised in Europe and North America.

In Part 1, Chapter 1 of this thesis, various factors involved in the revival of interest in phytomedicines, current UK and EU regulations in place regarding phytomedicines, the efficacy and safety of herbal medicines were discussed in length. Furthermore, the importance of phytochemicals in drug discovery and renewed interests exhibited by the pharmaceutical industry in concordant with the emergence of new technologies, allowing new approaches in research and development of new chemical entities isolated from plants. However, this increased interests in harnessing the hidden knowledge described in ancient medical manuscripts or those trapped within the memory of its practitioners, are not always welcome by the developing countries who claimed that they are being subjected to bio-piracy. These countries have various reasons to believe so due to their rich biodiversity, local socio-economic status and the high percentage of the local population that still trust and rely on traditional herbal medications. Brazil and Malaysia for example, armed themselves with strict legislation regarding the sample collection and exports of flora from

the rainforests. India on the other hand had embarked on an expensively ambitious project, christened the Traditional Knowledge Digital Library with the objective of compiling a 30-million-page electronic encyclopaedia of ancient Indian medical systems of ayurveda, unani and siddha which date back thousands of years. This initiative is perfectly understandable in ensuring such knowledge remained in public hands rather than corporate patents, as the Indian government has been embroiled in many high-profile patent litigation cases challenging individuals and companies alike in the US and European Patent Offices.

Part 1 of the first chapter also detailing the importance of safety assessment of phytomedicines and phytochemicals for the benefit of both the general public and the industry. Introduction to the compound of interest, andrographolide and previous studies on the potential toxicity and genotoxicity of this phytochemical was also discussed.

As elaborated previously, the increased consumption of traditional herbal products by the general public in conjunction with the perception that such products are entirely safe due to its 'natural' status and the paucity of reliable scientific data on their safety as well as their efficacy, should be immediately addressed. The author also believes that such opinions and attitudes by the public towards herbal products consumption would continue as the trend of leading a natural and 'green' lifestyle is currently in vogue. Data are lacking on various aspects of herbal medicines including subtle detrimental effects such as mutations, their impact on biotransformation as well as possible drug-herb interactions.

Computer-assisted structure activity relationship programmes based on expert knowledge, namely DEREK and METEOR were employed to provide semi-qualitative predictions on the toxicity and possible metabolites of andrographolide. The *in vitro* cytokinesis-block micronucleus assay (CBMA) was used to investigate the potential of andrographolide to induce micronuclei, a reliable genotoxic biomarker in metabolically competent cell lines. The assay was also combined with kinetochore labelling using CREST antibodies to elucidate the mechanisms responsible in micronuclei induction (see Chapter 3). Cytotoxicity of andrographolide was also examined using microscopical identification of necrotic and apoptotic cells as well as trypan-blue exclusion assay. After andrographolide was found to act primarily in an aneugenic manner as opposed to being a clastogen, assessment of the compound's capacity to disrupt mitotic machinery and causing chromosome aberrations were assessed (see Chapter 4). In relation to disruption to mitotic

apparatus, mitotic outcome and cellular recovery after andrographolide exposure were also looked into. The data obtained on these studies assisted in providing better comprehension of andrographolide's possible mode of action. It is generally accepted that aneugenic compounds possess a threshold of genotoxicity (COM, 2002), thus the underlying mode of action would also show a threshold of activity. HPRT forward mutation assay was chosen because it was suitably robust for qualitative and quantitative determination of genotoxic potential (see Chapter 5).

In Silico Screening of Toxicity and Prediction of Andrographolide Biotransformation

The existence of high number of phytochemicals with wide structural diversity and the paucity of data on their various properties are some of the factors that is slowing down the research & development including safety assessment procedures. Computer-assisted structure activity relationship (CSAR) assessment allows semi-qualitative assessment and priority setting for testing strategies on high number of compounds before embarking on laboratory-based experiments. Two expert-knowledge-based programmes namely DEREK and METEOR were used to predict *in silico* the toxicity and biotransformation of andrographolide respectively. The results obtained using DEREK showed that andrographolide is capable of causing nephropathy in rodents as well as skin sensitisation and chromosome damage in mammals *in vitro*, where the latter is attributed to the presence α-alkylidene γ-butyrolactone moiety detected as α, β-unsaturated ester or thioester by DEREK. Indeed, this particular part of the chemical structure among others was supported by experimental data to be responsible for the phytochemical's cytotoxic activity *in vitro* (Nanduri *et al*, 2004). It is worth pointing out that DEREK regarded the cytotoxic and genotoxic potential of andrographolide to be plausible *in vitro* because the programme is examining the chemical structure of andrographolide whereas *in vivo*, the compound would be subjected to biotransformation where the metabolites can either be more reactive or vice-versa. Thus METEOR was utilised to providing possible Phase I and II biotransformation routes of andrographolide. The various possible metabolites anticipated by METEOR exhibited similar outcome compared to those obtained experimentally. Previous studies involving rodents and small sample of human volunteers showed a variety of metabolites and all of these were anticipated by METEOR. However, the programme was not capable of determining whether these possible metabolites are more or less reactive

than the parent compound. As discussed previously, CSAR programmes are useful in certain aspects but they can only complement but not overrule experimental findings.

DEREK, METEOR or any other expert-knowledge-based programme can also be useful in priority setting for testing strategies, for example the European Union adopted a legislative proposal for a new chemical management system known as REACH that for one aspect, requires thousands of chemicals in cosmetics to be tested against skin irritation and yet the EU also warrants that testing of chemicals for cosmetic products in animals to end by 2009.

6.2 Elucidating the Genotoxic Potential of Andrographolide *In Vitro*

The results obtained using the CSAR programmes provided a sketch on andrographolide's toxicity portrait. The *in vitro* cytokinesis-block mironucleus assay (CBMA) in combination with anti-kinetochore labelling using CREST antibodies was used to paint a better picture of the portrait and it was revealed that andrographolide induced statistically significant micronuclei frequency at the lower concentrations tested, primarily in an aneugenic manner in V-79, AHH-1 and MCL-5 cell lines. There was significant difference in the frequency of micronuclei induction between the three cell lines tested and this may be attributed to the difference in metabolic capacity. Although V-79 cells are not metabolically competent, attributing the higher micronuclei frequency observed mainly due to biotransformation deficit might not be flawless. Ideally, data comparison between andrographolide-treated V-79 cells supplemented with S9-liver extract and those that are not might provide a better picture on the effect metabolic enzymes upon andrographolide genotoxicity potential. However, the presence of external metabolic capacity such as S9 poses disadvantages of its own since the low levels of certain P450 cytochromes and high levels of others, does not necessarily represent normal animal or human biotransformation process (Tweats et al 2007). Nonetheless, these data provided valuable insights into andrographolide biotransformation in human cell lines that also augment the *in silico* predictions derived from DEREK and METEOR. The V-79 cell line is deficient in p53 activity whereas AHH-1 and MCL-5 cells are capable of undergoing normal DNA repair process and judging by available data on the frequency of micronuclei induction, the cells' p53 status were considered to be not of significant influence in cellular response towards andrographolide. Rajagopal *et al.* (2003) reported that the p53 status of cancer cells exposed to

andrographolide did not account for the anti-proliferative properties exerted by the compound.

Andrographolide was also found to cause cell death in a dose-dependent fashion mainly via necrosis rather than apoptosis. Different methods were employed to assess the cytotoxicity of the phytochemical of interest and the trend observed was similar. Cellular toxicity exerted by andrographolide was demonstrated to be dependent on dose and incubation time. When MCL-5 cells were treated with andrographolide for 8 hours, the frequency of apoptotic cells was most prominent at 30 and 50μM but was still not as high as cells that suffered necrosis. Prolonging the treatment period from 8 to 24 hours caused even more cells to undergo necrotic cell death whereas neither increment nor reduction was recorded for apoptotic cells and the value still lingered less than 2% of the cell population scored. Cell death induced by andrographolide was recently suggested to be independent of cellular caspase activities (Li *et al.*, 2007). As discussed previously, andrographolide's influence on apoptosis is still not clear. There were reports of anti-apoptotic properties (Burgos *et al.*, 2004; Chen *et al.*, 2004) as well as pro-apoptotic effects in cells (Cheung *et al.*, 2005; Kim & Milner, 2005) treated with andrographolide. Furthermore, the molecular mechanisms of these effects remained largely unexplored and it is still to be determined whether andrographolide impose its anti/pro-apoptotic effects via direct or indirect action on cellular target(s).

The concentrations of andrographolide at 30 and 50μM administered to cells that elicited relatively high apoptotic response also educed comparatively high micronuclei incidence, suggesting a possible link between these doses, micronucleation and apoptotic responses. Decordier *et al.*, (2005) proposed that increased caspase-3 activity has a direct role in micronuclei formation. Indeed, caspase-3 activity, which is a distinguishing factor in apoptosis execution, was observed to be up-regulated in the presence of andrographolide (Li *et al.*, 2007). It may be possible that this phytochemical only exert micronucleation at these concentrations after the cellular defense mechanisms has been overwhelmed or sufficient cellular target(s) has been damaged leading limited apoptotic reaction since cells die mainly via necrosis. Damage to cytoskeleton and other mitotic machinery may also initiate apoptosis (Decordier *et al.*, 2002).

The phytochemical was demonstrated to inhibit cell growth and elicit cell death primarily via necrosis as the dose increased. Apoptosis was found to be a minor form of cell demise. Andrographolide exerts it cellular toxicity in time- and dose-dependent manner, where necrotic response was witnessed to be increased between 8 and 24 hours, in contrast to apoptosis which remained fairly stagnant during the same period. It seemed andrographolide has higher propensity to incite necrosis than the programmed cell death. Necrosis results from damage to a number of cellular constituents, including the plasma membrane. Several mechanisms alone or in combination can trigger and promote necrosis. These include plasma membrane permeability changes, which lead to a collapse of ion homeostasis, followed by cell and organelle swelling, and culminating in rupture of the cell membrane. For a given xenobiotic, the exact mechanisms leading to necrosis are not always known because the sequence of events is complex and many of these molecular events are causally interrelated with other mechanisms. Cause and effect cannot always be dissected from each other. Whether andrographolide inhibit apoptosis thus forcing damaged cells to die via necrosis, or various cellular targets were damaged by the compound and lead to necrosis, or a combination of both, is still not entirely clear.

Although the genotoxicity portrait of this main phytochemical from *Andrographis paniculata* is clearer than before, it is still lacking refined colours. Since andrographolide act primarily in an aneugenic manner when inducing micronuclei, it may not directly acting on the DNA itself but exert its genotoxic influence indirectly by targeting various other cellular targets including but not limited to the mitotic machinery. The study on Chinese hamster lung fibroblast V-79 cells showed that andrographolide caused the numerical amplification of the microtubule organising centres (MTOCs) with corresponding aberration in chromosome segregation, which supported the data on micronuclei induction observed in V-79 cells as well as those in AHH-1 and MCL-5. This concentration-dependent effect also caused accruement of cells experiencing mitotic arrest. As the cells challenged with andrographolide harbours abnormal polarity during mitosis, it was deemed an interesting venture to see if such anomaly would give rise to cells with more than one nuclei. MCL-5 and V-79 cells were exposed to andrographolide for one and two cell cycles, subsequently cell fate and cell death frequency were determined microscopically. The presence of multiple MTOCs promoted aberrant mitoses. MCL-5 cells were also exposed to andrographolide for a longer period of 5 cell cycles in order to compare the mitotic outcome and cytotoxicity levels with cells challenged with the phytochemical in a

shorter treatment period. The data showed that longer treatment period elicit mitotic aberration, cell death and reduction in cell number. As andrographolide was shown to induce damage in aneugenic manner and aneugens are known to involve threshold of damage, the possibility of cells to recover after andrographolide exposure was also examined and the data revealed that the effect generally persisted.

The visual determination of MTOCs number is not hard and most studies rely on antibody-labelling followed by fluorescent microscopy. Although currently this is the preferred method, data has to be interpreted cautiously. Factors to be taken into account include antibody quality, the orientation of the centrosome relative to viewing and the fact that not every particle staining with anti-PCM antibodies necessarily represents a complete centrosome.

The author believes that andrographolide may exerts it influence on mammalian cells as a parent compound and metabolism of the aglycone may reduced its genotoxicity, as shown by the observed differences in micronuclei induction between the cell lines adopted in these studies and various past publications cited in this thesis point to the same conclusion. However, it is inappropriate to speculate further until genotoxic experiments involving the possible metabolites of the compound can be performed and it is also remain to be seen if extensive metabolism (Phase I and II) would have an impact on the cytotoxicity of the compound without diminishing its reported medical properties.

Andrographolide was shown to cause reduced sperm count, giant multinucleated cells formation and necrotic cell death in male rats (Akbarsha & Murugaian, 2000) and the author decided to elucidate the compounds possible mechanism of action(s) as part of the genotoxicity assessment. Furthermore, the phytochemical was previously demonstrated to be able to halt the growth of various cancer cells (Siripong *et al.*, 1992; Rajagopal *et al.*, 2003; Kumar *et al.*, 2004) and it was hoped that by understanding the mode of action(s) and the effect on cell division kinetics would pave the way to the discovery of a possible pharmacological lead if not a potential anti-mitotic compound on its own or in combination with existing treatment.

The measurements of replication and mitotic indexes after exposure to andrographolide for one cell cycle may underestimate the compound's cytotoxicity since these endpoints only

take into account the percentage of cell population that proliferated and attempting to progress through mitosis. The proportion of dead and dying cells were excluded. These short-term cytotoxicity parameters and the trypan-blue exclusion assay were reported to underestimate cytotoxicity (Fellowes & Donovan, 2007). Andrographolide was demonstrated to cause necrotic cell death in a dose- and exposure time-dependent manner rather than a prominent apoptotic response. At the top dose, andrographolide caused more than 50% cytotoxicity in the cell lines as indicated by RI, MI and trypan-blue measurements and significant reduction in cell number. Continuous exposure of MCL-5 cells to andrographolide for five cell cycles also showed that the compound maintain its cytotoxicity. Even though the *in vitro* micronucleus assay was not exclusively design for cell death measurement, the estimation of necrotic/apoptotic cell population after andrographolide exposure provided a valuable mechanistic information.

The incidence of condensed chromatin, considered to be an indication of cell death was determined in V-79 cells exposed to andrographolide. The data revealed a dose-dependent pattern of dead cell population even after the treated cells were allowed to recover for one cell cycle in the absence of andrographolide and the percentage of dead cells was similar to those treated continuously (see Table 4.6). The incidence of aberrant centrosome number measured directly after exposure and the incremental increases in mitotic index even after the removal of andrographolide indicated that it profoundly affected the cell cycle mechanism, which in the long term may affect cell division and cell number.

Furthermore, cell viability determined using the plating efficiency as discussed in Chapter 5, demonstrated a dose-dependent reduction in growing AHH-1 cell colonies after 14-days of initial inoculation with the same cell concentration. Thus, based on the available data, andrographolide affected cell cycle kinetics via disruption to normal chromosome segregation and increased the mitotic index while a proportion of cell population exposed to the compound died primarily via necrosis in a dose-dependent manner. Disruption to normal cell division and chromosome damage as well as the cytotoxicity of the compound effectively reduced cell number. Furthermore, depending on the dose of exposure, the treated mammalian cells' ability to segregate normally might have been impeded evident from the persistence of cell cycle delay even in the absence of the phytochemical. The author believes that andrographolide may have a higher cytotoxicity than those measured using the previously stated parameters and even though the Relative Total Growth

calculation was not determined, it can be proposed that based on the observation and plating efficiency figures that this phytochemical will inhibit normal cell proliferation.

The results obtained would be more meaningful if the concentration of andrographolide presence in human serum is known or to what extent human exposure *in vivo* would be. At the moment, reliable data on this aspect is lacking. As stated earlier, many published works on this phytochemical tend to concentrate on the possible medical and therapeutic benefits of andrographolide, often overlooking the possible risks it might pose and the current lack of evidence in toxicity particularly genotoxicity may place the health of the public in jeopardy unless more information is obtained. History may not exactly repeat itself but it does tend to rhyme. Previous examples of herbal products that were not tested for its genotoxic potential such as *Aristolochia fangchi, Piper methysticum* and *Teuchrium chamaedrys*, to name a few, has been costly to public health and confidence.

6.3 Further Studies

Based on the findings made in this thesis, various further studies can be carried out but not limited to those described below.

- Since the methods employed to elucidate cell fate after aberrant mitosis due to centrosome amplification after andrographolide exposure is not very specific, time-lapsed video-microscopy on cell should be used to obtain a clearer picture.

- Another round of *in silico* assessment using both DEREK and METEOR can be performed on the predicted metabolites of andrographolide, which will provide valuable additional insights.

- In relation to the previous point and the results obtained, experiments to characterise the possible metabolites of andrographolide from AHH-1, MCL-5 and V-79 cell cultures can be performed for example by using mass spectrometry.

- Test the metabolites of this phytochemical to determine whether they can pose as a genotoxic threats and studies should also be performed on normal diploid human cells and cells with competent p53 activity.

- Conducting microarray studies on gene expression for cells exposed to andrographolide to determine its impact on genes involved in cell death mainly apoptosis, centrosome duplication and the mitotic checkpoint genes. Such studies would shed more lights on how andrographolide is affecting centrosome multiplication and cell death.

- Experiments to further examine and quantitate the effects of andrographolide on mammalian cells using apoptosis specific assays such as the TUNEL and caspases-oriented technique can be performed. Several cell types should be employed to provide a better picture since andrographolide is known to exert cell-specific response.

- Performing the *in vitro* cytokinesis-block micronucleus assay on larger samples with the aim of finding the threshold level of exposure since andrographolide behaves in an aneugenic manner.

- Sequencing the HPRT $^{-}$ mutants to obtain more information of the type of damage.

6.4 Conclusion

Major conclusions that can be drawn from these studies are:

- *In silico* assessment utilising expert knowledge-based program harnessing quantitative structure activity relationship such as DEREK and METEOR was useful in providing general initial information about andrographolide, where paucity of data exist. DEREK predicted that andrographolide is capable of causing skin sensitisation and chromosome damage in mammals *in vitro*. Whereas, METEOR predicted plausible Phase I and Phase II biotransformation routes of andrographolide that were in agreement with past published works.

- Andrographolide induced micronuclei formation *in vitro* in all three cell lines tested, primarily at the lower doses of the compound. Difference in cellular metabolic capabilities may explain the difference in the level of micronuclei incidence.

- Andrographolide induced kinetochore positive micronuclei, hence may act in aneugenic manner.

- The doses between 30 and 50μM induced high micronuclei frequency compared to other concentration tested and these doses also caused relatively high apoptotic response in scored cells.

- Cytotoxicity measurement performed using replicative index calculation, microscopical identification and trypan-blue exclusion assay showed a similar trend in that andrographolide cytotoxicity is both time- and dose-dependent. Cell death was observed to be primarily via necrosis as opposed to programmed cell death. Micronuclei frequency was observed to generally increase in tandem with cytotoxicity, except at the top two concentrations of 70 and 90μM. This phytochemical also reduced cell growth as the concentration increased. However, the compound's cytotoxicity might have been underestimated.

- Andrographolide instigated centrosome amplifications as the treatment dose increased and the presence of multiple MTOCs affected chromosomal segregation fidelity with corresponding increases in the mitotic index.

- V-79 cells challenged with andrographolide for 24 hours and subsequently allowed to grow for a further 24 and 48 hours post-treatment still retained abnormal MTOCs number.

- Centrosome numerical aberrations in V-79 cells challenged with andrographolide lead to anomalous mitoses where cells failed to undergo cytokinesis due to abnormal centrosome number, producing bi-, tri-, tetra- and multinucleated cells.

Even in the absence of the phytochemical after the initial insult, there was still significant presence of abnormal mitoses.

- Andrographolide elicited *HPRT* $^{-}$ mutants formation between 5 to 50μM and the induction is dose-related with 30μM induced the highest mutagenic response. Cell viability measured as plating efficiency showed that andrographolide affected cell growth and supported cytotoxicity assessment conducted earlier.

All the studies completed in this thesis were conducted with the aim of adding value to the existing knowledge on andrographolide by determining its potential genotoxicity, cytotoxicity and shed more lights into its possible mode of action. There are various windows of opportunity in terms of necessary further work that can be pursued in the future, some of which have been outlined by the author earlier as there are still more questions need to be answered. Recently, self-organising map (SOM) analysis performed on andrographolide suggested that this phytochemical may possess novel mechanism(s) of action (Jada *et al.*, 2007). Therefore the author would like to end his thesis as the novelist and lepidopterist, Vladimir Nabokov once put it, "The greater one's science, the deeper the sense of mystery".

BIBLIOGRAPHY AND APPENDIX

List of Research Publications Cited in This Thesis

A

Aardema, M.J., S. Albertini, P. Arni, L.M. Henderson, M. Kirsch-Volders, J.M. Mackay, A.M. Sarrif, D.A. Stringer and R.D. Taalman, 1998. Aneuploidy: a report of an ECETOC task force. *Mutation Research*, **410:** 3-79.

Abou Eisha, A. and M. Afifi, 2004. Genotoxic evaluation of the anti-malarial drug Fansidar in cultured human lymphocytes. Cell Biology and Toxicology, 20(5): 1573-6822.

Akbarsha, M.A. and P. Murugaian, 2000. Aspects of the male reproductive toxicity/male antifertility property of andrographolide in albino rats: Effect on the testis and the cauda epididymidal spermatozoa. *Phytotherapy Research*, **14(6):** 431-435.

Akiyama H., S. Barger, S. Barnum, B. Bradt, J. Bauer, G.M. Cole, N.R. Cooper, P. Eikelenboom, M. Emmerling, B.L. Fiebich, C.E. Finch, S. Frautschy, W.S. Griffin, H. Hampel, M. Hull, G. Landreth, L. Lue, R. Mrak, I.R. Mackenzie, P.L. McGeer, M.K. O'Banion, J. Pachter, G. Pasinetti, C. Plata-Salaman, J. Rogers, R. Rydel, Y. Shen, W. Streit, R. Strohmeyer, I. Tooyoma, F.L. Van Muiswinkel, R. Veerhuis, D. Walker, S. Webster, B. Wegrzyniak, G. Wenk, T. Wyss-Coray, 2000. Inflammation and Alzheimer's disease. *Neurobiology Aging*, **21:** 383–421.

Albertini, D. Anderson, G.R. Douglas, L. Hagmar, K. Hemminki, F. Merlo, A.T. Natarajan, H. Norppa, D.E. Shuker, R. Tice, M.D. Waters, A. Aitio, 2000. IPCS guidelines for the monitoring of genotoxic effects of carcinogens in humans, International Programme on Chemical Safety.*Mutation Research*, **463:** 111-172.

Ames, B.N., F.D. Lee, W.E. Dunston, 1973. An improved bacterial test system for the detection and classification of mutagens and carcinogens. *PNAS*, **70(3):** 782-786.

Andreakos, E.T., Foxwell, B.M., Brennan, F.M., Maini, R.N. and Feldmann, M., 2002. Cytokines and anti-cytokine biologicals in autoimmunity: present and future. *Cytokine & Growth Factor Reviews*, **13:** 299-313.

Andreassen, P.R., O.D. Lohez, F.B. Lacroix and R.L. Margolis, 2001. Tetraploid state induces p53-dependent arrest of non-transformed mammalian cells in G1. *Molecular Cell Biology*, **12(5):** 1315-1328.

Antoccia., A. F. Degrassi, P.C. Battistoni and C. Tanzarella, 1991. In vitro micronucleus test with kinetochore staining: evaluation of test performance. *Mutagenesis,* **6:** 319-324.

Antoccia., A., C. Tanzarella, D., Modesti and F. Degrassi, 1993. Cytokinesis-block micronucleus assay with kinetochore detection in colchicine-treated human fibroblasts. *Mutation Research*, **287:** 93-99.

Ashby, J., R.W. Tennant, 1994. Prediction of rodent carcinogenicity for 44 chemicals: results. *Mutagenesis*, **9(1):** 7-15.

Atkinson, E.A., M. Barry, A.J. Darmon, I. Shostak, P.C. Turner, R.W. Moyer, and R.C. Bleackley, 1998. Cytotoxic t-lymphocyte-assisted suicide. *Journal of Biological Chemistry,* **273:** 21261-21266.

Aula, P. and W.W. Nichols, 1967. The cytogenetic effects of mycoplasma in human leukocyte cultures. *J. Cell Physiology*, **70:** 281-290.

B

Bailly, E., M. Doree, P. Nurse and M. Bornens, 1989. p34cdc2 is located in both nucleus and cytoplasm; part is centrosomally-associated at G2/M and enters vesicles at anaphase. *EMBO Journal*, **8(13)**: 3985-3995.

Baker, D.J., K.B. Jeganathan, J.D. Cameron, M. Thompson, S. Juneja, A. Kopecka, R. Kumar, R.B. Jenkins et al., 2004. BubR1 insufficiency causes early onset of aging-associated phenotypes and infertility in mice. *Nature Genetics*, **36:** 744-749.

Balint, G.A., 2001. Artemisinin and its derivatives, an important new class of anti-malarial agents. *Pharmacology and Therapeutics*, **90:** 261-264.

Barber, R.C., P. Hickenbotham, T. Hatch, D. Kelly, N. Topchiy, G.M. Almeida, G.D. James, G.E. Johnson, J.M. Parry, K. Rothkamm, Y.E. Dubrova, 2006. Radiation-induced transgenerational alterations in genome stability and DNA damage. *Oncogene*, (1-7):

Barrera, J.E., H. Ai, Z. Pan, A.D. Meyers, and M. Varella, 1998. Malignancy detection by molecular cytogeneics in clinically normal mucosa adjacent to head and neck tumours. *Arch. Otolaryngol. Head Neck Surg.*, **124:** 847-851.

Barrera, J.E., M.E. Miller, S. Said, B.W. Jafek, J.P. Campana and K.R. Shroyer, 1999. Detection of occult cervical micrometastases in patients with head and neck squamous cell cancer. *Laryngscope*, **113:** 892-896.

Barkla, D.H. and P.R. Gibson, 1999. The fate of epithelial cells in the human large intestine. *Pathology*, **31:** 230–238.

Barnes, J., 1998. Herbal safety high on European phytotherapy agenda. *Inpharma*,**1164:** 20-21.

Barnes, P.J., 2002. Cytokine modulators as novel therapies for asthma. *Annual Review in Pharmacology and Toxicology*, **42:** 81-88.

Barone, G.W., Gurley, B.J., Ketel, B.L., Lightfoot, M.L., Abul-Ezz, S.R., 2000. Drug interaction between St John's wort and cyclosporine. *Annals Pharmacotherapy,* **34**: 1013-1016.

Basto, R., J. Lau, T. Vinogradova, A. Gardiol, G.G. Woods, A. Khodjakov and J.W. Raff., 2006.

Batkhuu, J., K. Hattori, F. Takano, S. Fushiya, K. Oshiman and Y. Fujimiya, 2002. Suppression of NO production in activated macrophages in vitro and ex vivo by neoandrographolide and andrographolide isolated from *Andrographis paniculata. Biol Pharm Bull,* **25(9):** 1169-1174.

Benninger J., Schneider H.T., Schuppan D., Kirchner T., Hahn EG, 1999. Acute hepatitis induced by greater celandine (*Chelidonium majus*). *Gastroenterology*, **117:** 1234-7.

Bentley, K.S., D. Kirkland, M. Murphy and R. Marshall, 2000. Evaluation of thresholds for benomyl- and carbendazim-induced aneuploidy in cultured human lymphocytes using FISH. *Mutation Research*, **464:** 41-51.

Beijnen J.H. and J.H., Schellens, 2004. Drug interactions in oncology. *Lancet Oncology*, **5:** 489–496.

Berridge, M.J., P. Lipp and M.D. Bootman, 2000. The versatility and universality of calcium signaling. *Nature Review Molecular Cell Biology*, **1:**11-21.

Bhan, M.K., A.K. Dhar, S.K. Lattoo et al., 2006. Screening and optimisation of Andrographis paniculata for total andrographolide content, yield and its components. *Scientia Horticulturae*, **107:** 386-391.

Blaskovich, M.A., J. Sun, A. Cantor, J. Turkson, R. Jove and S.M. Sebti, 2003. Discovery of JSI-124 (cucurbitacin 1), a selective Janus kinase/signal transducer and activator of transcription 3 signalling pathway inhibitor with potent anti-tumour activity against human and murine cancer cells in mice. *Cancer Research*, **63(6):** 1270-1279.

Blenkinsopp, A. and C Bradley, 1996. Patients, society and the increase in self-medication. *British Medical Journal*, **312(7031):** 629-632.

Blumenthal, M., ed 1998. The complete German Commission E monographs- therapeutic guide to herbal medicines. Austin, Texas: American Botanical Council.

Blom, W.M., H.J. De Bont, I. Meijerman, P.J. Kuppen, G.J. Mulder, J.F. Nagelkerke, Interleukin-2-activated natural killer cells can induce both apoptosis and necrosis in rat hepatocytes. *Hepatology,* **29:** 785–792.

Bonassi, S., Z. Cavalieri, S. Viaggi and A. Abbondandolo, 1992. The analysis of 10 potential spindle poisons for their ability to induce Crest-positive micronuclei in human diploid fibroblasts. *Mutagenesis*, **7:** 111-114.

Bolten, B.M. and T. DeGregorio, 2002. Trends in development cycles. *Nature Review Drug Discovery*, **1(5):** 335-336.

Boller, K. and W. Schmid, 1970. Chemical mutagenesis in mammals, the Chinese hamster bone marrow as an in vivo test system. Hematological findings after treatment with trenimon. *Humangenetik*, **11(1):** 35-54.

Bonacker, D., T. Stoiber, K.J. Bohm, E. Unger, G.H. Degen, R. Thier and H.M. Bolt, 2004. Chromosomal genotoxicity of nitrobenzene and benzonitrile. *Arch Toxicology*, **78:** 49-57.

Borthwick, N.J., R.G. Wickremasinghe, J. Lewin, L.D. Fairbanks, M. Bofill, Activation-associated necrosis in human immunodeficiency virus infection. *J. Infect Dis.*, **179:** 352–360.

Bornens, 2002. Centrosome composition and microtubule anchoring mechanisms. *Current Opinion in Cell Biology,* **14:** 25-34.

Bradley, M.O., B. Bhuyan, M.C. Francis, R. Langenbach, A. Peterson and E. Huberman, 1981. Mutagenesis by chemical agents in V79 chinese hamster cells: a review and analysis of the literature. A report of the Gene-Tox program. *Mutation Research*, **87:** 81-142.

Brennan, M.A. and B.T. Cookson, 2000. Salmonella induces macrophage death by caspase-1-dependent necrosis. *Molecular Microbiology*, **38:** 31–40.

Brinkley, B.R., A Tousson and M.M. Valdivia, 1985. The kinetochore of mammalian chromosomes: structure and function in normal mitosis and aneuploidy. *Basic Life Sci*, **36:** 243-67.

Brinkley, B.R., 2001. Managing the centrosome numbers game: from chaos to stability in cancer cell division. *Trends in Cell Biology*, **11:** 18-21.

Brooks, R.F. and R. Shields, 1985. Cell growth, cell division and cell size homeostasis in Swiss 3T3 cells. *Experimental Cell Research*, **156:** 1-6.

Brown, T.A., 2002. Genomes (2nd Edition), BIOS.

Burkhart, C.A., M. Kavallaris and S.B. Horvitz, 2001. The role of β-tubulin isotopes in resistance to anti-mitotic drugs.

C

Calabrese, C., SH Bernan, J.G. Babish, X. Ma, L. Shinto, M. Durr, K. Wells, C.A. Werner, L.J. Standish, 2000. A phase I trial of andrographolide in HIV positive patients and normal volunteers. *Phytotherapy Research.*

Carlile, G.W., Smith, D.H. and Wiedman, M., 2004. Caspase-3 has a non-apoptotic function in erythroid maturation. *Blood*, **103:** 4310-4316.

Carmichael, J., DeGraff, W.G., Gasdar, A.F., Minna, J.D., Mitchell, J.B., 1987. Evaluation of tetrazolium-based semiautomated colorimetric assay: assessment of chemosensitivity testing. *Cancer Research*, **47:** 936– 942.

Carroll. P.E., M. Okuda, H.F. Horn, P. Biddinger, P.J. Stambrook et al., 2000. Centrosome hyperamplification in human cancer: chromosome instability induced by p53 mutation and/or Mdm2 overexpression. *Oncogene*, **18(11):** 1935-1944.

Carter, S.B., 1967. Effects of cytochalasins on mammalian cells. *Nature*, **213:** 261-264.

Casenghi, M., R. Mangiacasale, M. Tuynder, P. Caillet-Fauquet et al., 1999. p53-independent apoptosis and p53-dependent block of DNA re-replication following mitotic spindle inhibition in human cells. *Experimental Cell Research*, **250(2):** 339-350.

Casenghi, M., P. Meraldi, U. Weinhart, P.I. Duncan, R. Korner and E.A. Nigg, 2003. Polo-like kinase 1 regulates Nlp, a centrosome protein involved in microtubule nucleation. *Dev Cell*, **5:** 113-125.

Caskey, C.T. and G.D. Kruh, 1979. The HPRT locus. *Cell*, **16:** 1-9.

Chang, R.S. *et al.*, 1991. Dehydroandrographolide succinic acid monoester as an inhibitor against the human immunodeficiency virus (43225). *Proceedings of the Society of Experimental Biology and Medicine*, **197:** 59-66.

Chaung, W., L.J. Mi and R.J. Boorstein, 1997. The p53 status of Chinese hamster V79 cells frequently used for studies on DNA damage and DNA repairs. *Nucleic Acids Research*, **25(5):** 992-994.

Chen W., L.L. Koenigs, S.J. Thompson, R.M. Peter, A.E. Rettie, W.F. Trager and S.D. Nelson, 1998. Oxidation of acetaminophen to its toxic quinone imine and non-toxic catechol metabolites by baculovirus-expressed and purified human cytochromes P450 2E1 and 2A6. *Chemical Research in Toxicology*, **11:** 295-301.

Chen, T., K. Harrington-Brock and M.M. Moore, 2002. Mutant frequency and mutational spectra in the TK and HPRT genes of N-ethyl-N-nitrosourea- treated mouse lymphoma cells. *Environmental and Molecular Mutagenesis*, **39:** 296-305.

Chen, J.H., G. Hsiao, A.R. Lee, C.C. Wu and M.H. Yao, 2004. Andrographolide suppresses endothelial cell apoptosis via activation of phosphotidyl inositol-3-kinase/Akt pathway. *Biochemical pharmacology*, **67:** 1337-1345.

Cheung, H.Y., S.H Cheung, J. Li, C.S. Cheung, W. Lai, W.F. Fong and F.M. Leung, 2005. Andrographolide isolated from *Andrographis paniculata* induces cell cycle arrest and mitochondrial-mediated apoptosis in human leukemic HL-60 cells. *Planta Medica*, **71:** 1106-1111.

Choudhary, B.R. and M.K Poddar, 1984. Andrographolide and kalmegh (*Andrographis paniculata*) extract: *in vivo* and *in vitro* effect on lipid peroxidation. *Findings in Experimental and Clinical Pharmacology*, **6:** 481-485.

Choudhuri, S. and L.G. Valerio Jr., 2005. Usefulness of studies on the molecular mechanism of action of herbals/botanicals: the case of St. John's wort. *Journal of Biochemical and Molecular Toxicology,* **19:** 1–11.

Clark, D.E. and S.D. Pickett, 2000. Computational methods for the prediction of drug-likeness. *Drug Discovery Today*, **5:** 49-58.

Clarke, P.G., 2002. Apoptosis: from morphological types of cell death to interacting pathways. *Trends Pharmacol. Sci.*, **23:** 308–309

Cichewicz, R.H. and S.A. Kouzi, 2004. Chemistry, biological activity and chemotherapeutic potential of betulinic acid for the prevention and treatment of cancer and HIV infection. *Medical Research Reviews*, **24(1):** 90-114.

Cipriani G., E. Rapizzi, A. Vannacci, R. Rizzuto, F. Moroni, and A. Chiarugi, 2005. Nuclear poly(ADP-ribose) polymerase-1 rapidly triggers mitochondrial dysfunction. *J. Biol. Chem.*, **280:** 17227–17234.

Collins, T., M. A. Read, A. S. Neish, M. Z. Whitley, D. Thanos, and T. Maniatis, 1995. Transcriptional regulation of endothelial cell adhesion molecules: NF-κB and cytokine-inducible enhancers. *FASEB J.* **9:**899.

COM, 2000. Guidance on the strategy for testing of chemicals for mutagenicity. *Department of Health*, London, UK.

Cordell, G.A., 2000. Biodiversity and drug discovery, a symbiotic relationship. *Phytochemistry,* **55:** 463-480.

Cochrane, J.E. and T.R. Skopek, 1994. Mutagenicity of butadiene and its epoxide metabolites: I. Mutagenic potential of 1,2-epoxybutene, 1,2,3,4-diepoxybutane and 3,4-epoxy-1,2-butanediol in cultured human lymphoblasts. *Carcinogenesis*, **15(4):** 713-717.

Coon, J.T. and E. Ernst, 2004. Andrographis paniculata in the treatment of upper respiratory tract infections: a systematic review of safety and efficacy. *Planta medica*, **70(4):** 293-298.

Corso, C. and E.M. Parry, 1999. The application of comparative genomic hybridisation and fluorescence *in situ* hybridisation. *Mutagenesis,* **14(4):** 417-426.

Countryman, P.I. and J.A. Heddle, 1976. The production of micronuclei from chromosome aberrations in irradiated cultures of human lymphocytes. *Mutation Research*, **41(2-3):** 321-332.

Cox, R., J. Thacker and D.T. Goodhead, 1977a. Inactivation and mutation of cultured mammalian cells by aluminium characteristic ultrasoft X-rays. Dose responses of Chinese hamster and human diploid cells to aluminium X-rays and radiation of different LET. *Int J. Radiat Biol Relat Stud Phys Chem Med,* **31:** 561-576.

Cox., R. J. Thacker, D.T. Goodhead and R.J. Munson, 1977b. Mutation and inactivation of mammalian cells by various ionising radiations. *Nature*, **267:** 425-427.

Crespi, C.L. and W.G. Thilly, 1984. Assay for gene mutation in a human lymphoblast line, AHH-1 competent for xenobiotic metabolism. *Mutation Research*, **128:** 221-230.

Crespi, C.L., C.G. Ryan, G.M. Sixas, T.R. Turner, B.W. Penman, 1985. Tests for mutagenic activity using mutation assays at two loci in the human lymphoblast cell lines TK-6 and AHH-1. *Prog. Mut Res*, **5:** 197-216.

Crespi, C.L., F.J. Gonzalez, D.T. Steimel, T.R. Turner, H.V. Gelboin, B.W. Penman and R. Langerbach, 1991. A metabolically competent human cell line expressing five cDNAs encoding pro-carcinogen-activating enzymes: application to mutagenicity testing. *Chem. Res. Tox.*, **4:** 566-572.

Crofton-Sleigh, C., A. Doherty, S. Ellard, E.M. Parry, S. Venitt, 1993. Micronucleus assay using cytochalasin-blocked MCL-5 cells, a proprietary human cell line expressing five human cytochromes P-450 and microsomal epoxide hydrolase. *Mutagenesis*, **8:** 363-372.

Crombie, I. K. and H.J. McQuay, (1998). The systematic review: a good guide rather than a guarantee. *Pain*, **76:** 1-2.

Cui L., F. Qiu, N. Wang and X. Yao, 2004. Four new andrographolide metabolites in human urine. *Chem Pharm Bulletin*, **52(6):** 772-775.

Cui L., F. Qiu and X. Yao, 2005. Isolation and identification of seven glucuronide conjugates of andrographolide in human urine. *Drug Metabolism and Disposition*, **33(4):** 555-562.

D

D'Assoro, A.B., S.L. Barrett, C. Folk, et al., 2002. Amplified centrosomes in breast cancer: a potential indicator of tumour aggressiveness. *Breast Cancer Res Treat*, **75(1):** 25-34.

Decordier, I., L. Dillen, E. Cundari and M. Kirsch-Volders, 2002. Elimination of micronucleated cells by apoptosis after treatment with inhibitors of microtubules. *Mutagenesis*, **17:** 337-344.

Decordier, I., E. Cundari and M. Kirsch-Volders, 2005. Influence of caspase activity on micronuclei detection: a possible role for caspase-3 in micronucleation. *Mutagenesis*, **20(3):** 173-179.

Degrassi, F. and C. Tanzarella, 1988. Immunofluorescent staining of kinetochores in micronuclei: a new assay for the detection of aneuploidy. *Mutation Research*, **203:** 339-345.

Dellarco, V.L., K.H. Mavournin and R.R. Tice, 1985. Aneuploidy and health-risk assessment: current status and future directions. *Environmental Mutagenesis*, **7(3):** 405-424.

Denell, R.E., M.C. Lim, C. Auerbach, 1978. Diepoxybutane-induced male-transmissable X-autosome translocations in Drosophila melanogaster: a test of the supporting evidence for the Lifschytz-Lindsley model of spermatogenesis. *Mutation Research*, **49(2):** 219-224.

De Smet P.A.G.M., 1995. Health risks of herbal remedies. *Drug Safety*, **13:** 81-93.

Dinarello, C.A., 2000. Pro-inflammatory cytokines. *Chest*, **118:** 503-508.

Duensing, A., Y. Liu, S.A. Perdreau, J. Kleylein-Sohn, E.A. Nigg and S. Duensing, 2007. Centriole overduplication through the concurrent formation of multiple daughter centrioles at single maternal templates. *Oncogene*, **26:** 6280-6288.

Duesberg, P. and D.N. Rasnick, 2000. Aneuploidy, the somatic mutation that makes cancer a species of its own. Cell Motil. *Cytoskeleton*, **47:** 81-107.

Duesberg, P. and R. Li, 2003. Multistep carcinogenesis: a chain reaction of aneuploidisations. *Cell Cycle*, **2(3):** 202-210.

Duesberg, P. A. Fabarius, R. Hehlmann, 2004. Aneuploidy, the primary cause of the multilateral genomic instability of neoplastic and pre-neoplastic cells. *IUBMB Life*, **56:** 65-81.

Duke, R.C., Chervenak, R., Cohen, J.J., 1983. Endogenous endonuclease induced DNA fragmentation: an early event in cell-mediated cytolysis. *Proc. Natl. Acad. Sci. U.S.A.*, **80:** 6361– 6365.

Dunkelberg. H., 1979. On the oncogenic activity of ethylene oxide and propylene oxide in mice. *British Journal of Cancer*, **39(5):** 588-589.

Durkin, W.J., Ghanta, V.K., Balch, C.M., Davis, D.W., Hiramoto, R.N., 1979. A methodological approach to the prediction of anticancer drug effect in humans. *Cancer Research*, **39:** 402– 407.

Doak, S.H., G.J. Jenkins, G.E. Jonhson, E. Queik, E.M. Parry, J.M. Parry, 2007. Mechanistic influences for mutation induction curves after exposure to DNA-reactive carcinogens. *Cancer Research*, **67(8):** 3904-3911.

Dodson, H., E. Bourke, L.J. Jeffers, P. Vagnarelli, E. Sonoda, S. Takeda, W.C. Earnshaw, A. Mendes, C. Morrison, 2004. Centrosome amplification induced by DNA damage occurs during a prolonged G2 phase and involves ATM. *EMBO*, **23(19):** 3864-3873.

Doherty, A.T., S. Ellard, E.M. Parry and J.M. Parry, 1996. An investigation into the activation of chlorinated hydrocarbons to genotoxins in metabolically competent human cells. *Mutagenesis*, **11:** 247-274.

Domon, O.E., L.J. McGarrity, M. Bishop, M. Yoshika, J.J. Chen, S.M. Morris, 2001. Evaluation of the genotoxicity of the phytoestrogen, coumastrol in AHH-1 TK(+/-) human lymphoblastoid cells. *Mutation Research*, **474(1-2):** 129-137.

Doxsey, S., 2001. Re-evaluating centrosome function. *Nature Reviews Molecular Cell Biology*, **2(9):** 688-698.

E

Eastmond, D.A. and J.D. Tucker, 1989. Identification of aneuploidy-inducing agents using cytokinesis-blocked human lymphocytes and an antikinetochore antibody. *Environmental Molecular Mutagenesis*, **13:** 34-43.

Edinger, A.L. and C.B. Thompson, 2004. Death by design: apoptosis, necrosis and autophagy. *Current Opinion in Cell Biology*, **16:** 663–669.

Eggert, U.S., T.J. Mitchison and C.M. Field, 2006. Animal cytokinesis: from parts list to mechanisms. *Annual Review Biochemistry*, **75:** 543-566.

Ellard, S., Y. Mohammed, S. Dogra, C. Wolfel, J. Doehner, J.M. Parry, 1991. The use of genetically engineered V-79 Chinese hamster cultures expressing rat liver CYP1A1, 1A2 and 2B1 cDNAs in micronucleus assays. *Mutagenesis*, **6:** 461-470.

Eliasson, M.J., K. Sampei, A.S. Mandir, P.D. Hurn, R.J. Traystman, J. Bao, A. Pieper, Z.Q. Wang, T.M. Dawson, S.H. Snyder, V.L. Dawson, 1997. Poly(ADP-ribose) polymerase gene disruption renders mice resistant to cerebral ischemia. *Nature Medicine*, **3:** 1089–1095.

Elhajouji, A., Van Hummelen, P. and Kirsch-Volders, M., 1995. Indications for a threshold of chemically induced aneuploidy *in vitro* in human lymphocytes. *Environ. Mol. Mutagen.*, **26**: 292–304.

Elhajouji, A., Tibaldi, F. and Kirsch-Volders, M., 1997. Indication for thresholds of chromosome non-disjunction versus chromosome lagging induced by spindle inhibitors *in vitro* in human lymphocytes. *Mutagenesis*, **12**: 133–140.

Elhajouji, A., M. Cunha and M. Kirsch-Volders, 1998. Spindle poisons can induce polyploidy by mitotic slippage and micronucleate mononucleates in the cytokinesis-block assay. *Mutagenesis*, **13:** 193–198.

Escher M., Desmules J., Giostra E., Mentha G., 2001. Hepatitis associated with Kava, a herbal remedy associated with anxiety. *British Medical Journal*, **322:** 139.

Eisenbrand, G., F.Hippe, S. Jakobs and S. Muehlbeyer, 2004. Molecular mechanisms of indirubin and its derivateives: novel anticancer molecules with their origin in traditional Chinese phytomedicine. *Journal of Cancer Research and Clinical Oncology*, **130(11):** 627-635.

Erickson H.P. and E.T., O'Brien, 1992. Microtubule dynamic instability and GTP hydrolysis. *Annu Rev Biophys Biomol Structure.* **21**: 145–166.

F

Farah MH, Edwards R, 2000. International monitoring of adverse health effects associated with herbal medicines. *Pharmacoepidomiol Drug Safety*, **9:**105-112.

Fau, D., Lekehal, M., Farrell, G., Moreau, A., Moulis, C., Feldmann, G., Haouzi, D., Pessayre, D., 1997. Diterpenoids from germander, an herbal medicine, induce apoptosis in isolated rat hepatocytes. *Gastroenterology*, **113 (4):** 1334–1346.

Fava, F., B. Raynaud-Messina, J. Leung-Tack, L. Mazzolini, M. Li, J.C. Guillemot, D. Cachot, Y. Tollon, P. Ferrara and M. Wright, 1999. Human 76p: A new member of the gamma-tubulin-associated protein family. *Journal of Cell Biology*, **147:** 857-868.

FDA Press Release, 1992. Withdrawal of omniflox from the market.

Fellowes, M.D. and M.R. O'Donovan, 2007. Cytotoxicity in cultured cells is a function of the method used to estimate it. *Mutagenesis*, **22(4):** 275-280.

Fenech, M. and A.A. Morley, 1985. Measurement of micronuclei in lymphocytes. *Mutation Research*, **147:** 29-36.

Fenech, M., 2000. The *in vitro* micronucleus technique. *Mutation Research*, **455:** 81-95.

Fenech, M., 2002. Chromosomal biomarkers of genomic instability relevant to cancer. *Drug Discovery Today*, **7:** 1128-1137.

Fenech, M., W.P. Chang, M. Kirsch-Volders, N. Holland, S. Bonassi and E. Zeiger, 2003. HUMN project: detailed description of the scoring criteria for the cytokinesis-block micronucleus assay using isolated human lymphocyte cultures. *Mutation Research*, **534:** 65-75.

Fenech, M., 2005. The Genome Health Clinic and Genome Health Nutrgenomics concepts: diagnosis and nutritional treatment of genome and epigenome damage on an individual basis. *Mutagenesis*, **20:** 255-269

Fenech, M., P. Baghurst, W. Luderer, J. Turner, S. Record, M. Ceppi and S. Bonassi, 2005. Low intake of calcium, folate, nicotinic acid, vitamin E, retinol, beta-carotene and high intake of pantothenic acid, biotin and riboflavin are significantly associated with increased genome instability-results from a dietary intake and micronucleus index survey inSouth Australia. *Carcinogenesis*, **26:** 991-999.

Fiers, W., R. Beyaert, W. Declercq, P. Vandenabeele, 1999. More than one way to die: apoptosis, necrosis and reactive oxygen damage. *Oncogene,* **18:** 7719–7730.

Fisk, H.A. and M. Winey, 2001. The mouse Mps1p-like kinase regulates centrosome duplication. *Cell,* **106(1):** 95-104.

Fisk, H.A, C.P. Mattison and M. Winey, 2002. Centrosomes and tumour suppressors. *Current Opinion in Cell Biology*, **14(6):** 700-705.

Francois, M., V. Le Cabec, M.A. Dupont, P.J. Sansonetti, I. Maridonneau-Parini, 2000. Induction of necrosis in human neutrophils by *Shigella flexneri* requires type III secretion, IpaB and IpaC invasins, and actin polymerization. *Infect. Immun.*, **68:** 1289–1296.

Frederick CB, Potter DW, Midey IC, Andersen ME., 1992. A Physiologically based Pharmacokinetic and Pharmacodynamic Model to Describe the Oral Dosing of Rats with Ethyl Acrylate and its Implications for Risk Assessment. *Toxicol. Appl. Pharmacol.* **114:** 246-260.

Freshney, I.R., 2000. Culture of animal cells: a manual of basic technique. 4th Edition, Wiley-Liss, New York. pp. 330-332.

Friedberg, E.C., G.C. Walker, W. Siede, 1995. DNA repair and mutagenesis. ASM Press, Washington D.C.

Fry, A.M., T. Mayor, P. Meraldi, Y.D Stierhof, K. Tanaka and E.A. Nigg, 1998. C-Nap1, a novel centrosomal coiled-coil protein and candidate substrate of the cell cycle-regulated protein kinase Nek2. *Journal of Cell Biology*, **141:** 1563-1574.

Frost V, Delikat S, Al-Mehairi S, Sinclair AJ. Regulation of p27KIP1 in Epstein-Barr virus immortalized lymphoblastoid cell lines involves non-apoptotic caspase cleavage, 2001. *J Gen Virol*, **82:** 3057–3066.

Fujikawa, D.G., 2000. Confusion between neuronal apoptosis and activation of programmed cell death mechanisms in acute necrotic insults. *Trends Neurosci.*, **23:** 410–411.

Fukasawa, K., T. Choi, R. Kuriyama, S. Rulong, G.F. Woude, 1996. Abnormal centrosome amplification in the absence of p53. *Science*, **271(5256):** 1744-1747.

Fukasawa K, F. Wiener, G.F. Vande Woude, S. Mai, 1997. Genomic instability and apoptosis are frequent in p53 deficient young mice. *Oncogene*, **15:**1295-1302.

Fukasawa, K., 2005. Centrosome amplification, chromosome instability and cancer development. *Cancer Letters*, **230(1):** 6-19.

Furth, E., W.G. Thilly, B.W. Penman, H.L. Liber, W.M. Rand, 1981. Quantitative assay for mutation in diploid human lymbphoblasts using microliter plates. *Anal Biochem*, **160:** 1-8.

Fogh,J. and H. Fogh, 1965. Chromosome changes in PPLO-infected FL human amnion cells. *Proc. Soc. Exp. Biol and Med.*, **119:** 233-238.

G

Galipeau P.C., D.S. Cowan, C.A. Sanchez, M.T. Barrett, M.J. Emond, D.S. Levine, P.S. Rabinovitch, B.J. Reid, 1996. 17p (p53) allelic losses, 4N (G2/tetraploid) populations, and progression to aneuploidy in Barrett's esophagus. *PNAS USA*, **93:** 7081-7084.

Galloway, S.M., M.J. Armstrong, C. Reuben, S. Colman, B.C.C. Brown, A.D. Bloom, F. Nakamura, M. Ahmed, S. Duk, J. Rimpo, B.H. Margolin, M.A. Resnick, B. Anderson, E. Zeiger, 1987. Chromosome aberrations and sister chromatid exchanges in Chinese hamster ovary cells: evaluation of 108 chemicals. *Environ. Mol. Mutagen.* **10:**1–175.

Galloway, S., 2000. Cytotoxicity and chromosome aberrations in vitro: experience in industry and the case for an upper limit on toxicity in the aberration assay. *Environ. Mol. Mutagenesis*, **35:** 191–201.

Gentest Corporation Manual, 1994. AHH-1 TK+/- human lymphoblastoid cells: Routine cell culture, metabolite production and gene-locus mutation assay, procedures for use. Version 9.

Ghadimi, B.M., D.L. Sackett, M.J. Difilippantonio et al., 2000. Centrosome amplification and instability occurs exclusively in aneuploid but not in diploid colorectal cancer cell lines and correlates with numerical chromosome aberrations. *Genes Chromosomes Cancer*, **27:** 183-190.

Goshima, G., F. Nedelec and R.D. Vale, 2005. Mechanisms for focusing mitotic spindle poles by minus end-directed motor proteins. *Journal of Cell Biology*, **171:** 229-240.

Ghosh, S., M. J. May, and E. B. Kopp. 1998. NF-κB and Rel proteins: evolutionarily conserved mediators of immune responses. *Annual Rev. Immunolology*, **16:** 225.

Gibson G.G. and P. Skett, 2001. *Introduction to drug metabolism, 3rd edition.* Nelson Thornes, Cheltenham, UK.

Gibbs, R.A., P.N. Nguyen, A. Edwards, A.B. Civitello, and C.T. Caskey, 1990. Multiplex DNA deletion and exon sequencing of the HPRT gene in Lesch-Nyan families. *Genomics*, **7:** 235-244.

Grabsch, H., S. Takeno, W.J. Parsons, N. Pomjanski, A. Boecking, H.E. Gabbert and W. Muller, 2003. Overexpression of the mitotic checkpoint genes BUB1, BUBR1 and BUB3 in gastric cancer-association with tumour proliferation. *Journal of Pathology*, **200:** 16-22.

Granetto,C., L. Ottaggio, A. Abbondandolo and S. Bonatti, 1996. p53 accumulates in micronuclei after treatment with a DNA breaking chemical, methylnitrosourea, and with the spindle poison, vinblastine. *Mutation Research,* **352:** 61-64.

Grandis, J.R., 2006. Prognostic biomarkers in head and neck cancer. *Clinical Cancer Research*, **12(17):** 5005-5006.

Greene, N. et al., 1999. Knowledge-based expert systems for toxicity and metabolism prediction: DEREK, StAR and METEOR. *SAR QSAR Environ, Res.* **10**: 299–314.

Greenwood, S.K., R.B. Hill, J.T. Sun, M.J. Armstrong, T.E. Johnson, J.P. Gara and S.M. Galloway, 2004. A simple and more accurate estimation of cell growth suppression in the *in vitro* assay for chromosomal aberrations that reduces irrelevant positive results. *Environmental and Molecular Mutagenesis*, **43:** 36-44.

Greim H, Ahlers J, Bias R, Broecker B, Hollander H, Gelbke HP, Jacobi S, Klimisch HJ, Mangelsdorf I, Mayr W, Schön N, Stropp G, Stahnecker P, Vogel R, Weber C, Ziegler-Skylakakis K, Bayer E., 1995. Assessment of structurally related chemicals: Toxicity and ecotoxicity of acrylic acid and acrylic acid alkyl esters (Acrylates), Methacrylic acid and methacrylic acid alkyl esters (Methacrylates). *Chemosphere,* **31:** 2637-2659.

Griffiths, A.J.F, W.M. Gelbart, R.C. Lewontin, S.R. Wessler, D.T. Suzuki and J.H. Miller, 2004. *An Introduction to Genetic Analysis*, 8th Edition, pp.800.

Guest, R.D. and J.M. Parry, 1999. p53 integirty in the genetically engineered mammalian cell lines AHH-1 and MCL-5. *Mutation Research*, **423(1-2):** 39-46.

Guengerich, F.P. and T. Shimada, 1998. Activation of procarcinogens by human cytochrome P450 enzymes. *Mutation Research*, **400:** 201-213.

Gupta, R.S. and B. Singh, 1982. Mutagenic responses of five independent genetic loci in CHO cells on a variety of mutagens. Development and characteristics of a mutagen screening system based on selection for multiple drug-resistant markers. *Mutation Research,* **94:** 449–466.

Gupta, S. *et al.*, 1990. Antidiarrhoeal activity of diterpenes of *Andrographis paniculata* (kalmegh) against *Escherichia coli* enterotoxin in in vivo models. *International Journal of Crude Drug Research*, **28;** 273-283.

Gupta, J.B. and K. Prasad, 1992. Mechanism of hydrogen peroxide-induced modulation of airway smooth muscle. *Am J. Physiol.*, **263:** 714-722.

Gupta, S. *et al.*, 1993. Antisecretory (antidiarrhoeal) activity of Indian medicinal plants against *Escherichia coli* enterotoxin-induced secretion in rabbit and guinea-pig ileal loop models. *International Journal of Pharmacognosy*, **31:** 198-204.

H

Haaf, T., E. Raderschall, G. Reddy, D.C. Ward, C.M. Radding, E.I. Golub, 1999. Sequestration of mammalian Rad51-recombination protein into micronuclei. *Journal of Cell Biology,* **144:** 11–20.
Habtemariam, S., 1998. Andrographolide inhibits the tumour necrosis factor-α-induced up-regulation of ICAM-1 expression and endothelial monocyte adhesion. *Phytotherapy Research,* **12:** 37-40.

Haddad, J.J., 2002. Cytokines and related receptor-mediated signalling pathways. *Biochemical and Biophysical Communications*, **297:** 700-713.

Hallworth, R., R.F. Luduena, 2000. Differential expressions of beta-tubulin isotopes in the adult gerbil cochlea. *Hear Res.*, **148(1-2):** 161-172.

Hahn, W.C., C.M. Counter, A.S. Lundberg, R.L. Beijersbergen, M.W. Brooks and R.A. Weinberg, 1999. Creation of human tumour cells with defined genetic elements. *Nature*, **400:** 464-468.

Hanahan, D and R. A. Weinberg, 2000. The hallmarks of cancer. *Cell*, **100:** 57-70.

Handa, S.S. and A. Sharma, 1990a. Hepatoprotective activity of andrographolide from *Andrographis paniculata* against carbon tetrachloride. *Indian Journal of Medical Research*, **92**: 276-283.

Handa, S.S. and A. Sharma, 1990b. Hepatoprotective activity of andrographolide against galactosamine and paracetamol intoxication in rats. *Indian Journal of Medical Research*, **92:** 284-292.

Hagan, I.M. and R.E. Palazzo, 2006. Warming up at the poles. *EMBO Reports*, **7:** 364-371.

Heald, R., R. Tournebize, T. Blank et al., 1996. Self-organisation of microtubules into bipolar spindles around artificial chromosomes in *Xenopus* egg extracts. *Nature*, **382:** 420-425.

He, K., Iyer, K.R., Hayes, R.N., Sinz, M.W., Woolf, T.F., Hollenberg, P.F., 1998. Inactivation of cytochrome P450 3A4 by bergamottin, a component of grapefruit juice. *Chemical Research and Toxicology*, **11 (4):** 252–259.

He, X.J., J.K. Li, H. Gao, F. Qiu, K. Hu, X.M. Cui and X.S. Yao, 2003a. Four new andrographolide metabolites in rats. *Tetrahedron,* **59:** 6603-6607.

He, X.J., J.K. Li, H. Gao, F. Qiu, K. Hu, X.M. Cui and X.S. Yao, 2003b. Six new andrographolide metabolites in rats. *Chem Pharm Bulletin*, **51:** 586-589.

He, X.J., J.K. Li, H. Gao, F. Qiu, K. Hu, X.M. Cui and X.S. Yao, 2003c. Identification of a rare sulfonic acid metabolite of andrographolide in rats. *Drug Metabolism and Disposition*, **31:** 983-985.

Heddle, J.A. and W.R. Bruce, 1977. Comparison of the micronucleus sperm assay for mutagenicity with the carcinogenic activity of 61 different agents, in: H.H. Hiatt, J.D. Watson, J.A. Winsten (Eds.), Origins of Human Cancer, vol. 4, Cold Spring Harbor Conferences.

Heddle, J.A., P.B. Shepson, J.D. Gingerich, K.W. So, 1993. Mutagenicity of peroxyacetylnitrate in vivo: tests for somatic mutations and chromosomal aberrations. *Environmental Molecular Mutagen*, **21(1):** 58-66.

Hidalgo, M.A., A. Romero, J. Figuera, P. Cortes, I. Concha, J.L. Hancke and R.A. Burgos, 2005. Andrographolide interferes with binding of nuclear factor-κB to DNA in HL-60-derived neutrophilic cells. *British Journal of Pharmacology*, **144:** 680-686.

Hinchcliffe, E.H., C. Li, E.A. Thompson, J.L. Maller and G. Sluder, 1999. Requirement of Cdk2-cyclin E activity for repeated centrosome reproduction in Xenopus egg extracts. *Science*, **283(5403):** 851-854.

Hinchcliffe, E.H., F.J. Miller, M. Cham, A. Khodjakov and G. Sluder, 2001. Requirement of a centrosomal activity for cell cycle progression through G1 into S phase. *Science*, **291 (5508):** 1547-1550.

Hirata, H., Takahashi,A., Kobayashi,S., Yonehara,S., Sawai,H., Okazak.i, T., Yamamoto,K. and Sasada M., 1998. Caspases are activated in a branched protease cascade and control distinct downstream processes in Fas-induced apoptosis. *J. Exp. Med.*, **187:** 587-600.

Hoessel, R., S. Leclerc, J.A. Endicott, M.E. Nobel, A. Lawrie, P. Tunnah, M. Leost, E. Damiens, D. Marie, D. Marko, E. Niederberger, W. Tang, G. Eisenbrand and L. Meijer, 1999. Indirubin, the active constituent of a Chinese anti-leukaemia medicine inhibits cyclin-dependent kinases. *Nature Cell Biology*, **1(1):** 60-67.

Hoffman, M.E., A.C. Mello-Filho and R. Meneghini, 1984. Correlation between cytotoxic effect of hydrogen peroxide and the yield of DNA strand breaks in cells of different species. *Biochim Biophys Acta*, **781:** 234-238.

Hollander, M.C., M.S. Sheikh, D.V. Bulavin, K. Lundgren et al., 1999. Genomic instability in Gadd45a-deficient mice. *Nature Genetics*, **23(2):** 176-184.

Hollander, M.C. and A.J. Fornace Jr., 2002. Genomic instability, centrosome amplification, cell cycle checkpoints and Gadd45a. *Oncogene*, **21:** 6228-6233.

Holmes, A.L., S.S. Wise, S.J. Sandwick, W.L. Lingle, V.C. Negron, W.D. Thompson and J.P. Wise Sr., 2006. Chronic exposure to lead chromate causes centrosome abnormalities and anueploidy in human lung cells. *Cancer Research*, **66:** 4041-4048.

Honma, M, M. Hayashi, H. Shimada, N. Tanaka, S. Wakuri, T. Awogi, K.I.Yamamoto, N.-U.Kodani,Y. Nishi, M. Nakadate, T. Sofuni, 1999a. Evaluation of the mouse lymphoma tk assay (microwell method) as an alternative to the in vitro chromosomal aberration test, *Mutagenesis*, **14:** 5–22.

Honma, M., L.-S. Zhang, H. Sakamoto, M. Ozaki, K. Takeshita, M. Momose, M. Hayashi, T. Sofuni, 1999b. The need for long-term treatment in the mouse lymphoma assay. *Mutagenesis* **14:** 23–29.

Hsiang, P and K. Lewis, 2000. Synergy in medicinal plants: antimicrobials potentiated by multidrug pump inhibitors. *Proceedings of the National Academy of Sciences U.S.A*, **97:** 1433-1437.

Hughes, M.F., 2002. Arsenic toxicity and potential mechanisms of action. *Toxicology Letters*, **133:** 1-16.

Hypericum Depression Trial Study Group, 2002. Effect of *Hypericum perforatum* (St. John's wort) in major depressive disorder: A Randomized, Controlled Trial. *Journal of the American Medical Association*, **287:** 1807-14.

I

IARC monographs on the evaluation of the carcinogenic risk of chemicals to humans. International Agency for Research on Cancer, Lyon, France, p. V10 171 Y76.

IARC, 1999. Summaries and evaluations. Vol. 71, p.1059.

Ishidate Jr., M., M.C. Harnois, T. Sofuni,Acomparative analysis of data on the clastogenicity of 951 chemical substances tested in mammalian cell cultures, 1988. *Mutation Research*, **195:** 151–213.

Izzo, M., Antoccia, A., Degrassi, F., Tanzarella, C., 1998. Immunofluorescence analysis of diazepam-induced mitotic apparatus anomalies and chromosome loss in Chinese hamster cells. *Mutagenesis,* **13:** 445–451.

ICH, 1995. ICH Topic S2A. Genotoxicity: Guidance on Specific Aspects of Regulatory Genotoxicity Tests for Pharmaceuticals. International Conference on Harmonisation of Technical Requirements for Registration of Pharmaceuticals for Human Use. Geneva.

J

Jaattela, M and J. Tschopp, 2003. Caspase-independent cell death in T lymphocytes. *Nature Immunology*, **4:** 416–423.

Jackman, M., C. Linde, E.A. Nigg, J. Pies,

Jada, S.R., G.S. Subur, C. Matthews, A.S. Hamzah, N. Lajis, M.S. Saad, M.F.G. Stevens and J. Stanslas, 2007. Semisynthesis and in vitro anticancer activities of andrographolide analogues. *Phytochemistry*, **68:** 904-912.

Jaruchotikamol, A., K. Jarukamjorn, W. Sirisangtrakul, T. Sakuma, Y. Kawasaki and N. Nemoto, 2007. Strong synergistic induction of CYP1A1 expression by andrographolide plus typical CYP1A inducers in mouse hepatocytes. *Toxicol Appl Pharmacol*, **224(2):** 156-162.

Jarukamjorn, K., K. Don-in, C. Makejaruskul, T. Laha, S. Daodee, P. Pearaksa and B. Sripanidkulchai, 2006. Impact of *Andrographis paniculata* crude extract on mouse hepatic cytochrome P450 enzymes. *Journal of Ethnopharmacology*, **105(3):** 464-467.

Johnson, D.E. and A.D. Rodgers, 2006. Computational toxicology: heading toward more relevance in drug discovery and development. *Current Opinion in Drug Discovery and Development*, **9:** 29-37.

K

Kaplowitz, N., 2000. Mechanisms of liver cell injury. *Journal of Hepatology*, **32:** 39–47.

Kasprzak, K.S., F.W. Sunderman Jr. and K. Salnikow, 2003. Nickel carcinogenesis. *Mutation Research*, **533:** 67-97.

Kass, G.E.N. and S. Orrenius, 1999. Calcium signaling and cytotoxicity. *Environmental Health Perspective*, **107(1):** 25-35.

Kayani, M.A. and J.M. Parry, 2008. The detection and assessment of the aneugenic potential of selected oestrogens, progestines and androgens using the *in vitro* CBMA. *Mutation Research*, **651**: 40-45.

Khan, I.A., I. Tomita, F. Mizuhashi and R.F. Luduena, 2000. Differential interaction of tubulin isotopes with the anti-mitotic compound IKP-104.

Khodjakov, A. and C.L. Rieder, 1999. The sudden recruitment of gamma-tubulin to the centrosome at the onset of mitosis and its dynamic exchange throughout the cell cycle, do not require microtubule. *Journal of Cell Biology*, **146:** 585-596.

Khodjakov, A., R.W. Cole, B.R. Oakley et al., 2000. Centrosome-independent mitotic spindle formation in vertebrates. *Curr Biol.*, **10(2):** 59-67.

Khodjakov, A. and C.L. Rieder, 2001. Centrosomes enhance the fidelity of cytokinesis in vertebrates and are required for cell cycle progression. *Journal of Cell Biology*, **153:** 237-242.

Kim, Y.S. and J.A. Milner, 2005. Targets for indole-3-carbinol in cancer prevention. *Journal Nutrition Biochemistry*, **16:** 65-73.

Kirkland, D. J., 1992. Chromosomal aberration tests *in vitro*: problems with protocol design and interpretation of results. *Mutagenesis*, **7:** 95–106.

Kirsch-Volders, M., A. Elhajouji, E. Cundari and P.V. Hummelen, 1997. The *in vitro* micronucleus test: a multi-endpoint assay to detect simultaneously mitotic delay, apoptosis, chromosome breakage, chromosome loss and non- disjunction. *Mutation Research*, **392:** 19-30.

Kirsch-Volders, M, E. Cundari and B. Verdoodt, 1998. Towards a unifying model for the metaphase/anaphase transition. *Mutagenesis*, **13:** 321-335.

Kirsch-Volders, M., M. Aardema and A. Elhajouji, 2000. Concepts of threshold in mutagenesis and carcinogenesis. *Mutation Research*, **464:** 3-11.

Kirsch-Volders, M. and M. Fenech, 2001. Inclusion of micronuclei in non-divided mononuclear lymphocytes and necrosis/apoptosis may provide a more comprehensive cytokinesis block micronucleus assay for biomonitoring purposes. *Mutagenesis*, **16:** 51–58.

Kirsch-Volders, M., A. Vanhauwert, M. De Boeck and I. Decordier, 2002. Importance of detecting numerical versus structural chromosome aberrations. *Mutation Research*, **504(1-2):** 137-148.

Kirsch-Volders, M., A. Vanhauwaert, U. Eichenlaub-Ritter and I. Decordier, 2003. Indirect mechanisms of genotoxicity. *Toxicology Letters*, **140/141:** 63-74.

Kirsch-Volders, M., T. Sofuni, M. Aardema, S. Albertini et al., 2003. Report from the *in vitro* micronucleus assay-working group. *Mutation Research*, **540:** 153-163.

Klayman, D.L., 1985. Qinghaosu (artemisinin): an antimalarial drug from China. *Science*, **228**: 1049–1055.

Kleipool, R.J.C., 1952. Constituents of *Andrographis paniculata* Nees. *Nature*, **169:** 33-34.

Klug, W.S. and M.R. Cummings, 2005. *Essentials of Genetics (5th Edition),* Pearson, pp. 568.

Koehn, F.E. and G.T. Carter, 2005. The evolving role of natural products in drug discovery. *Nature Reviews Drug Discovery*, **4(3):** 206-220.

Kops, G.J., D.R. Foltz and D.W. Cleveland, 2004. Lethality to human cancer cells through massive chromosome loss by inhibition of the mitotic checkpoint. *PNAS USA*, **101:** 8699-8704.

Kops, G.J., B.A. Weaver and D.W. Cleveland, 2005. On the road to cancer: Aneuploidy and the mitotic checkpoint. *Nature Reviews Cancer*, **5:** 773-785.

Kottke,T.J., Blajeski,A.L., Meng,X.W. et al., 2002. Lack of correlation between caspase activation and caspase activity assays in paclitaxel-treated MCF-7 breast cancer cells. *J. Biol. Chem.*, **277:** 804-815.

Kouri, T., M. Jalkanen, H. Turakainen, R.H. Leach and R. Pettinen, 1983. Effect of Mycoplasma pulmonis infection on protein and glycosaminoglucan synthesis of cultured connective tissue cells. *Exptl.Cell Res.*, **148:** 1-10.

Kracht, M. and J., Saklatvala, 2002. Transcriptional and post-transcriptional control of gene expression in inflammation. *Cytokine*, **20:** 91-106.

Kramer , R. and D. Cohen, 2004. Functional genomics to new drug targets. *Nature Reviews Drug Discovery*, **3(11):** 965-972.

Kroemer, G., Dallapotta, B., Resche-Rigon, M., 1998. The mitochondrial death/life regulator in apoptosis and necrosis. *Annu. Rev. Physiol.* **60:** 619–642.

Krysko, D.V. et al., 2006. Macrophages use different internalization mechanisms to clear apoptotic and necrotic cells. *Cell Death and Differentiation*, **13:** 2011–2022.

Kumar, R.A., K. Sridevi, N.V. Kumar, S. Nanduri and S. Rajagopal, 2004. Anticancer and immunostimulatory compounds from *Andrographis paniculata*. *Journal of Ethnopharmacology,* **92(2-3):** 291-295.

L

Lacey, K.R., P.K. Jackson and T. Stearns, 1999. Cyclin-dependent kinase control of centrosome duplication. *PNAS USA*, **96(6):** 2817-2822.

Langowski, J. and A. Long, 2002. Computer systems for the prediction of xenobiotic metabolism. *Adv. Drug Deliv. Rev.* **54**: 407–415.

Lanni, J.S. and T. Jacks, 1998. Characterisation of the p-53-dependent post-mitotic checkpoint following spindle disruption. *Mol. Cell. Biol.*, **18(2):** 1055-1064.

Lawley, P.D., 1979. Approaches to chemical dosimetry in mutagenesis and carcinogenesis: the relevance of reactions of chemical mutagens and carcinogens in DNA, in P.C. Grover (Ed), Chemical carcinogens and DNA. CRC Press, Florida, pp. 1-79.

Lawrence, T., D. W. Gilroy, P. R. Colville-Nash, and D. A. Willoughby. 2001. Possible new role for NF-κB in the resolution of inflammation. *Nature Medicine*, **7:**1291.

Leach, N.T. and C. Jackson-Cook, 2004. Micronuclei with multiple copies of the chromosome: Do chromosomes replicate in micronuclei? *Mutation Research*, **554:** 89-94.

Lee, J.H., T.H. Koo, B.Y. Hwang, J.J. Lee, 2002. Kaurane diterpene, kamebakaurin inhibits NF-kappa B by directly targeting the DNA-binding activity of p50 and blocks the expression of NF-kappa B target genes. *Journal of Biological Chemistry*, **277(21):** 18411-18420.

Lekehal, M., Pessayre, D., Lereau, J.M., Moulis, C., Fouraste, I., Fau, D., 1996. Hepatotoxicity of the herbal medicine germander: metabolic activation of its furano diterpenoids by cytochrome P450 3A depletes cytoskeleton-associated protein thiols and forms plasma membrane blebs in rat hepatocytes. *Hepatology*, **24 (1):** 212–218.

Leist, M and M. Jaattela, 2001. Four deaths and a funeral: from caspases to alternative mechanisms. *Nat. Rev., Mol. Cell. Biol.* **2:** 589–598.

Lenardo, M.J., S.B. Angleman, V. Bounkeua, J. Dimas, M.G. Duvall, M. B. Graubard, F. Hornung, M.C. Selkirk, C.K. Speirs, C. Trageser, J.O. Orenstein, D.L. Bolton, 2002. Cytopathic killing of peripheral blood CD4(+) T lymphocytes by human immunodeficiency virus type 1 appears necrotic rather than apoptotic and does not require env. *Journal of Virology,* **76:** 5082–5093.

Li, Q., and I. M. Verma. 2002. NF-κB regulation in the immune system. *Nature Review Immunolology,* **10:** 725.

Li, Y., X. Sun, J.T. LaMont, A.B. Pardee, and C.J. Li, 2003. Selective killing of cancer cells by beta-lacaphone: direct checkpoint activation as a strategy against cancer. *Proceedings of the National Academy of Sciences U.S.A*, **100(5):** 2674-2678.

Li, J., H.Y. Cheung, Z. Zhang, G.K.L. Chan and W.F. Fong, 2007. Andrographolide induces cell cycle arrest at G_2/M phase and cell death in HepG2 cells via alteration of reactive oxygen species. *European Journal of Pharmacology*, **568(1-3):** 31-44.

Liang, J.C. and B.R. Brinkley, 1985. Chemical probes and possible targets for the induction of aneuploidy, In: Dellarco, V.L., P.E. Voytek and A. Hollaender. Aneuploidy: Etiology and mechanisms. Plenum Press, NY pages 491-506.

Liebler, D.C. and F.P. Guengerich, 2005. Elucidating mechanisms of drug-induced toxicity. *Nature Reviews Drug Discovery*, **4:** 410-420.

Liu, D.X. *et al.*, 1990. Antimutagenicity screening of water extracts from 102 kinds of Chinese medical herbs. Chung-kuo Chung Yao Tsa Chi Li, 15: 617-622.

Linde K, Ramirez G, Mulrow CD, Pauls A, Weidenhammer W, Melchart D, 1996. St. John's wort for depression – an overview and meta-analysis of randomised clinical trials. *BMJ*, **313:** 253-8.

Lingle, W.L., W.L. Lutz, J.N. Ingle, N.J. Maihle and J.L. Salisbury, 1998. Centrosome hypertrophy in human breast tumours: implications for genomic stability and cell polarity. *PNAS USA*, **95(6):** 2950-2955.

Lingle, W.L. and J.L. Salisbury, 2001. Methods for the analysis of centrosome reproduction in cancer cells. *Methods in Cell Biology*, **67:** 325-336.

Lingle, W.L., S.L. Barrett, V.C. Negron et al., 2002. Centrosome amplification drives chromosomal instability in breast tumour development. *PNAS USA*, **99:** 1978-1983.

Loeper, J., Descatoire, V., Letteron, P., Moulis, C., Degott, C., Dansette, P., Fau, D., Pessayre, D., 1994. Hepatotoxicity of germander in mice. *Gastroenterology*, **106 (2):** 464–472.

Loeper, J., De Berardinis, V., Moulis, C., Beaune, P., Pessayre, D., Pompon, D., 2001. Human epoxide hydrolase is the target of germander autoantibodies on the surface of human hepatocytes: enzymatic implications. *Advances in Experimental and Medical Biology*, **500:** 121–124.

Lodish, H., D. Baltimore, A. Berk., S.L. Zipursky, P. Matsudaira and J. Darnell, 1995. Molecular cell biology. Scientific American Books, Oxford.

Lomax LG, Krivanek ND, Frame SR., 1997. Chronic inhalation toxicity and oncogenicity of methyl methacrylate in rat and hamsters. *Food Chem. Toxicol.* **35:** 393-407.

Lord, G.M, Cook T, Arlt VM, Schmeiser HH, Williams G and C.D. Pusey, 2001. Urothelial malignant disease and Chinese herbal nephropathy. *Lancet*, **358:**1515-6.

Lynch, A.M. and J.M. Parry, 1993. The cytochalasin-B micronucleus/kinetochore assay in vitro: studies with 10 suspected aneugens. *Mutation Research*, **287(1):** 71-86.

M

Madav, S. *et al.*, 1995. Analgesic and antiulcerogenic effects of andrographolide. *Indian Journal of Pharmaceutical Science*, **57:** 121-125.

Mahoney, N.M., G. Goshima, A.D. Douglass and R.D. Vale, 2006. Making microtubules and mitotic spindles in cells without functional centrosomes. *Current Biology*, **16:** 564-569.

Mailhes, J.B. and P.Y. Zhin, 1987. Differential sensitivity of mouse oocytes to colchicine-induced aneuploidy. *Environmental Molecular Mutagenesis*, **10:** 183-188.

Mantel, C., S.E. Braun, S. Reid et al., 1999. p21 deficiency causes deformed nuclear architecture, centriole overduplication, polyploidy and relaxed microtubule damage checkpoints in human hematopoietic cells. *Blood*, **93(4):** 1390-1398.

Marx, J., 2002. Debate surges over the origins of genomic defects in cancer. *Science*, **297:** 544-546.

Masood, E., 1997. Medicinal plants threatened by over-use. *Nature*, **385:** 570.

Mathijssen, R.H., J. Verweij, P. de Bruijn, W.J. Loos and A. Sparreboom, 2002. Effects of St. John's wort on irinotecan metabolism. *J. National Cancer Institute*, **94(16):** 1247-1249.

Matsushima, T., M. Hayashi, A. Matsuoka, M. Ishidate Jr., K.F. Miura, H. Shimizu,Y. Suzuki, K. Morimoto, H. Ogura, K. Mure, K.Koshi,T. Sofuni,Validation study of the in vitro micronucleus test in a Chinese hamster lung cell line (CHL/IU), 1999a. *Mutagenesis*, **14:** 569–580.

Matzke, M.A., M.F. Mette, et al., 2003. Does the intrinsic instability of aneuploid genomes have a causal role in cancer? *Trends in Genetic*, **19:** 253-256.

Mavournin, K.H., D.H. Blakey, M.C. Cimino, M.F. Salamone, J.A. Heddle, 1990. The in vivo micronucleus assay in mammalian bone marrow and peripheral blood. A report of the U.S. Environmental Protection Agency Gene-Tox Program. *Mutation Research*, **239:** 29–80.

Mayor T., P. Meraldi, Y.D. Stierhof, E.A. Nigg and A.M. Fry, 1999. Protein kinases in control of the centrosome cycle. *FEBS Letters*, **452(1-2):** 92-95.

McCarthy TJ and Witz G., 1997. Structure-activity relationships in the hydrolysis of acrylate and methacrylate esters by carboxylesterase in vitro. *Toxicology* **116:**153-158.

McGarrity, G.J., V. Vanaman and J. Sarama, 1984. Cytogenetic effects of mycolasmal infection of cell cultures: a review. *In Vitro*, **20:** 1-18.

McGregor, D.B., C. Riach, P. Cattanach, I. Edwards, W. Shepherd and W.J. Casparry, 1989. Mutagenic responses of L5178Y mouse cells at the TK and HPRT loci. *Toxicology in vitro*, **10:** 643-647.

Meraldi, P and E.A. Nigg, 2001. Centrosome cohesion is regulated by a balance of kinase and phosphatase activities. *Journal of Cell Science*, **114(20):** 3749-3757.

Merdes A., R. Heald, K Samejima, W.C. Earnshaw and D.W. Cleveland, 2000. Formation of spindle poles by dynein/dynactin-dependent transport of NuMA. *Journal of Cell Biology*, **149:** 851-862.

Meshnick, S.R., 1998. Artemisinin antimalarials: mechanism of action and resistance. *Medicine Tropicale*, **58(3):** 13-17.

Michel, L.S., V. Liberal, A. Chatterjee, R. Kirchwegger, B. Pasche, W. Gerald, M. Dobles, P.K. Sorger, V.V. Murty and R. Benezra, 2001. MAD2 haplo-insufficiency causes premature anaphase and chromosome instability in mammalian cells. *Nature*, **409:** 355-359.

Michel, L., E. Diaz-Rodriguez, G. Narayan, E. Hernando, V.V. Murty, R. Benezra, 2004. Complete loss of tumour suppressor MAD2 causes premature cyclin B degradation and mitotic failure in human somatic cells. *PNAS USA*, **101:** 4459-4464.

Miller, B.M. and I.D. Adler, 1989. Spindle poisons: analysis of c-mitotic effects in mouse bone marrow cells. *Mutagenesis*, **4:** 208-215.

Miller,B, F. P¨otter-Locher, A. Seelbach, H. Stopper, D. Utesch, S. Madle, Evaluation of the in vitro micronucleus test as an alternative to the in vitro chromosomal aberration assay: position of the GUM working group on the in vitro micronucleus test, 1998. *Mutation Research*, **410:**81–116.

Mintel International Group, 1997. Complementary medicines. Mintel International Group Ltd, UK.

Misra, P. *et al.*, 1992. Antimalarial activity of *Andrographis paniculata* (kalmegh) against *Plasmodium berghei* NK65 in *Mastomys natalensis*. *International Journal of Pharmacognosy*, **30:** 263-274.

Mitchison, T. and M. Kirschner, 1984. Dynamic instability of microtubule growth. *Nature,* **312**: 237–242.

Miura K, Bowman ED, Simon R, Peng AC, Robles AI, Jones RT, Katagiri T, He P, Mizukami H, Charboneau L et al., 2002. Laser capture microdissection and microarray expression analysis of lung adenocarcinoma reveals tobacco smoking- and prognosis-related molecular profiles. *Cancer Research*, **62:** 3244-3250.

Montagna, C., Andrechek, E.R., Padilla-Nash, H., Muller, W.J., Ried, T., 2002. Centrosome abnormalities, recurring deletions of chromosome 4, and genomic amplification of HER2/neu define mouse mammary gland adenocarcinomas induced by mutant HER2/neu. *Oncogene*, **21:** 890–898.

Moritz, M., M.B. Braunfeld, J.C. Fung, J.W. Sedat, B.M. Alberts and D.A. Agard, 1995a. Three dimensional characterisation of centrosomes from early Drosophila embryos. *Journal of Cell Biology*, **130:** 1149-1159.

Moritz, M.B. Braunfeld, J.W. Sedat, B. Alberts and D.A. Agard, 1995b. Microtubule nucleation by gamma-tubulin-containing rings in the centrosome. *Nature*, **378:**638-640.

Moroi, Y., C. Peebles, M.J. Frizler, J. Steigerwald and E.M. Tan, 1980. Autoantibody to centromere (kinetochore) in scleroderma sera. *Proceedings of the National Academy of Sciences U.S.A*, **77:** 1627-1631.

Morris, S. M., O.E. Domon, K.B. Delclos, J.J. Chan, D.A. Casciano, 1994. Induction of mutations at the hypoxanthine phosphoribosyl transferase (HPRT) locus in AHH-1 human lymphoblastoid cells. *Mutation Research*, **310(1):** 45-54.

Mosmann, T., 1983. Rapid colorimetric assay for cellular growth and survival: application to proliferation and cytotoxicity assays. *Journal of Immunological Methods*, **65:** 55– 63.

Moudjou, M., N. Bordes, M. Paintrand and M. Bornens, 1996. Gamma-tubulin in mammalian cells: the centrosomal and the cytosolic forms. Journal of Cell Science, 109: 875-887.

Murdoch, W.J, C. Wilken, D.A. Young, 1999. Sequence of apoptosis and inflammatory necrosis within the formative ovulatory site of sheep follicles. *J. Reprod. Fertil.*, **117:** 325–329.

Murphy, S.M., L. Urbani and T. Stearns, 1998. The mammalian γ-tubulin complex contains homologues of the yeast spindle body components spc97p and spc98p. *Journal of Cell Biology*, **141:** 663-674.

Murphy, S.M., A.M. Prebble, U.K. Patel, K.L. O'Connell, D.P. Dias, M. Moritz, D. Agard, J.T. Stults and T. Stearns, 2001. GCP5 and GCP6: Two new members of the human gamma-tubulin complex. *Molecular Cell Biology*, **12:** 3340-3352.

Mussman, J.G., H.F. Horn, P.E. Carroll, M. Okuda et al., 2000. Synergistic induction of centrosome hyperamplification by loss of p53 and cyclin E overexpression. *Oncogene*, **19(13):** 1635-1646.

N

Nanduri, S., Nyavanadi, V.K., Thunuguntla, S.S.R., Kasu, S., Pallerla, M.K., Ram, P.S., Rajagopal, S., Kumar, R.A., Ramanujam, R., Babu, J.M., Vyas, K., Devi, A.S., Reddy, G.O., Akella, V., 2004. Synthesis and structure-activity relationships of andrographolide analogues as novel cytotoxic agents. *Bioorg. Med. Chem. Lett.* **14:** 4711–4717.

Nebert, D.W. and D.W. Russell, 2002. Clinical importance of the cytochromes P450. *Lancet,* **360:** 1155 - 1162 .

Nelson, D.R., 2003. Comparison of P450s from human and fugu: 420 million years of vertebrate P450 evolution. *Arch Biochem Biophys,* **409(1):** 18-24.

Newall, CA, Anderson LA and Phillipson JD, 1996. Herbal Medicines, a guide for healthcare professionals. The Pharmaceutical Press.

Newman, D.J., G.M. Cragg and K.M. Snader, 2003. Natural products as a source of new drugs over the period 1981-2002. *Journal of Natural Products*, **66:** 1002-1037.

Nicotera, P., Leist, M., Ferrando-May, E., 1999. Apoptosis and necrosis: different execution of the same death. *Biochem. Soc. Symp.* **66:** 69– 73.

Nicholson, D.W., Ali, A., Thornberry, N.A., Vaillancourt, J.P., Ding, C.K., Gallant, M., Gareau, Y., Griffin, P.R., Labelle, M., Lazebnik, Y.A., Munday, N.A., Raju, S.M., Smulson, M.E., Yamin, T.-T., Yu, V.L., Miller, D.K., 1995. Identification and inhibition of the ICE/CED-3 protease necessary for mammalian apoptosis. *Nature*, **376:** 37–43.

Nigg, E.A., 2007. Centrosome duplication: of rules and licenses. *Trends in Cell Biology*, **17(5):** 215-221.

Nik A. Rahman, N.N., T. Furuta, S. Kojima, K. Takane and Mohd, M.A., 1999. Antimalarial activity of extracts of Malaysian medicinal plants. *Journal of Ethnopharmacology*, **64:** 249-254.

Nortier JL, Martinez M-CM, Schmeiser HH, et al. Urothelial carcinoma associated with the use of a Chinese herb (*Aristolochia fangchi*). *New England J. Med*, **342:** 1686-92.

O

Ochi, T., 2002. Methylmercury, but not inorganic mercury, causes abnormality of centrosome integrity (multiple foci of gammatubulin), multipolar spindles and multinucleated cells without microtubule disruption in cultured Chinese hamster V79 cells. *Toxicology*, **175:** 111–121.

OECD, 1997. Guideline for the Testing of Chemicals. No. 473. *In Vitro* Mammalian Chromosome Aberration Test. Organisation for Economic Cooperation and Development. Paris.

OECD, 1997. Guideline for the Testing of Chemicals. No. 476. *In Vitro* Mammalian Cell Gene Mutation Test. Organisation for Economic Cooperation and Development. Paris.

Okuda, M., H.F. Horn, P. Tarapore et al., 2000. Nucleophosmin/B23 is a target of CDK2/cyclin E in centrosome duplication. *Cell*, **103(1):** 127-140.

Okuyama R, Nguyen BC, Talora C, Ogawa E, Tommasi di Vignano A, Lioumi M et al., 2004. High commitment of embryonic keratinocytes to terminal differentiation through a Notch1-caspase 3 regulatory mechanism. *Dev Cell*, **6:** 551–562.

O' Neil, M.J. *et al.*, 2001. The Merck Index: An encyclopedia of chemicals, drugs and biologicals, 13th edition. Merck Research Laboratory, NJ, pp. 106-107.

Opal, S.M. and V.A. DePalo, 2000. Anti-inflammatory cytokines. *Chest*, **117:** 1162-1172.

P

Panossian, A. *et al.*, 1999. Effect of *Andrographis paniculata* extract on progesterone in blood plasma of pregnant rats. *Phytomedicine*, **6:** 157-161.

Parry, J.M. and E.M. Parry, 1987. Comparison of tests for aneuploidy. *Mutation Research*, **181:** 267-287.

Parry, J.M. and A. Sors, 1993. The detection and assessment of the aneugenic potential of environmental chemicals: the European Community Aneuploidy Project. *Mutation Research*, **287:** 3-15.

Parry, J.M., E.M. Parry, S. Ellard, T. Warr, J. O'Donovan and A. Lafi, 1993. The detection, definition and regulation of aneugenic chemicals, in: Vigg, B.K. (Ed), Chromosome Segregation and Aneuploidy. BK NATO ASI Series, Vol.H12, Springer Berlin, pp. 391-415.

Parry, J.M., E.M. Parry, R. Bourner, A. Doherty, S. Ellard, J. O'Donovan, B. Hoebee et al., 1996. The detection and evaluation of aneugenic chemicals. *Mutation Research*, **353:** 11-46.

Parry, E.M., J.M. Parry, C. Corso, A. Doherty, F. Haddad, T.F. Hermine, G. Johnsen, M. Kayani, E. Quikc, T. Warr and J. Williamson, 2002. Detection and characterisation of mechanisms of action of aneugenic chemicals. *Mutagenesis*, **17(6):** 509-521.

Paton, G.R., J.P. Jacobs and F.T. Perkins, 1965. Chromosome changes in human diploid cell cultures infected with mycoplasma.

Patten C.J., P.E. Thomas, R.L. Guy, M. Lee, F.J. Gonzalez, F.P Guengerich and C.S. Yang, 1993. Cytochrome P450 enzymes involved in acetaminophen activation by rat and human liver microsomes and their kinetics. *Chemical Research in Toxicology*, **6:** 511-518.

Piel, M., J. Nordberg, U. Euteneuer and M. Bornens, 2001. Centrosome-dependent exit of cytokinesis in animal cells. *Science*, **2001:** 1550-1553.

Pihan G.A. and S.J. Doxsey, 1999. The mitotic machinery as a source of genetic instability in cancer. *Semin Cancer Biol*, **9:** 289–302.

Pihan, G.A., A. Purohit, J. Wallace, R. Malhotra, L. Liotta and S.J. Doxsey, 2001. Centrosome defects can account for cellular and genetic changes that characterise prostate cancer progression. *Cancer Research*, **61(5):** 2212-2219.

Pihan, G.A., J. Wallace, Y. Zhou and S.J. Doxsey, 2003. Centrosome abnormalities and chromosome instability occur together in pre-invasive carcinomas. *Cancer Research*, **63(6):** 1398-1404.

Pisha, E., H. Chai, I.S. Lee, T.E. Chagwedera, N.R. Farnsworth, G.A. Cordell, C.W. Beecher, H.H. Fong, A.D. Kinghorn, D.M. Brown, M.C. Wani, M.E. Wall, T.J. Heiken, T.K. Das Gupta and J.M. Peruzzo, 1995. Discovery of betulinic acid as a selective inhibitor of human melanoma that functions by induction of apoptosis. *Nature Medicine*, **1(10):** 1046-1051.

Pittler MH, Ernst E, 2003. Kava extract for treating anxiety. Cochrane Database Syst Rev, 1: CD003383.

Plymale, D.R., D.S. Tang, A.M. Comardelle, C.D. Fermin, D.E. Lewis, R.F. Garry, 1999. Both necrosis and apoptosis contribute to HIV-1-induced killing of CD4 cells. *Aids*, **13:** 1827–1839.

Pratt and Taylor (eds.), Principles of Drug Action, Third Edition, 1990, Churchill Livingstone.

Puri, A. *et al.*, 1993. Immunostimulant agents from *Andrographis paniculata*. *Journal of Natural Products*, 56: 995-999.

Purves, W.K., G.H. Orians, H.G. Heller and D. Sadava, 1998. Life: The science of biology. Sinauer Associates.

Pockwinse, S.M., G. Krockmalnic, S.J. Doxsey, J. Nickerson et al., 1997. Cell cycle independent interaction of CDC2 with the centrosome which is associated with the nuclear matrix-intermediate filament scaffold. *PNAS USA*, **94(7):** 3022-3027.

Polphana, N., N. Rangkadilok, S. Thongnest, S., Ruchirawat, M. Ruchirawat and J. Satayavivad, 2004. Determination and variation of three active diterpenoids in *Andrographis paniculata*. *Phytochemical Analysis*, **15(6):** 365-371.

Q

Qin, L.H., L. Kong, G.J. Shi, Z.T. Wang and B.X. Ge, 2006. Andrographolide inhibits the production of TNF-a and interleukin-12 in lipopolysaccharide-stimulated macrophages: role of mitogen-activated protein kinases. *Biol Pharm Bull*, **29(2):** 220-224.

Quintyne, N.J., J.E. Reing, D.R. Hoffelder, S.M. Gollin and W.S. Saunders, 2005. Spindle multipolarity is prevented by centrosomal clustering. *Science*, **307:** 127-129.

Quillardet, P., C. de Bellecombe, M. Hofnung, 1985. The SOS Chromotest, a colorimetric bacterial assay for genotoxins: validation study with 83 compounds. *Mutation Research*, **147:** 79–95.

Quo, L.Q., K. Fukuda, T. Ohta and Y. Yamazoe, 2000. Role of furanocoumarin derivatives on grapefruit mediated inhibition CYP3A activity. *Drug Metabolism and Disposition*, **28:** 766-771.

R

Raff, J.W., 2002. Centrosomes and cancer: lessons from a TACC. *Trends Cell Biol*, **12(5):** 222-225.

Rajagopal, S., R.A. Kumar, D.S. Deevi, C. Satyanarayana and R. Rajagopalan, 2003. Andrographolide, a potential cancer therapeutic agent isolated from *Andrographis paniculata*. *Journal of Experimental Therapeutics and Oncology*, **3:** 147-158.

Rates, S.M.K., 2001. Plants as sources of drugs. *Toxicon*, **39:** 603-613.

Recio, L. and T.R. Skopek, 1988. Mutagenicity of acrylonitrile and its metabolite 2-cyanoethylene oxide in human lymphoblasts in vitro. *Mutation Research*, **206:** 297-305.

Recio L, Steen A.M, Pluta L.J, Meyer K.G, Saranko C.J, 2001. Mutational spectrum of 1,3-butadiene and metabolites 1,2-epoxybutene and 1,2,3,4-diepoxybutane to assess mutagenic mechanisms. *Chem Biol Interact,* **135–136:** 325–341.

Reif S, Nicolson M.C, Bisset D et al., 2002. Effect of grapefruit juice intake on etoposide bioavailability. *Eur J Clin Pharmacol*, **58:** 491–494.

Ridler, M.A. and G.F. Smith, 1968. The response of human cultured lymphocytes to cytochalasin-B. *Journal of Cell Science*, **3:** 595-602.

Rieder, C.L., A. Schultz, R. Cole and G. Sluder, 1994. Anaphase onset on vertebrate somatic cells is controlled by a checkpoint that monitors sister kinetochore attachement to the spindle. *Journal of Cell Biology*, **127:** 1301-1310.

Rieder, C.L., R.W. Cole, A. Khodjakov and G. Sluder, 1995. The checkpoint delaying anaphase in response to chromosome monoorientation is mediated by an inhibitory signal produced by unattached kinetochores. *Journal of Cell Biology*, **130:** 941-948.

Ring, D., M. Hubble and M. Kirschner, 1982. Mitosis in a cell with multiple centrioles. *Journal of Cell Biology*, **94:** 549-556.

Rowinsky, E.K. and R.C Donehower, 1995. Paclitaxel (taxol). *New England Journal of Medicine*, **332:** 1004–1014.

Russo, A. and F. Pachierotti, 1988. Meiotic arrest and aneuploidy induced by vinblastine in mouse oocytes. *Mutation Research*, **202:** 215-221.

S

Sablina, A.A., G.V. Ilyinskaya, S.N., Rubtsova, L.S. Agapova, P.M. Chumakov and B.P. Kopnin, 1998. Activation of p53-mediated cell cycle checkpoint in response to micronuclei formation. *J. Cell Sci.*, **111:** 977-984

Salisbury, J.L., W.L. Lingle, A.R. White, L.E. Cordes, S. Berrett, 1999. Microtubule nucleating capacity of centrosomes in tissue sections. *Journal of Histochemistry and Cytochemistry,* **47(10):** 1265-1274.

Satyanarayana, C., D.S. Deevi, R. Rajagopalan, N. Srinivas and S. Rajagopal, 2004. *BMC, Cancer*, **4:** 26.

Sato, N., K. Mizumoto, M. Nakamura, K. Nakamura, M. Kusumoto, H. Niiyama et al., 1999. Centrosome abnormalities in pancreatic ductal carcinoma. *Clinical Cancer Research*, **5(5):** 963-970.

Sato, N., K. Mizumoto and M. Tanaka, 2004. Radiation therapy and centrosome anomalies in pancreatic cancer. In Nigg, E.A. (Ed.), Centrosomes in Development and Disease, Weiheim. pp. 337-352.

Sankaran, S. and J.D. Parvin, 2006. Centrosome function in normal and tumor cells. *Journal of Cellular Biochemistry*, **99:** 1240-1250.

Saunders, W.S., M. Shuster, X. Huang, B. Gharaibeh et al., 2000. Chromosomal instability and cytoskeletal defects in oral cancer cells. *PNAS USA,* **97:** 303-308.

Savill, J. and V. Fadok, 2000. Corpse clearance defines the meaning of cell death. *Nature*, **407:** 784–788.

Schippmann, U., D.J. Leaman and A.B. Cunningham, 2002. Impact of cultivation and gathering of medicinal plants on biodiversity. Biodiversity and the Ecosystem Approach in Agriculture, Forestry and Fisheries (FAO): 1-21.

Schmit, A.C., 2002. Acentrosomal microtubule nucleation in higher plants. *Int Rev Cytol*, **220:** 257-289.

Schreiber, S.L., 2000. Target-oriented and diversity-oriented organic synthesis in drug discovery. *Science*, **287:** 1964-1969.

Schuler, M., D.S. Rupa and D.A. Eastmond, 1997. A critical evaluation of centromeric labelling to distinguish micronuclei induced by choromosomal loss and breakage *in vitro*. *Mutation Research*, **392(1-2):** 81-95.

Schulze J., Raasch W, Siegers CP, 2003. Toxicity of kava pyrones, drug safety and precautions – a case study. *Phytomedicine*, **10:** Suppl 4:68-73.

Schwabe, R.F. and D.A. Brenner, 2006. Mechanisms of Liver Injury. I. TNF-{alpha}-induced liver injury: role of IKK, JNK, and ROS pathways. *Am. J. Physiol.: Gastrointest. Liver Physiol.*, **290:** G583–G589.

Schwarz, U.I., Buschel, B., Kirch, W., 2003. Unwanted pregnancy on self-medication with St John's Wort despite hormonal contraception. *British Journal of Clinical Pharmacology* **55,** 112–113.

Sega, G.A., 1984. A review of the genetic effects of ethylmethanesulfonate. *Mutation Research*, **134:** 113-142.

Shaw D *et al.*, 1997. Traditional remedies and food supplements: A 5-year toxicological study (1991-1995). *Drug Safety*, **17:** 342-56.

Shelton RC, Keller MB, Gelenberg AJ, et al., 2002. Effectiveness of St. John's wort in major depression. *Journal of the American Medical Association*, **285:** 1978-86.

Shen, Y.C., C.F. Chen and W.F. Chiou, 2002. Andrographolide prevents oxygen radical production by human neutrophils: possible mechanism(s) involved in its anti-inflammatory effects. *British Journal of Pharmacology*, **135:** 399-406.

Sluder, G., E.A. Thompson, F.J. Miller, J. Hayes and C.L. Rieder, 1997. The checkpoint control for anaphase onset does not monitor excess numbers of spindle poles or bipolar spindle symmetry. *Journal of Cell Science*, **110 (Pt4):** 421-429.

Singh, R.P., S. Banerjee and A.R. Rao, 2001. Modulatory influence of Andrographis paniculata on mouse hepatic and extrahepatic carcinogen metabolising enzymes and antioxidant status. *Phytotheraphy Research*, **15:**382-390.

Singha, P.K., S. Roy and S. Dey, 2003. Antimicrobial activity of *Andrographis paniculata. Fitoterapia,* **74:** 692-694.

Siripong, P., B. Kongkathip, K. Preechanukool, P. Picha, K. Tunsuwan and W.C. Taylor, 1992. Cytotoxic diterpenoid constituents from *Andrographis paniculata. J. Sci. Soc Thailand*, **18:** 187-194.

Snyder, R.D. *et al.* (2004) Assessment of the sensitivity of the computational programs DEREK, TOPKAT and MCASE in the prediction of the genotoxicity of pharmaceutical molecules. *Environ. Mol. Mutagen.* **43:** 143–158

Sofuni, T., M. Honma, M. Hayashi, H. Shimada, N. Tanaka, S. Wakuri, T. Awogi, K.I. Yamamoto, Y. Nishi, M. Nakadate, 1996. Detection of in vitro clastogens and spindle poisons by the mouse lymphoma assay using the microwell method: interim report of an international collaborative study. *Mutagenesis*, **11:** 349-355.

Southern S.A., M.F. Evans, C.S. Herrington, 1997. Basal cell tetrasomy in low-grade cervical squamous intraepithelial lesions infected with high-risk human papillomaviruses. *Cancer Research*, **57:** 4210-4213.

Sparreboom A, Cox MC, Acharya MR et al., 2004. Herbal remedies in the United States: potential adverse interactions with anticancer agents. *Journal of Clinical Oncology*, **22:** 2489–2503.

Stevinson, C and Ernst E., 1999. Hypericum for depression: an update of the clinical evidence. *Eur Neuropscyhopharmacology*, **9(6):** 501-505.

Stopper, H. and S.O. Muller, 1997. Micronuclei as a biological endpoint for genotoxicity: a minireview. *Toxicology in vitro*, **11:** 661-667.

Storer, R.D., T.W. McKelvey, A.R. Kraynek, M.C. Elia, J.E. Barman, L.S. Hormon, W.W. Nicholas, J.K. Lorca, 1996. Revalidation of the in vitro alkaline elution/rat hepatocyte assay for DNA damage: compound criteria for assessment of cytotox and genetox and results for 81 compounds. *Mutation Research*, **368:** 59-101.

T

Tan, Y.R. Yu and J.M. Peruzzo, 2003. Betulinic acid-induced programmed cell death in human melanoma cells involves mitogen-activated protein kinase activation. *Clinical Cancer Research*, **9(7):** 2866-2875.

Tanaka, T. and N. Shimizu, 2000. Induced detachment of acentric chromatin from mitotic chromosomes leads to their cytoplasmic localization at G_1 and the micronucleation by lamin reorganization at S phase. *J. Cell Sci.*, **113:** 697-707.

Tarapore, P., H.F. Horn, Y. Tokuyama and K. Fukasawa, 2001a. Direct regulation of the centrosome duplication cycle by the p53-p21Waf1/Cip1 pathway. *Oncogene*, **20(25):** 3173-3184.

Tarapore, P. Y. Tokuyama, H.F. Horn and K. Fukasawa, 2001b. Difference in the centrosome duplication regulatory activity among p53 'hot spot' mutants: potential role of Ser 315 phosphorylation-dependent centrosome binding of p53. *Oncogene*, **20(47):** 6851-6863.

Teodori, L., W. Gohde, M. Persiani, F. Ferrario, D.D. Tirindelli, D. Scarpignato, U. Di Tondo, P. Alo, L. Laparso, 1998. DNA/protein flow cytometry as a predictive marker of malignancy in dysplasia-free Barret's esophagus: thirteen-year follow-up study on a cohort of patients. *Cytometry,* **34(6):** 257-263.

Tewari, M., Quan, L.T., O'Rourke, K., Desnoyers, S., Zeng, Z., Beidler, D.R., Poirie, G.G., Salvesen, G.S., Dixit, V.M., 1995. Yama/CPP32h, a mammalian homolog of CED-3, is a CrmA-inhibitable protease that cleaves the death substrate poly (ADP-ribose) polymerase. *Cell*, **81:** 801– 809.

Thomas, P., K. Umegaki and M. Fenech, 2003. Nucleoplasmic bridges are a sensitive measure of chromosome rearrangement in the cytokinesis-block micronucleus assay. *Mutagenesis*, **18:** 187-194.

Tsai, H.R., L.M. Yang, W.J. Tsai and W.F. Chiou, 2004. Andrographolide acts through inhibition of ERK1/2 and Akt phosphorylation to suppress chemotactic migration. *European Journal of Pharmacology*, **498(1-3):** 45-52.

Touil, N., P.V. Aka, J.P. Buchet, H. Thierens and M. Kirsch-Volders, 2002. Assessment of genotoxic effects related to chronic low level exposure to ionising radiation using biomarkers for DNA damage and repair. *Mutagenesis*, **17(3):** 223-232.

Tsou, MF and T. Stearns, 2006. Controlling centrosome number: Licenses and blocks. *Current Opinion in Cell Biology*,**18:** 74-78.

Trapp, S. and R. Croteau, 2001. Defensive resin biosynthesis in conifers. *Annual Review Plant Physiology Plant Molecular Biology*, **52:** 689-724.

Trump, B.F. and I.K. Berezesky. 1995. Calcium-mediated cell injury and cell death, J. FASEB, 9: 219-228.

Trivedi, N. and U.M. Rawal, 2000. Hepatoprotective and toxicological evaluation of Andrographis paniculata on severe liver damage. *Indian Journal of Pharmacology*, **32:** 288-293.

Turlings, T.C. and J.H. Tumlinson, 1992. Systemic release of chemical signals by herbivore-injured corn. *PNAS*, **89(17):** 8399-8402.

Tweats, D.J., A.D. Scott, C. Westmoreland, P.L. Carmichael, 2007. Determination of genetic toxicology and potential carcinogenicity in vitro- challenges post the 7th Amendment to EU cosmetics Directive. *Mutagenesis*, **22(1):**5-13.

U

Umegaki, K and M. Fenech, 2000. Cytokinesis-block micronucleus assay in WIL2-NS cells: a sensitive system to detect chromosomal damage induced by reactive oxygen species and activated human neutrophils. *Mutagenesis*, **15(3):** 261–269.

United Nations Conference on Trade and Development (UNCTAD), 2000. Systems and national experiences for protecting traditional knowledge, innovations and practices. Background note by the UNCTAD Secretariat, Geneva. Document reference TD/B/COM.1/EM.13/2).

United States Food and Drug Administration (US FDA), Center for Drug Evaluation and Research (CDER), Draft 2005. Guidance for Industry: Safety Testing of Drug Metabolites.

Upender, M.B., J.K. Habermann, L.M. McShane, E.L. Korn, J.C. Barrett, M.J. Difillipantonio and T. Ried, 2004. Chromosome transfer induced aneuploidy results in complex dysregulation of the cellular transcriptome in immortalized and cancer cells. *Cancer Research*, **64:** 6941-6949.

V

Vral., A., H. Thierens and L. De Ridder, 1997. In vitro micronucleus-centromere assay to detect radiation-damage induced by low doses in human lymphocytes. *International Journal of Radiation Biology*, **71(1):** 61-68.

von der Hude, W., S. Kalweit, G. Engelhardt, S. McKiernan, P. Kasper, R. Slacik-Erben, H.G. Miltenburger, N. Honarvar, R. Fahrig, B. G¨orlitz, S. Albertini, S. Kirschner, D. Utesch, F. Potter-Locher,H. Stopper, S.Madle, 2000. In vitro micronucleus assay with Chinese hamster V79 cells—results of a collaborative study with in situ exposure to 26 chemical substances. *Mutation Research*, **468:** 137–163.

W

Wadsworth, P. and A. Khodjakov, 2004. E pluribus unum: towards a universal mechanism for spindle assembly. *Trends in Cell Biology*, **14:** 413-419.

Wall, M.E. and M.C. Wani, 1996. Campthothecin and taxol: from discovery to clinic. *Journal of Ethnopharmacology*, **51:** 239-254.

Wang, X.W., Q Zhan, J.D. Coursen et al., 1999. GADD45 induction of a G2/M cell cycle checkpoint. *PNAS USA*, **96(7):** 3706-3711.

Wang, Y.J, J.T. Wang, Q.X. Fan and J. G.Geng, 2007. Andrographolide inhibits NF-κB activation and attenuates neointimal hyperplasia in arterial restenosis. *Cell Research*, 1-9.

Williams G, O.I. Arouma, 2000. Molecular Drug Metabolism and Toxicology. London.

Wienkers, L.C. and T.G. Heath, 2005. Predicting in vivo drug interactions from in vitro drug discovery data. *Nature Reviews Drug Discovery*, **4:** 825-833.

Wissinger, W.L., D.N. Estervig and J. Wang, 1981. A differential staining technique for simultaneous visualisation of mitotic spindle and chromosomes in mammalian cells. *Stain technology*, **56:** 221-226.

Wong, M.M. and E.N. Fish, 2003. Chemokines: attractive mediators of the immune response. *Seminar in Immunology*, **15:** 5-14.

World Health Organisation, WHO Traditional Medicine Strategy 2002-2005 (online). Geneva, 2002 (cited 10 October 2003) PDF format available from: http://www.who.int/medicines/library/trm/trm_strat-eng.pdf

Woo, Y.T., DY. Lai, M.F. Argus, J.C. Arcos, 1995. Development of structure-activity relationships rules for predicting carcinogenic potential of chemicals. *Toxicology Letters*, **79(1-3):** 219-228.

Woo M, Hakem R, Furlonger C, Hakem A, Duncan GS, Sasaki T et al. Caspase-3 regulates cell cycle in B cells: a consequence of substrate specificity, 2003. *Nature Immunology*, **4:** 1016–1022.

Wyllie, A.H., Kerr, J.F., Currie, A.R., 1980. Cell death: the significance of apoptosis. *Int. Rev. Cytol.*, **68:** 251– 306.

X

Xia, Y.F., B.Q. Ye, Y.D. Li, J.G. Wang, X.J. He, X. Lin, X. Yao, D. Ma, A. Slungaard, R.P. Hebbel, N.S. Key and J.G. Geng, 2004. Andrographolide attenuates inflammation by inhibition of NF-kB activation through covalent modification of reduced cysteine 62 of p50. *Journal of Immunology*, **173:** 4207-4217

Y

Yamamoto, Y., and R. B. Gaynor, 2001. Therapeutic potential of inhibition of the NF-_B pathway in the treatment of inflammation and cancer. *J. Clin. Invest.* **107:** 135.

Yamamoto, Y. H. Matsuyama, T. Furuya, A. Oga, S. Yoshihiro, M. Okuda, S. Kawauchi, K. Sasaki, K. Naito, 2004. Centrosome hyperamplification predicts progression and tumour recurrence in bladder cancer. *Clinical Cancer Research*, **10(19):** 6449-6455.

Yan, XX, Najbauer J, Woo CC, Dashtipour K, Ribak CE, Leon M, 2001. Expression of active caspase-3 in mitotic and postmitotic cells of the rat forebrain. *J Comp Neurol*, **433:** 4–22.

Yeowell-O_Connell K., N. Rothman, M.T. Smith, R.B. Hayes, G. Li, S. Waidyanatha, M. Dosemeci, L. Zhang, S. Yin, N. Titenko-Holland, S.M. Rappaport, 1998. Hemoglobin and albumin adducts of benzene oxide among workers exposed to high levels of benzene. *Carcinogenesis*, **19:** 1565–1571.

Yin, X., D.X. Liu, H. Wang and Y. Zhou, 1991. A study on the mutagenicity of 102 raw pharmaceuticals used in Chinese traditional medicine. *Mutation Research*, **260(1):** 73-82.

Young, P.R., 1998. Pharmacological modulation of cytokine action and production through signalling pathways. *Cytokine & Growth Factor Reviews*, **9:** 239-257.

Yuen, K.W., B. Montpetit and P. Hieter, 2005. The kinetochore and cancer: what the connection? *Current Opinion in Cell Biology*, **17:** 576-582.

Yuan B, Xu Y, Woo JH, Wang Y, Bae YK, Yoon DS, Wersto RP, Tully E, Wilsbach K, Gabrielson E, 2006. Increased expression of mitotic checkpoint genes in breast cancer cells with chromosomal instability. *Clinical Cancer Research*, **12:** 405-410.

Yuan, J., 2006. Divergence from a dedicated cellular suicide mechanism: exploring evolution of cell death. *Molecular Cell*, **23:** 1–12.

Z

Zatsepina, O.V., A. Rousselet, P.K. Chan, M.O. Olson, E.G. Jordon and M. Bornens, 1999. The nucleolar phosphoprotein B23 redistributes in part to the spindle polse during mitosis. *J. Cell Sci*, **112(4):** 455-466.

Zimonjic, D., M.W. Brooks, N. Popescu, R.A. Weinberg and W.C. Hahn, 2001. Derivation of human tumour cells *in vitro* without widespread genomic instability. *Cancer Research*, **61:** 8838-8844.

Zitvogel, L. et al., 2004. The immune response against dying tumor cells. *Adv. Immunology*, **84:** 131–179.

Zong, W-X. and C.B. Thompson, 2006. Necrotic death as a cell fate. *Genes and Development*, **20:** 1–15.

APPENDIX

Data for Chapter 3.

Table A1. Raw data on cell count for the three cell lines used in cell doubling time determination experiments.

Hours	AHH-1 Cell count (Cells/ml)			MCL-5 Cell count (Cells/ml)			V-79 Cell count (Cells/ml)		
	A	B	C	A	B	C	A	B	C
16h	1.70E+05	1.52E+05	1.44E+05	1.64E+05	1.66E+05	1.58E+05	1.75E+05	1.66E+05	1.60E+05
17h	1.72E+05	1.58E+05	1.45E+05	1.74E+05	1.68E+05	1.63E+05	1.73E+05	1.65E+05	1.63E+05
18h	1.73E+05	1.55E+05	1.48E+05	1.70E+05	1.72E+05	1.70E+05	3.61E+05	3.52E+05	3.55E+06
19h	3.50E+05	3.03E+05	3.12E+05	1.72E+05	1.75E+05	1.65E+05	3.60E+05	3.45E+05	3.56E+05
20h	3.50E+05	3.10E+05	3.12E+05	1.72E+05	1.80E+05	1.66E+05	3.63E+05	3.52E+05	3.54E+05
21h	3.53E+05	3.12E+05	3.20E+05	1.75E+05	1.78E+05	1.66E+05	3.63E+05	3.54E+05	3.52E+05
22h	3.52E+05	3.12E+05	3.21E+05	1.89E+05	1.80E+05	1.71E+05	3.56E+05	3.53E+05	3.58E+05
23h	3.55E+05	3.10E+05	3.23E+05	3.30E+05	3.40E+05	3.23E+05	3.64E+05	3.53E+05	3.54E+05
24h	3.55E+05	3.16E+05	3.21E+05	3.43E+05	3.44E+05	3.22E+05	3.63E+05	3.57E+05	3.55E+05

Table A2. Raw data on *in vitro* CBMA for AHH-1 cells treated with andrographolide for dose setting assay.

Dose (µM)	Mono	Bi	Tri	Tetra	Multi	Total	Total Mn	% Bi	% Mn/Bi	RI
0	1520	2000	7	7	7	3541	3	56.48	0.15	0.58
	1555	2000	9	10	3	3577	2	55.91	0.10	0.57
	1596	2000	7	9	4	3616	3	55.31	0.15	0.56
	1475	2000	8	8	4	3495	4	57.22	0.20	0.58
Mean value								56.23	0.15	0.57
DMSO	1496	2000	8	11	6	3521	3	56.80	0.15	0.58

	1510	2000	8	9	4	3531	2	56.64	0.10	0.58
	1449	2000	7	9	3	3468	3	57.67	0.15	0.59
	1500	2000	6	8	4	3518	4	56.85	0.20	0.58
Mean value								56.99	0.15	0.58
10	943	1000	6	3	2	1954	3	51.18	0.30	0.52
	934	1000	6	4	2	1946	3	51.39	0.30	0.53
	922	1000	5	5	2	1934	4	51.71	0.40	0.53
	925	1000	4	3	4	1936	3	51.65	0.30	0.53
Mean value								51.48	0.33	0.53
20	962	1000	6	3	2	1973	4	50.68	0.40	0.52
	978	1000	5	4	3	1990	2	50.25	0.20	0.51
	992	1000	6	4	4	2006	3	49.85	0.30	0.51
	983	1000	7	3	2	1995	4	50.13	0.40	0.51
Mean value								50.23	0.33	0.51
30	1197	1000	6	5	3	2211	4	45.23	0.40	0.46
	1256	1000	7	3	3	2269	4	44.07	0.40	0.45
	1278	1000	6	5	2	2291	3	43.65	0.30	0.45
	1236	1000	4	5	3	2248	5	44.48	0.50	0.46
Mean value								44.36	0.40	0.46
40	1276	1000	9	5	4	2294	3	43.59	0.30	0.45
	1320	1000	8	5	5	2338	4	42.77	0.40	0.44
	1424	1000	6	5	3	2438	3	41.02	0.30	0.42
	1435	1000	10	3	2	2450	4	40.82	0.40	0.42
Mean value								42.05	0.35	0.43

50	1668	1000	12	6	5	2691	3	37.16	0.30	0.39
	1754	1000	8	5	4	2771	4	36.09	0.40	0.37
	1823	1000	7	8	4	2842	3	35.19	0.30	0.37
	1895	1000	12	7	5	2919	4	34.26	0.40	0.36
Mean value								35.67	0.35	0.37
60	1788	1000	9	6	4	2807	2	35.63	0.20	0.37
	1825	1000	9	5	3	2842	2	35.19	0.20	0.36
	1964	1000	10	5	3	2982	1	33.53	0.10	0.35
	1980	1000	8	4	2	2994	2	33.40	0.20	0.34
Mean value								34.44	0.18	0.36
70	3467	1000	4	4	2	4477	2	22.34	0.20	0.23
	3510	1000	3	5	3	4521	3	22.12	0.30	0.23
	3624	1000	3	3	4	4634	1	21.58	0.10	0.22
	3543	1000	3	4	1	4551	1	21.97	0.10	0.22
Mean value								22.00	0.18	0.22
80	3603	1000	2	2	2	4609	2	21.70	0.20	0.22
	3566	1000	3	3	1	4573	1	21.87	0.10	0.22
	3520	1000	2	3	2	4527	0	22.09	0.00	0.22
	3535	1000	2	2	1	4540	2	22.03	0.20	0.22
Mean value								21.92	0.13	0.22
90	5012	1000	2	2	0	6016	1	16.62	0.10	0.17
	4796	1000	2	4	0	5802	0	17.24	0.00	0.17
	4899	1000	3	1	1	5904	1	16.94	0.10	0.17
	5023	1000	2	2	1	6028	0	16.59	0.00	0.17
Mean value								16.85	0.05	0.17

100	5431	1000	2	3	0	6436	0	15.54	0.00	0.16
	5323	1000	2	3	0	6328	0	15.80	0.00	0.16
	5241	1000	3	2	1	6247	0	16.01	0.00	0.16
	5236	1000	3	2	0	6241	1	16.02	0.10	0.16
Mean value								15.84	0.03	0.16

N.B. Mono= Mononucleated cells, Bi= Binucleated cells, Tri= Trinucleated cells, Tetra= Tetranucleated cells, Multi= Multinucleated cells, Mn= Micronuclei, Mn/Bn=Micronuclei in binucleated cells, RI= Replication index.

Table A3. Raw data on *in vitro* CBMA for AHH-1 cells treated with andrographolide.

Dose (µM)	Mono	Bi	Tri	Tetra	Multi	Total	Total Mn	% Bi	% Mn/Bi	RI
0	1452	2000	8	11	6	3477	2	57.52	0.10	0.59
	1486	2000	9	10	4	3509	3	57.00	0.15	0.58
	1428	2000	10	9	3	3450	3	57.97	0.15	0.59
	1462	2000	10	8	3	3483	3	57.42	0.15	0.59
Mean value								57.48	0.14	0.59
DMSO	1510	2000	8	12	4	3534	3	56.59	0.15	0.58
	1515	2000	7	10	3	3535	3	56.58	0.15	0.58
	1492	2000	7	9	3	3511	4	56.96	0.20	0.58
	1502	2000	9	7	4	3522	4	56.79	0.20	0.58
Mean value								56.73	0.18	0.58
10	945	1000	8	4	2	1959	3	51.05	0.30	0.52
	941	1000	7	4	2	1954	2	51.18	0.20	0.53
	930	1000	6	5	3	1944	3	51.44	0.30	0.53
	938	1000	7	5	4	1954	4	51.18	0.40	0.53

Mean value								51.21	0.30	0.53
30	1291	1000	10	5	3	2309	5	43.31	0.50	0.45
	1258	1000	10	3	3	2274	4	43.98	0.40	0.45
	1164	1000	6	6	4	2180	4	45.87	0.40	0.47
	1275	1000	7	9	2	2293	3	43.61	0.30	0.45
Mean value								44.19	0.40	0.46
50	1765	1000	11	7	5	2788	3	35.87	0.30	0.38
	1821	1000	12	8	5	2846	3	35.14	0.30	0.37
	1911	1000	8	7	4	2930	4	34.13	0.40	0.35
	1788	1000	8	5	3	2804	3	35.66	0.30	0.37
Mean value								35.20	0.33	0.37
70	3367	1000	4	3	3	4377	2	22.85	0.20	0.23
	3450	1000	3	6	2	4461	1	22.42	0.10	0.23
	3621	1000	4	4	2	4631	1	21.59	0.10	0.22
	3677	1000	3	4	3	4687	3	21.34	0.30	0.22
Mean value								22.05	0.18	0.23
90	4820	1000	2	2	0	5824	0	17.17	0.00	0.17
	4758	1000	1	3	1	5763	1	17.35	0.10	0.18
	4965	1000	4	1	1	5971	1	16.75	0.10	0.17
	5095	1000	2	3	1	6101	0	16.39	0.00	0.17
Mean value								16.92	0.05	0.17

N.B. Mono= Mononucleated cells, Bi= Binucleated cells, Tri= Trinucleated cells, Tetra= Tetranucleated cells, Multi= Multinucleated cells, Mn= Micronuclei, Mn/Bn=Micronuclei in binucleated cells, RI= Replication index.

Table A4. Raw data on *in vitro* CBMA for MCL-5 cells treated with andrographolide.

Dose (μM)	Mono	Bi	Tri	Tetra	Multi	Total	Total Mn	% Bi	% Mn/Bi	RI
0	1506	2000	7	19	6	3538	2	56.53	0.10	0.58
	1650	2000	10	6	6	3672	4	54.47	0.20	0.56
	1672	2000	12	10	3	3697	2	54.10	0.10	0.55
	1536	2000	9	12	7	3564	3	56.12	0.15	0.58
Mean value								55.30	0.14	0.57
DMSO	1668	2000	9	12	6	3695	2	54.13	0.10	0.56
	1675	2000	10	8	5	3698	3	54.08	0.15	0.55
	1650	2000	8	11	4	3673	3	54.45	0.15	0.56
	1655	2000	8	8	4	3675	3	54.42	0.15	0.56
Mean value								54.27	0.14	0.56
10	943	1000	9	11	2	1965	2	50.89	0.20	0.53
	950	1000	9	9	4	1972	1	50.71	0.10	0.53
	980	1000	10	7	5	2002	1	49.95	0.10	0.52
	968	1000	10	9	8	1995	2	50.13	0.20	0.53
Mean value								50.42	0.15	0.53
30	1388	1000	11	11	3	2413	3	41.44	0.30	0.44
	1490	1000	9	5	4	2508	4	39.87	0.40	0.41
	1502	1000	7	5	2	2516	3	39.75	0.30	0.41
	1420	1000	5	8	2	2435	3	41.07	0.30	0.42
Mean value								40.53	0.33	0.42
50	1789	1000	10	6	4	2809	4	35.60	0.40	0.37

	1820	1000	9	7	3	2839	4	35.22	0.40	0.37
	1862	1000	12	5	3	2882	5	34.70	0.50	0.36
	1938	1000	10	12	2	2962	3	33.76	0.30	0.35
Mean value								34.82	0.40	0.36
70	3238	1000	5	2	1	4246	2	23.55	0.20	0.24
	3560	1000	6	3	0	4569	1	21.89	0.10	0.22
	3497	1000	4	2	0	4503	1	22.21	0.10	0.22
	3602	1000	4	2	1	4609	1	21.70	0.10	0.22
Mean value								22.34	0.13	0.23
90	4520	1000	3	2	0	5525	1	18.10	0.10	0.18
	4557	1000	4	3	0	5564	0	17.97	0.00	0.18
	4401	1000	4	1	2	5408	2	18.49	0.20	0.19
	3976	1000	2	0	1	4979	0	20.08	0.00	0.20
Mean value								18.66	0.08	0.19

N.B. Mono= Mononucleated cells, Bi= Binucleated cells, Tri= Trinucleated cells, Tetra= Tetranucleated cells, Multi= Multinucleated cells, Mn= Micronuclei, Mn/Bn=Micronuclei in binucleated cells, RI= Replication index.

Table A5. Raw data on *in vitro* CBMA for V-79 cells treated with andrographolide.

Dose (μM)	Mono	Bi	Tri	Tetra	Multi	Total	Total Mn	% Bi	% Mn/Bi	RI
0	2132	2000	10	6	3	4151	3	48.18	0.15	0.49
	2035	2000	9	5	3	4052	3	49.36	0.15	0.50
	2192	2000	12	8	5	4217	2	47.43	0.10	0.49
	2167	2000	13	10	4	4194	2	47.69	0.10	0.49
Mean value								48.16	0.13	0.49
DMSO	1350	1000	14	8	5	2377	2	42.07	0.20	0.44
	1408	1000	12	5	3	2428	1	41.19	0.10	0.43
	1280	1000	10	6	3	2299	1	43.50	0.10	0.45
	1249	1000	10	4	4	2267	2	44.11	0.20	0.46
Mean value								42.72	0.15	0.45
10	1320	1000	14	10	3	2347	3	42.61	0.30	0.45
	1448	1000	12	9	5	2474	4	40.42	0.40	0.43
	1361	1000	12	12	6	2391	3	41.82	0.30	0.44
	1460	1000	10	5	5	2480	3	40.32	0.30	0.42
Mean value								41.29	0.33	0.43
30	1675	1000	16	11	6	2708	5	36.93	0.50	0.39
	1698	1000	20	11	5	2734	6	36.58	0.60	0.39
	1720	1000	17	9	8	2754	4	36.31	0.40	0.39
	1676	1000	15	10	8	2709	5	36.91	0.50	0.39
Mean value								36.68	0.50	0.39

50	2464	1000	19	10	7	3500	4	28.57	0.40	0.31
	2311	1000	21	9	6	3347	3	29.88	0.30	0.32
	2514	1000	17	8	5	3544	5	28.22	0.50	0.30
	2402	1000	20	10	8	3440	5	29.07	0.50	0.31
Mean value								28.93	0.43	0.31
70	3985	1000	3	3	3	4994	1	20.02	0.10	0.20
	4051	1000	3	4	1	5059	1	19.77	0.10	0.20
	4098	1000	4	5	3	5110	2	19.57	0.20	0.20
	4210	1000	3	4	2	5219	2	19.16	0.20	0.20
Mean value								19.63	0.15	0.20
90	4861	1000	2	2	3	5868	0	17.04	0.00	0.17
	4626	1000	3	1	1	5631	1	17.76	0.10	0.18
	4688	1000	2	2	0	5692	1	17.57	0.10	0.18
	5210	1000	2	2	2	6216	1	16.09	0.10	0.16
Mean value								17.11	0.08	0.17

N.B. Mono= Mononucleated cells, Bi= Binucleated cells, Tri= Trinucleated cells, Tetra= Tetranucleated cells, Multi= Multinucleated cells, Mn= Micronuclei, Mn/Bn=Micronuclei in binucleated cells, RI= Replication index.

Table A6. Raw data on cells challenged with mitomycin-C.

Cell Line	Mono	Bi	Tri	Tetra	Multi	Total	Total Mn	% Bi	% Mn/Bi	RI
AHH-1	960	1000	7	9	5	1981	15	50.48	1.5	0.53
	982	1000	9	12	5	2008	19	49.80	1.9	0.52
	976	1000	8	10	4	1998	19	50.05	1.9	0.52
	964	1000	10	10	3	1987	22	50.33	2.2	0.53
Mean value								50.16	1.9	0.52

MCL-5	987	1000	9	8	5	2009	21	49.78	2.1	0.52
	982	1000	10	10	7	2009	22	49.78	2.2	0.52
	992	1000	8	8	4	2012	22	49.70	2.2	0.52
	989	1000	8	9	6	2012	25	49.70	2.5	0.52
Mean value								49.74	2.3	0.52
V-79	1420	1000	10	12	6	2448	25	40.85	2.5	0.43
	1359	1000	9	9	5	2382	23	41.98	2.3	0.44
	1393	1000	11	9	8	2421	20	41.31	2.0	0.44
	1464	1000	8	10	6	2488	20	40.19	2.0	0.42
Mean value								41.08	2.2	0.43

N.B. Mono= Mononucleated cells, Bi= Binucleated cells, Tri= Trinucleated cells, Tetra= Tetranucleated cells, Multi= Multinucleated cells, Mn= Micronuclei, Mn/Bn=Micronuclei in binucleated cells, RI= Replication index.

Table A7. The frequency of micronuclei in AHH-1 and MCL-5 mononucleated cells treated with andrographolide in CBMN *in vitro*.

	AHH-1			MCL-5		
Dose (μM)	Mono	Total Mn	% Mn/Mono	Mono	Total Mn	% Mn/Mono
0	1452	1	0.07	1506	2	0.13
	1486	0	0.00	1650	1	0.06
	1428	2	0.14	1672	1	0.06
	1462	2	0.14	1536	1	0.07
Mean value		5	0.09		5	0.08
DMSO	1510	1	0.07	1668	2	0.12
	1515	2	0.13	1675	1	0.06
	1492	1	0.07	1650	1	0.06
	1502	2	0.13	1655	1	0.06

Mean value		6	0.10		5	0.08
10	945	1	0.11	943	1	0.11
	941	1	0.11	950	1	0.11
	930	2	0.22	980	2	0.20
	938	1	0.11	968	1	0.10
Mean value		5	0.13		5	0.13
30	1291	2	0.15	1388	2	0.14
	1258	2	0.16	1490	1	0.07
	1164	1	0.09	1502	2	0.13
	1275	1	0.08	1420	2	0.14
Mean value		6	0.12		7	0.12
50	1765	2	0.11	1789	2	0.11
	1821	3	0.16	1820	2	0.11
	1911	2	0.10	1862	2	0.11
	1788	1	0.06	1938	3	0.15
Mean value		8	0.11		9	0.12
70	3367	2	0.06	3238	1	0.03
	3450	2	0.06	3560	2	0.06
	3621	1	0.03	3497	2	0.06
	3677	2	0.05	3602	1	0.03
Mean value		7	0.05		6	0.04
90	4820	1	0.02	4520	1	0.02
	4758	2	0.04	4557	0	0.00
	4965	1	0.02	4401	2	0.05

	5095	2	0.04	3976	1	0.03
Mean value		6	0.03		4	0.02

Table A8. Raw data on the frequency of necrotic and apoptotic AHH-1 cells treated with andrographolide for 24 hours.

Dose (μM)	Viable cells	Necrotic cells	Apoptotic cells	Total cells	% Necrotic cells	% Apoptotic cells
0	918	78	4	1000	7.80	0.40
	912	85	3	1000	8.50	0.30
	914	82	4	1000	8.20	0.40
	908	88	4	1000	8.80	0.40
Mean value					8.33	0.38
DMSO	903	92	5	1000	9.20	0.50
	912	84	4	1000	8.40	0.40
	911	85	4	1000	8.50	0.40
	914	81	5	1000	8.10	0.50
Mean value					8.55	0.45
10	871	120	9	1000	12.00	0.90
	877	115	8	1000	11.50	0.80
	863	128	9	1000	12.80	0.90
	865	125	10	1000	12.50	1.00
Mean value					12.20	0.90
30	635	355	10	1000	35.50	1.00
	648	341	11	1000	34.10	1.10
	614	376	10	1000	37.60	1.00

	623	362	15	1000	36.20	1.50
Mean value					35.85	1.15
50	589	399	12	1000	39.90	1.20
	568	420	12	1000	42.00	1.20
	554	436	10	1000	43.60	1.00
	567	422	11	1000	42.20	1.10
Mean value					41.93	1.13
70	471	520	9	1000	52.00	0.90
	494	498	8	1000	49.80	0.80
	490	502	8	1000	50.20	0.80
	526	466	8	1000	46.60	0.80
Mean value					49.65	0.83
90	323	672	5	1000	67.20	0.50
	341	656	3	1000	65.60	0.30
	366	632	2	1000	63.20	0.20
	314	682	4	1000	68.20	0.40
					66.05	0.35

Table A9. Raw data on the frequency of necrotic and apoptotic MCL-5 cells treated with andrographolide for 24 hours.

Dose (μM)	**Viable cells**	**Necrotic cells**	**Apoptotic cells**	**Total cells**	**% Necrotic cells**	**% Apoptotic cells**
0	921	75	4	1000	7.50	0.40
	925	70	5	1000	7.00	0.50

	923	73	4	1000	7.30	0.40
	913	82	5	1000	8.20	0.50
Mean value					7.50	0.45
DMSO	912	82	6	1000	8.20	0.60
	920	76	4	1000	7.60	0.40
	917	78	5	1000	7.80	0.50
	912	84	4	1000	8.40	0.40
Mean value					8.00	0.48
10	824	165	11	1000	16.50	1.10
	834	158	8	1000	15.80	0.80
	852	142	6	1000	14.20	0.60
	849	146	5	1000	14.60	0.50
Mean value					15.28	0.75
30	618	364	18	1000	36.40	1.80
	602	391	12	1005	38.91	1.19
	661	332	10	1003	33.10	1.00
	653	339	11	1003	33.80	1.10
Mean value					35.55	1.27
50	522	469	10	1001	46.85	1.00
	515	475	10	1000	47.50	1.00
	527	465	9	1001	46.45	0.90
	538	454	12	1004	45.22	1.20
Mean value					46.51	1.02
70	371	620	9	1000	62.00	0.90

	362	629	9	1000	62.90	0.90
	408	584	8	1000	58.40	0.80
	379	611	7	997	61.28	0.70
Mean value					61.15	0.83
90	316	678	6	1000	67.80	0.60
	345	650	5	1000	65.00	0.50
	351	645	4	1000	64.50	0.40
	335	662	3	1000	66.20	0.30
					65.88	0.45

Table A10. Raw data on the frequency of necrotic and apoptotic V-79 cells treated with andrographolide for 24 hours.

Dose (μM)	**Viable cells**	**Necrotic cells**	**Apoptotic cells**	**Total cells**	**% Necrotic cells**	**% Apoptotic cells**
0	921	76	3	1000	7.60	0.30
	919	78	3	1000	7.80	0.30
	915	82	3	1000	8.20	0.30
	906	89	5	1000	8.90	0.50
Mean value					8.13	0.35
DMSO	908	87	5	1000	8.70	0.50
	910	85	5	1000	8.50	0.50
	927	70	3	1000	7.00	0.30
	909	86	5	1000	8.60	0.50
Mean value					8.20	0.45
10	838	152	10	1000	15.20	1.00

	836	156	8	1000	15.60	0.80
	842	150	8	1000	15.00	0.80
	832	159	9	1000	15.90	0.90
Mean value					15.43	0.88
30	733	252	15	1000	25.20	1.50
	749	237	14	1000	23.70	1.40
	746	242	12	1000	24.20	1.20
	728	258	14	1000	25.80	1.40
Mean value					24.73	1.38
50	571	420	9	1000	42.00	0.90
	579	415	6	1000	41.50	0.60
	564	428	8	1000	42.80	0.80
	582	409	9	1000	40.90	0.90
Mean value					41.80	0.80
70	465	532	3	1000	53.20	0.30
	484	512	4	1000	51.20	0.40
	520	478	2	1000	47.80	0.20
	498	497	5	1000	49.70	0.50
Mean value					50.48	0.35
90	310	688	2	1000	68.80	0.20
	304	694	2	1000	69.40	0.20
	320	676	4	1000	67.60	0.40
	294	702	4	1000	70.20	0.40
					69.00	0.30

Table A11. Raw data on the frequency of necrotic and apoptotic cell death for MCL-5 cells treated with andrographolide for 8 hours.

Dose (μM)	Viable cells	Necrotic cells	Apoptotic cells	Total cells	% Necrotic cells	% Apoptotic cells
0	926	70	4	1000	7.00	0.40
	925	71	4	1000	7.10	0.40
	926	71	3	1000	7.10	0.30
	917	80	3	1000	8.00	0.30
Mean value					7.30	0.35
DMSO	912	83	5	1000	8.30	0.50
	923	74	3	1000	7.40	0.30
	913	83	4	1000	8.30	0.40
	921	74	5	1000	7.40	0.50
Mean value					7.85	0.43
10	870	109	8	987	11.04	0.81
	879	114	8	1001	11.39	0.80
	893	98	9	1000	9.80	0.90
	877	110	8	995	11.06	0.80
Mean value					10.82	0.83
30	787	201	12	1000	20.10	1.20
	827	159	14	1000	15.90	1.40
	809	178	13	1000	17.80	1.30
	802	185	13	1000	18.50	1.30
Mean value					18.08	1.30

50	793	194	13	1000	19.40	1.30
	795	190	15	1000	19.00	1.50
	776	211	13	1000	21.10	1.30
	765	219	16	1000	21.90	1.60
Mean value					20.35	1.43
70	645	350	5	1000	35.00	0.50
	675	320	5	1000	32.00	0.50
	661	336	3	1000	33.60	0.30
	654	342	4	1000	34.20	0.40
Mean value					33.70	0.43
90	610	387	3	1000	38.70	0.30
	575	421	4	1000	42.10	0.40
	563	433	4	1000	43.30	0.40
	582	415	3	1000	41.50	0.30
Mean value					41.40	0.35

Table A12. Trypan-blue exclusion cell viability assay for AHH-1 cells treated with andrographolide for 24 hours.

Dose	Alive	Dead (blue)	Total	Cell conc (cells/ml)	% Non-viable cells	% Viable cells	Mean cell concentration (cells/ml)	Mean % Non-viable cells	Mean % Viable cells
0	221	5	226	5.65E+05	2.21	97.79	6.14E+05	2.66	97.34
	236	5	241	6.03E+05	2.07	97.93			
	260	10	270	6.75E+05	3.70	96.30			
DMSO	238	4	242	6.05E+05	1.65	98.35	6.10E+05	2.45	97.55
	225	6	231	5.78E+05	2.60	97.40			

	251	8	259	6.48E+05	3.09	96.91			
10	220	15	235	5.88E+05	6.38	93.62	6.04E+05	6.89	93.11
	225	20	245	6.13E+05	8.16	91.84			
	230	15	245	6.13E+05	6.12	93.88			
30	205	48	253	6.33E+05	18.97	81.03	5.94E+05	21.54	78.46
	180	53	233	5.83E+05	22.75	77.25			
	175	52	227	5.68E+05	22.91	77.09			
50	164	62	226	5.65E+05	27.43	72.57	5.61E+05	31.97	68.03
	154	70	224	5.60E+05	31.25	68.75			
	140	83	223	5.58E+05	37.22	62.78			
70	85	96	181	4.53E+05	53.04	46.96	4.22E+05	54.40	45.60
	76	87	163	4.08E+05	53.37	46.63			
	70	92	162	4.05E+05	56.79	43.21			
90	47	93	140	3.50E+05	66.43	33.57	3.26E+05	66.22	33.78
	44	87	131	3.28E+05	66.41	33.59			
	41	79	120	3.00E+05	65.83	34.17			

Table A13. Trypan-blue exclusion cell viability assay for MCL-5 cells treated with andrographolide for 24 hours.

Dose	Alive	Dead (blue)	Total	Cell conc (cells/ml)	% Non-viable cells	% Viable cells	Mean cell concentration (cells/ml)	Mean % Non-viable cells	Mean % Viable cells
0	215	7	222	5.55E+05	3.15	96.85	5.84E+05	3.00	97.00
	235	8	243	6.08E+05	3.29	96.71			

	230	6	236	5.90E+05	2.54	97.46			
DMSO	226	8	234	5.85E+05	3.42	96.58	5.73E+05	3.20	96.80
	225	6	231	5.78E+05	2.60	97.40			
	215	8	223	5.58E+05	3.59	96.41			
10	195	12	207	5.18E+05	5.80	94.20	5.15E+05	5.54	94.46
	180	12	192	4.80E+05	6.25	93.75			
	209	10	219	5.48E+05	4.57	95.43			
30	145	38	183	4.58E+05	20.77	79.23	4.63E+05	20.53	79.47
	146	36	182	4.55E+05	19.78	80.22			
	150	40	190	4.75E+05	21.05	78.95			
50	98	75	173	4.33E+05	43.35	56.65	4.29E+05	40.27	59.73
	115	62	177	4.43E+05	35.03	64.97			
	95	70	165	4.13E+05	42.42	57.58			
70	45	63	108	2.70E+05	58.33	41.67	2.78E+05	59.90	40.10
	48	70	118	2.95E+05	59.32	40.68			
	41	67	108	2.70E+05	62.04	37.96			
90	38	72	110	2.75E+05	65.45	34.55	2.40E+05	69.86	30.14
	30	62	92	2.30E+05	67.39	32.61			
	20	66	86	2.15E+05	76.74	23.26			

Table A14. Trypan-blue exclusion cell viability assay for V-79 cells treated with andrographolide for 24 hours.

Dose	Alive	Dead (blue)	Total	Cell conc (cells/ml)	% Non-viable cells	% Viable cells	Mean cell concentration (cells/ml)	Mean % Non-viable cells	Mean % Viable cells
0	131	11	142	3.55E+05	7.75	92.25	3.63E+05	6.69	93.31
	145	9	154	3.85E+05	5.84	94.16			
	130	9	139	3.48E+05	6.47	93.53			
DMSO	120	10	130	3.25E+05	7.69	92.31	3.23E+05	6.97	93.03
	115	8	123	3.08E+05	6.50	93.50			
	125	9	134	3.35E+05	6.72	93.28			
10	112	8	120	3.00E+05	6.67	93.33	2.93E+05	7.08	92.92
	104	7	111	2.78E+05	6.31	93.69			
	111	10	121	3.03E+05	8.26	91.74			
30	74	10	84	2.10E+05	11.90	88.10	2.03E+05	14.45	85.55
	66	12	78	1.95E+05	15.38	84.62			
	68	13	81	2.03E+05	16.05	83.95			
50	48	31	79	1.98E+05	39.24	60.76	2.00E+05	38.25	61.75
	48	35	83	2.08E+05	42.17	57.83			
	52	26	78	1.95E+05	33.33	66.67			
70	12	18	30	7.50E+04	60.00	40.00	7.50E+04	61.10	38.90
	10	16	26	6.50E+04	61.54	38.46			
	13	21	34	8.50E+04	61.76	38.24			
90	4	15	19	4.75E+04	78.95	21.05	4.83E+04	75.76	24.24

	4	11	15	3.75E+04	73.33	26.67			
	6	18	24	6.00E+04	75.00	25.00			

Table A15. Trypan-blue exclusion cell viability assay for V-79 cells treated with andrographolide for 48 hours.

Dose	Alive	Dead (blue)	Total	Cell conc (cells/ml)	% Non-viable cells	% Viable cells	Mean cell concentration (cells/ml)	Mean % Non-viable cells	Mean % Viable cells
0	302	94	396	9.90E+05	23.74	76.26	8.93E+05	25.62	74.38
	240	81	321	8.03E+05	25.23	74.77			
	256	99	355	8.88E+05	27.89	72.11			
DMSO	265	103	368	9.20E+05	27.99	72.01	9.04E+05	27.39	72.61
	273	110	383	9.58E+05	28.72	71.28			
	249	85	334	8.35E+05	25.45	74.55			
10	112	110	222	5.50E+05	49.55	50.45	6.28E+05	44.98	55.02
	160	125	285	7.13E+05	43.86	56.14			
	145	103	248	6.20E+05	41.53	58.47			
30	17	60	77	1.93E+05	77.92	22.08	2.42E+05	81.41	18.59
	12	79	91	2.28E+05	86.81	13.19			
	25	97	122	3.05E+05	79.51	20.49			
50	3	38	41	1.03E+05	92.68	7.32	1.39E+05	91.08	8.92
	3	51	54	1.35E+05	94.44	5.56			
	10	62	72	1.80E+05	86.11	13.89			
70	5	26	31	7.75E+04	83.87	16.13	7.50E+04	83.82	16.18

	2	25	27	6.75E+04	92.59	7.41			
	8	24	32	8.00E+04	75.00	25.00			
90	3	15	18	4.50E+04	83.33	16.67	5.08E+04	83.63	16.37
	3	16	19	4.75E+04	84.21	15.79			
	4	20	24	6.00E+04	83.33	16.67			

Table A16. Raw data on kinetochore labelling with CREST antibodies in MCL-5 cells.

Dose (μM)	**Kinetochore +ve**	**Kinetochore - ve**	**Total**	**% Kin +ve**	**% Kin - ve**	**Mean % kin +ve**	**Mean % kin - ve**
0	29	31	60	48.33	51.67	48.33	51.67
	28	32	60	46.67	53.33		
	30	30	60	50.00	50.00		
10	33	27	60	55.00	45.00	52.78	47.22
	32	28	60	53.33	46.67		
	30	30	60	50.00	50.00		
30	42	18	60	70.00	30.00	63.89	36.11
	35	25	60	58.33	41.67		
	38	22	60	63.33	36.67		
50	43	17	60	71.67	28.33	72.22	27.78
	45	15	60	75.00	25.00		
	42	18	60	70.00	30.00		

Data for Chapter 4.

Table A17. Raw data on MTOCs integrity in V-79 cells treated with andrographolide for 24 hours.

Dose (μM)	Bipolar	Tripolar	Tetrapolar	Multipolar	Total Count
0	965	27	6	2	1000
DMSO	857	30	10	3	900
10	840	42	9	9	900
30	742	99	33	26	900
50	687	125	52	36	900
Colchicine	482	282	87	49	900

Three replicate experiments were conducted using freshly prepared stocks of andrographolide. For each replicate experiment, 100 cells were scored per slide and three slides per dose. Cells treated with 70 and 90μM of andrographolide were not counted due to high cell non-viability. An extra slide was scored for the negative control '0'. This dataset is for the immunofluorescently-stained cells.

Table A18. Raw data on mitotic index in V-79 cells treated with andrographolide for 24 hours.

Dose (μM)	Interphase Cells	Mitotic Cells	Total Count	Mitotic Index
0	11446	554	12000	4.84
DMSO	8616	384	9000	4.46
10	8514	486	9000	5.71
30	8462	538	9000	6.36
50	8530	470	9000	5.51
70	8855	145	9000	1.64
90	8983	17	9000	0.19

Three replicate experiments were conducted using freshly prepared stocks of andrographolide. For each replicate experiment, 1000 cells were scored per slide and three slides per dose. Extra slides were scored for the negative control '0'. This dataset is for the BBR/SO-stained cells.

Table A19. Raw data on MTOCs integrity in V-79 cells treated with andrographolide and allowed to recover for 24 hours post treatment.

Dose (μM)	Bipolar	Tripolar	Tetrapolar	Multipolar	Total Count
0	377	19	2	2	400
DMSO	378	15	5	2	400
10	367	23	5	5	400
30	333	44	13	10	400
50	327	45	15	13	400

Four replicate experiments were conducted using freshly prepared stocks of andrographolide. For each replicate experiment, 100 cells were scored per slide for every dose. Cells treated with 70 and 90μM of andrographolide were not counted due to high cell non-viability. This dataset is for the immunofluorescently-stained cells.

Table A20. Raw data on MTOCs integrity in V-79 cells treated with andrographolide and allowed to recover for 48 hours post treatment.

Dose (μM)	Bipolar	Tripolar	Tetrapolar	Multipolar	Total Count
0	371	22	4	3	400
DMSO	378	17	4	1	400
10	358	29	9	4	400
30	325	49	15	11	400
50	310	56	21	13	400

Four replicate experiments were conducted using freshly prepared stocks of andrographolide. For each replicate experiment, 100 cells were scored per slide for every dose. Cells treated with 70 and 90μM of andrographolide were not counted due to high cell non-viability. This dataset is for the immunofluorescently-stained cells.

Table A21. Raw data on mitotic index in V-79 cells treated with andrographolide and allowed to recover for 24 hours post treatment.

Dose (µM)	Interphase Cells	Mitotic Cells	Total Count	Mitotic Index
0	2852	148	3000	5.19
DMSO	2851	149	3000	5.23
10	2837	163	3000	5.75
30	2822	178	3000	6.31
50	2828	172	3000	6.08
70	2849	151	3000	5.30
90	2850	150	3000	5.26

Three replicate experiments were conducted using freshly prepared stocks of andrographolide. For each replicate experiment, 1000 cells were scored per slide for every dose.

Table A22. Raw data on mitotic index in V-79 cells treated with andrographolide and allowed to recover for 48 hours post treatment.

Dose (µM)	Interphase Cells	Mitotic Cells	Total Count	Mitotic Index
0	2835	165	3000	5.82
DMSO	2844	156	3000	5.49
10	2807	193	3000	6.88
30	2796	204	3000	7.30
50	2777	223	3000	8.03
70	2783	217	3000	7.82
90	2822	178	3000	6.31

Three replicate experiments were conducted using freshly prepared stocks of andrographolide. For each replicate experiment, 1000 cells were scored per slide for every dose.

Table A23. Raw data on the incidence of aberrant mitosis in V-79 cells treated with andrographolide for 24 hours.

Dose (μM)	Abnormal mitosis	Normal mitosis	Total count
0	22	878	900
DMSO	24	876	900
10	39	861	900
30	98	802	900
50	95	805	900

Three replicate experiments were conducted using freshly prepared stocks of andrographolide. For each replicate experiment, 100 cells were scored per slide and three slides per dose.

Table A24. Raw data on the incidence of condensed chromatin in V-79 cells treated with andrographolide for 24 hours.

Dose (μM)	Normal	Condensed chromatin	Total count	Mean % condensed chromatin
0	4497	4	4501	0.09
DMSO	4495	5	4500	0.11
10	4493	7	4500	0.16
30	4473	27	4500	0.60
50	4418	82	4500	1.82
70	4337	163	4500	3.62
90	4260	240	4500	5.33

Table A25. Raw data on the incidence of condensed chromatin in V-79 cells treated with andrographolide for 24 hours and allowed to recover for another one cell cycle.

Dose (μM)	Normal	Condensed chromatin	Total count	Mean % condensed chromatin
0	4495	5	4500	0.11
DMSO	4494	6	4500	0.13
10	4492	8	4500	0.18

30	4469	31	4500	0.69
50	4407	93	4500	2.07
70	4303	197	4500	4.38
90	4262	238	4500	5.29

Table A26. Raw data on mitotic outcome of V-79 cells treated with different doses of andrographolide for 24 hours.

Dose (μM)	Mononucleates	Binucleates	Trinucleates	Tetranucleates	Multinucleates	Total	%Bi	%Tri	%Tetra	%Multi
0	973	24	3	0	0	1000	2.40	0.30	0.00	0.00
0	957	40	1	1	1	1000	4.00	0.10	0.10	0.10
0	948	46	3	2	1	1000	4.60	0.30	0.20	0.10
0	965	32	2	1	0	1000	3.20	0.20	0.10	0.00
DMSO	973	25	2	0	0	1000	2.50	0.20	0.00	0.00
DMSO	958	36	3	2	1	1000	3.60	0.30	0.20	0.10
DMSO	955	40	1	3	1	1000	4.00	0.10	0.30	0.10
DMSO	966	28	4	1	1	1000	2.80	0.40	0.10	0.10
10	937	59	1	2	1	1000	5.90	0.10	0.20	0.10
10	923	70	3	2	2	1000	7.00	0.30	0.20	0.20
10	905	85	4	4	2	1000	8.50	0.40	0.40	0.20
10	933	60	4	2	1	1000	6.00	0.40	0.20	0.10
30	853	124	10	8	5	1000	12.40	1.00	0.80	0.50
30	863	114	12	9	2	1000	11.40	1.20	0.90	0.20
30	801	165	25	7	2	1000	16.50	2.50	0.70	0.20

30	845	128	15	10	2	1000	12.80	1.50	1.00	0.20
50	822	149	15	7	7	1000	14.90	1.50	0.70	0.70
50	837	140	14	7	2	1000	14.00	1.40	0.70	0.20
50	843	135	15	4	3	1000	13.50	1.50	0.40	0.30
50	859	125	10	4	2	1000	12.50	1.00	0.40	0.20
70	845	130	11	6	8	1000	13.00	1.10	0.60	0.80
70	895	90	8	1	6	1000	9.00	0.80	0.10	0.60
70	904	85	5	2	4	1000	8.50	0.50	0.20	0.40
70	894	92	4	5	5	1000	9.20	0.40	0.50	0.50
90	942	50	4	2	2	1000	5.00	0.40	0.20	0.20
90	943	48	6	0	3	1000	4.80	0.60	0.00	0.30
90	956	38	3	1	2	1000	3.80	0.30	0.10	0.20
90	956	42	2	0	0	1000	4.20	0.20	0.00	0.00

Table A27. Raw data on mitotic outcome of V-79 cells treated with different doses of andrographolide for 24 hours and then permitted to grow for another 24 hours in the absence of andrographolide.

Dose (μM)	**Mononucleates**	**Binucleates**	**Trinucleates**	**Tetranucleates**	**Multinucleates**	**Total**	**%Bi**	**%Tri**	**%Tetra**	**%Multi**
0	973	24	3	0	0	1000	2.40	0.30	0.00	0.00
0	970	26	4	0	0	1000	2.60	0.40	0.00	0.00
0	973	23	3	1	0	1000	2.30	0.30	0.10	0.00
0	970	25	4	0	1	1000	2.50	0.40	0.00	0.10
DMSO	964	30	4	1	1	1000	3.00	0.40	0.10	0.10

DMSO	973	25	2	0	0	1000	2.50	0.20	0.00	0.00
DMSO	972	25	3	0	0	1000	2.50	0.30	0.00	0.00
DMSO	970	26	3	0	1	1000	2.60	0.30	0.00	0.10
10	955	35	8	2	0	1000	3.50	0.80	0.20	0.00
10	951	34	12	1	2	1000	3.40	1.20	0.10	0.20
10	960	27	9	3	1	1000	2.70	0.90	0.30	0.10
10	960	27	10	2	1	1000	2.70	1.00	0.20	0.10
30	914	65	14	5	2	1000	6.50	1.40	0.50	0.20
30	920	58	15	5	2	1000	5.80	1.50	0.50	0.20
30	915	62	18	4	1	1000	6.20	1.80	0.40	0.10
30	917	60	16	6	1	1000	6.00	1.60	0.60	0.10
50	904	68	18	6	4	1000	6.80	1.80	0.60	0.40
50	906	70	15	6	3	1000	7.00	1.50	0.60	0.30
50	904	68	20	5	3	1000	6.80	2.00	0.50	0.30
50	896	75	18	8	3	1000	7.50	1.80	0.80	0.30
70	956	33	5	4	2	1000	3.30	0.50	0.40	0.20
70	954	38	4	3	1	1000	3.80	0.40	0.30	0.10
70	958	35	5	2	0	1000	3.50	0.50	0.20	0.00
70	954	35	6	3	2	1000	3.50	0.60	0.30	0.20
90	970	25	3	2	0	1000	2.50	0.30	0.20	0.00
90	971	24	3	1	1	1000	2.40	0.30	0.10	0.10
90	974	20	5	0	1	1000	2.00	0.50	0.00	0.10
90	975	20	4	1	0	1000	2.00	0.40	0.10	0.00

Table A28. Raw data on mitotic outcome of MCL-5 cells treated with different doses of andrographolide for 24 hours.

Dose	Mononucleates	Binucleates	Trinucleates	Tetranucleates	Multinucleates	Total	%Bi	%Tri	%Tetra	%Multi
0	940	50	4	6	0	1000	5.00	0.40	0.60	0.00
0	925	64	6	5	0	1000	6.40	0.60	0.50	0.00
0	937	60	1	2	0	1000	6.00	0.10	0.20	0.00
0	937	55	3	4	1	1000	5.50	0.30	0.40	0.10
DMSO	930	55	8	5	2	1000	5.50	0.80	0.50	0.20
DMSO	927	71	0	2	0	1000	7.10	0.00	0.20	0.00
DMSO	931	60	5	2	2	1000	6.00	0.50	0.20	0.20
DMSO	931	57	7	3	2	1000	5.70	0.70	0.30	0.20
10	922	72	6	3	0	1003	7.18	0.60	0.30	0.00
10	858	131	5	3	3	1000	13.10	0.50	0.30	0.30
10	894	95	9	2	0	1000	9.50	0.90	0.20	0.00
10	875	115	6	2	2	1000	11.50	0.60	0.20	0.20
30	859	132	6	3	0	1000	13.20	0.60	0.30	0.00
30	843	140	8	5	4	1000	14.00	0.80	0.50	0.40
30	853	128	10	9	0	1000	12.80	1.00	0.90	0.00
30	843	135	12	7	3	1000	13.50	1.20	0.70	0.30
50	875	116	4	3	2	1000	11.60	0.40	0.30	0.20
50	874	101	12	8	5	1000	10.10	1.20	0.80	0.50
50	904	92	1	3	0	1000	9.20	0.10	0.30	0.00
50	871	109	9	6	5	1000	10.90	0.90	0.60	0.50

70	921	73	3	0	3	1000	7.30	0.30	0.00	0.30
70	924	69	4	3	0	1000	6.90	0.40	0.30	0.00
70	945	50	1	2	2	1000	5.00	0.10	0.20	0.20
70	937	57	4	1	1	1000	5.70	0.40	0.10	0.10
90	938	52	5	2	3	1000	5.20	0.50	0.20	0.30
90	940	53	3	3	1	1000	5.30	0.30	0.30	0.10
90	975	21	2	2	0	1000	2.10	0.20	0.20	0.00
90	965	30	2	1	2	1000	3.00	0.20	0.10	0.20

Table 29. Raw data on mitotic outcome of MCL-5 cells treated with different doses of andrographolide for 48 hours.

Dose (μM)	Mononucleates	Binucleates	Trinucleates	Tetranucleates	Multinucleates	Total	%Bi	%Tri	%Tetra	%Multi
0	957	39	3	1	0	1000	3.90	0.30	0.10	0.00
0	969	27	1	3	0	1000	2.70	0.10	0.30	0.00
0	966	30	1	0	3	1000	3.00	0.10	0.00	0.30
0	968	28	2	2	0	1000	2.80	0.20	0.20	0.00
DMSO	940	55	3	1	1	1000	5.50	0.30	0.10	0.10
DMSO	962	31	4	1	2	1000	3.10	0.40	0.10	0.20
DMSO	974	25	1	0	0	1000	2.50	0.10	0.00	0.00
DMSO	972	25	2	0	1	1000	2.50	0.20	0.00	0.10
10	894	98	4	4	0	1000	9.80	0.40	0.40	0.00
10	918	77	3	2	0	1000	7.70	0.30	0.20	0.00
10	946	50	2	1	1	1000	5.00	0.20	0.10	0.10
10	940	55	3	1	1	1000	5.50	0.30	0.10	0.10
30	861	121	9	6	3	1000	12.10	0.90	0.60	0.30
30	897	95	2	5	1	1000	9.50	0.20	0.50	0.10
30	886	105	5	3	1	1000	10.50	0.50	0.30	0.10
30	907	86	4	3	0	1000	8.60	0.40	0.30	0.00
50	877	115	4	2	2	1000	11.50	0.40	0.20	0.20
50	913	80	3	2	2	1000	8.00	0.30	0.20	0.20
50	879	109	6	2	4	1000	10.90	0.60	0.20	0.40
50	897	93	5	3	2	1000	9.30	0.50	0.30	0.20

70	898	92	6	3	1	1000	9.20	0.60	0.30	0.10
70	891	99	6	4	0	1000	9.90	0.60	0.40	0.00
70	909	85	4	2	0	1000	8.50	0.40	0.20	0.00
70	917	79	3	0	1	1000	7.90	0.30	0.00	0.10
90	906	91	1	1	1	1000	9.10	0.10	0.10	0.10
90	926	70	2	1	1	1000	7.00	0.20	0.10	0.10
90	928	71	1	0	0	1000	7.10	0.10	0.00	0.00
90	917	81	0	2	0	1000	8.10	0.00	0.20	0.00

Table A30. Raw data on mitotic outcome of MCL-5 cells treated with different doses of andrographolide for 120 hours.

Dose (μM)	**Mononucleates**	**Binucleates**	**Trinucleates**	**Tetranucleates**	**Multinucleates**	**Total**	**%Bi**	**%Tri**	**%Tetra**	**%Multi**
0	926	65	3	6	0	1000	6.50	0.30	0.60	0.00
0	920	70	5	5	0	1000	7.00	0.50	0.50	0.00
0	924	69	4	3	0	1000	6.90	0.40	0.30	0.00
0	911	78	5	5	1	1000	7.80	0.50	0.50	0.10
10	855	121	11	7	6	1000	12.10	1.10	0.70	0.60
10	851	127	11	8	3	1000	12.70	1.10	0.80	0.30
10	876	117	6	1	0	1000	11.70	0.60	0.10	0.00
10	856	122	9	10	3	1000	12.20	0.90	1.00	0.30
30	813	115	22	15	5	970	11.86	2.27	1.55	0.52
30	829	103	16	6	5	959	10.74	1.67	0.63	0.52
30	825	98	13	4	4	944	10.38	1.38	0.42	0.42

30	772	111	19	14	6	922	12.04	2.06	1.52	0.65
50	830	93	19	5	6	953	9.76	1.99	0.52	0.63
50	817	95	17	9	5	943	10.07	1.80	0.95	0.53
50	804	96	15	12	4	931	10.31	1.61	1.29	0.43
50	808	94	20	8	4	934	10.06	2.14	0.86	0.43

Table A31. Raw data on the incidence of necrotic and apoptotic death in MCL-5 cells treated with different doses of andrographolide for 120 hours.

Dose (μM)	**Viable cells**	**Necrotic cells**	**Apoptotic cells**	**Total cells**	**% Viable cells**	**% Necrotic cells**	**% Apoptotic cells**
0	429	68	3	500	85.80	13.60	0.60
	431	65	4	500	86.20	13.00	0.80
	435	62	3	500	87.00	12.40	0.60
	432	64	4	500	86.40	12.80	0.80
DMSO	426	70	4	500	85.20	14.00	0.80
	431	65	4	500	86.20	13.00	0.80
	433	63	4	500	86.60	12.60	0.80
	432	65	3	500	86.40	13.00	0.60
10	375	120	5	500	75.00	24.00	1.00
	379	115	6	500	75.80	23.00	1.20
	370	125	5	500	74.00	25.00	1.00
	367	129	4	500	73.40	25.80	0.80
30	322	168	10	500	64.40	33.60	2.00

	334	159	7	500	66.80	31.80	1.40
	320	175	5	500	64.00	35.00	1.00
	332	161	7	500	66.40	32.20	1.40
50	245	247	8	500	49.00	49.40	1.60
	243	251	6	500	48.60	50.20	1.20
	234	259	7	500	46.80	51.80	1.40
	233	262	5	500	46.60	52.40	1.00

Data for Chapter 5.

Table A32. Raw data of andrographolide-treated AHH-1 cells with 6-thioguanine selection for HPRT⁻ mutant detection. Replicates A and B.

Dose (μM)	Replicate A					Replicate B				
	PE		*HPRT*⁻ mutants			PE		*HPRT*⁻ mutants		
	Positive	Total	Positive	Total	MF	Positive	Total	Positive	Total	MF
0	298	300	4	300	1.34	294	300	0	300	0.00
DMSO	296	300	4	300	1.55	295	300	2	300	0.82
1	291	300	7	300	3.37	294	300	2	300	0.85
5	291	300	6	300	2.88	292	300	5	300	2.32
10	291	300	10	300	4.83	290	300	8	300	3.97
30	290	300	64	300	35.27	286	300	75	300	46.93
50	281	300	8	300	4.90	275	300	14	300	9.62
MMS	294	300	117	300	63.18	291	300	115	300	68.93

Cells cultured for plating efficiency (PE) did not have 6-thioguanine added. HPRT= Hypoxanthine phosphoribosyl transferase, MMS= Methyl methane sulfonate (4μM)

Table A33. Raw data of andrographolide-treated AHH-1 cells with 6-thioguanine selection for HPRT⁻ mutant detection. Replicates C and D.

Dose (μM)	Replicate C					Replicate D				
	PE		*HPRT*⁻ mutants			PE		*HPRT*⁻ mutants		
	Positive	Total	Positive	Total	MF	Positive	Total	Positive	Total	MF
0	295	300	5	300	2.05	296	300	1	300	0.39
DMSO	295	300	2	300	0.82	296	300	1	300	0.39
1	294	300	1	300	0.43	295	300	3	300	1.23
5	291	300	7	300	3.37	288	300	11	300	5.80
10	288	300	11	300	5.80	285	300	15	300	8.56
30	280	300	68	300	47.46	277	300	79	300	59.50
50	270	300	10	300	7.36	272	300	10	300	7.15
MMS	292	300	121	300	71.24	292	300	119	300	69.71

Cells cultured for plating efficiency (PE) did not have 6-thioguanine added. *HPRT*⁻= Hypoxanthine phosphoribosyl transferase. MMS= Methyl methane sulfonate (4μM).